REPORT NO. GDC-DCB69-046
CONTRACT NAS 9-9207

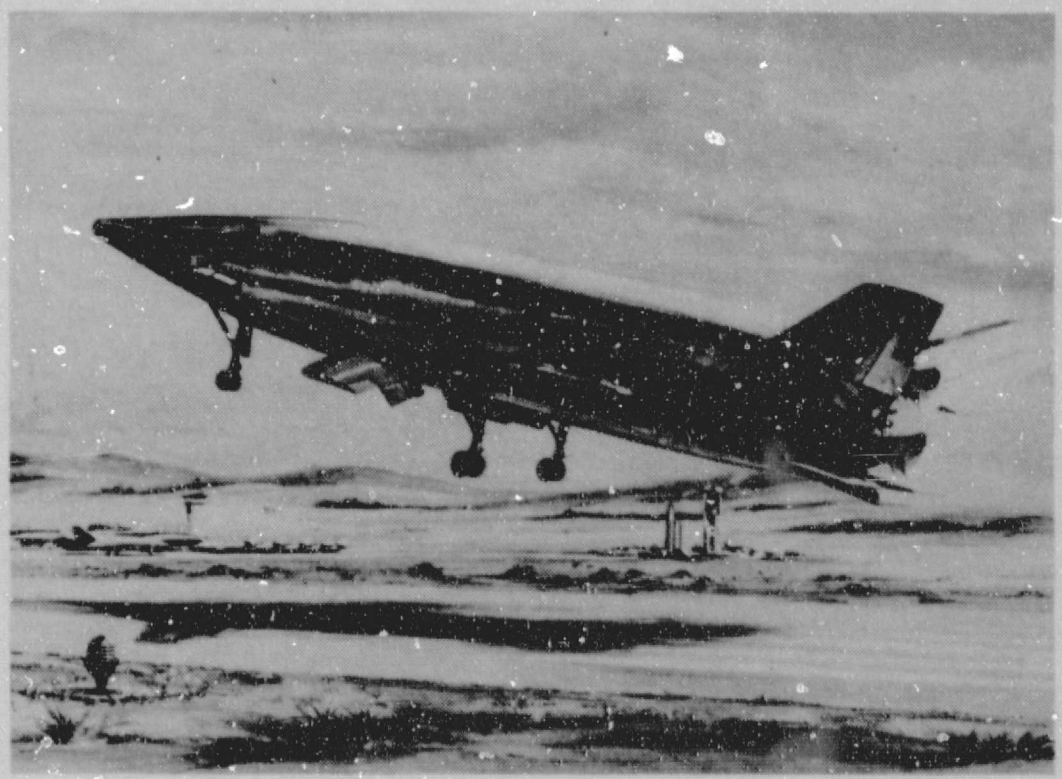

SPACE SHUTTLE
FINAL TECHNICAL REPORT

VOLUME III • INITIAL VEHICLE SPECTRUM AND PARAMETRIC EXCURSIONS

GENERAL DYNAMICS
Convair Division

REPORT NO. GDC-DCB69-046

SPACE SHUTTLE
FINAL TECHNICAL REPORT

VOLUME III • INITIAL VEHICLE SPECTRUM AND PARAMETRIC EXCURSIONS

31 October 1969

Prepared by
CONVAIR DIVISION OF GENERAL DYNAMICS
San Diego, California

FOREWORD

This volume of Convair Report No. GDC-DCB 69-046 constitutes a portion of the final report for the "Study of Integral Launch and Reentry Vehicles." The study was conducted by Convair, a division of General Dynamics Corporation, for National Aeronautics and Space Administration George C. Marshall Space Flight Center under Contract NAS 9-9207 Modification 2.

The final report is published in ten volumes:

Volume I	Condensed Summary
Volume II	Final Vehicle Configurations
Volume III	Initial Vehicle Spectrum and Parametric Excursions
Volume IV	Technical Analysis and Performance
Volume V	Subsystems and Weight Analysis
Volume VI	Propulsion Analysis and Tradeoffs
Volume VII	Integrated Electronics
Volume VIII	Mission/Payload and Safety/Abort Analyses
Volume IX	Ground Turnaround Operations and Facility Requirements
Volume X	Program Development, Cost Analysis, and Technology Requirements

Convair gratefully acknowledges the cooperation of the many agencies and companies that provided technical assistance during this study:

NASA-MSFC	Aerojet-General Corporation
NASA-MSC	Rocketdyne
NASA-ERC	Pratt and Whitney
NASA-LaRC	Pan American World Airways

The study was managed and supervised by Glenn Karel, Study Manager, C. P. Plummer, Principal Configuration Designer, and Carl E. Crone, Principal Program Analyst (all of Convair) under the direction of Charles M. Akridge and Alfred J. Finzel, NASA study co-managers.

ABSTRACT

A study was made to obtain a conceptual definition of reusable space shuttle systems having multimission capability. The systems as defined can deliver 50,000-pound payloads having a diameter of 15 feet and a length of 60 feet to a 55-degree inclined orbit at an altitude of 270 n.mi. The following types of missions can be accommodated by the space shuttle system: logistics; propellant delivery; propulsive stage delivery; satellite delivery, retrieval, and maintenance; short-duration missions, and rescue missions.

Two types of reusable space shuttle systems were defined: a two-element system consisting of a boost and an orbital element and a three-element system consisting of two boost elements and an orbital element. The vehicles lift off vertically using high pressure oxygen/hydrogen rocket engines, land horizontally on conventional runways, and are fully reusable. The boost elements, after staging, perform an aerodynamic entry and fly back to the launch site using conventional airbreathing engines. Radiative thermal protection systems were defined to provide for reusability. Development programs, technology programs, schedules, and costs have been defined for planning purposes.

During the study, special emphasis was given to the following areas: System Development Approaches, Ground Turnaround Operations, Mission Interfaces and Cargo Accommodations/Handling, Propulsion System Parameters, and Integrated Electronics Systems.

TABLE OF CONTENTS

TABLE OF CONTENTS, Contd

TABLE OF CONTENTS, Contd

LIST OF FIGURES

LIST OF FIGURES, Contd

LIST OF FIGURES, Contd

LIST OF FIGURES, Contd

LIST OF FIGURES, Contd

LIST OF FIGURES, Contd

LIST OF TABLES

LIST OF TABLES, Contd

SUMMARY

The vehicle configurations are summarized in the figure below. The three-element systems have elements of identical size and shape. The two-element vehicles are optimized for minimum weight and have larger booster elements. Section 2 contains a description of each vehicle.

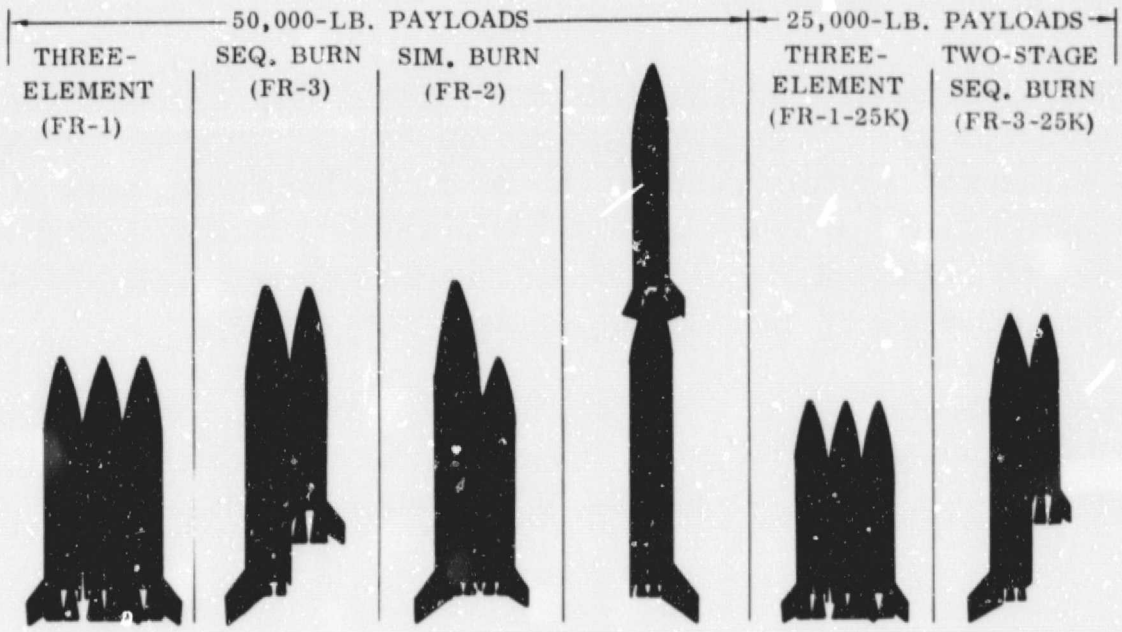

LIFTOFF WT. (10^6 LB.)	4.53	4.00	3.53	3.86	2.81	2.76
THRUST/ENG. (10^6 LB.)	1.070	0.710	0.497	0.681	0.670	0.488
COMMON AERO SHAPE	YES	NO	NO	NO	YES	NO
CROSS-FEED	YES	NO	YES	NO	YES	NO

Performance trade studies were conducted using the two-element, sequential-burn vehicle (second from left in the figure) as a baseline. The results, discussed in Section 3, indicate that the vehicle will stage at approximately 11,000 ft/sec. The booster element has a thrust-to-weight ratio of 1.45 and the orbiter 1.30 for optimum performance. Orbiter engine failure considerations, however, indicate that the thrust-to-weight ratio should be increased to approximately 1.60 to achieve a once-around abort capability. Development costs make it attractive to use a common rocket engine for both stages of the two-element system. The program costs follow the weight trends. The nonrecurring costs follow the total dry system weight trends, and the recurring costs follow the gross weight trends (see Section 3.1.3).

Section 4 provides a summary of the FR-1 (three-element with crossfeed) developed during the study period. As shown in the vehicle spectrum, this vehicle has a higher gross weight than any of the two-element configurations; however, it has the basic advantage of a common stage shape, which can substantially reduce development costs. A sensitivity comparison shows the three-element (FR-1) gross liftoff weight more sensitive to orbiter weight and ΔV maneuver requirements when compared with a two-element vehicle.

In Section 5, vehicles with and without propellant crossfeed are compared. It was determined that for a given vehicle configuration, (such as "common" elements) the use of crossfeed reduces launch weight six to nine percent. However, if the vehicles are optimized for either crossfeed or no crossfeed, differences in weight are minor.

Section 6 contains a preliminary comparison of fixed and deployable-wing space shuttle configurations. It was concluded that the weight difference was small. The fixed wing is inherently simpler in concept; however, the fixed wing needs to satisfy subsonic, transonic, and hypersonic entry flight conditions, including entry heating. Deployable wings eliminate entry wing problems at some expense in structural complexity. The deployable-wing cross-range capability is also greater.

Section 7 contains studies of space shuttle configurations with the gross liftoff weight fixed at 3.0 and 3.5M pounds. It was necessary to relax the basic study ground rules (contingency) to meet the 50,000-pound payload requirement.

SECTION 1

INTRODUCTION

This volume contains the initial definition of the vehicle spectrum defined by NASA and evaluated by Convair in this study. This spectrum is shown in Figure 1-1 and includes the following concepts.

The term "element" is used to denote a complete "flyable" entity. All configurations studied have either two or three elements. The two booster elements of the three-element FR-1 are simultaneously staged from the orbiter element.

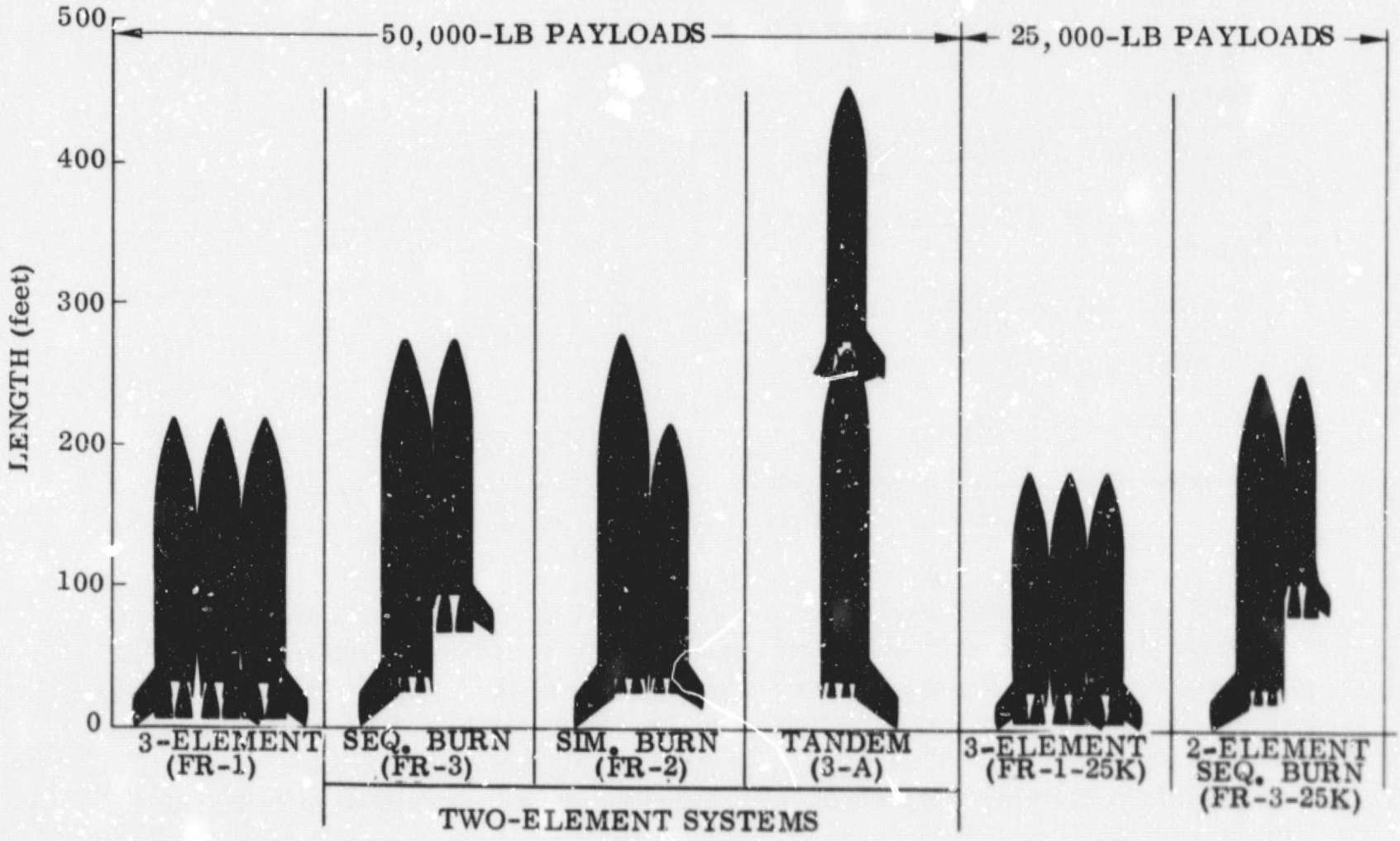

Figure 1-1. Vehicle Spectrum

a. Two-element systems:

   1. 50,000 pound payload vehicles:

      a) Parallel staged, sequential burn concept (Vehicle FR-3)

      b) Tandem staged concept (Vehicle 3A)

      c) Parallel staged, simultaneous burn (with crossfeed) concept (Vehicle FR-2)

   2. 25,000 pound payload vehicles:

      a) Parallel staged, sequential burn concept (Vehicle FR-3-25K)

b. Three-element systems:

   1. 50,000 pound payload vehicle (with crossfeed) (Vehicle FR-1-25K).

   2. 25,000 pound payload vehicle (with crossfeed) (Vehicle FR-1-25K).

All of the vehicles were sized to satisfy the following requirements (see Figure 1-2).

a. A 55-degree, 270-n. mi. orbit; launch from ETR.

b. An on-orbit ΔV capability of 1800 fps using the main propulsion system suitably throttled.

c. An orbital and entry attitude control subsystem ΔV of 200 fps.

d. A 3/4 of 1 percent contingency on the ideal ΔV to orbit including backpressure losses.

e. A 10 percent contingency on dry weight across the board.

f. An orbit staytime of 7 days maximum.

g. A 3g axial load limit.

h. Payload size: 15 feet diameter and 60 feet long (50,000 lb),
   15 feet diameter and 15 feet long (25,000 lb).

A typical two-stage flight profile is summarized in Figure 1-3. A major problem in examining the large number of vehicle configurations listed was to derive meaningful and consistent supporting data on the characteristics of each stage. The approach used to solve this problem was to establish a baseline stage configuration compatible with the basic requirements. This baseline stage was then sized and modified as required for each of the above arrangements. The baseline stage is described in Section 2.

A flow diagram of the initial vehicle design process is shown in Figure 1-4. An initial vehicle is synthesized to the given groundrules using inputs to the synthesis program (Volume IV) based on preliminary design layouts and experience. The results of this

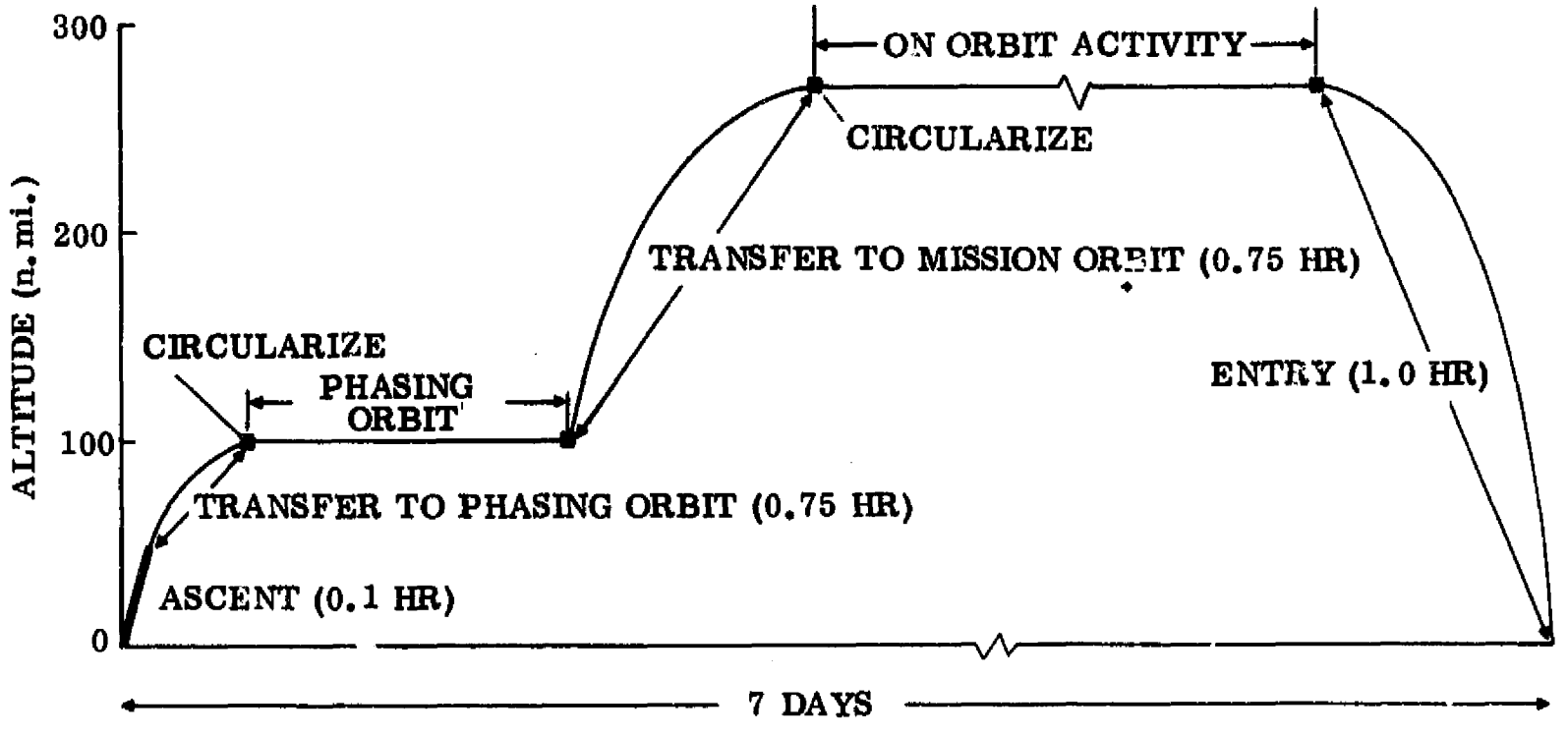

Figure 1-2. Mission Profile

synthesis, based on a selected geometry, are packaged in terms of preliminary weight bogies, initial trajectory, and a vehicle layout with preliminary dimensional data. This package is analyzed by the various technical groups as indicated on the schematic. The results of these investigations result in inputs to a new iteration from which the "final" vehicle layouts are made. Sensitivies and vehicle mass properties are then generated. This is a very simplified flow diagram, there being in fact many internal iterations; the entire loop must be traversed more than once or twice, depending on the degree of iteration closure in performance, loads, weights, and vehicle balance required.

By agreement with MSFC a two-element and a three-element system without propellant crossfeed and with a 50,000 pound payload capability were selected for a more detailed definition. These systems are described in Volume II.

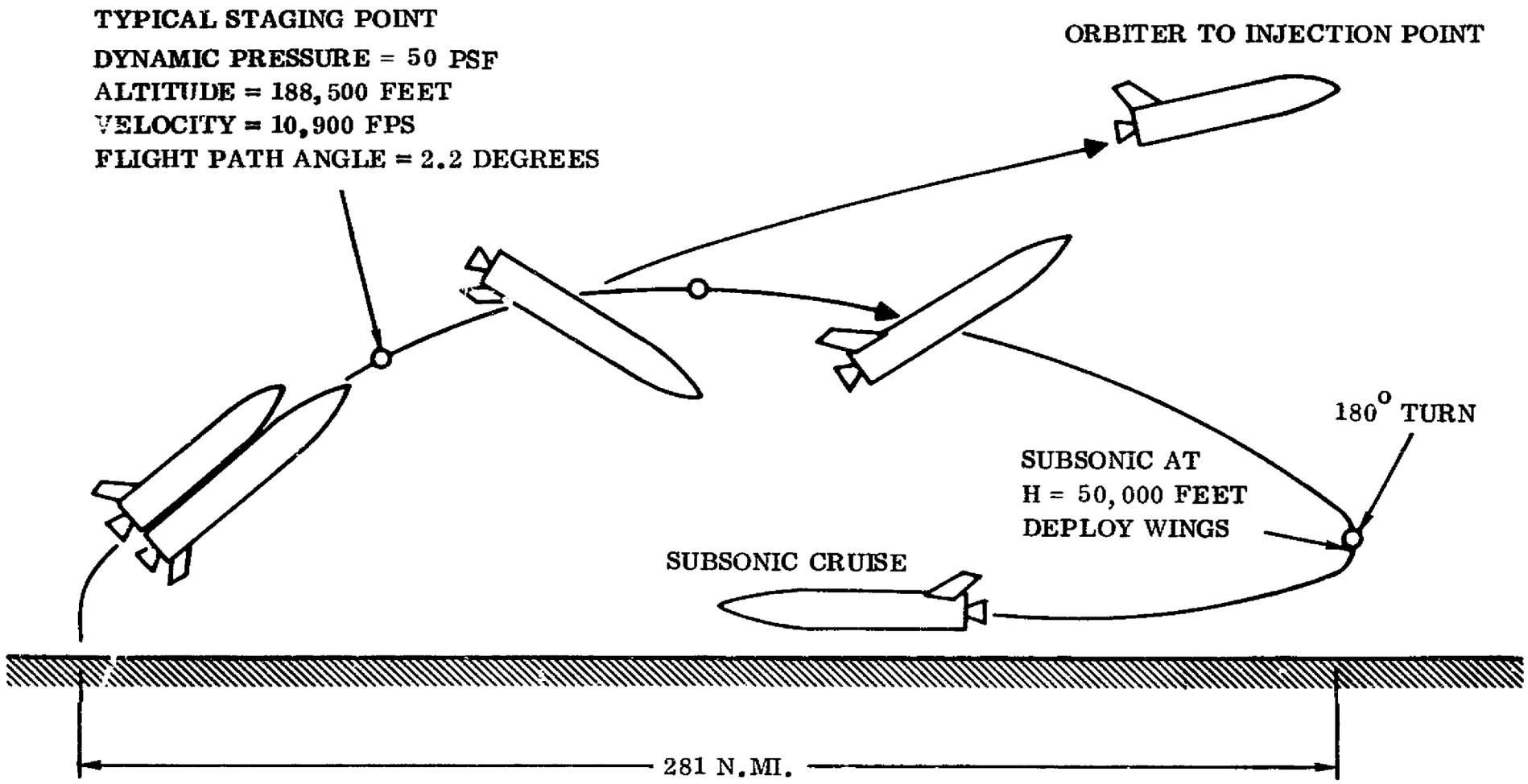

Figure 1-3. Two-Stage Flight Profile

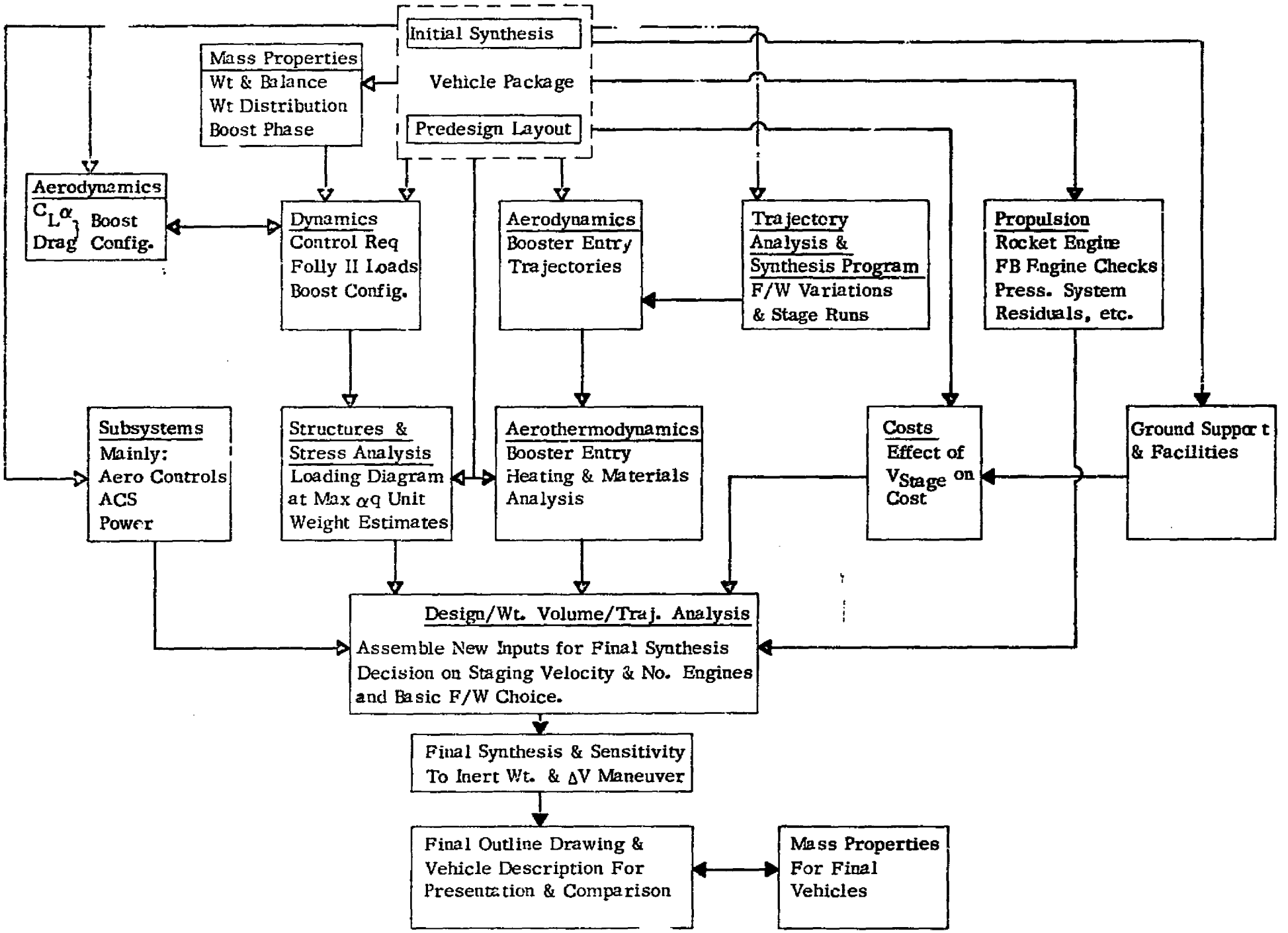

Figure 1-4. NASA ILRV Design Process

SECTION 2

VEHICLE DESIGN AND DESCRIPTION

This section contains a general description of the baseline element configuration. Paragraphs 2.1 through 2.7 then describe the two- and three-element arrangements shown in Figure 1-1.

All vehicles have the following common characteristics: high performance, bell type, LO_2/LH_2 engines, flyback air-breathing propulsion systems, and vertical takeoff and horizontal landing (VTOHL).

Vehicle staging arrangements and operations were investigated for all candidate systems. The aerodynamic configuration was optimized considering the overall flight regime and performance requirements.

Figure 2-1 shows the general arrangement of the baseline element with stowable wings. The cross-section has a flat bottom and semicircular upper surface. The flat bottom improves hypersonic lift/drag ratio and provides convenient stowage for the wings. The sides are sloped slightly, both to improve the hypersonic lift/drag ratio and to reduce entry heating. The semicircular upper surface is compatible with circular propellant tanks. The nose of the body is parabolic in both the side and plan view. The Vee tail is attached high up on the aft body for subsonic stability and to provide adequate hypersonic directional stability.

The element shown was modified as required for specific applications. Overall size varied as a result of propellant requirements. The payload bay and subsystems require modification when used as a boost element. Specific arrangements of booster and orbiter elements are described further in subsequent paragraphs.

2.1 SEQUENTIAL BURN 50K POUND PAYLOAD, VEHICLE FR-3

The two-stage sequential burn baseline vehicle is shown in Figure 2-2 in the mated (launch) configuration. The booster and orbiter stages are shown separately in Figures 2-3 and 2-4.

The vehicle shapes are derived from the baseline configuration. All stages have variable geometry stowable wings. The vehicle size was based on a series of runs made on the Convair weight/volume/performance synthesis program as were all the vehicles in the spectrum. The objective was to treat all the vehicles on the same basis and to the same ground rules so that the comparisons would be valid.

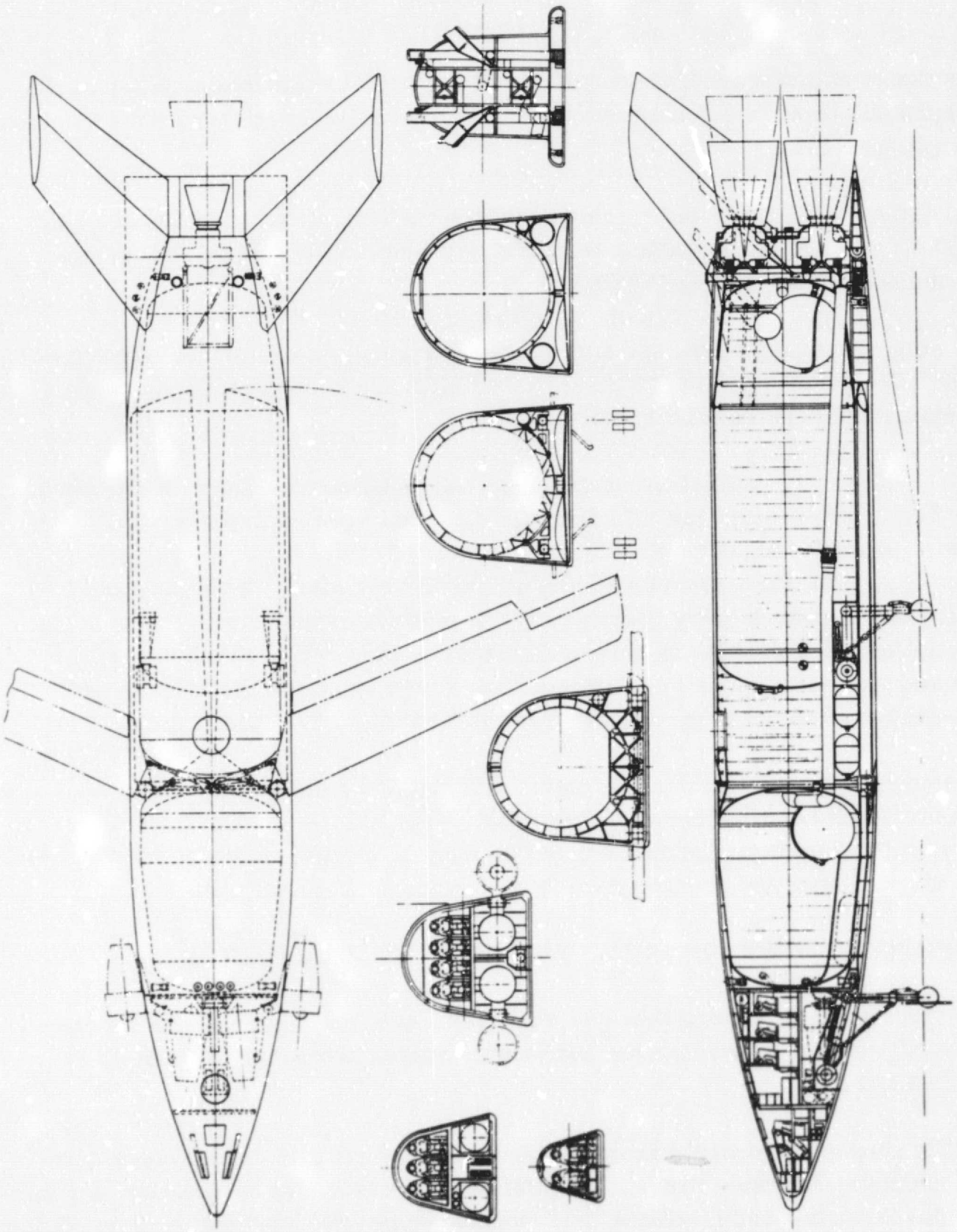

Figure 2-1. Baseline Element

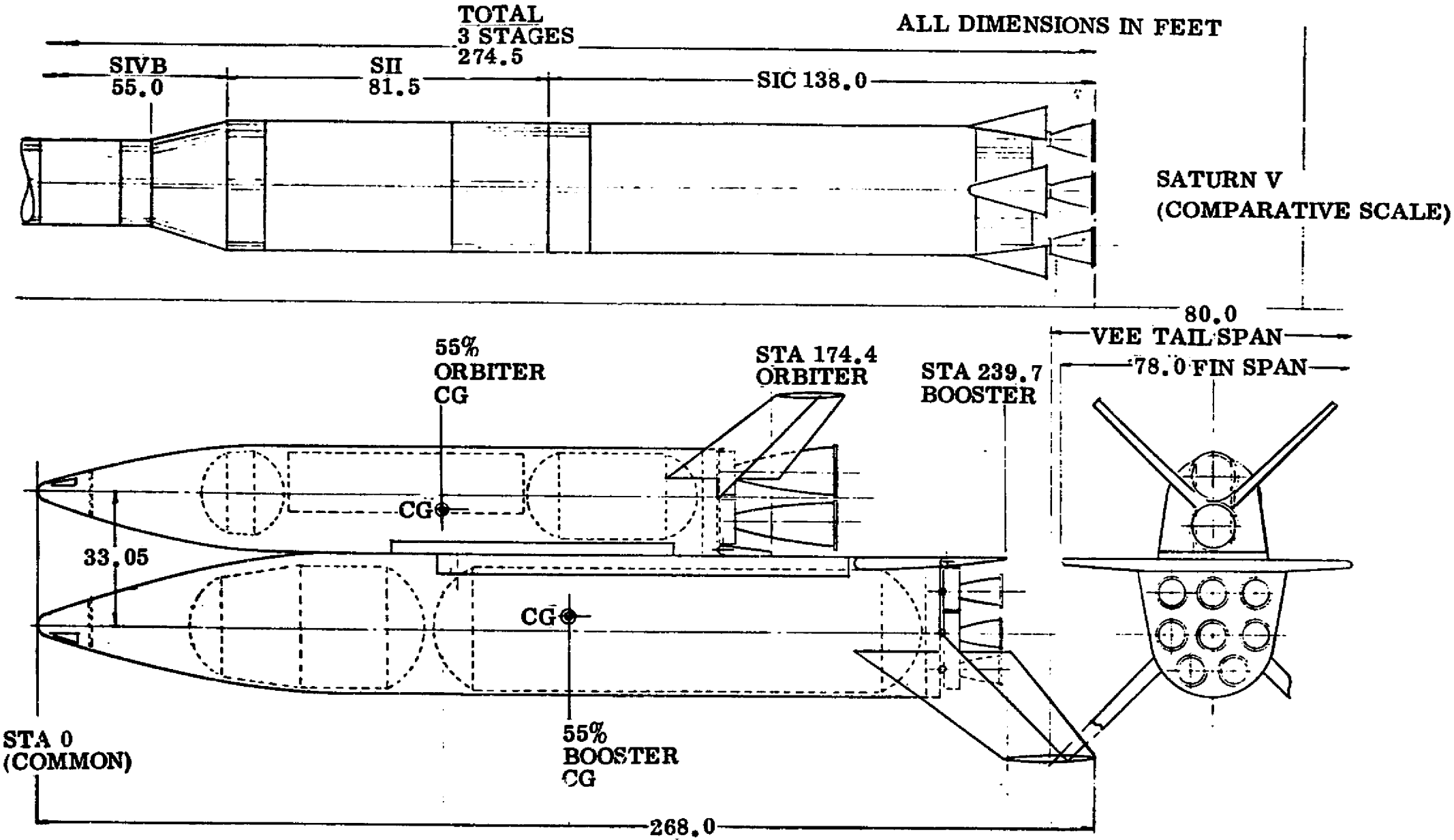

Figure 2-2. Vehicle FR-3 Baseline

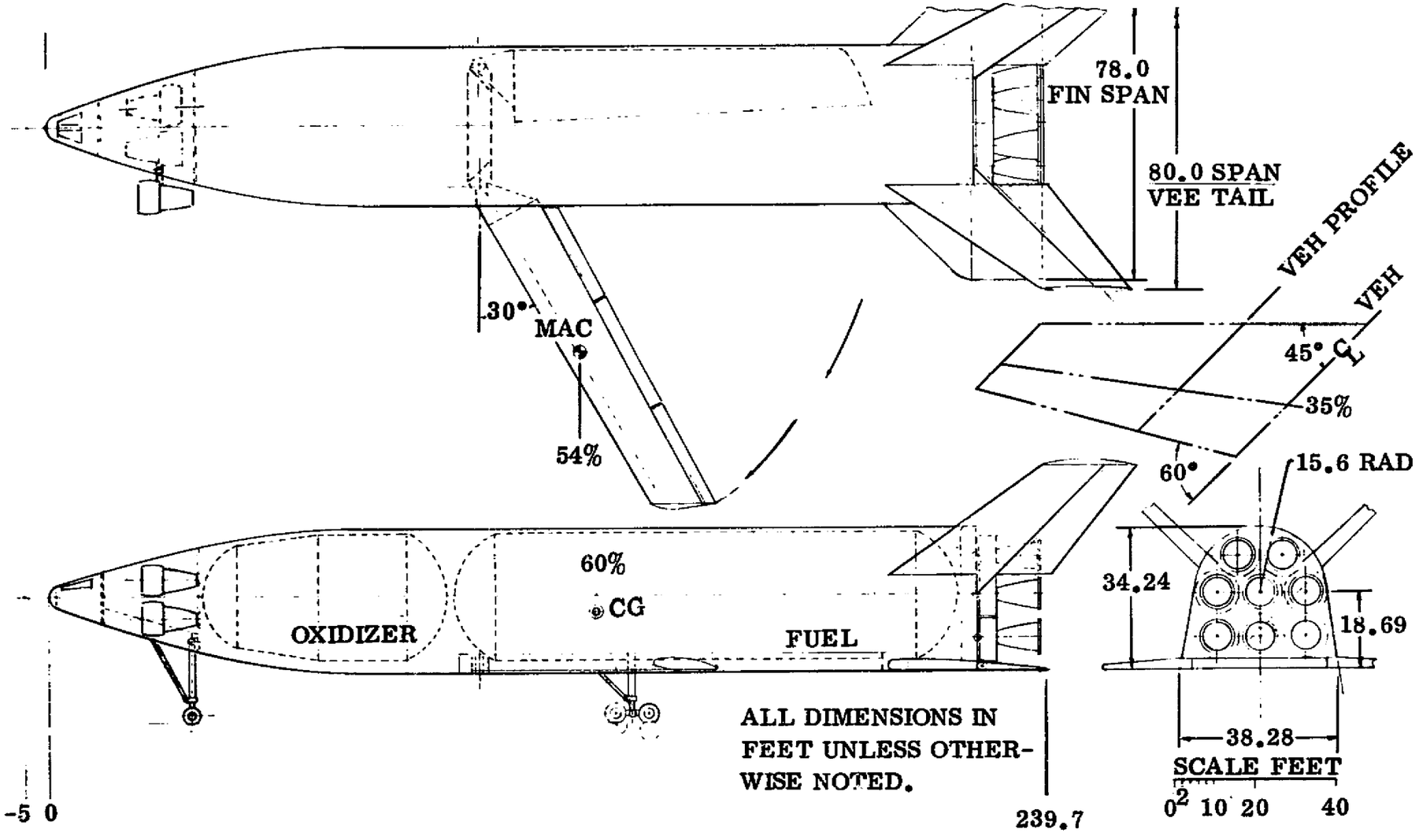

Figure 2-3. Booster — Vehicle FR-3

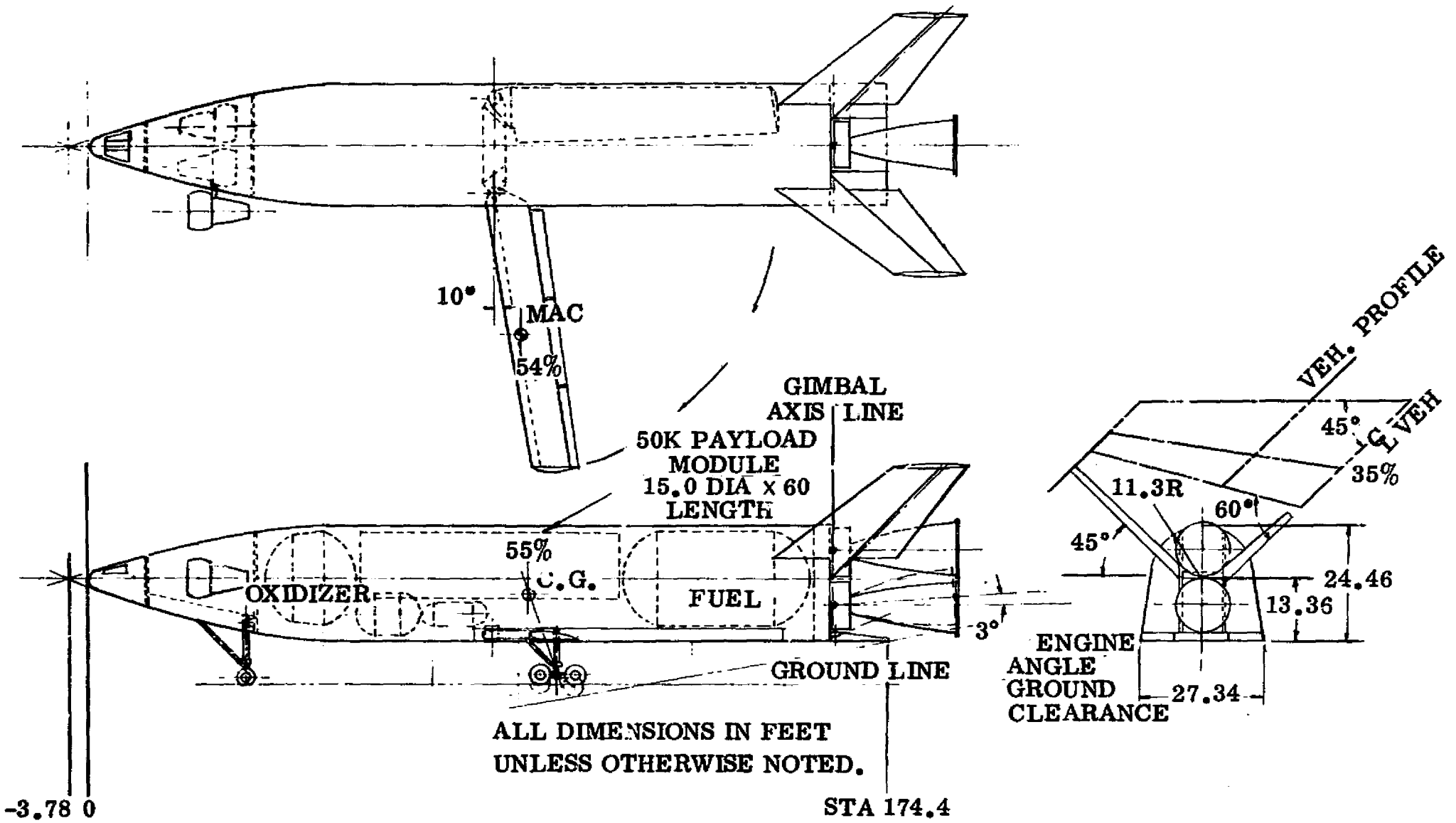

Figure 2-4. Orbiter — Vehicle FR-3

The staging velocity for Vehicle FR-3 was selected from the following synthesis results:

Staging Velocity (fps)	Gross Liftoff Weight (lb)	Total System Dry Weight (lb)
10,642	3,996,000	712,830
11,089	4,007,000	711,420
11,617	4,030,000	711,011

The design point was selected at 11,089 fps - a compromise between gross liftoff weight and total hardware weight.

The boost trajectory adopted was one where the second stage was injected at an altitude of 260,000 feet (43 n. mi.), representing the perigee of an elliptical orbit whose apogee was at 100 nautical miles. Thus, the vehicle has approximately 100 fps excess velocity above the circular velocity requirement at the 260,000 foot altitude initial boost burnout injection point. After approximately 45 minutes of coast time the orbit is circularized at 100 n. mi. by reigniting a single main engine and providing a circularizing "kick" of approximately 105 fps.

A staging dynamic pressure of 50 psf was adopted for all vehicles in the spectrum. This was shown at the time to be the minimum system gross liftoff weight value for the FR-1 series of vehicles. Subsequent work reported in Volume II, Section 4 indicates that a somewhat lower staging dynamic pressure, in the order of 40 psf, would minimize GLOW but the differences are not great.

The synthesis summary run is shown in Table 2-1. (Only the summary run is shown here.) In Paragraph 6.7 of this volume a more complete weight, dimension, and trajectory printout is given for an updated version of the two-stage sequential burn 50K pound payload vehicle.

The booster is about four times the weight of the orbiter and about three times the volume. Typical planform loadings are 61 psf for the booster and 59 psf for the orbiter elements. The rocket engines have common thrust chamber and primary nozzles. The nozzles are compromised to give the orbiter vehicle the additional expansion ratio. The booster expansion ratio is 35/80 (two position) and the orbiter is 150. Four flyback engines are used in the booster and two in the orbiter.

Table 2-1. FR-3 Two-Stage Sequential, 50K Pound Payload Vehicle Synthesis Summary

	BOOSTER ELEMENT	ORBITER	VEHICLE
WEIGHT			
FUEL	352858	64903	
OXIDIZER	2258288	454319	
PROPELLANT	2611146	519221	
FLYBACK FUEL	45921	2992	
PAYLOAD		50000	
STRUCTURE	513042	198380	711422
TOTAL	3190525	816941	4007467
IN ORBIT	0	302315	
RETURN CONDITION	579393	293714	
ENTRY	0	253591	
LANDING	513996	249297	
VOLUME			
FUEL	87740	13134	
OXIDIZER	33460	6728	
PROPELLANT	121200	19861	
PAYLOAD		10638	
OTHER	71533	43773	
TOTAL	192733	74272	
GEOMETRY			
LENGTH	239.7	174.4	
BODY WETTED AREA	25144.5	13315.5	
BODY PLANFORM AREA	9174.6	4299.6	
ENTRY PLANFORM LOADING	61.1	59.0	
PROPULSION			
THRUST-TO-WEIGHT		1.73110	1.39238
NO. OF ENGINES	8	2	
THRUST PER ENGINE (SL)	697491 UPRATED		
THRUST PER ENGINE (VAC)	O/F = 6.4	707103 NOMINAL	
SPECIFIC IMPULSE (SL)	395.0	357.4 O/F = 7.0	395.0
SPECIFIC IMPULSE (VAC)	451.7	456.5	451.7
TRAJECTORY			
MASS RATIO		2.70102	2.47000
MAXIMUM DYNAMIC PRESSURE			669.2
STAGING DYNAMIC PRESSURE			50
STAGING VELOCITY (RELATIVE)			11089
STAGING ALTITUDE			188351
STAGING FLIGHT PATH ANGLE (RELATIVE)			1.860
INJECTION VELOCITY (INERTIAL)		25897	
INJECTION ALTITUDE		259985	
INJECTION FLIGHT PATH ANGLE (INERTIAL)		.001	
INJECTION INCLINATION		54.56	
FLYBACK RANGE	283.7		

2.2 TANDEM 50K POUND PAYLOAD, VEHICLE 3A

The tandem two-stage baseline vehicle, sized to a staging velocity of 10,977 ft/sec, is shown in Figure 2-5. The staging velocity was selected on the basis of the following synthesis results:

Staging Velocity (fps)	Gross Liftoff Weight (lb)	Total System Dry Weight (lb)
10,474	3,877,000	689,810
10,987	3,860,000	684,140
11,485	3,870,000	682,250

Vehicle sizing is based on the synthesis run summary shown in Table 2-2. Since the overall vehicle is performance optimized, the first stage is larger than the orbital stage (booster weight/orbiter weight = 3.56). As a result, the sizes of the major structural components (tanks, wings, etc.) are not similar. Commonality of the rocket engines was obtained by using the same basic engine on both stages with different expansion ratio nozzles. A weight summary is shown in Table 2-3.

The truss adapter shown in Figure 2-5 was selected as a baseline due to its inherent simplicity and reliability. Stage separation is accomplished by releasing four explosive bolts attaching the truss adapter to the orbiter base. The truss is permanently attached to the booster in this concept and is recovered with it.

The two-stage tandem concept is well over 400 feet high in the launch configuration. Because of this, the configuration was not considered acceptable by NASA and was discontinued on 19 August 1969.

2.3 SIMULTANEOUS BURN 50K POUND PAYLOAD, VEHICLE FR-2

The simultaneous burn two-stage ILRV baseline is shown in Figure 2-6 in the launch configuration. The booster and orbiter stages are shown separately in Figures 2-7 and 2-8.

The relative staging velocity of 11,050 ft/sec was selected on the basis of synthesis runs with the following results:

Staging Velocity (fps)	Gross Liftoff Weight (lb)	Total System Dry Weight (lb)
10,546	3,581,000	596,080
11,046	3,533,000	588,510
11,533	3,513,000	582,890

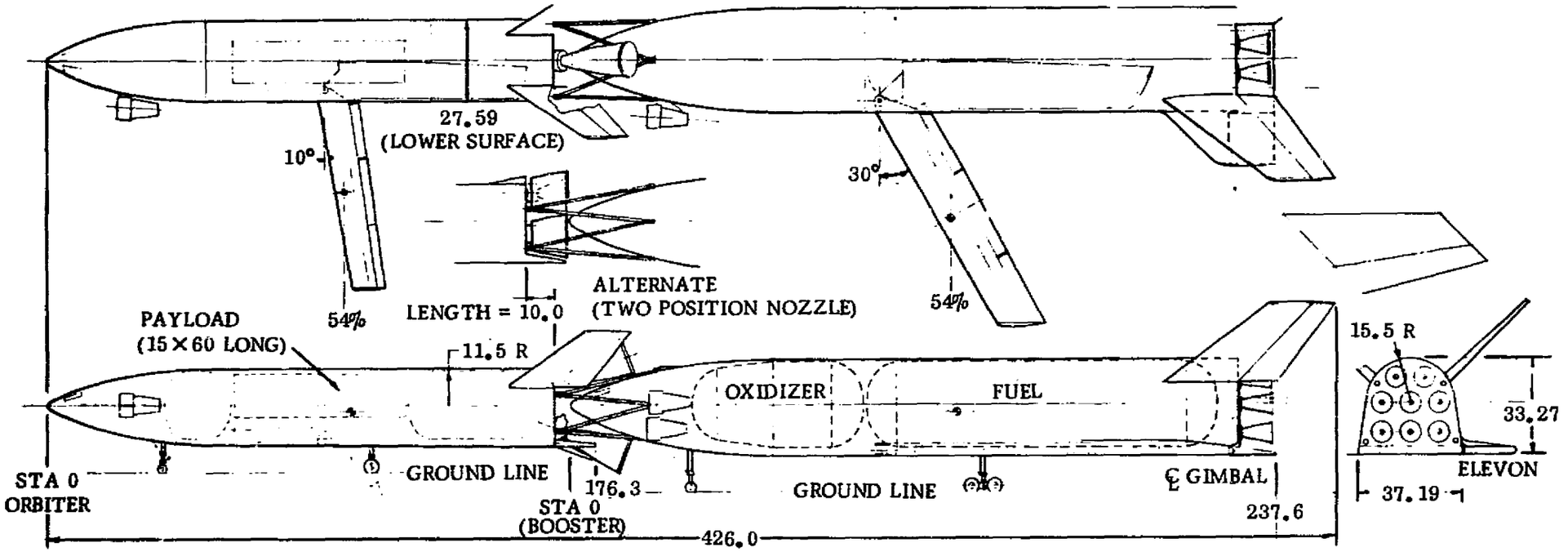

ALL DIMENSIONS IN FEET
UNLESS OTHERWISE INDICATED

Figure 2-5. Vehicle 3A (Tandem)

Table 2-2. 3A Two-Stage Tandem Vehicle Synthesis Summary

	BOOSTER ELEMENT	ORBITER	VEHICLE
WEIGHT			
FUEL	334675	67456	
OXIDIZER	2141922	472192	
PROPELLANT	2476597	539648	
FLYBACK FUEL	42653	3076	
PAYLOAD		50000	
STRUCTURE	478697	205439	684137
TOTAL	3014544	845626	3860170
IN ORBIT	0	310700	
RETURN CONDITION	537948	302049	
ENTRY	0	260792	
LANDING	479607	256356	
VOLUME			
FUEL	82794	13765	
OXIDIZER	31717	6992	
PROPELLANT	114512	20757	
PAYLOAD		10638	
OTHER	73321	45272	
TOTAL	187833	76667	
GEOMETRY			
LENGTH	237.6	176.3	
BODY WETTED AREA	24716.5	13600.2	
BODY PLANFORM AREA	9018.5	4391.5	
ENTRY PLANFORM LOADING	58.0	59.4	
PROPULSION			
THRUST-TO-WEIGHT		1.61020	1.39176
NO. OF ENGINES	8	2	
THRUST PER ENGINE (SL)	671556(UPRATED)		
THRUST PER ENGINE (VAC)		O/F = 6.4) 680810 (O/F = 7.0)	
SPECIFIC IMPULSE (SL)	395.0	357.4	395.0
SPECIFIC IMPULSE (VAC)	451.7	456.5	451.7
TRAJECTORY			
MASS RATIO		2.72175	2.79000
MAXIMUM DYNAMIC PRESSURE			755.0
STAGING DYNAMIC PRESSURE			50
STAGING VELOCITY (RELATIVE)			10987
STAGING ALTITUDE			187914
STAGING FLIGHT PATH ANGLE (RELATIVE)			2.162
INJECTION VELOCITY (INERTIAL)		25897	
INJECTION ALTITUDE		260004	
INJECTION FLIGHT PATH ANGLE (INERTIAL)		-.000	
INJECTION INCLINATION		54.96	
FLYBACK RANGE	282.5		

Table 2-3. 3A Two-Stage Tandem Summary Weight

SPACECRAFT SUMMARY WEIGHT STATEMENT

CONFIGURATION: 3A Two Stage Tandem	BY	DATE

CODE	SYSTEM	ITEM OR MODULE						SPACECRAFT	
		A	B	C	D	E	F	M	U
1.0	AERODYNAMIC SURFACES	62366						29691	
2.0	BODY STRUCTURE	211919						66978	
3.0	INDUCED ENVIR PROT	27331						40829	
4.0	LNCH RECOV & DKG	28489						11695	
5.0	MAIN PROPULS'ON	128127						35463	
6.0	ORIENT CONTROL SEP & ULL	14302						15127	
7.0	PRIME POWER SOURCE	948						1832	
8.0	POWER CONV & DISTR	4004						2109	
9.0	GUIDANCE & NAVIGATION	220						310	
10.0	INSTRUMENTATION	320						275	
11.0	COMMUNICATION	220						240	
12.0	ENVIRONMENTAL CONTROL	330						616	
13.0	(RESERVED)								
14.0	PERSONNEL PROVISIONS								
15.0	CREW STA CONTRL & PAN	220						275	
16.0	RANGE SAFETY & ABORT								
SUBTOTALS (DRY WEIGHT)		478698						205440	
17.0	PERSONNEL	900						920	
18.0	CARGO							50000	
19.0	ORDNANCE								
20.0	BALLAST								
21.0	RESID PROP & SERV ITEMS	15297						3927	
SUBTOTALS (INERT WEIGHT)		16197						54847	
22.0	RES PROP & SERV ITEMS								
23.0	INFLIGHT LOSSES	43052						11581	
24.0	THRUST DECAY PROPELLANT								
25.0	FULL THRUST PROPELLANT	2476597						573758	
26.0	THRUST PROP BUILDUP								
27.0	PRE-IGNITION LOSSES								
TOTALS (GROSS WEIGHT) (LB)		3014544						845626	
DESIGN ENVELOPE VOLUME (FT^3)		187833						76667	
PRESSURIZED VOLUME (FT^3)									
DESIGN ENVEL SURF AREA (FT^2)		24716						13600	
PRESSURIZED SURF AREA (FT^2)									
DESIGN q, MAX (LB/FT^2)		755						755	
DESIGN g, MAX		4						4	
DESIGN POWER, MAX (KW)									
DESIGN NO. MEN/DAYS		2/.1						2/7	

DESIGNATIONS:

CODE, SYSTEM: REF. MIL-M-38310A OR SP-6004

ITEM OR MODULE

A - Booster

B

C

D

E

F

SPACECRAFT

M MANNED LAUNCH - Orbiter

U UNMANNED LAUNCH

NOTES & SKETCHES:

Thrust decay propellants are included in residual weights.

Tanks are over-sized to account for thrust build-up and pre-ignition losses.

MSC Form 1523 (Jul 69)

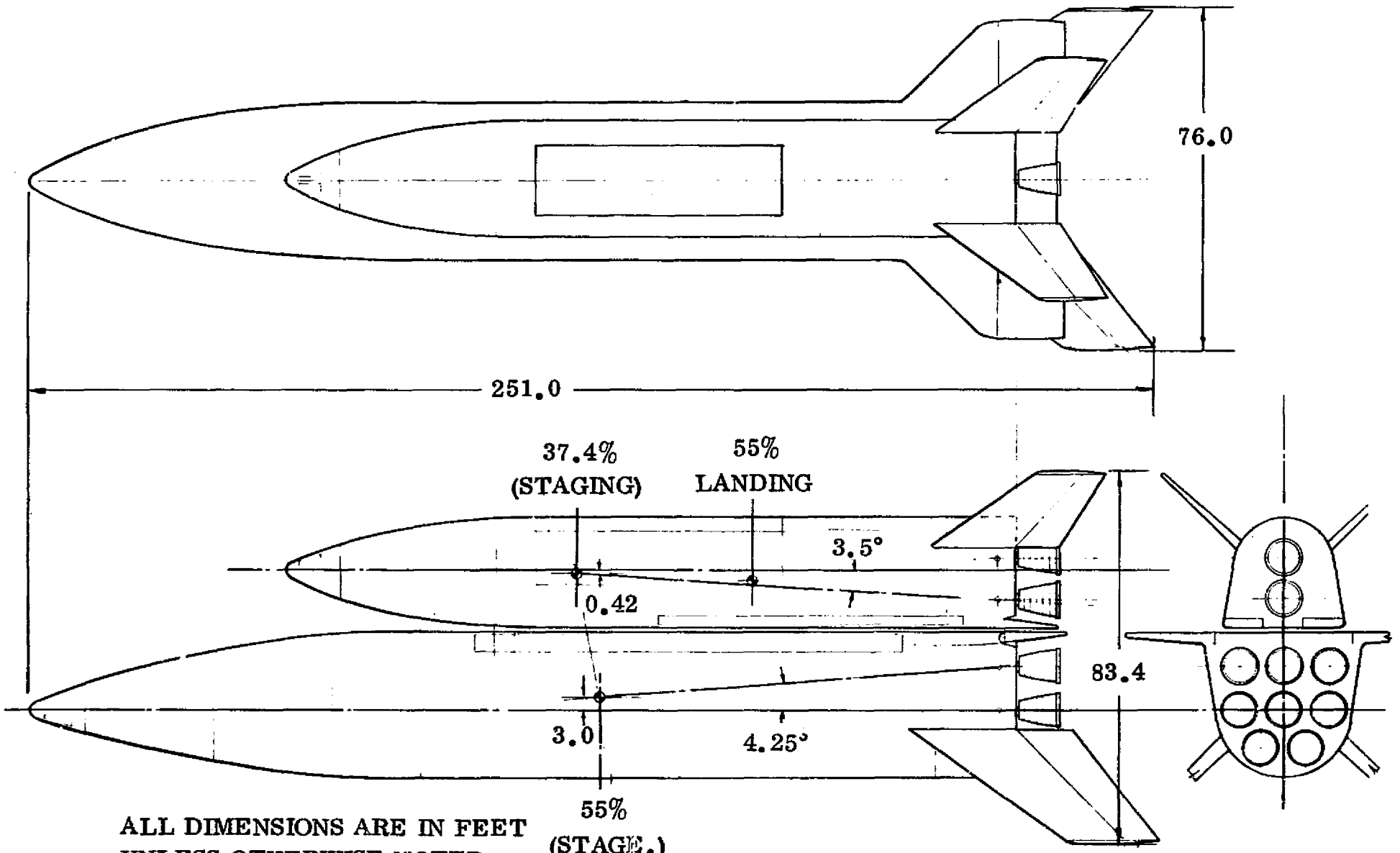

ALL DIMENSIONS ARE IN FEET
UNLESS OTHERWISE NOTED.

Figure 2-6. Vehicle FR-2

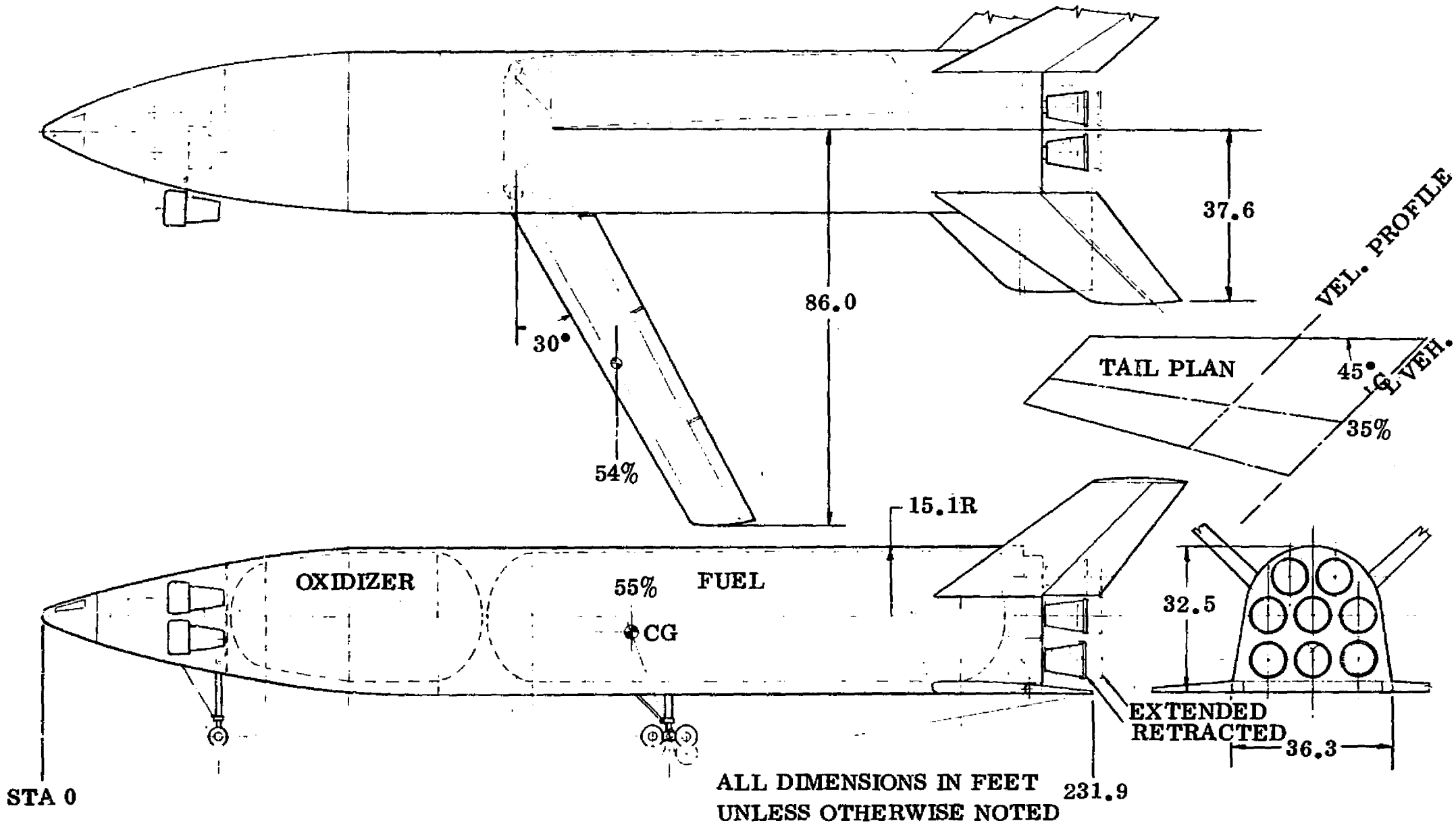

Figure 2-7. Booster — Vehicle FR-2

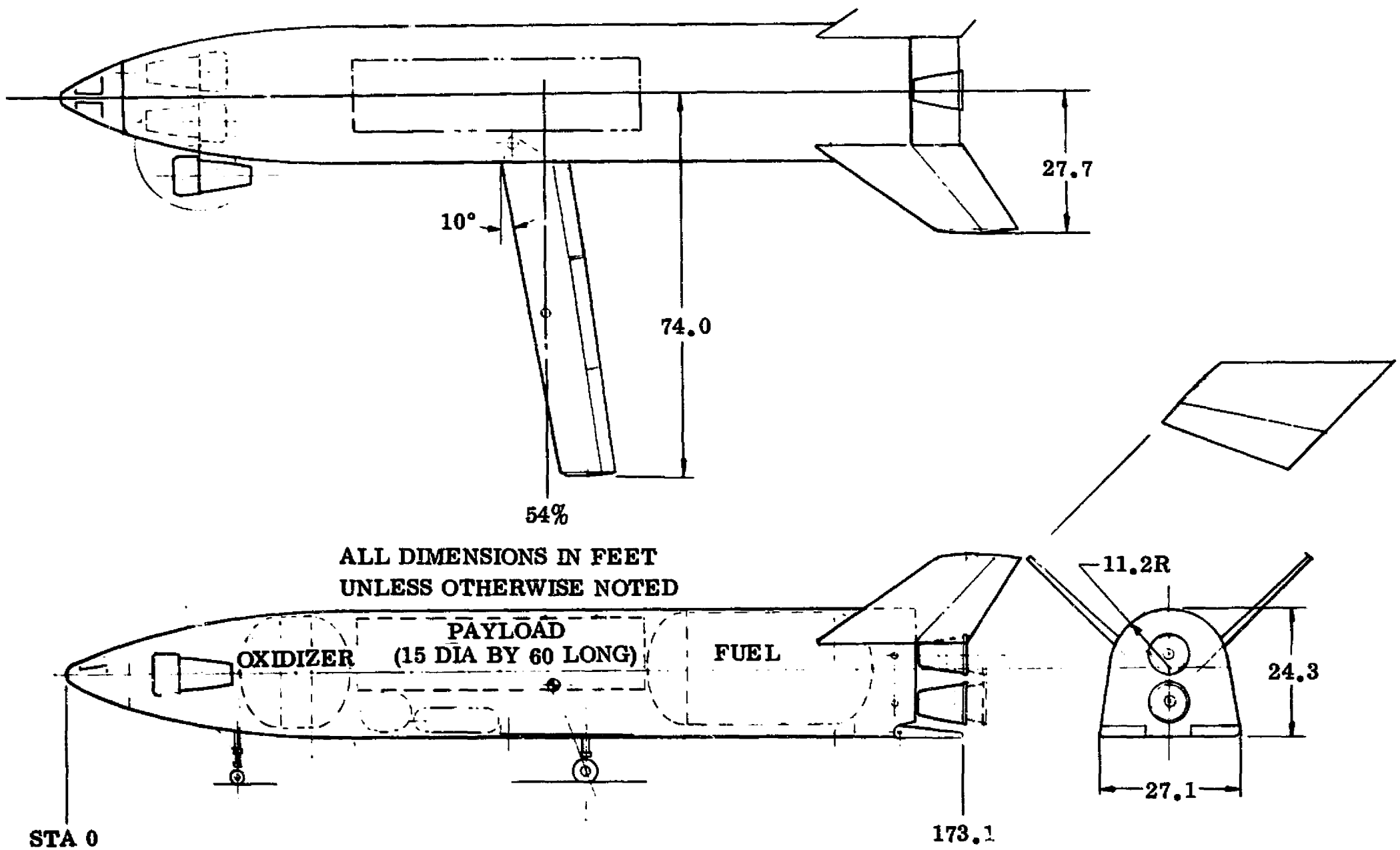

Figure 2-8. Orbiter — Vehicle FR-2

Here the minimum weights at staging were not reached since a constraint of 11,000 fps was held for aerodynamic heating reasons, as explained later in Paragraph 3.6. Future iterations could, however, allow an increase in staging velocity with some minor thermal protection subsystem modifications.

At liftoff both orbiter and booster engines are operating; therefore, the bases of the two stages are aligned to minimize plume impingement. The engines of the orbiter are being fed with propellants from the booster tanks so that at staging the tanks of the booster are empty while the tanks of the orbiter are full. After staging, the booster separates from the orbiter, which then accelerates to orbital velocity using propellants from its own tanks. As in all the other vehicles in the spectrum, both stages are equipped with subsonic wings, turbofan engines, and landing gear to permit conventional airplane-type landing.

Since the overall vehicle was performance optimized, the booster is much larger than the orbital stage (booster weight/orbiter weight = 3.5). As a result, the size of the major structural components (tanks, wings, etc.) are not similar.

Commonality of all rocket engines was obtained by using the same engine on both stages. A two-position nozzle is used to increase expansion ratio and minimize performance losses.

Table 2-4 shows the synthesis summary for the FR-2 vehicle. A summary weight statement is shown in Table 2-5.

This vehicle employed an 8-2 system, that is, eight engines in the booster and two in the orbiter. This led to a deficiency of thrust in the orbiter element for the once-around abort case. Therefore, a 7-2 arrangement was run as summarized in Table 2-6. The indications are that this is probably still marginal and that, had crossfeed been pursued, a 6-2 arrangement or a 9-3 arrangement would have been logical candidates for future examination.

2.4 SEQUENTIAL BURN 25K POUND PAYLOAD, VEHICLE FR-3-25K

The two-element sequential burn baseline vehicle is shown in Figure 2-9 in the launch configuration. The booster and orbiter stages are shown separately in Figures 2-10 and 2-11. This is the only two-element candidate with a 25K pound payload. The payload is shown in the 15-foot-diameter by 30-foot-long payload bay of the orbiter. The booster vehicle is still large in dimensions. The Saturn V is shown for comparison. While a nose-to-nose arrangement of booster and orbiter is shown here, alternate arrangements have been investigated, as indicated in Figure 2-12, for the 50K pound payload vehicle.

Table 2-4. FR-2 Two-Stage Simultaneous Burn Vehicle Synthesis Summary (Eight Engine Booster)

	BOOSTER ELEMENT	ORBITER	VEHICLE
'EIGHT			
FUEL	309300	63230	
OXIDIZER	1979517	442610	
PROPELLANT	2288817	505840	
FLYBACK FUEL	36204	2860	
PAYLOAD		50000	
STRUCTURE	401104	187408	588512
TOTAL	2742726	790008	3532734
IN ORBIT	0	288541	
RETURN CONDITION	453914	280870	
ENTRY	0	242517	
LANDING	402009	238328	
'OLUME			
FUEL	76868	12708	
OXIDIZER	29321	6553	
PROPELLANT	106189	19260	
PAYLOAD		10638	
OTHER	68307	42760	
TOTAL	174496	72658	
IEOMETRY			
LENGTH	231.9	173.1	
BODY WETTED AREA	23532.2	13121.9	
BODY PLANFORM AREA	8586.3	4237.1	
ENTRY PLANFORM LOADING	51.1	57.2	
'ROPULSION			
THRUST-TO-WEIGHT		1.25928	1.39149
NO. OF ENGINES	8	2	
THRUST PER ENGINE (SL)	494600	UPRATED	
THRUST PER ENGINE (VAC)	O/F = 6.4	497417	NOMINAL
SPECIFIC IMPULSE (SL)	393.2	381.0	O/F = 7.0 392.1
SPECIFIC IMPULSE (VAC)	454.0	457.5	455.2
'RAJECTORY			
MASS RATIO		2.73820	2.84000
MAXIMUM DYNAMIC PRESSURE			689.8
STAGING DYNAMIC PRESSURE			50
STAGING VELOCITY (RELATIVE)			11046
STAGING ALTITUDE			188264
STAGING FLIGHT PATH ANGLE (RELATIVE)			2.420
INJECTION VELOCITY (INERTIAL)		25897	
INJECTION ALTITUDE		260040	
INJECTION FLIGHT PATH ANGLE (INERTIAL)		.000	
INJECTION INCLINATION		54.90	
'LYBACK RANGE	285.9		

Table 2-5. Two-Stage Simultaneous Burn (Eight Engine Booster) Summary Weight

SPACECRAFT SUMMARY WEIGHT STATEMENT

CONFIGURATION: 2-Stage Simultaneous(8 Eng. Booster) | BY: | DATE:

CODE	SYSTEM	ITEM OR MODULE						SPACECRAFT	
		A	B	C	D	E	F	M	U
1.0	AERODYNAMIC SURFACES	57585						38591	
2.0	BODY STRUCTURE	168882						60838	
3.0	INDUCED ENVIR PROT	26028						39402	
4.0	LNCH RECOV & DKG	23711						10891	
5.0	MAIN PROPULSION	106497						82038	
6.0	ORIENT CONTROL SEP & ULL	12951						9979	
7.0	PRIME POWER SOURCE	810						2473	
8.0	POWER CONV & DISTR	3431						1984	
9.0	GUIDANCE & NAVIGATION	220						310	
10.0	INSTRUMENTATION	220						275	
11.0	COMMUNICATION	220						240	
12.0	ENVIRONMENTAL CONTROL	330						616	
13.0	(RESERVED)								
14.0	PERSONNEL PROVISIONS								
15.0	CREW STA CONTRL & PAN	220						275	
16.0	RANGE SAFETY & ABORT								
SUBTOTALS (DRY WEIGHT)		401105						187400	
17.0	PERSONNEL	900						920	
18.0	CARGO							50000	
19.0	ORDNANCE								
20.0	BALLAST								
21.0	RESID PROP & SERV ITEMS	15295						3296	
SUBTOTALS (INERT WEIGHT)		16195						54216	
22.0	RES PROP & SERV ITEMS								
23.0	INFLIGHT LOSSES	96609						10826	
24.0	THRUST DECAY PROPELLANT								
25.0	FULL THRUST PROPELLANT	2288817						537559	
26.0	THRUST PROP BUILDUP								
27.0	PRE-IGNITION LOSSES								
TOTALS (GROSS WEIGHT) (LB)		2742726						791008	
DESIGN ENVELOPE VOLUME (FT^3)		174496						72658	
PRESSURIZED VOLUME (FT^3)									
DESIGN ENVEL SURF AREA (FT^2)		23532						13122	
PRESSURIZED SURF AREA (FT^2)									
DESIGN q, MAX (LB/FT^2)		690						590	
DESIGN n, MAX		4						4	
DESIGN POWER, MAX (KW)									
DESIGN NO. MEN/DAYS		2/.1						2/7	

DESIGNATIONS:
CODE, SYSTEM: REF. MIL-M-38310A OR SP-6004
ITEM OR MODULE
A - Booster
B
C
D
E
F
SPACECRAFT
M MANNED LAUNCH - Orbiter
U UNMANNED LAUNCH

NOTES & SKETCHES:
Thrust decay propellants are included in residual weights.
Tanks are over-sized to account for thrust build-up and pre-ignition losses.

MSC Form 1523 (Jul 68)

Table 2-6. FR-2 Two-Stage Simultaneous Burn Vehicle Synthesis Summary (Seven Engine Booster)

	BOOSTER ELEMENT	ORBITER	VEHICLE
WEIGHT			
FUEL	309794	63651	
OXIDIZER	1982681	445560	
PROPELLANT	2292474	509211	
FLYBACK FUEL	35897	2883	
PAYLOAD		50000	
STRUCTURE	360134	172121	532255
CONTINGENCY	37513	17212	
OTHER	16436	44500	
TOTAL	2742455	795928	3538383
IN ORBIT		201164	
RETURN CONDITION	449982	283146	
ENTRY	0	244474	
LANDING	398526	240261	
VOLUME			
FUEL	76987	12815	
OXIDIZER	29368	6597	
PROPELLANT	106355	19412	
PAYLOAD		10638	
OTHER	68406	43014	
TOTAL	174761	73064	
GEOMETRY			
LENGTH	232.0	173.5	
BODY WETTED AREA	23556.0	13170.6	
BODY PLANFORM AREA	8595.1	4252.8	
ENTRY PLANFORM LOADING	50.6	57.5	
PROPULSION	ϵ = 35/100	ϵ = 35/150	
THRUST-TO-WEIGHT		1.39478	1.39196
NO. OF ENGINES	7	2	
THRUST PER ENGINE (SL)	551300 UPRATED		
THRUST PER ENGINE (VAC)	O/F = 6.4	555076 NOMINAL	
SPECIFIC IMPULSE (SL)	390.5	377.7 O/F = 7.0	389.6
SPECIFIC IMPULSE (VAC)	453.5	455.0	454.8
TRAJECTORY			
MASS RATIO		2.73195	2.84000
MAXIMUM DYNAMIC PRESSURE			699.5
STAGING DYNAMIC PRESSURE			50
STAGING VELOCITY (RELATIVE)			11027
STAGING ALTITUDE			187959
STAGING FLIGHT PATH ANGLE (RELATIVE)			2.513
INJECTION VELOCITY (INERTIAL)		25897	
INJECTION ALTITUDE		259975	
INJECTION FLIGHT PATH ANGLE (INERTIAL)		-.000	
INJECTION INCLINATION		54.93	
FLYBACK RANGE	285.9		

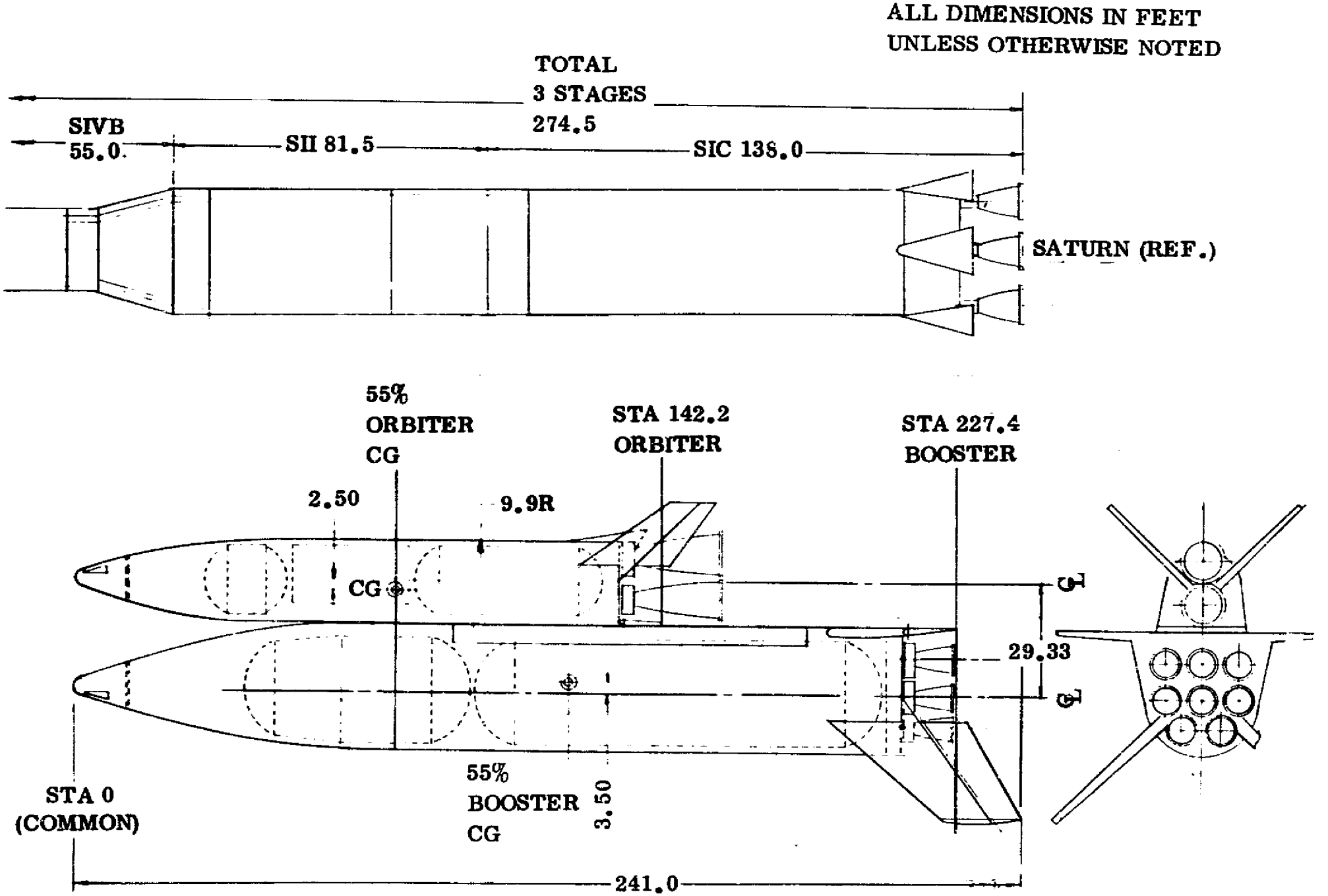

Figure 2-9. Vehicle FR-3-25K

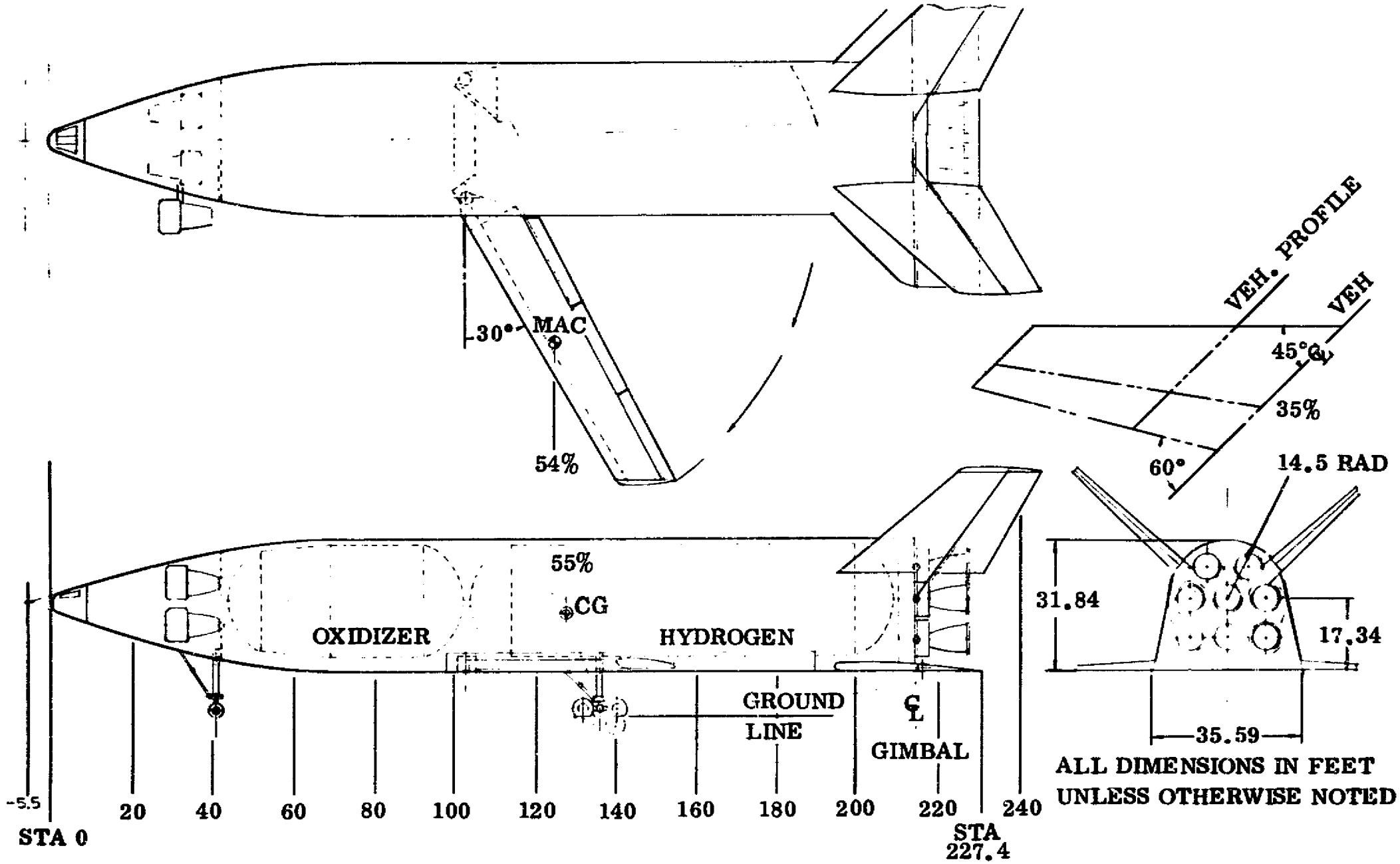

Figure 2-10. Booster — Vehicle FR-3-25K

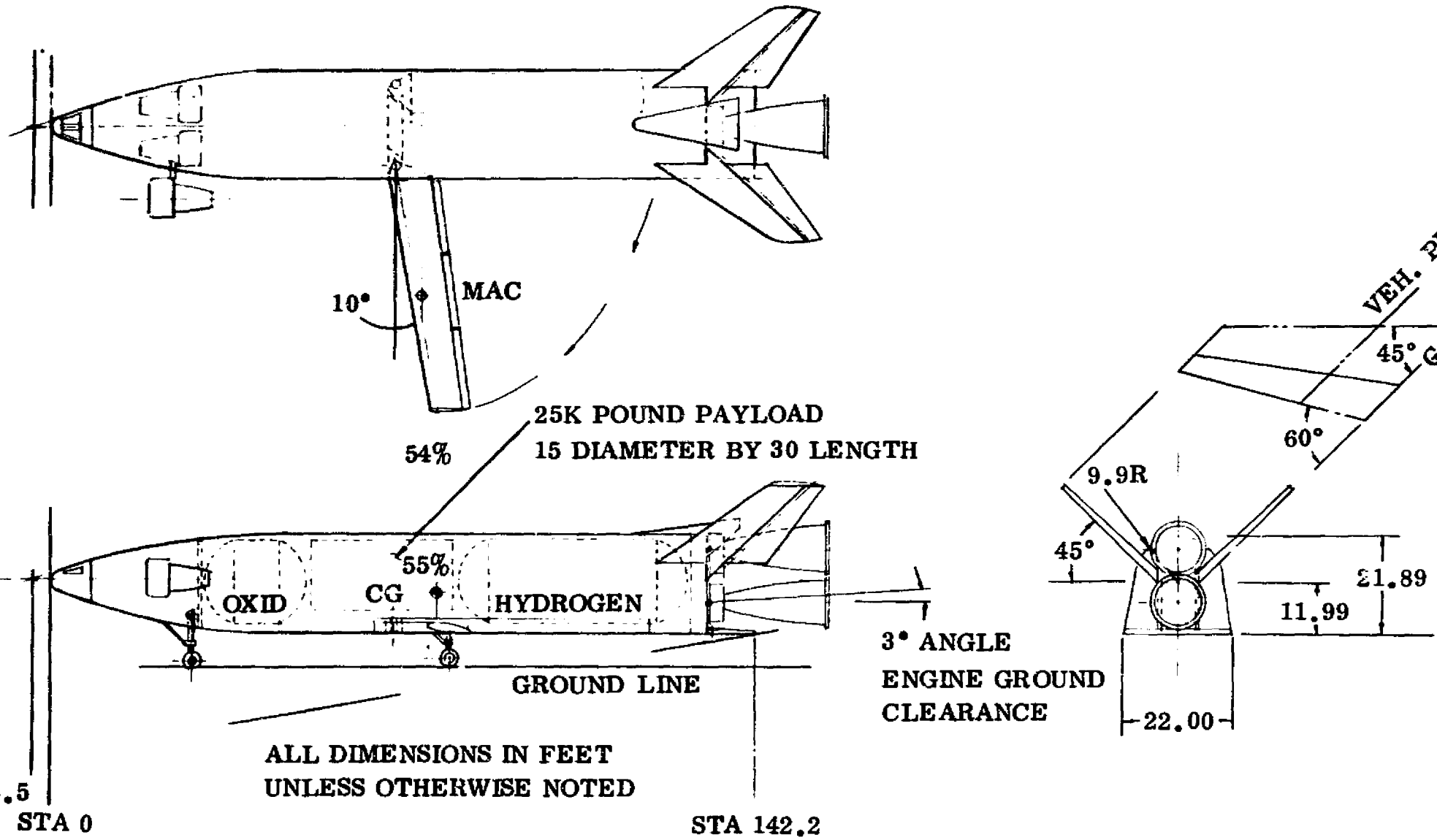

Figure 2-11. Orbiter — Vehicle FR-3-25K

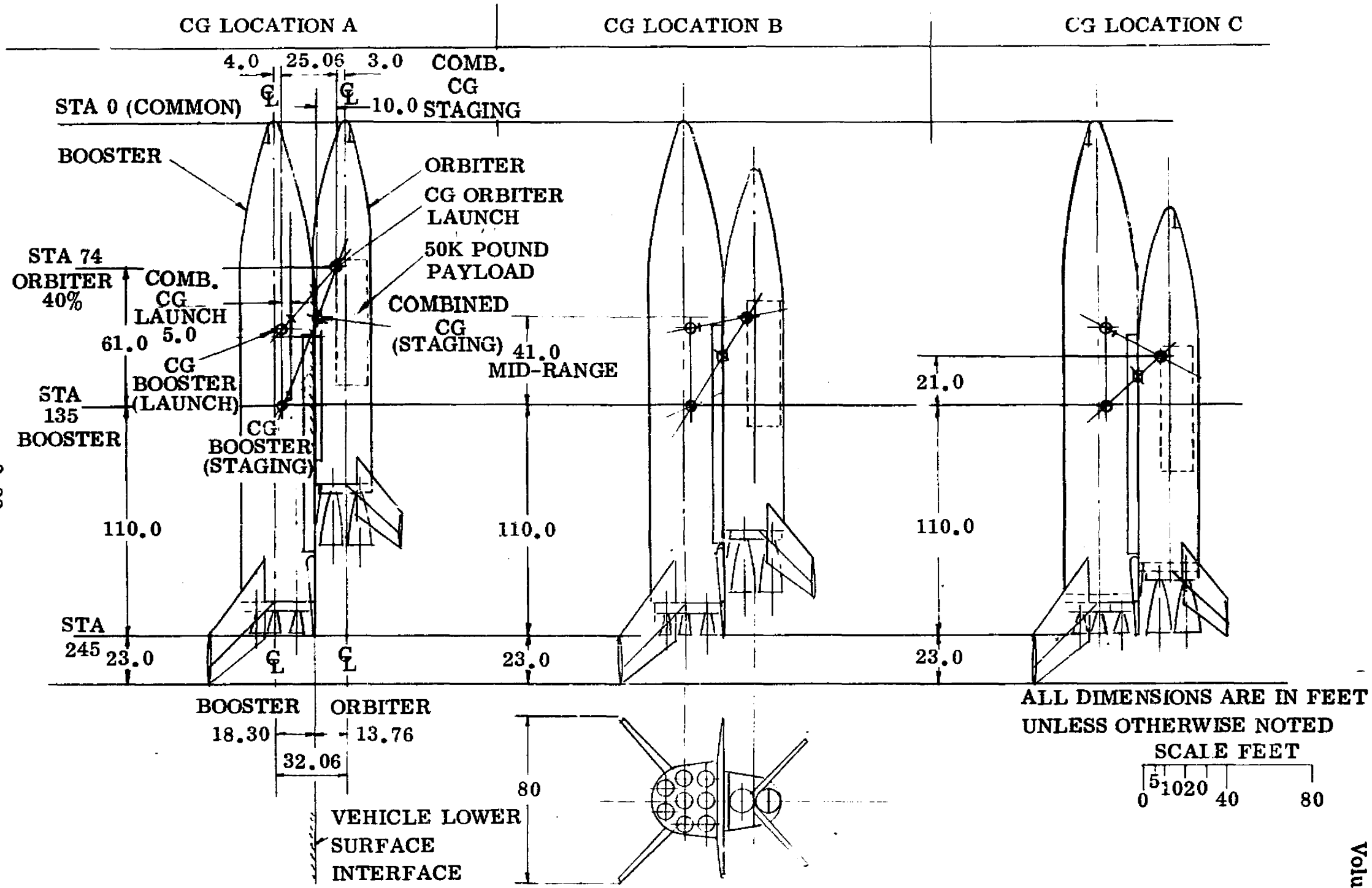

Figure 2-12. Vehicle CG Relationship

The major factors that must be considered are:

a. Booster/orbiter cg and geometric relation.

b. Engine thrust vector/gimbaling angle.

c. Stage separation.

The interrelationship of these influential design factors determines the magnitude of drag forces, stability, control, aerodynamic heating, and structural design. Figure 2-12 illustrates three different geometric relationships of the booster/orbiter vehicles relative to their longitudinal axes.

Location A in Figure 2-12 is considered the maximum that the orbiter should be forward, and although it requires the minimum of thrust vector angle it also requires the maximum structural support length when mounted on a launch pad. Location C is the maximum aft position of the orbiter considering booster engine burn. The range of these extreme locations is 43 feet. The combined cg of each of the three concepts is approximately 5 feet below the booster cg W/L, and varies longitudinally according to the orbiter vehicle's location. This is approximately 6 feet forward for the A location, 2 feet for B location, and 2 feet aft for the C location.

Considering booster thrust line performance relative to all three locations, although location A requires the minimum gimbal angle, between location A and B the resultant cg's are within 10 minutes of arc. This points to the fact that longitudinal location of the orbiter is not sensitive regarding engine thrust line performance.

The staging velocity was selected from a series of synthesis runs, namely:

Staging Velocity (fps)	Gross Liftoff Weight (lb)	Total System Drag Weight (lb)
10,369	2,765,000	531,210
10,862	2,788,000	532,424
11,343	2,823,000	535,700

The selected run was at 10,369 fps staging velocity, with the indication that it might be slightly lower.

The synthesis summary printout for the system is shown in Table 2-7. The vehicle summary weight statement is shown in Table 2-8.

Table 2-7. Two-Stage, Sequential Burn, 25K Pound Payload Vehicle Synthesis Summary

	BOOSTER ELEMENT	ORBITER	VEHICLE
WEIGHT			
FUEL	238800	45188	
OXIDIZER	1528321	316317	
PROPELLANT	1767121	361505	
FLYBACK FUEL	33332	1930	
PAYLOAD		25000	
STRUCTURE	396301	134909	531210
TOTAL	2211192	554297	2765488
IN ORBIT	0	195765	
RETURN CONDITION	444077	190019	
ENTRY	0	164056	
LANDING	397218	160823	
VOLUME			
FUEL	59383	11233	
OXIDIZER	22645	4684	
PROPELLANT	82028	15917	
PAYLOAD		5319	
OTHER	82604	23350	
TOTAL	164633	44586	
GEOMETRY			
LENGTH	227.4	142.2	
BODY WETTED AREA	22636.8	8982.3	
BODY PLANFORM AREA	8259.7	2821.3	
ENTRY PLANFORM LOADING	52.2	58.1	
PROPULSION			
THRUST-TO-WEIGHT		1.76129	1.39244
NO. OF ENGINES	8	2	
THRUST PER ENGINE (SL)	481348	UPRATED	
THRUST PER ENGINE (VAC)		O/F = 6.4 488136	NOMINAL
SPECIFIC IMPULSE (SL)	394.0	356.4	O/F = 7.0 394.0
SPECIFIC IMPULSE (VAC)	450.7	455.5	450.7
TRAJECTORY			
MASS RATIO		2.83146	2.77000
MAXIMUM DYNAMIC PRESSURE			624.8
STAGING DYNAMIC PRESSURE			50
STAGING VELOCITY (RELATIVE)			10369
STAGING ALTITUDE			184686
STAGING FLIGHT PATH ANGLE (RELATIVE)			2.731
INJECTION VELOCITY (INERTIAL)		25897	
INJECTION ALTITUDE		260003	
INJECTION FLIGHT PATH ANGLE (INERTIAL)		-.001	
INJECTION INCLINATION		54.96	
FLYBACK RANGE	267.1		

Table 2-8. FR-3-25K Two-Stage, Sequential Burn
25K Pound Payload Summary Weight

SPACECRAFT SUMMARY WEIGHT STATEMENT

M-5A Two Stage, Sequential Burn 25K Payload | BY | DATE

CODE	SYSTEM	ITEM OR MODULE A	B	C	D	E	F	SPACECRAFT M	U
1.0	AERODYNAMIC SURFACES	61125						19987	
2.0	BODY STRUCTURE	166453						43122	
3.0	INDUCED ENVIR PROT	25044						27062	
4.0	LNCH RECOV & DKG	22823						7438	
5.0	MAIN PROPULSION	101398						34269	
6.0	ORIENT CONTROL SEP & ULL	14186						8326	
7.0	PRIME POWER SOURCE	796						1560	
8.0	POWER CONV & DISTR	3269						1427	
9.0	GUIDANCE & NAVIGATION	220						310	
10.0	INSTRUMENTATION	220						275	
11.0	COMMUNICATION	220						242	
12.0	ENVIRONMENTAL CONTROL	330						616	
13.0	(RESERVED)								
14.0	PERSONNEL PROVISIONS								
15.0	CREW STA CONTRL & PAN	220						275	
16.0	RANGE SAFETY & ABORT								
SUBTOTALS (DRY WEIGHT)		396302						134909	
17.0	PERSONNEL	900						920	
18.0	CARGO							25000	
19.0	ORDNANCE								
20.0	BALLAST								
21.0	RESID PROP & SERV ITEMS	13124						2770	
SUBTOTALS (INERT WEIGHT)		14024						28690	
22.0	RES PROP & SERV ITEMS								
23.0	INFLIGHT LOSSES	33745						7734	
24.0	THRUST DECAY PROPELLANT								
25.0	FULL THRUST PROPELLANT	1767121						382964	
26.0	THRUST PROP BUILDUP								
27.0	PRE-IGNITION LOSSES								
TOTALS (GROSS WEIGHT) (LB)		2211192						554297	
DESIGN ENVELOPE VOLUME (FT^3)		164633						44586	
PRESSURIZED VOLUME (FT^3)									
DESIGN ENVEL SURF AREA (FT^2)		22637						8982	
PRESSURIZED SURF AREA (FT^2)									
DESIGN q, MAX (LB/FT^2)		625						625	
DESIGN n, MAX		4						4	
DESIGN POWER, MAX (KW)									
DESIGN NO. MEN/DAYS		2/.1						2/7	

DESIGNATIONS:
CODE, SYSTEM: REF. MIL-M-38310A OR SP-6004
ITEM OR MODULE
A - Booster
B
C
D
E
F
SPACECRAFT
M MANNED LAUNCH - Orbiter
U UNMANNED LAUNCH

NOTES & SKETCHES:
Thrust decay propellants are included in residual weights.
Tanks are over-sized to account for thrust build-up and pre-ignition losses.

MSC Form 1523 (Jul 68)

2.5 STAGING CONCEPTS

This section documents the alternate staging concepts considered for the two-element integral launch and reentry vehicle (ILRV) baselines. Tandem, simultaneous burn, and sequential burn arrangements were investigated to establish staging techniques for each baseline vehicle. (Three-element staging is discussed in Section 10 of Volume V).

2.5.1 TANDEM VEHICLE. It appears that the lower ballistic coefficient of the empty booster will cause the two stages to separate without auxiliary thrust devices. It may be desirable to deflect the control surfaces of the booster to increase drag and reduce the time required for separation prior to orbiter ignition. Also, the negative acceleration experienced by the orbiter during coast may require special propellant feed provisions to ensure main engine start.

2.5.2 SIMULTANEOUS BURN VEHICLES. Four candidate separation concepts are described in subsequent paragraphs. (See Figure 2-13.)

a. Longitudinal separation.

b. Pure lateral separation.

c. Lateral-rotational separation.

d. "Lofting" separation.

2.5.2.1 Longitudinal Separation. One element drops or eliminates thrust and drops back on a rail or guide through the plume. Problems in addition to plume force/heating are large overturning moments due to plume impingement on the aft-located element that must be reacted through the rail or guide (beefy structure) and the forward elements control system. These problems, in addition to the inherent problems of passing a manned-reusable vehicle through the plume, make this a very poor candidate. A more attractive method appears to be a passive staging approach using the higher ballistic coefficient of the orbiter element at staging. Both elements eliminate thrust and use aerodynamics to drag one (the lighter or empty booster) back on a rail or guide. This maneuver requires moderate q (50 to 100 psf) to accomplish staging in a reasonable time. The larger, lighter vehicle having less mass and larger cross-section will have considerably larger drag acceleration to accomplish separation. Advantages are:

a. Can burn to depletion (no planned residuals).

b. Passive system (slide off rail once released).

c. Reliable.

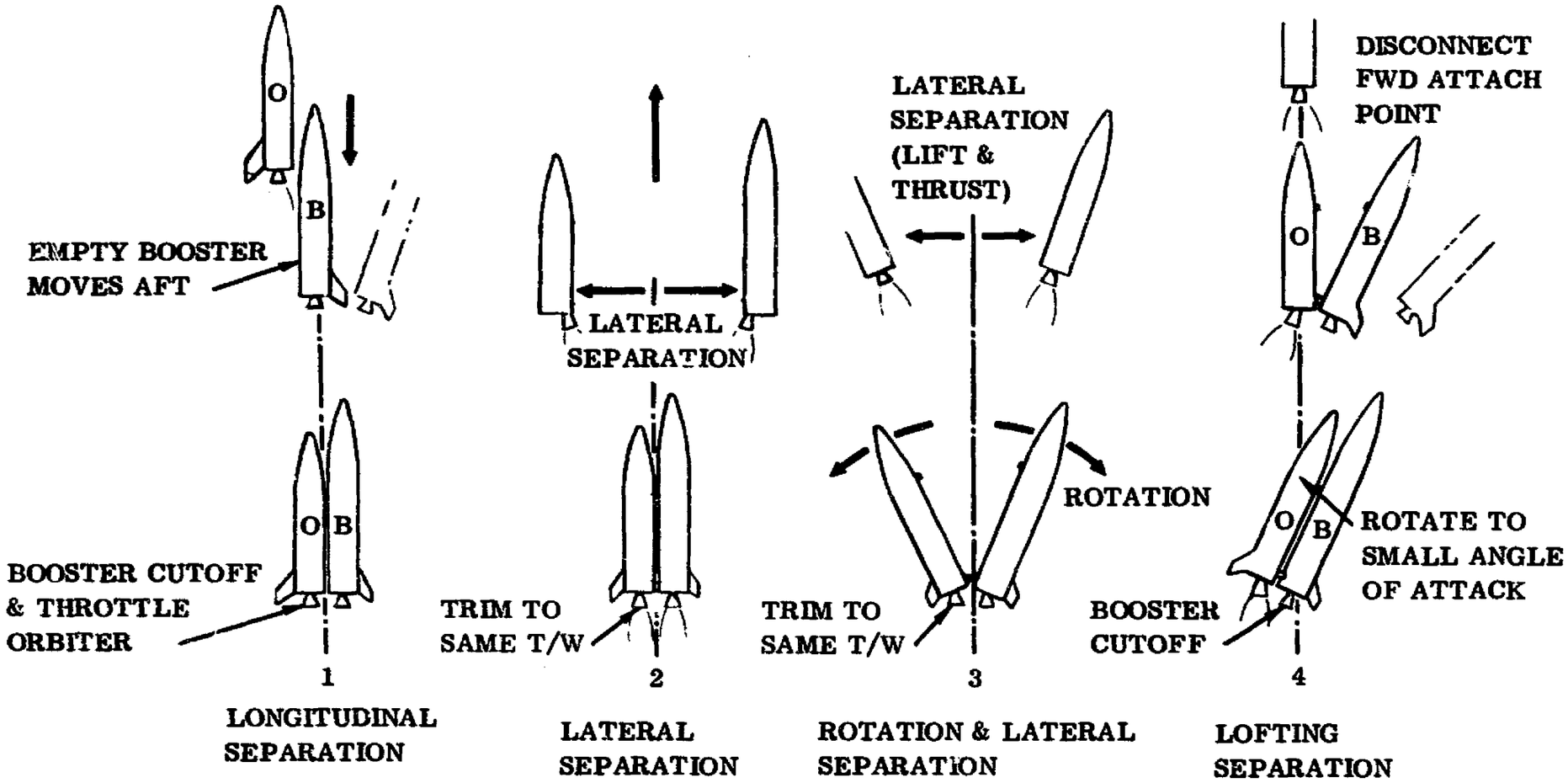

Figure 2-13. Staging Concepts

Disadvantages are:

a. Orbiter engines must be shut down and restarted. (Simultaneous burn vehicle only.)

b. Both elements are noncontrolled during separation and must recover aerodynamically from disturbance. (Actually a very minor problem.)

c. Orbiter restart must be accomplished under negative g (although small negative g due to its very high mass.

d. A moderate to high q is required for this concept. Since the orbiter engines must be restartable for many in-orbit tasks, this is a very attractive candidate.

2.5.2.2 Pure Lateral Separation. (See Figure 2-13(2).) Both elements:

a. Trim thrust to approximately same longitudinal g.

b. Disengage engine thrust vector control (TVC) system and trim thrust slightly inboard of worse center of mass dispersion to ensure slight outward moment.

c. Rotate-translate outward until sufficient clearance is obtained, then reactivate control.

d. Fly to adequate separation before cutting off booster engines, etc.

Advantages are:

a. Large vehicle separation can be obtained.

b. Engine cutoff not required.

Disadvantages are:

a. Low q is required so as not to provide reconnecting disturbance thrusts, <20 psf.

b. An aft bumper or bumper-alignment mechanism is required.

c. Booster must be provided with run-time propellants plus adequate pad (a serious performance loss).

d. Non-workable if engine cutoff required (fire).

With the advantage/disadvantage ratio shown above, this appears to be a moderately poor candidate.

2.5.2.3 Lateral-Rotational Separation. (See Figure 2-13(3).) Both elements:

a. Trim thrust to same g (approximately).

b. Disengage TVC and trim thrust considerably inboard to ensure good rotation.

c. Rotate until desired angle is obtained (moderate angle of attack) and initial disengagement.

d. Rotate-translate (using aerodynamics) until adequate clearance is obtained, then reactivate control.

e. Fly to adequate separation before cutting off booster engines, etc.

Advantages are:

a. Large vehicle separation can be obtained.

b. Engine cutoff not required.

c. High or low q can be accommodated (high q being preferred).

d. Can accommodate high q, engine cutoff case.

Disadvantages are:

a. An aft hinge is required.

b. Booster must be provided with run-time propellants plus adequate pad (a severe performance loss).

c. Engine-out problem severe.

This modification to the pure-lateral separation scheme is moderately attractive and can be considered a candidate.

2.5.2.4 Lofting Separation. At booster cutoff and with orbiter at thrust, the orbiter rotates nose-down to slight negative angle of attack (positive for booster), disconnects forward attach point with hard nose-up orbiter TVC, pivots on aft hinge to desired disconnect angle, and booster flies off aerodynamically. (See Figure 2-13(4).)

Advantages are:

a. No booster engine run required.

b. Partially extendable to abort condition (not max q).

Disadvantages are:

a. Moderate (not large) separation clearance.

b. Requires thrust on orbiter element.

c. Large thrust vector deflections required by orbiter and orbiter engine-out problem severe.

d. Large rotational accelerations required by orbiter and booster.

e. Non-workable without orbiter thrust.

With the advantages/disadvantages ratio shown above, this is a moderately poor candidate system.

In summary, the passive longitudinal system and the lateral-rotational system are the prime candidates with the longitudinal system appearing to be the most attractive.

2.5.3 SEQUENTIAL BURN. When the orbiter is moved aft (to align the bases of both vehicles), the concepts discussed above are applicable.

It would appear that the sequential burn configuration with noncoplanar bases may be subjected to heavy buffet loading and some heating downstream of a relatively sharp discontinuity, the base of the orbiter. This would require further investigation.

The longitudinal passive technique discussed in Paragraph 2.5.2.1 would work well in this situation. Since the orbiter engine is not started until after separation, disadvantages (a) and (c) would be the normal mode and should not be considered in this case.

The lofting separation concept is also workable, with extendable links or actuators to force a large angle of attack on the booster, which can then fly away aerodynamically.

Staging the sequential burn vehicle is discussed further in Paragraph 6.5 of Volume II.

2.6 25K POUND PAYLOAD, VEHICLE FR-1-25K

This vehicle is shown in Figure 2-14. The orbiter element is shown in plan and side view. The booster element is identical except that the space occupied by the 15-foot-diameter by 30-foot-long payload bay in the orbiter is occupied by extensions of the main propellant tanks as shown. The shorter payload bay requires that the main landing gear attach in the hydrogen tank region; however, with this requirement met, a very efficient tankage arrangement results.

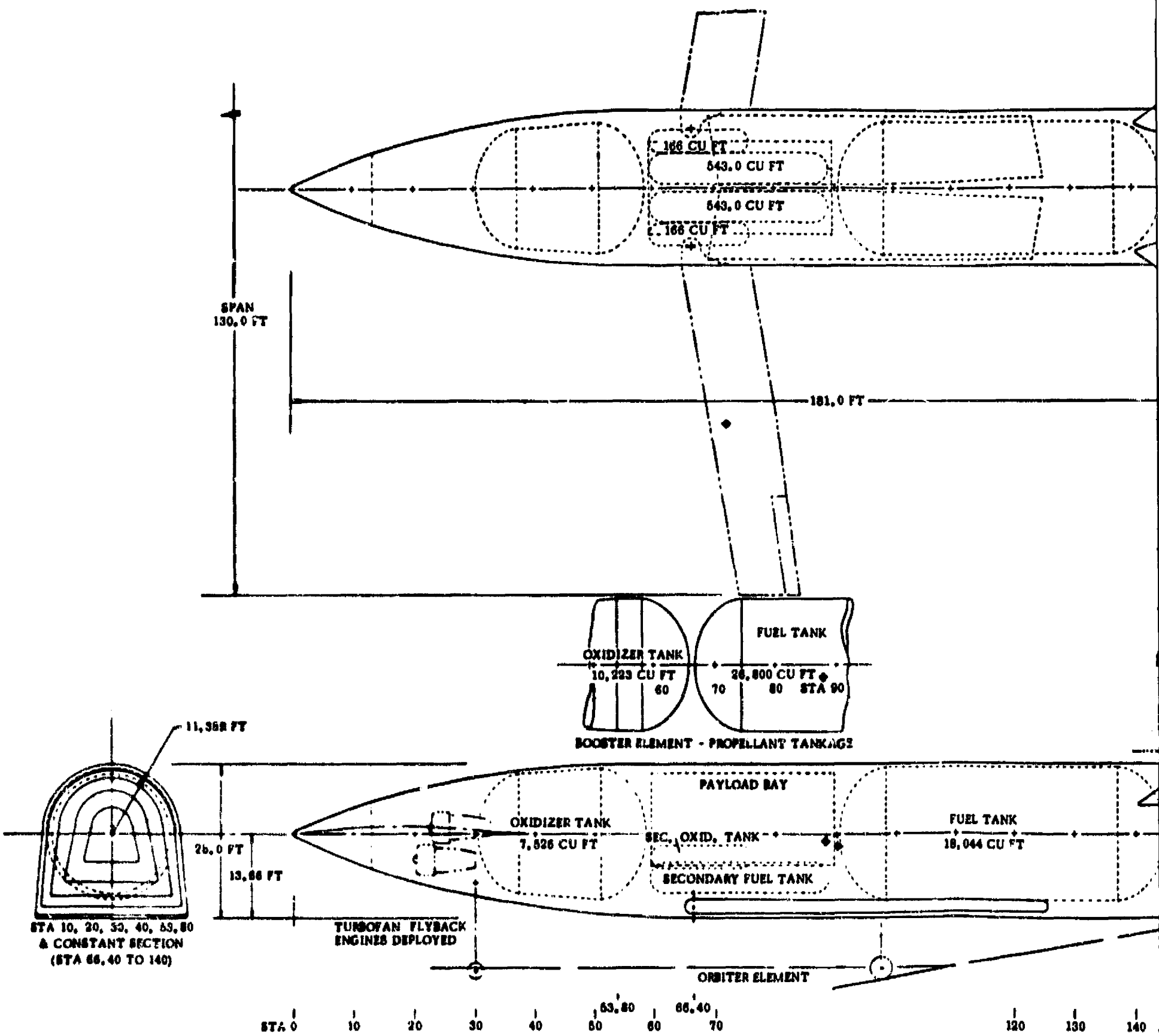

FOLDOUT FRAME 1

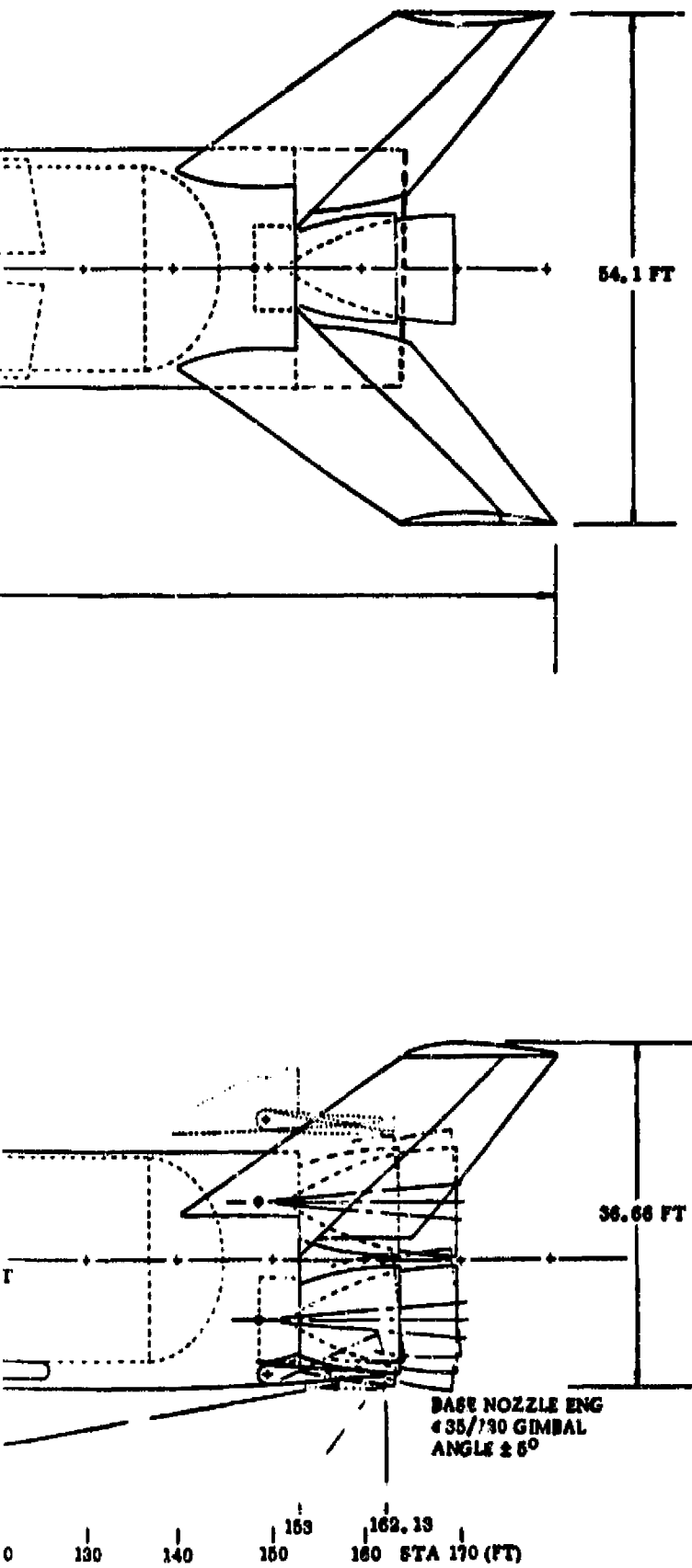

Figure 2-14. FR-1-25K Vehicle Orbiter Element

FOLDOUT FRAME 2

The main tanks are integral (nulled waffle pattern) with external frames and stringers. These members transmit the main bending and axial loads. The payload bay and intertank section is basically a skin/stringer assembly of conventional design. Polyurethane or open face honeycomb insulation is used inside the hydrogen tank. The major structure is of 2021 or 2219 aluminum alloy protected by a thermal protection system of dynaflex and microquartz insulation with external shingle-type cover skin primarily L605 alloy on the lower surface and 811 titanium on the upper surface.

The liquid-oxygen tank is placed forward to increase the forward cg location during boost and to reduce gimbal requirements. All the tanks have 1.414 to 1 end closures. The thrust structure consists of paired parallel beams supported by a cylindrical thrust skirt, which is a simple extension of the main hydrogen tank.

The orbiter payload bay area is shown. Stowed beneath this are the secondary fuel and oxidizer tanks used for the on-orbit maneuver and retro propellants. These are heavily insulated tanks that contain propellants for up to seven days in space. The payload bay doors run the full 30-foot length and provide a 1-foot clearance at each end also. The doors are on top of the orbiter body, symmetrical about the vehicle centerline. A swing nose payload access method was discarded primarily because of orbital attitude control problems with the door open.

The wing pivot bulkhead and carryover structure runs around the payload bay section in the orbiter and between the main tanks in the booster. The wings are protected by segmented doors in the stowed position. The wings are not deployed until subsonic flight is achieved. The deployment mechanism is similar to that of the F-111, namely, screwjacks driven by hydraulic motors.

Two bell nozzle engines with two position nozzles of expansion ratio 35/130 are incorporated in each of the configuration elements (six total). The extensions are retracted at entry, and the nozzles are gimballed upward to protect them from heating. The orbiter and booster nominal cg location is at 55% of the length from the nose to the elevon trailing edge.

In general the FR-1-25K vehicle is an extension of the initial point design (IPD) vehicle presented to NASA in April 1969 except that the payload bay size and ΔV requirements have increased. Four flyback turbofan engines are proposed instead of two to enhance engineout performance. These are currently parametric extensions of the GE T34 Step III. Future work on this configuration would evaluate the penalty of installing off-the-shelf engines. Figure 2-15 shows the 25K pound payload vehicle FR-1-25K launch configuration and overall dimensions.

The synthesis summary for this vehicle is shown in Table 2-9. The summary weight statement is shown in Table 2-10.

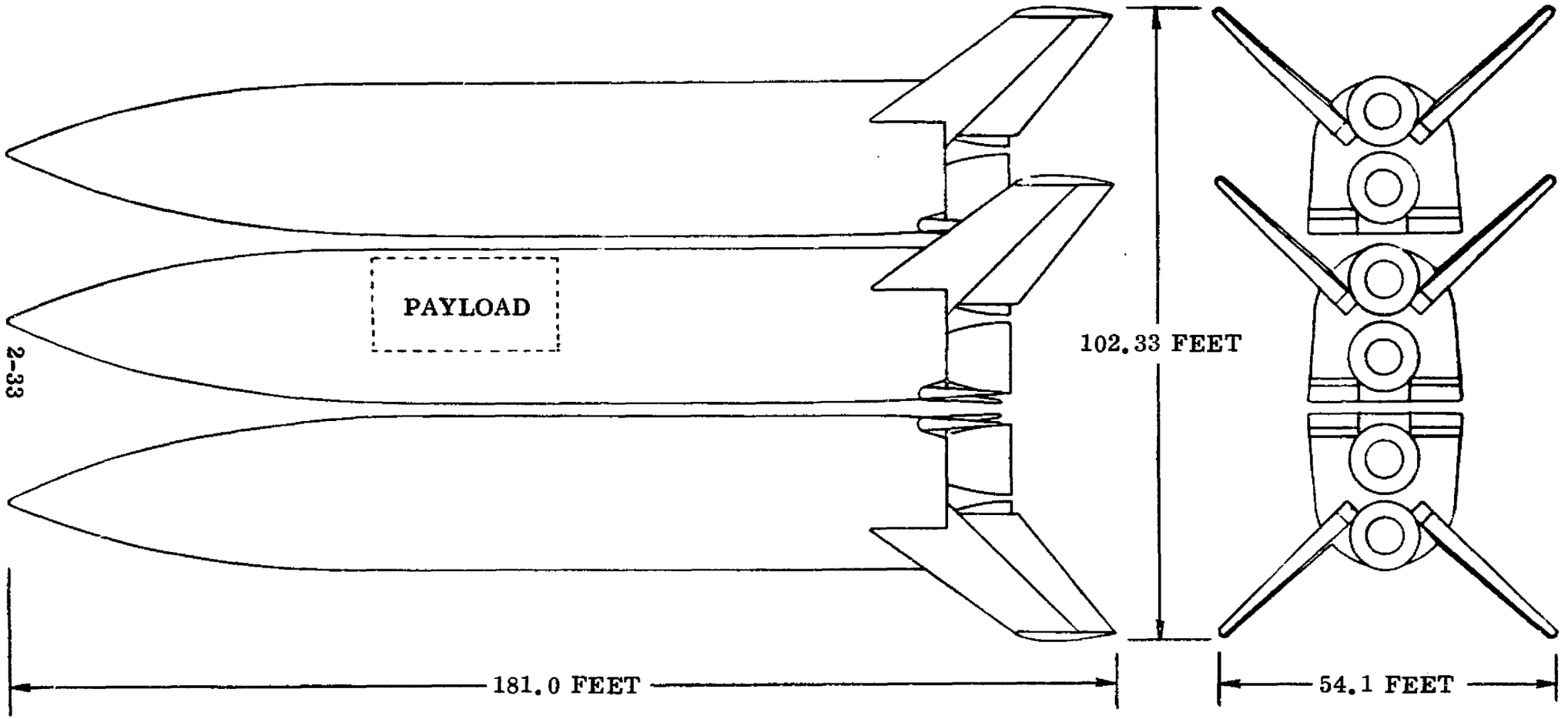

Figure 2-15. 25K Pound Payload Vehicle FR-1-25K Launch Configuration

Table 2-9. FR-1-25K Pound Payload Vehicle Synthesis Summary

	BOOSTER ELEMENT	ORBITER	VEHICLE
WEIGHT			
FUEL	107842	72612	
OXIDIZER	690189	508284	
PROPELLANT	798031	580896	
FLYBACK FUEL	12226	2423	
PAYLOAD		25000	
STRUCTURE	176496	176040	529031
TOTAL	993525	823524	2810574
IN ORBIT	0	246400	
RETURN CONDITION	195484	237913	
ENTRY	0	205551	
LANDING	177392	201958	
VOLUME			
FUEL	26798	18044	
OXIDIZER	10223	7526	
PROPELLANT	37021	25570	
PAYLOAD		5319	
OTHER	29522	35659	
TOTAL	66544	66548	
GEOMETRY			
LENGTH	162.1	162.1	
BODY WETTED AREA	11730.7	11731.1	
BODY PLANFORM AREA	3684.6	3684.7	
ENTRY PLANFORM LOADING	51.5	55.8	
PROPULSION			
THRUST-TO-WEIGHT		1.62800	1.39183
NO. OF ENGINES	2	2	
THRUST PER ENGINE (SL)	652000 UPRATED		
THRUST PER ENGINE (VAC)	O/F = 6.4 670351 NOMINAL		
SPECIFIC IMPULSE (SL)	390.3	381.6 O/F = 7.0	390.3
SPECIFIC IMPULSE (VAC)	457.5	453.7	457.5
TRAJECTORY			
MASS RATIO		3.34086	2.31418
MAXIMUM DYNAMIC PRESSURE			606.5
STAGING DYNAMIC PRESSURE			50
STAGING VELOCITY (RELATIVE)			7882
STAGING ALTITUDE			169657
STAGING FLIGHT PATH ANGLE (RELATIVE)			9.265
INJECTION VELOCITY (INERTIAL)		25897	
INJECTION ALTITUDE		259967	
INJECTION FLIGHT PATH ANGLE (INERTIAL)		-.000	
INJECTION INCLINATION		55.01	
FLYBACK RANGE	221.0		

Table 2-10. FR-1-25K Vehicle Summary Weight

SPACECRAFT SUMMARY WEIGHT STATEMENT

CONFIGURATION: FR-1-25K | BY: | DATE:

CODE	SYSTEM	ITEM OR MODULE A	B	C	D	E	F	SPACECRAFT M	U
1.0	AERODYNAMIC SURFACES	22485						24629	
2.0	BODY STRUCTURE	64319						57539	
3.0	INDUCED ENVIR PROT	32790						35256	
4.0	LNCH RECOV & DKG	9044						9264	
5.0	MAIN PROPULSION	39208						37267	
6.0	ORIENT CONTROL SEP & ULL	5310						6961	
7.0	PRIME POWER SOURCE	399						1675	
8.0	POWER CONV & DISTR	1731						1731	
9.0	GUIDANCE & NAVIGATION	220						310	
10.0	INSTRUMENTATION	220						275	
11.0	COMMUNICATION	220						242	
12.0	ENVIRONMENTAL CONTROL	330						616	
13.0	(RESERVED)								
14.0	PERSONNEL PROVISIONS								
15.0	CREW STA CONTRL & PAN	220						275	
16.0	RANGE SAFETY & ABORT								
SUBTOTALS (DRY WEIGHT)		176496						176040	
17.0	PERSONNEL	900						920	
18.0	CARGO							25000	
19.0	ORDNANCE								
20.0	BALLAST								
21.0	RESID PROP & SERV ITEMS	5661						4716	
SUBTOTALS (INERT WEIGHT)		6561						30636	
22.0	RES PROP & SERV ITEMS								
23.0	INFLIGHT LOSSES	12437						9260	
24.0	THRUST DECAY PROPELLANT								
25.0	FULL THRUST PROPELLANT	798031						607588	
26.0	THRUST PROP BUILDUP								
27.0	PRE-IGNITION LOSSES								
TOTALS (GROSS WEIGHT) (LB)		993525						823524	
DESIGN ENVELOPE VOLUME (FT^3)		66544						66548	
PRESSURIZED VOLUME (FT^3)									
DESIGN ENVEL SURF AREA (FT^2)		11731						11731	
PRESSURIZED SURF AREA (FT^2)									
DESIGN q, MAX (LB/FT^2)		607						607	
DESIGN g, MAX		4						4	
DESIGN POWER, MAX (KW)									
DESIGN NO. MEN/DAYS		2/1						2/7	

DESIGNATIONS:
CODE, SYSTEM: REF. MIL-M-38310A OR SP-6004
ITEM OR MODULE
A - Booster
B
C
D
E
F
SPACECRAFT
M MANNED LAUNCH - Orbiter
U UNMANNED LAUNCH

NOTES & SKETCHES:
Thrust decay propellants are included in residual weights.
Tanks are over-sized to account for thrust build-up and pre-ignition losses.

MSC Form 1523 (Jul 69)

2.7 50K POUND PAYLOAD, VEHICLE FR-1

The configuration inboard is shown in Figure 2-16. The synthesis summary is shown in Table 2-11 for the vehicle as presented in August. As in all the vehicles in the spectrum the boost phase mixture ratio was selected at 6.4 to allow use of the 14% uprating. The orbit phase was made at the nominal mixture ratio of 7.0, the same as for all the other vehicles. The 50K FR-1 vehicle is described in more detail in Section 4 of this report for an updated version that included structural weight changes and the incorporation of off-the-shelf flyback engines.

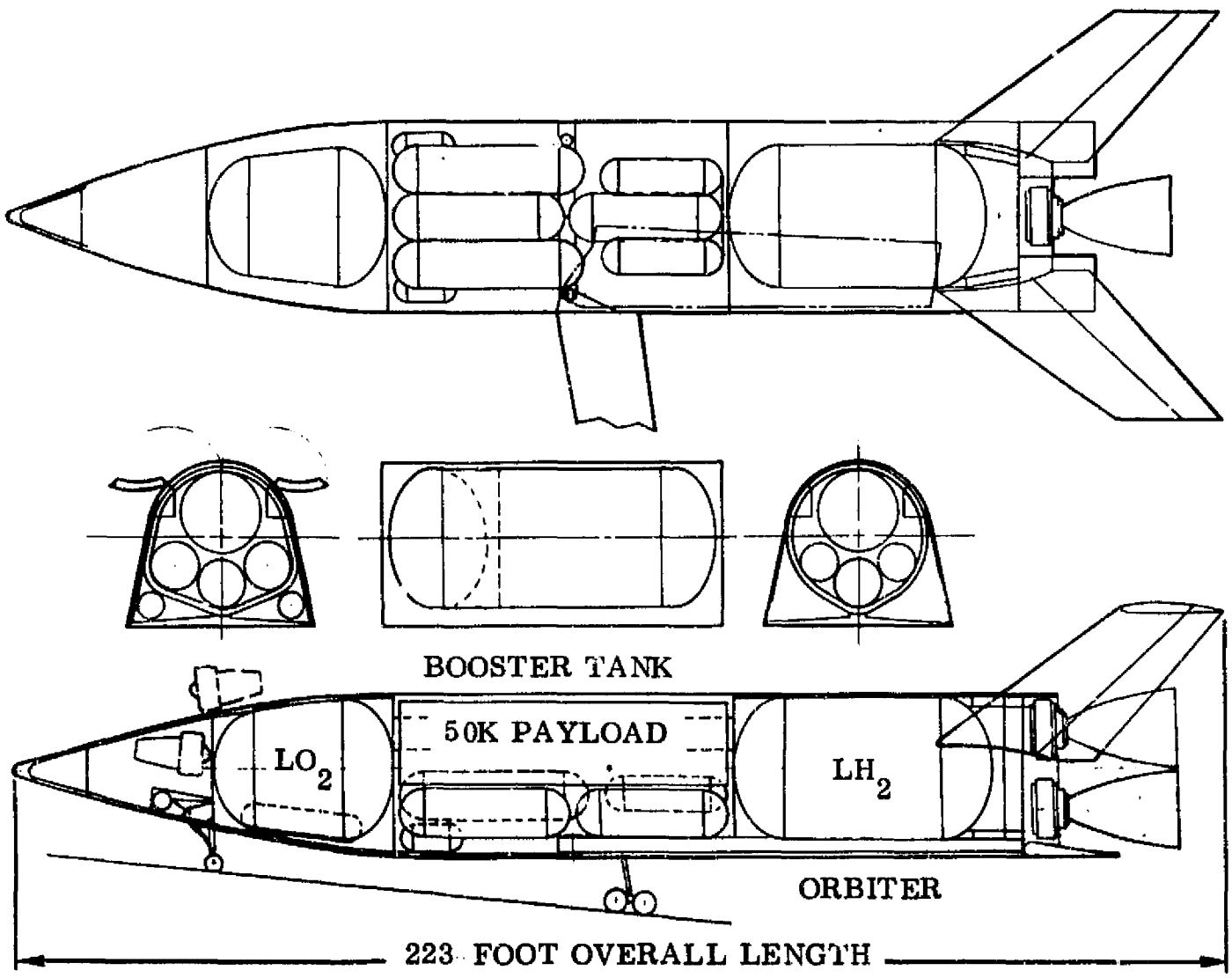

Figure 2-16. FR-1 Element

Table 2-11. FR-1 Vehicle 50K Pound Payload Synthesis Summary

	BOOSTER ELEMENT	ORBITER	VEHICLE
WEIGHT			
FUEL	177339	115128	
OXIDIZER	1134968	805896	
PROPELLANT	1312307	921024	
FLYBACK FUEL	18797	3963	
PAYLOAD		50000	
STRUCTURE	262944	279367	805255
TOTAL	1604332	1317681	4526345
IN ORBIT	0	402851	
RETURN CONDITION	292006	389132	
ENTRY	0	335723	
LANDING	263835	330281	
VOLUME			
FUEL	40065	24609	
OXIDIZER	16810	11932	
PROPELLANT	56875	36542	
PAYLOAD		10638	
OTHER	59881	69585	
TOTAL	116757	116764	
GEOMETRY			
LENGTH	202.8	202.8	
BODY WETTED AREA	18002.4	18003.0	
BODY PLANFORM AREA	5813.0	5813.2	
ENTRY PLANFORM LOADING	48.7	57.8	
PROPULSION			
THRUST-TO-WEIGHT		1.62695	1.39196
NO. OF ENGINES	2	2	
THRUST PER ENGINE (SL)	1,050,800 UPRATED O/F = 6.4	1071904 NOMINAL O/F = 7.0	
THRUST PER ENGINE (VAC)			
SPECIFIC IMPULSE (SL)	391.7	383.0	391.7
SPECIFIC IMPULSE (VAC)	455.8	451.7	455.8
TRAJECTORY			
MASS RATIO		3.27007	2.38015
MAXIMUM DYNAMIC PRESSURE			606.8
STAGING DYNAMIC PRESSURE			50
STAGING VELOCITY (RELATIVE)			8273
STAGING ALTITUDE			172179
STAGING FLIGHT PATH ANGLE (RELATIVE)			7.952
INJECTION VELOCITY (INERTIAL)		25897	
INJECTION ALTITUDE		259986	
INJECTION FLIGHT PATH ANGLE (INERTIAL)		.000	
INJECTION INCLINATION		54.99	
FLYBACK RANGE	228.2		

SECTION 3

TWO-ELEMENT PARAMETRIC DESIGN ANALYSIS

3.1 PERFORMANCE

Parametric synthesis runs were made on the 50K payload two-stage sequential burn vehicle to investigate the effects of staging velocity, thrust-to-weight at liftoff and thrust-to-weight of the orbiter at staging on the vehicle weights, and the impact on engine thrust requirements and numbers of engines. The staging velocity was also tempered by aerodynamic heating considerations as discussed in Section 3.6. The mixture ratio was held at 7.0 and nominal thrust was used in both booster and orbiter elements for this study. Uprating of liftoff thrust was not employed.

Figure 3-1 shows the weight relationships to staging velocity. Note that the gross liftoff weight at all thrust-to-weight levels tends to be minimum at approximately 10,500 fps staging velocity. The total system dry weight has reached a minimum at approximately 12,000 fps. The scale on the ordinates relative to the total amounts is

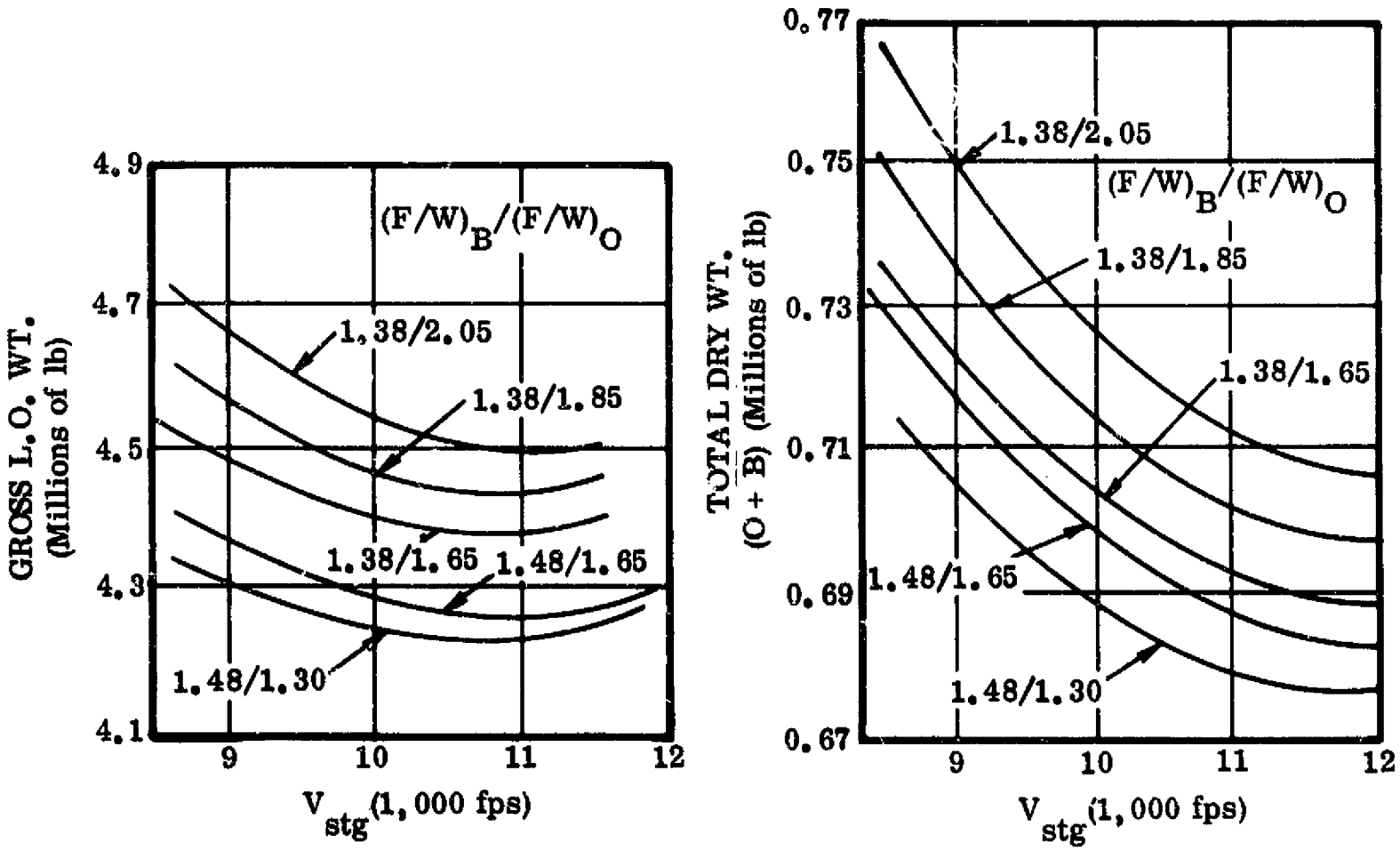

Figure 3-1. Weight versus Staging Velocity

a coarse one and the differences in dry weight are not as severe as the visual indication from the plot. As the figure indicates, weight will be reduced with increasing thrust-to-weight at liftoff and weights increase with increasing thrust-to-weight at orbiter ignition (over the range investigated).

A minimum thrust-to-weight at liftoff of 1.16 with one engine out was established as a system ground rule to ensure safe liftoff without excessive drift in this condition. The thrust-to-weight in the orbiter is fixed by the "once around" abort philosophy whereby the orbiter, in case of engine out, proceeds to low orbit using the mission maneuver propellants to overcome the performance loss of the engine out. The top half of Figure 3-2 shows the effects, which indicate that a thrust to weight (F/W) of about 0.825 (min.) is needed.

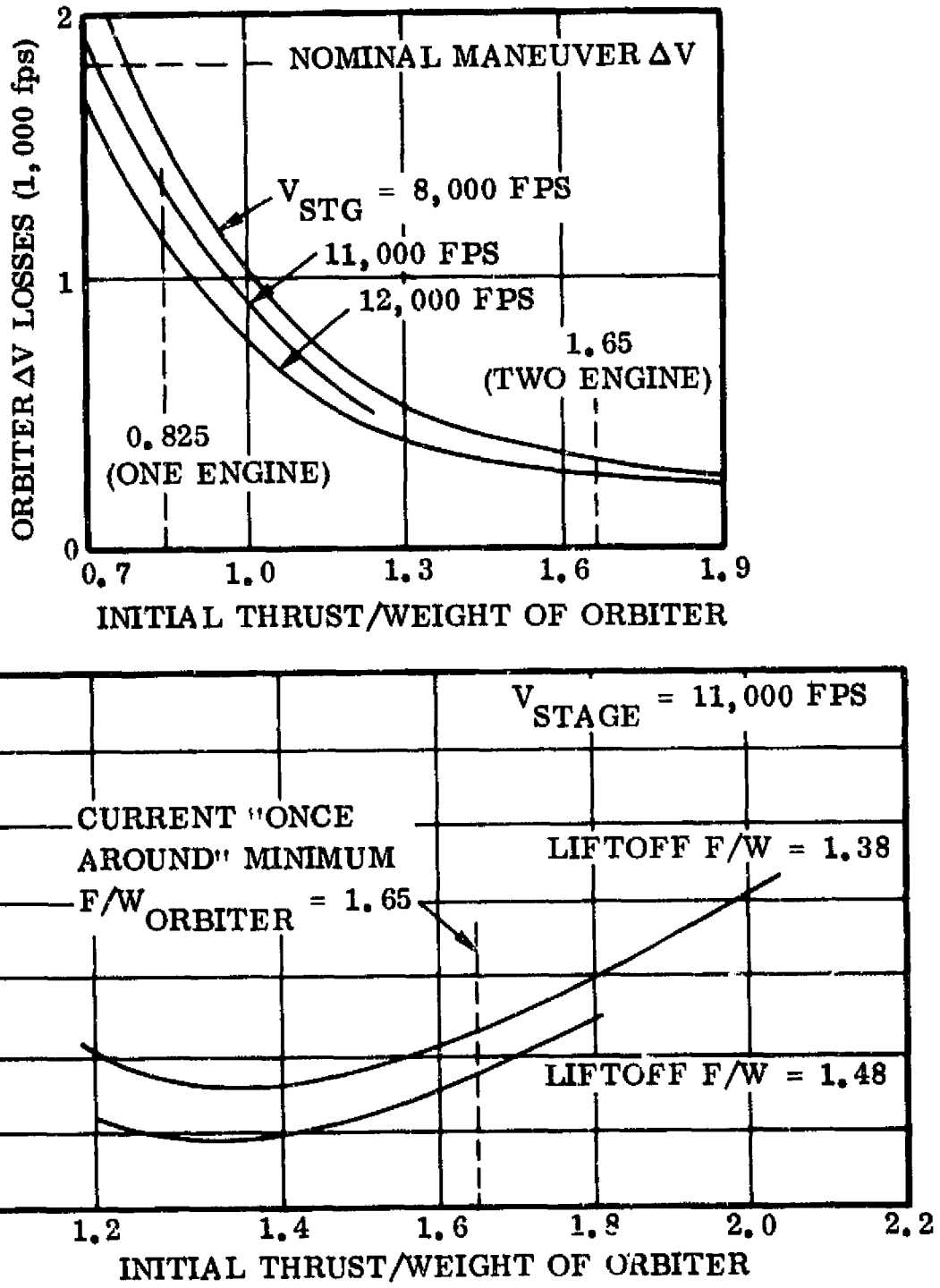

Figure 3-2. Two-Stage Parameter Study — Effect of Orbiter Initial Thrust/Weight Ratio

For a two-engine orbiter this results in a 1.65 F/W at ignition of both engines. (These are initial estimates which are currently being revised for the NASA and the USAF missions. Indications are that the requirements will be more severe than anticipated here, and that it may be necessary to go to three-engine orbiters to maintain a higher F/W orbiter with one engine out, and thus reduce the effect of misalignment ΔV losses.)

Figure 3-2 (bottom) shows that there is a minimum dry weight associated with the orbiter F/W at ignition and that the safety aspects of once-around abort with a return to the launch site involve a weight penalty. The crossrange associated with this abort philosophy is about 800 n.mi. for the 55-deg orbit and ETR launch site.

The data was converted to numbers of engines versus staging velocity and plotted as shown in Figure 3-3. The approximate temperature limit at 11,000 fps staging

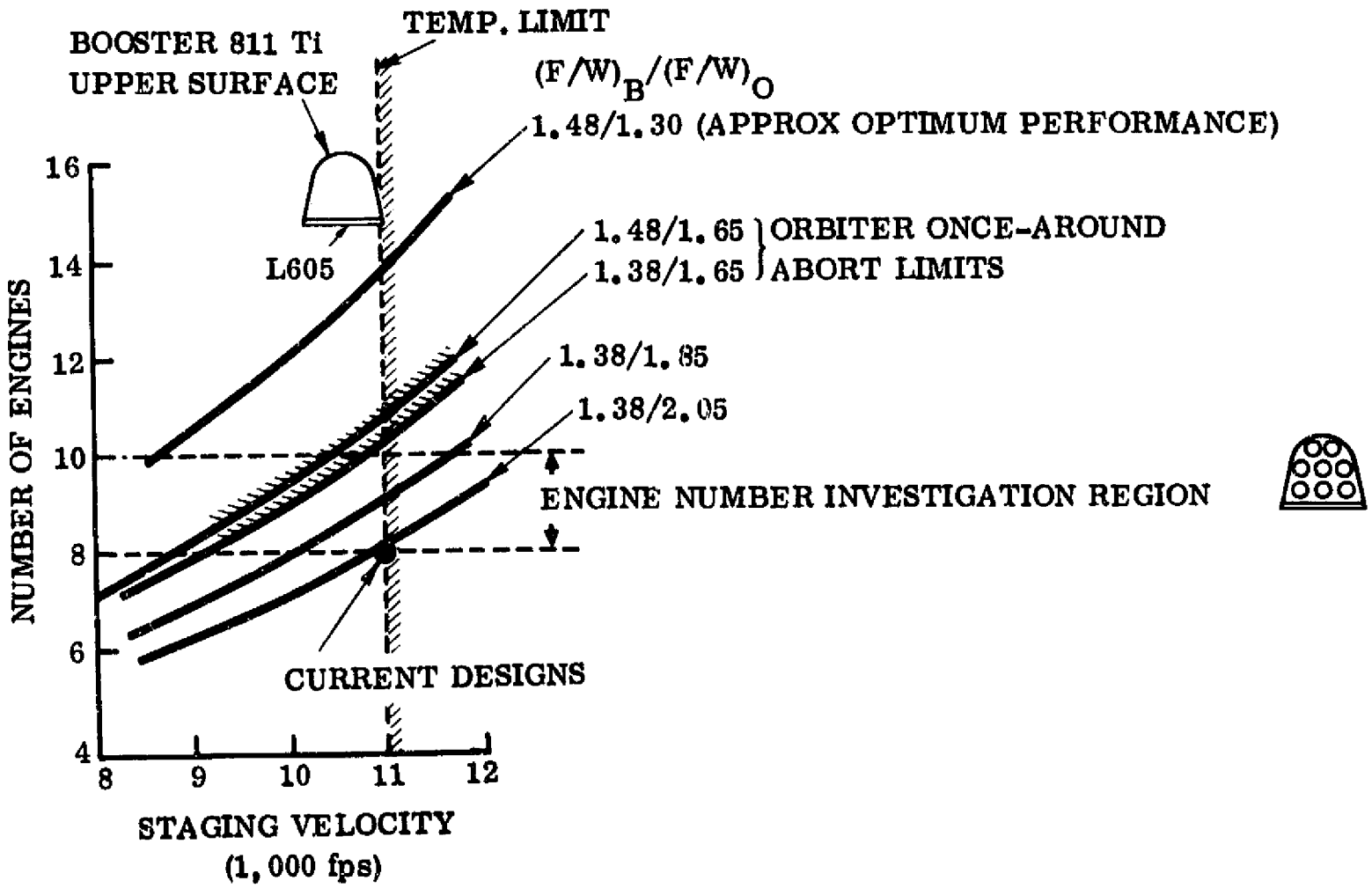

Figure 3-3. V_{stg} vs. F/W vs. Number of Engines

velocity is shown. Selected curves to show the trend with F/W are also shown. The orbiter once-around abort limits as presently used are indicated. Note that increasing the number of engines at a fixed orbiter F/W and constant staging velocity increases the liftoff F/W of the booster. The number of engines investigated at this point was held between eight and ten. The minimum-weight solution tends to increase the number of engines, as shown on Figure 3-4.

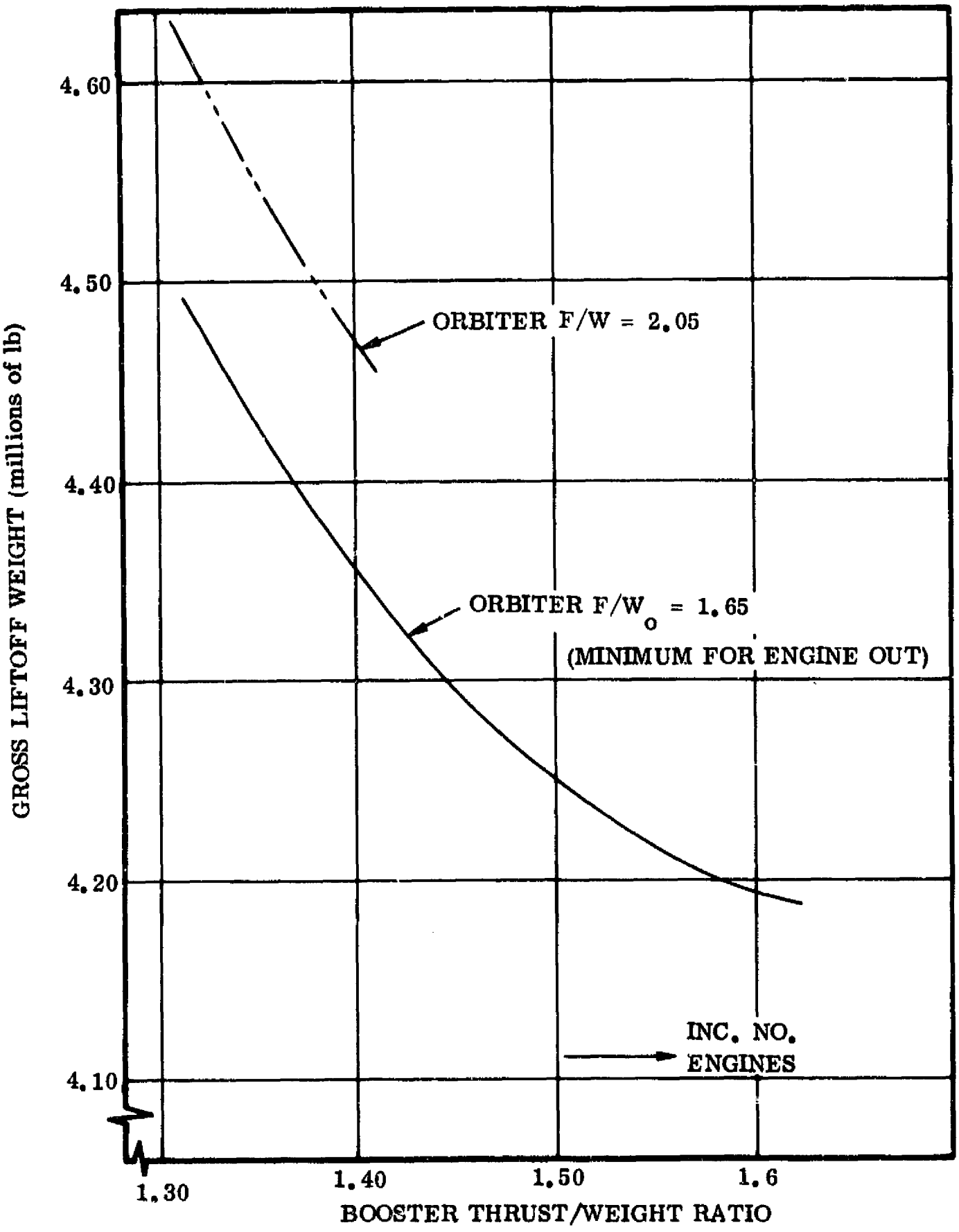

Figure 3-4. Liftoff Weight vs. Booster Thrust/Weight

One method of obtaining a high booster F/W with fewer engines is to increase the F/W of the orbiter (bigger engine). However, as shown in Figure 3-5 (an extension of Figure 3-2), increasing orbiter F/W above 1.30 increases gross liftoff weight (GLOW) as the orbiter engine weight effects overcome the reduction in ΔV misalignment loss effects to the right of this minimum.

To summarize, the maximum thrust of the common engine is limited by orbiter performance considerations (Figure 3-5); therefore, increasing the number of engines on the booster is the best way to increase the F/W and reduce GLOW. See Figure 3-6. It should be noted, however, that increasing the number of booster engines beyond eight reduces reliability (Ref. Section 3.1.2.3).

3.1.1 ENGINE SIZES, ARRANGEMENTS, AND NUMBERS

3.1.1.1 Engine Size Required. The variation in engine size when 8, 9, and 10 engines are used on the booster is summarized in Table 3-1.

Table 3-1. Engine Size

Number of Engines	$(F/W)_B / (F/W)_O$	Thrust/ Eng	Nozzle Exit Dia (ft)	Engine Dia (ft) (Power Pack)
8	1.38 / 2.05	775,000	7.08	10.1
9	1.38 / 1.85	675,000	6.40	9.5
10	1.38 / 1.65	602,000	6.06	9.0

3.1.1.2 Engine Space Available. The engine space available on the baseline booster is limited by the basic shape of the vehicle and the arrangement or pattern used in grouping the engines. The basic shape assumed in this investigation was based on early FR-1 (T-14) lines. The engine arrangements are discussed below:

a. Eight-Engine Arrangement. The optimum pattern for eight engines is shown in Figure 3-7. It maximizes the engine space available when eight identical engines are used and results in a reasonable thrust vector/vehicle cg relationship.

b. Nine-Engine Arrangement. Figure 3-8 shows four candidate engine arrangements. The packaging efficiency of each arrangement was evaluated by comparing the ratio of maximum engine diameter to vehicle diameter (De/Dv). As shown, arrangement D has the highest ratio and allows the maximum engine diameter for a given vehicle size. This pattern also has a favorable thrust vector/cg relationship.

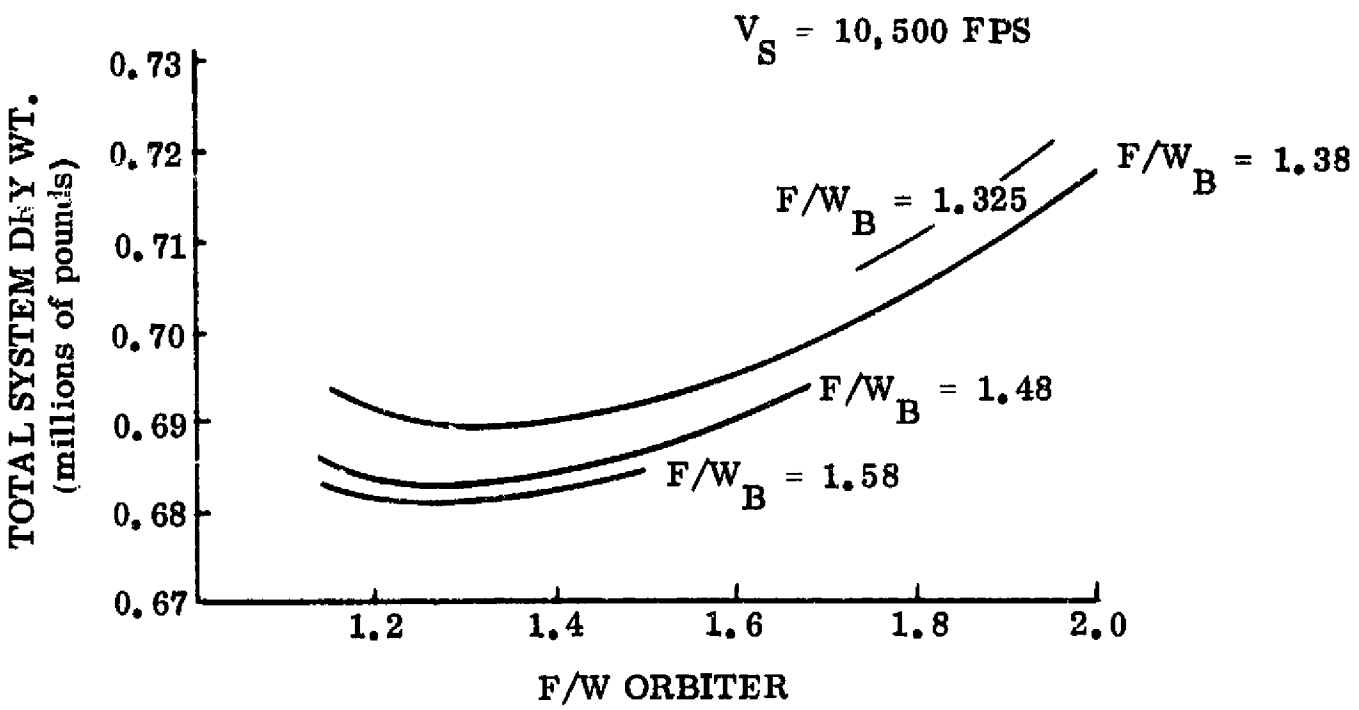

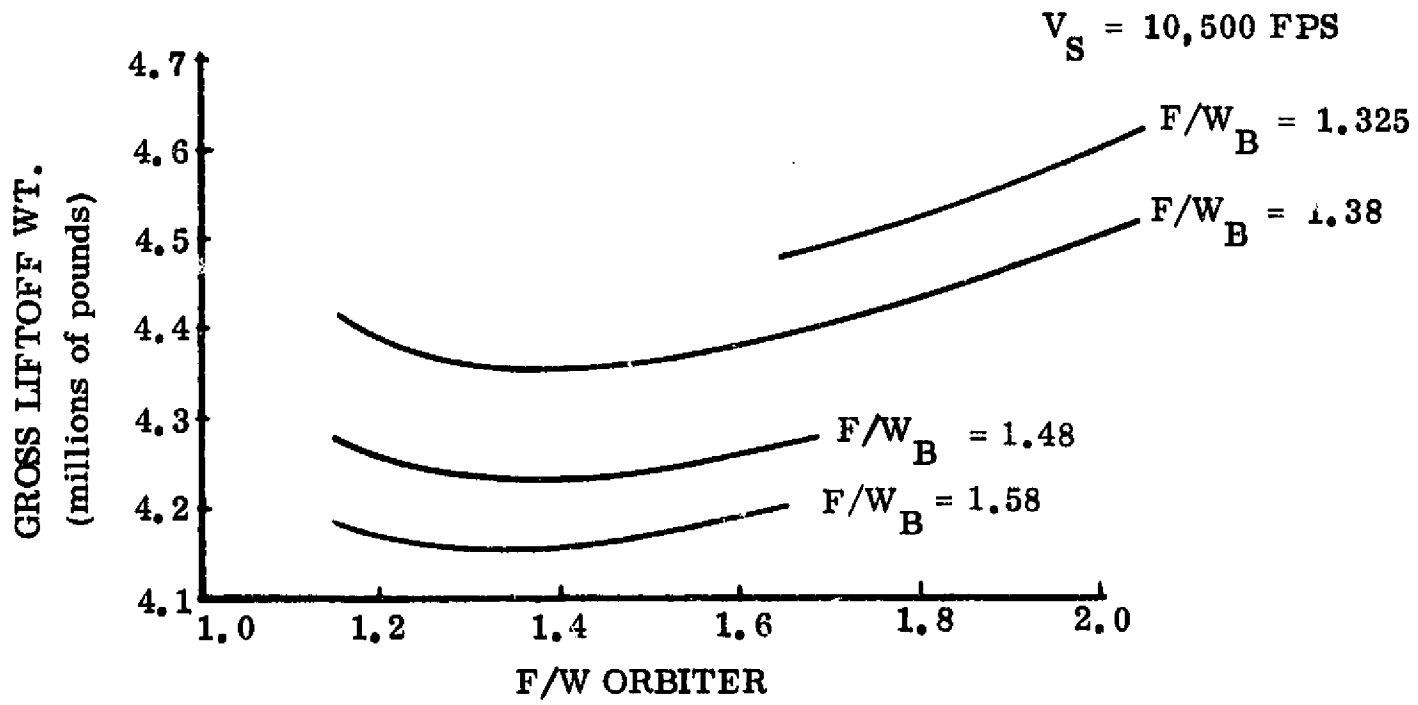

Figure 3-5. Effect of Orbiter F/W on Total System Dry Weight and GLOW

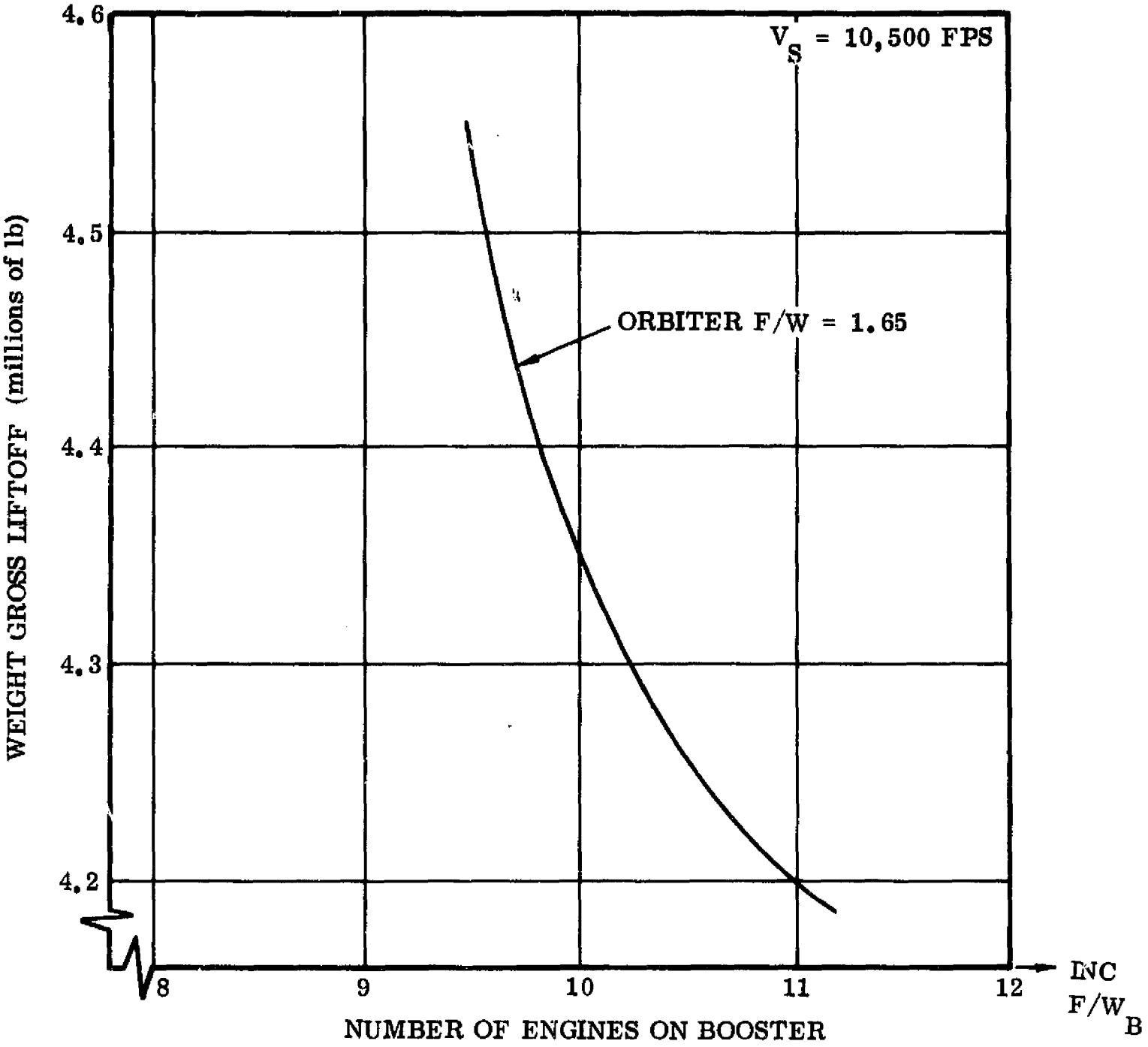

Figure 3-6. Liftoff Weight vs. Number of Engines

c. Ten-Engine Arrangement. Figure 3-9 shows four candidate engine arrangements. The De/Dv ratio favors arrangement D; however, when compared to arrangement B, the small space advantage may not outweigh the mounting and boattail advantages of B. All arrangements except A have a favorable thrust line, with C the best for side/side stage mounting as it has the lowest thrust line (nearest the vehicle base). This will minimize the engine bulkhead cant angle required to align the booster thrust line through the combined center of mass of both stages.

3.1.1.3 Comparison of Space Available and Required. Engine space available and space required is compared in Table 3-2. The comparison is based on best pattern

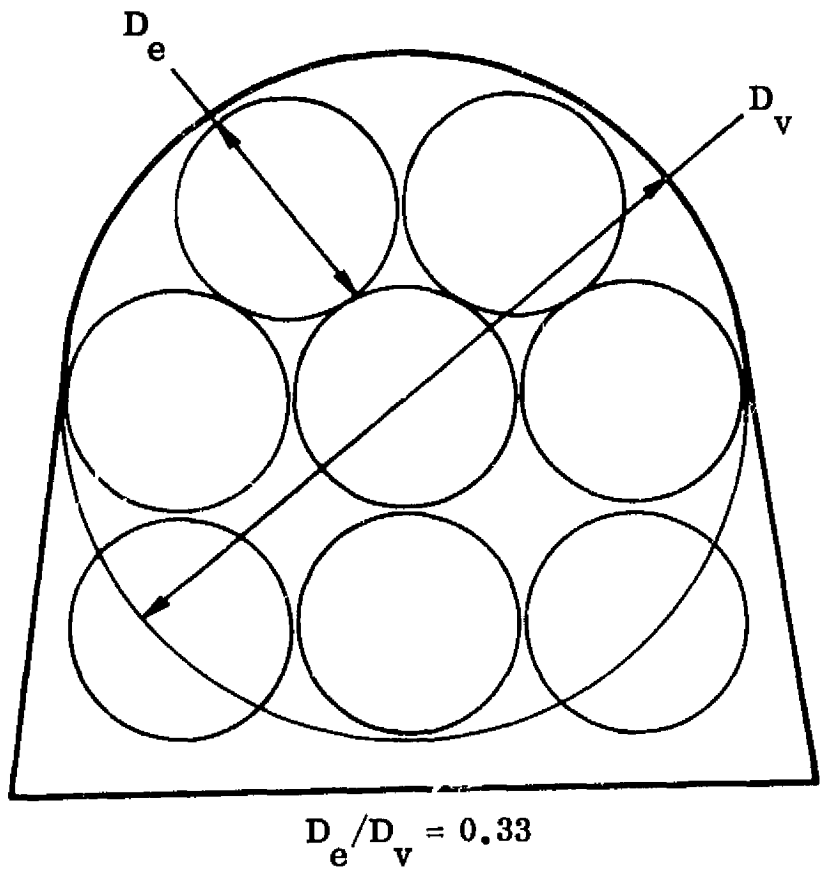

Figure 3-7. Eight-Engine Arrangement

and Baseline Booster, L = 245.0 ft, D_V = 32.2 ft. At an expansion ratio ϵ = 35, power pack diameter is critical. At ϵ = 80, nozzle diameter is critical.

Table 3-2. Clearance Comparison

Number Engines	Dia. Avail.	Diameter Required: No Gimbal ϵ = 35 / ϵ = 80	Diameter Required: Gimbal 7 Deg ϵ = 35 / ϵ = 80	Clearance: No Gimbal ϵ = 35 / ϵ = 80	Clearance: Gimbal 7 Deg ϵ = 35 / ϵ = 80
8	10.70	10.1/11.0	10.1/13.0	+0.6/-0.3	+0.6/-1.3
9	9.50	9.5/10.25	9.5/12.25	+0/-0.75	+0.0/-2.75
10	9.20	9.0/9.75	9.0/11.75	+0.2/-0.55	+0.2/-2.55

clear — no clearance

Note: All Dimensions in Feet

a. Expansion. Engines with nozzle expansions of 35 have clearance regardless of the number used (up to 10), and permit 7.0-deg gimbaling. Expansion ratios of 35/80 (two-position) will not stay within the base outline of the vehicle; however, this protrusion is small when 7.0-deg gimbal clearance is not required between engines.

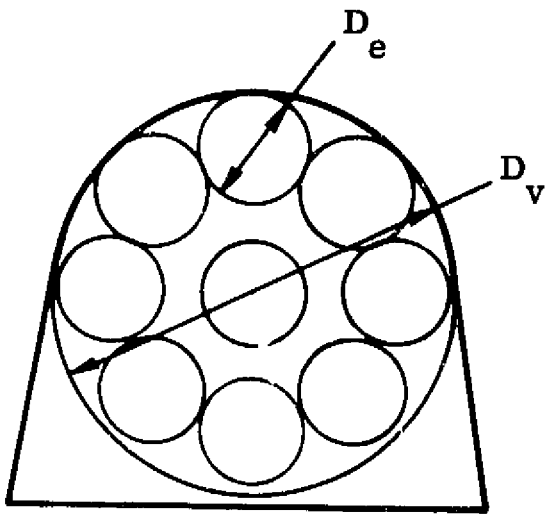

(A)

$D_e/D_v = 0.281$

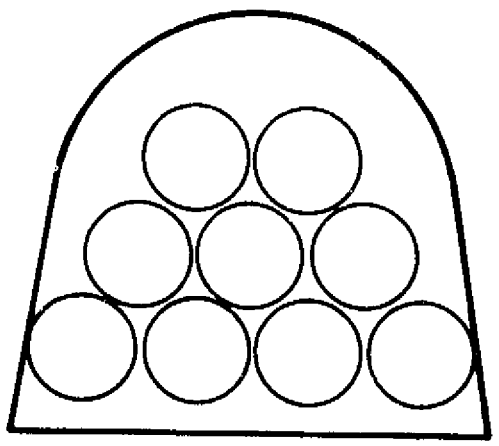

(B)

$D_e/D_v = 0.283$

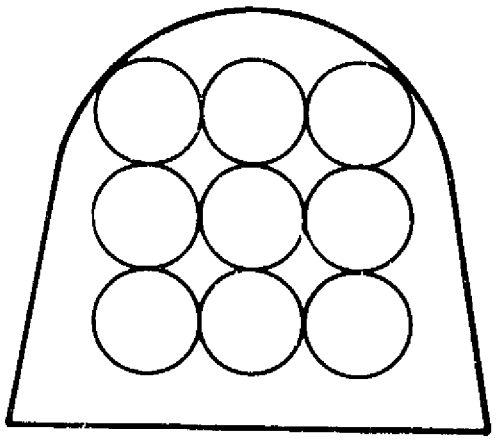

(C)

$D_e/D_v = 0.283$

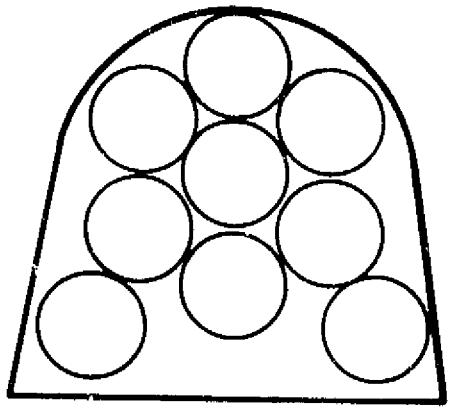

(D)

$D_e/D_v = 0.294$

Figure 3-8. Nine-Engine Arrangement

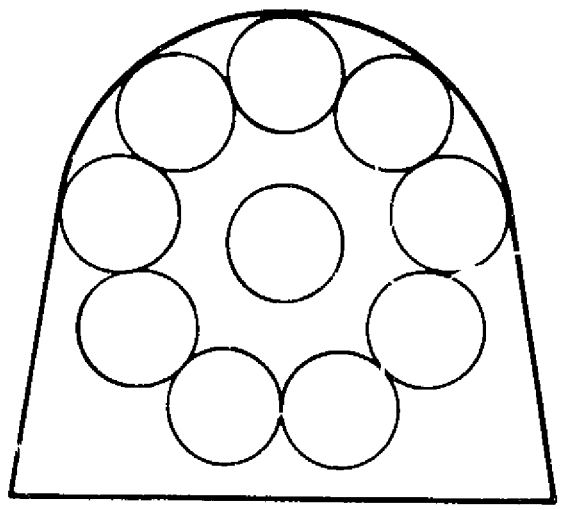

(A)

$D_e/D_v = 0.260$

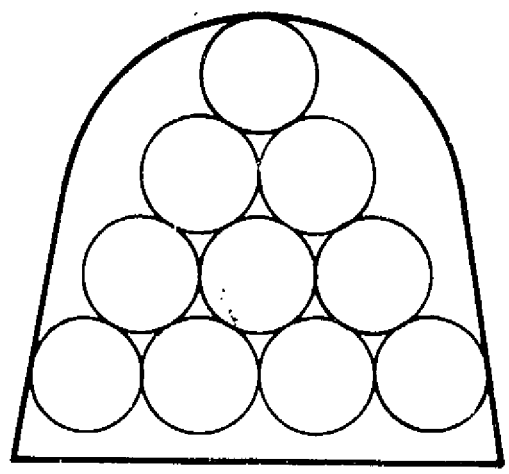

(B)

$D_e/D_v = 0.280$

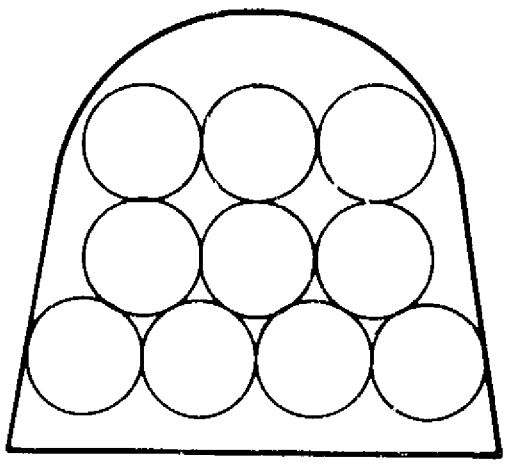

(C)

$D_e/D_v = 0.280$

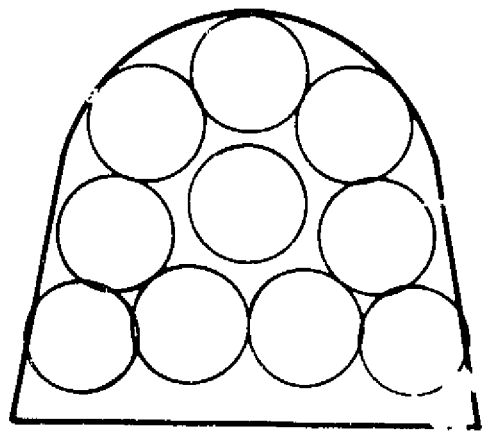

(D)

$D_e/D_v = 0.286$

Figure 3-9. Ten-Engine Arrangement

b. Number of Engines. Eight-engine arrangements have the best clearance when compared at a fixed expansion, with gimbaling requirement. Nine-engine arrangements are acceptable with $\epsilon = 35$ but will have large protrusions outside the base outline at $\epsilon = 80$ with 7.0 deg gimbaling. The ten-engine arrangement is better with regard to space than nine, but not as good as eight.

3.1.1.4 Summary. Increasing the number of booster engines from eight to ten is desirable from a performance standpoint (see Figure 3-10) and is acceptable from a design standpoint if the engine expansion is limited to 35 to 1 (S. L.).

However, if two-position (35/80) nozzles are used, the protrusion beyond the base outline will be greather with nine or ten engines than with eight. The larger-expansion nozzle will also make gimbaling all engines (or thrust modulation) more attractive for thrust vector control (TVC), because individual engine gimbaling (for checkout) now determines engine spacing (not so with $\epsilon = 35$).

3.1.2 SAFETY AND RELIABILITY

3.1.2.1 Gross Failure and Mission Termination Analysis. Section 8, "Safety Analysis," of Convair Report GDC-DCB69-027 presents information on safety and reliability for a fully reusable launch vehicle concept. The objectives of the analysis were:

a. Investigate safety in the operation.

b. Establish abort philosophies and mission termination procedures, subsystem design requirements, and requirements for redundancy.

The analysis shows that intact abort following subsystem failure can be accomplished; vehicles can be returned to the launch site with the orbiter executing a "once around the earth" maneuver and return to the launch site, and with the boosters depleting propellant, separating, and flying back to the launch site in a normal manner.

It was determined that mission losses (incompleted missions) do not represent a large operational cost factor. However, vehicle losses are a major cost factor and fail-safe capability is required. Rocket engines, propellant feed and gimbaling are major contributing factors in defining a safe vehicle. The analysis also considered the use of LO_2/LH_2 propellant combinations and indicated what design actions are required to minimize fire and explosion by the use of pressurization and purge of critical compartments with an inert gas.

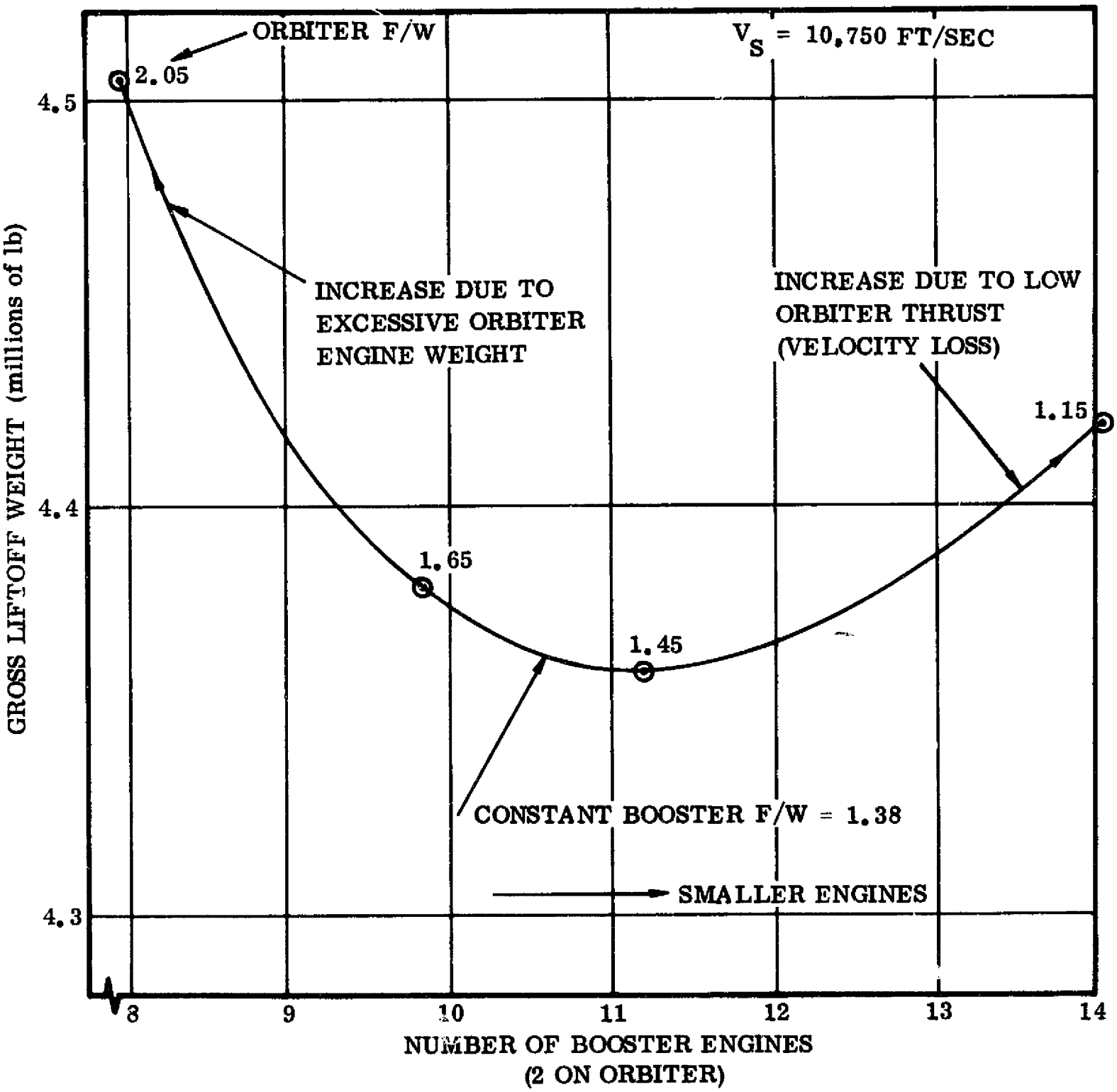

Figure 3-10. GLOW vs. Number of Engines (F/W_b = 1.38)

Abort procedures following failures occurring in each trajectory phase were defined and design recommendations for improved safety were made.

3.1.2.2 Safety Considerations in Selection of Number of Rocket Engines for the Two-Stage (FR-3) System. An analysis was conducted to determine the effect on crew and passenger safety and mission success for a range of booster engines (6-12) and for one and two orbiter engines installed in the vehicles.

The analysis was based on:

a. Data and information from Convair Report GDC-DCB69-027, Section 8, "Safety Analysis", where

   1. A mission success goal of ≈ 0.97 (mission losses = 30/1000 flights) was established, and

   2. A vehicle intact abort success goal ≈ 0.9994 was established (vehicle losses = 0.6/1000 flights) for mechanical failures.

b. Engine reliability = 0.997.

c. Liftoff to staging burn time = 0.066 hr.

d. Liftoff thrust to weight (F/W) = 1.16 required for intact abort.

e. Liftoff F/W $\approx$ 1.16 with n-1 engines operating (one engine out) is provided.

f. Orbiter can accomplish intact abort with n-1 engines operating.

3.1.2.3 Summary. Results of the analysis are summarized below and in Table 3-3.

As the number of booster engines used increases from 6 to 12:

a. Total mission losses increase from 30 to 38.

b. Total vehicle losses increase from 0.6 to $\approx$ 0.7.

As the number of orbiter engines used increases from one to two:

a. Total mission losses increase from 28.7 to 30.

b. Total vehicle losses decrease from 1.9 to 0.6.

For a basic goal for vehicle losses < 0.6 total, a minimum of two orbiter engines are required.

Table 3-3. Variation of Losses With Engine Quantity

	Number of Engines	Mission Losses/1000 Flights Total, All Causes	Mission Losses/1000 Flights Due To Engines Only	Vehicle Losses/1000 Flights Total, All Causes	Vehicle Losses/1000 Flights All Causes Except Fire & Explosion
Booster	6	30	(8)	0.6	(0.025)
	12	38	(16)	0.7	(0.11)
Orbiter	1	28.7	(1.3)	1.9	(1.3)
	2	30	(2.6)	0.6	(0.0018)

3.1.2.4 Conclusions and Recommendations. The conclusions and recommendations are:

a. Booster Engines

1. The number of booster engines should be greater than six and less than 12.
2. Thrust to weight at liftoff with one engine out ≥ 1.16.
3. Results with these recommendations incorporated:

   Vehicle losses* $\approx 0.03/1000$ to $0.1/1000$

   Mission losses* ≈ 8 to $16/1000$

b. Orbiter Engines

1. A minimum of two orbiter engines should be used.
2. Thrust to weight

   $F/W_{seq.\ burn} = 1.2$ (at staging)

   $F/W_{par.\ burn} = 1.8$ (at staging)

3. Results

   Vehicle losses* $\approx 0.002/1000$

   Mission losses* $\approx 3/1000$

c. Commonality of Engines. It is suggested that n_b be determined from sizing $n_o = 2$ to achieve commonality or, if penalties are too great, select $n_o = 2$ for orbiter and optimize n_b for booster with uncommon engines.

*Due to engines only.

3.1.3 PARAMETRIC COST STUDY. A parametric cost study was performed for the 50K lb two-stage sequential burn (FR-3) configuration. The purpose of the study was to determine the effects on system cost of booster F/W, orbiter F/W, number of booster rocket engines, and staging velocity. The number of orbiter rocket engines was fixed at two.

The relationships developed for the above variables are shown in Figures 3-11 and 3-12. In Figure 3-11 the costs are shown broken down into recurring costs and non-

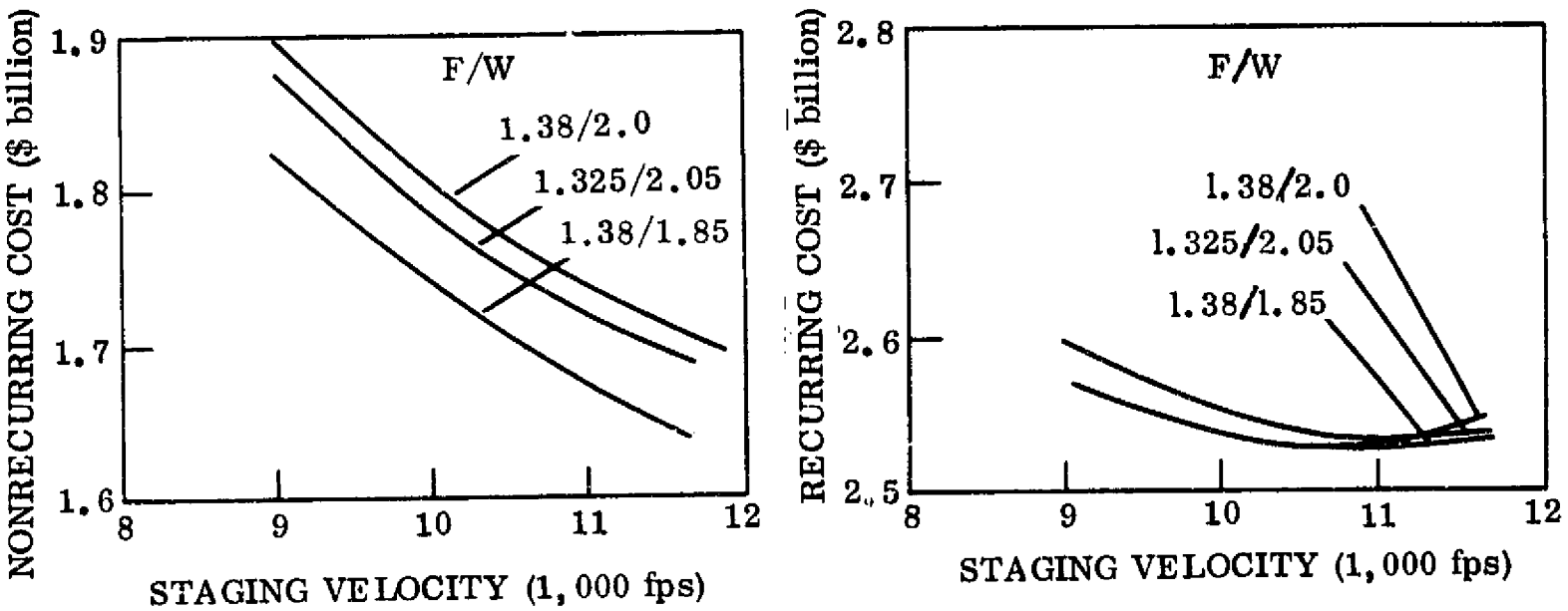

Figure 3-11. Two-Stage Vehicle Program Cost Trends
(100 Launches Per Year for 10 Years)

recurring costs. Nonrecurring costs are made up entirely of development costs, but do not include the cost of flight test hardware that is passed on to the operational program. Recurring costs include the investment in operational hardware, spares, propellants, and operations costs. The nonrecurring cost plot shows that with the F/W of both the booster and orbiter set at fixed values the development cost can be reduced by increasing the staging velocity. Also shown is a decrease in development cost associated with increasing F/W of the booster and/or decreasing F/W of the orbiter when the staging velocity is set at a fixed value. The recurring cost plot shows relative insensitivity to both F/W and staging velocity, although there appears to be a bucket in the recurring costs curve at about 10,500 fps to 11,000 fps.

In Figure 3-12 the nonrecurring and recurring costs have been combined and plotted to show total program cost versus the same parameters. Constant number of

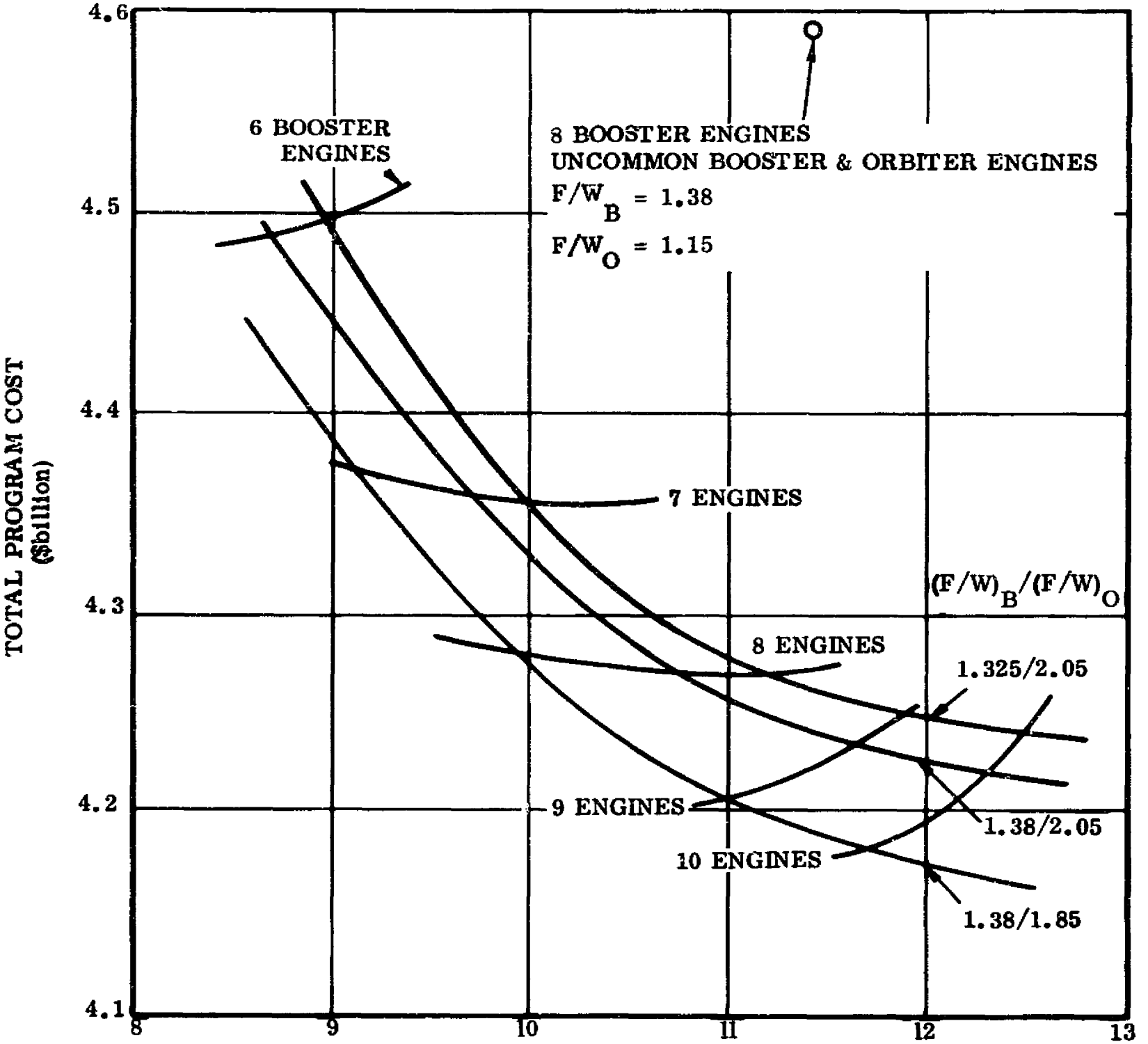

Figure 3-12. Two-Stage Vehicle Program Cost Trends for Total Program (100 Launches Per Year for 10 Years)

engine lines have also been identified. Due to the relative insensitivity of recurring costs, the trends in total program cost tend to parallel those of the nonrecurring costs. In determining the relative advantage of varying F/W, $V_{staging}$ and number of booster engines, the impact of a constraint on any one of these variables on the others must be understood. For instance, there is no cost advantage to increasing the staging velocity unless there is a real constraint against going to a F/W relationship that lies further toward the lower left corner of the plot. Likewise, depending on the relationship of one constraint to another, different conclusions can be drawn about numbers of engines and staging velocity. If the configuration were constrained to no more than eight engines, from a total program cost point of view staging velocity would not matter. If, however, there is a constraint of nine engines maximum and there is also a constraint of 1.38/1.85 on the F/W relationship, then staging velocity should be 11,000 fps to achieve minimum total program cost. The plot shows a general tendency toward decreasing costs with increasing numbers of engines, but this trend can be counteracted if the F/W relationship is allowed to vary. As can be seen from the plot, nine engines with F/W set at 1.38/1.85 is cheaper on a total program basis than 10 engines with F/W set at 1.325/2.05.

The point shown at the upper portion of the graph at about 11,500 fps illustrates the effect on cost of optimizing the vehicle primarily on performance and not constraining the configuration to use the same rocket engine in both booster and orbiter. As can be seen, this results in significantly higher total program costs.

3.1.4 TWO-STAGE SEQUENTIAL BURN 50K LB PAYLOAD PARAMETRIC STUDY CONCLUSIONS. The following general trends were observed:

a. The optimized vehicles will stage in the neighborhood of 11,000 to 12,000 fps.

b. Temperature limits currently set at 11,000 fps could probably be extended to 12,000 fps without significant penalty.

c. A F/W of about 1.45 in the booster and 1.30 in the orbiter is optimum for performance, but the common engine requirement makes this unachievable. The F/W of the orbiter must be higher than optimum in order to achieve the staging velocity required within the 8- to 10-engine limits which seem to be practical for the booster. Part of the increase in F/W of the orbiter is desirable, however, to achieve the once-around abort requirement.

d. Vehicle safety or mission success increases slightly by going from 12 to 6 engines in the two-stage sequential system. (Catastrophic failures were not considered as a percentage of all engine failures in this work, however, and for these effects Convair Report GDC-DCB69-032 should be consulted.)

e. Development costs make it desirable to use a common rocket engine with a single development program for both stages of the two-stage system.

f. Program costs follow the weight trends versus staging velocity. Nonrecurring costs follow the total dry system weight trends; recurring costs, for the selected conditions, follow the gross weight trends. Costs reduce with numbers of engines and with the thrust-to-weight ratios which give lowest weights. Staging velocity and number of engines are interrelated, with 10 engines showing the least cost.

g. The parametric study was for nominal engine thrusts. Uprated liftoff thrust at a mixture ratio of O/F = 6.4 would reduce the number of booster engines and improve the total system.

3.2 TWO-STAGE THRUST VECTOR CONTROL GIMBAL ANGLE REQUIREMENTS

Simulated flights using 99 percentile winds have demonstrated the need for engine gimbaling. Figure 3-13 presents the gimbal requirements for each configuration. These requirements are dictated by 1) one engine out, 2) center of gravity offset, and 3) maximum αq conditions. A unique feature which heavily influences the gimbal angle requirement is that all of the vehicles under consideration are aerodynamically stable throughout the boost phase of flight. With an aerodynamically stable vehicle, maximum αq loads can be relieved by limiting the gimbal angle. For the limited gimbal angle conditions at maximum αq, the vehicle "weathercocks" (rotates into the wind) to reduce the angle of attack, thereby reducing the airloads on the vehicle. Gimbal angle requirements were established by limiting the attitude error (command attitude minus actual attitude) to less than three degrees. The gimbal angle limiting is unconventional when compared to the control systems on operational unstable boost vehicles; for these vehicles, a gimbal angle limit can produce a catastrophic failure and load relief can only be provided by sophisticated control system electronics.

3.3 TWO-ELEMENT VEHICLE LOADS

Net loads were determined for four two-element vehicle configurations. These configurations were nose-to-nose sequential burn, tail-to-tail sequential burn, simultaneous burn, and tandem.

The net loads presented herein are net body shears, bending moments and axial loads for various ground, flight and landing conditions. All loads shown in this section are limit. Net loads were determined by means of computer programs which handle airloads and mass distributions, cruise and booster thrust vectors, concentrated loads, and translational and rotational inertia loads. Rigid-body analysis was used and the vehicles are in quasi-static equilibrium in all cases. Details relative to airloads, mass distributions, and net loads are given in the following paragraphs.

3.3.1 AIRLOADS. Vehicle airloads were obtained for conditions of maximum boost dynamic pressure, subsonic cruise gust, landing, and launch pad ground winds. The

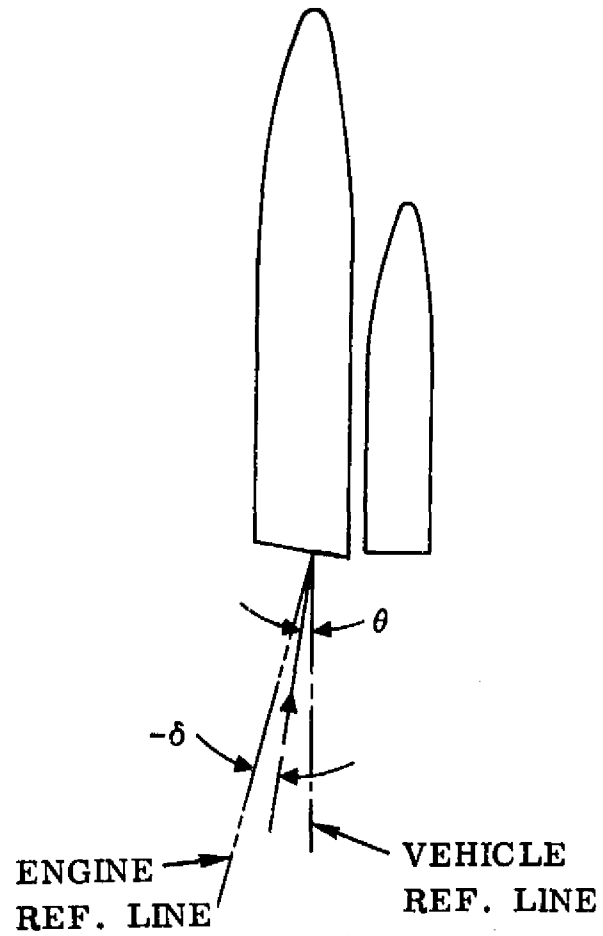

Configuration	θ Cant Angle	δ Gimbal Angle	δ Liftoff	δ Max q	δ Burnout	δ One Engine Out
Two-Stage Seq-Burn	8	±5	-3.8	4	3.5	4.5
Two-Stage Sim-Burn	5	±5	-3.5	4.7	4.8	4.7
Fixed-Wing Two-Stage Seq-Burn (see Section 6 of this report)	8	±7.5	-3.8	7.5	3.5	4.5

All units in degrees.
*Gimbal angle is the engine rotation about the cant angle.

Figure 3-13. Gimbal Angle* Requirements for Two-Stage Space Shuttle Configuration

surface winds were assumed to act normal to the longitudinal axis of the vehicle on the launch pad and to be from the most critical direction. The winds were 99 percentile surface wind speed envelopes for the Eastern Test Range. Maximum boost dynamic pressure loads were obtained by a three-degree-of-freedom simulation. The vehicle was flown through 99 percentile Marshall synthetic winds for the most critical direction with the peak gust occurring at maximum dynamic pressure. Subsonic cruise gust loads were for a 50 ft/sec sharp-edge gust as specified in MIL-SPEC-8861. Airloads on the wing, fin, and body were determined. The landing loads are for a 12 ft/sec touchdown sink speed and a rigid body analysis. Both two-point and three-point touchdown attitude conditions were considered.

All air loads are for a rigid body. Maximum dynamic pressure loads were computed for an elastic body and the elastic body amplification factor was found equal to 1.026. The first bending frequency for this class of vehicles was found to be between 3.0 and 3.5 cps.

3.3.2 MASS DISTRIBUTIONS. Mass distributions used in the calculation of net loads were those for the dry weight and the propellant weight corresponding to each of the conditions analyzed. Summaries of the total weights used with these mass distributions are given in Section 2.

3.3.3 BODY NET LOADS. Net loads for the body were determined for various ground and flight conditions. These include ground winds, max αq, booster burnout, subsonic gust, and landing. Plots of net axial loads, shears and bending moments for those conditions are shown in Figures 3-14 through 3-33 for the orbiter and the booster of each configuration. Subsonic gust and two-point landing loads shown in Figures 3-30 through 3-33 are typical of all configurations. In order to visualize the effects of configuration on loads, plots of net axial loads and net bending moments for maximum αq and booster burnout conditions are presented in Figures 3-34 through 3-41 for orbiter and booster elements. Furthermore, peak compression load intensities were also plotted for the nose-to-nose and tail-to-tail sequential burn configurations to enable identification of critical load conditions. These plots, which include the effects of internal pressure in the orbiter's integral tanks, are shown in Figures 3-42 through 3-45.

3.4 VEHICLE MASS PROPERTIES

Tables 3-4, 3-5, and 3-6 are mass property summaries for the FR-3 two-element, sequential burn, (3A) two-element tandem, and FR-1 50K lb payload. The two-element simultaneous burn mass properties data was not calculated separately, because of its similarity to the (3A) configuration. Load data, balance, and inertias for the FR-3-25K were therefore obtained by using FR-3 data with appropriate modification. In like manner, FR-1-25K mass properties were obtained when needed by ratioing FR-1 data.

Shown in the FR-3 and (3A) mass property summaries are preliminary weights, not current weights. The FR-1 summary reflects current weight status. Current weight summaries for the five configurations — FR-3, (3A), FR-3-25K, FR-1-25K and FR-1 — are shown in Section 2. These weights were obtained through use of the space shuttle synthesis program, with program inputs constantly modified to reflect the developing designs, load data, etc.

3.5 TWO-STAGE VEHICLE AERODYNAMICS

Certain studies, such as tail sizing versus vehicle length and side slope, are applicable to both the booster and the orbiter vehicles. These are covered in Section 3.5.1. The studies specifically for the two-stage booster are covered in Section 3.5.2.

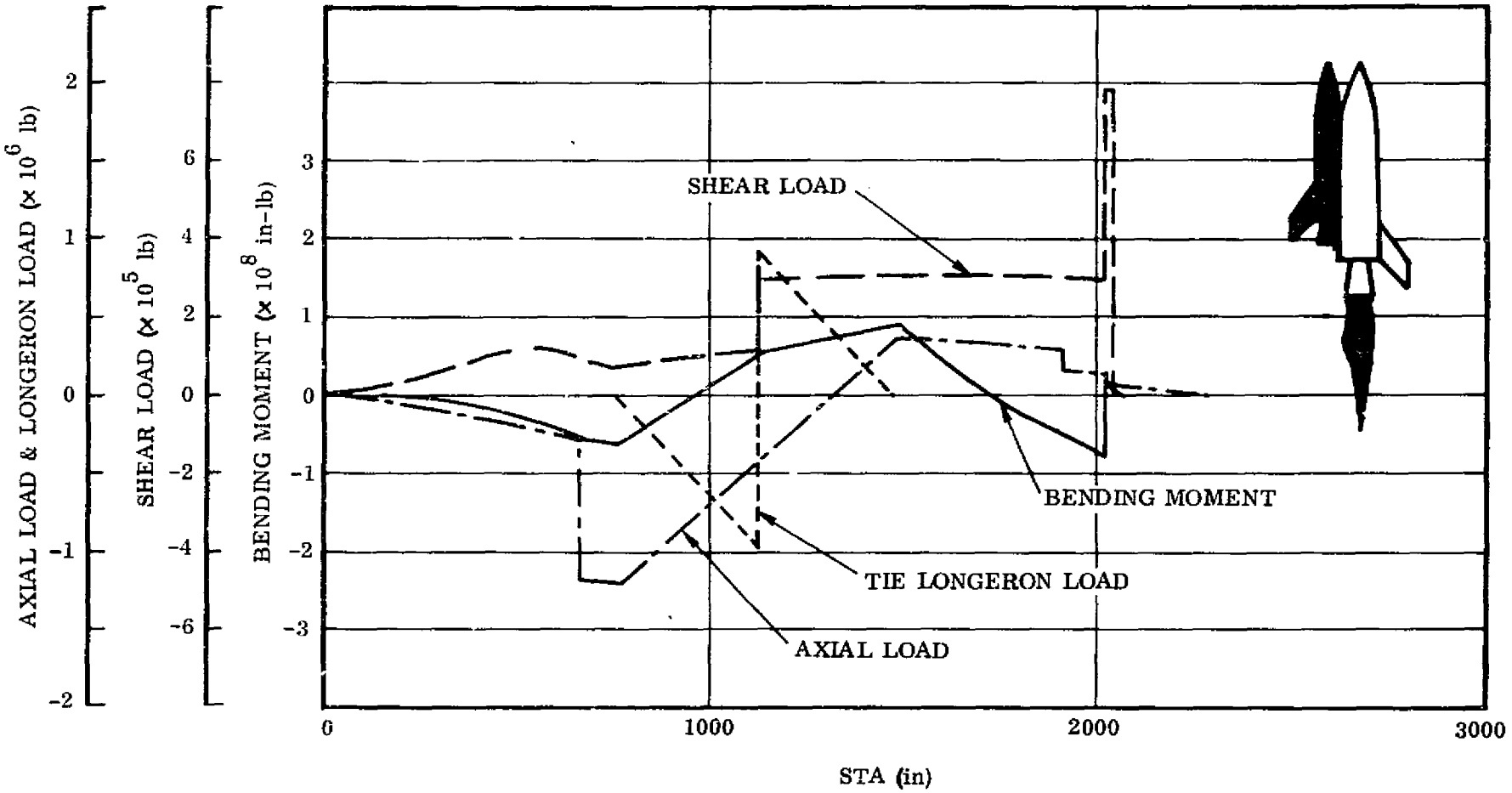

Figure 3-14. Two-Element (Nose-to-Nose) Sequential Burn 50K Lb Payload Orbiter at Max α q

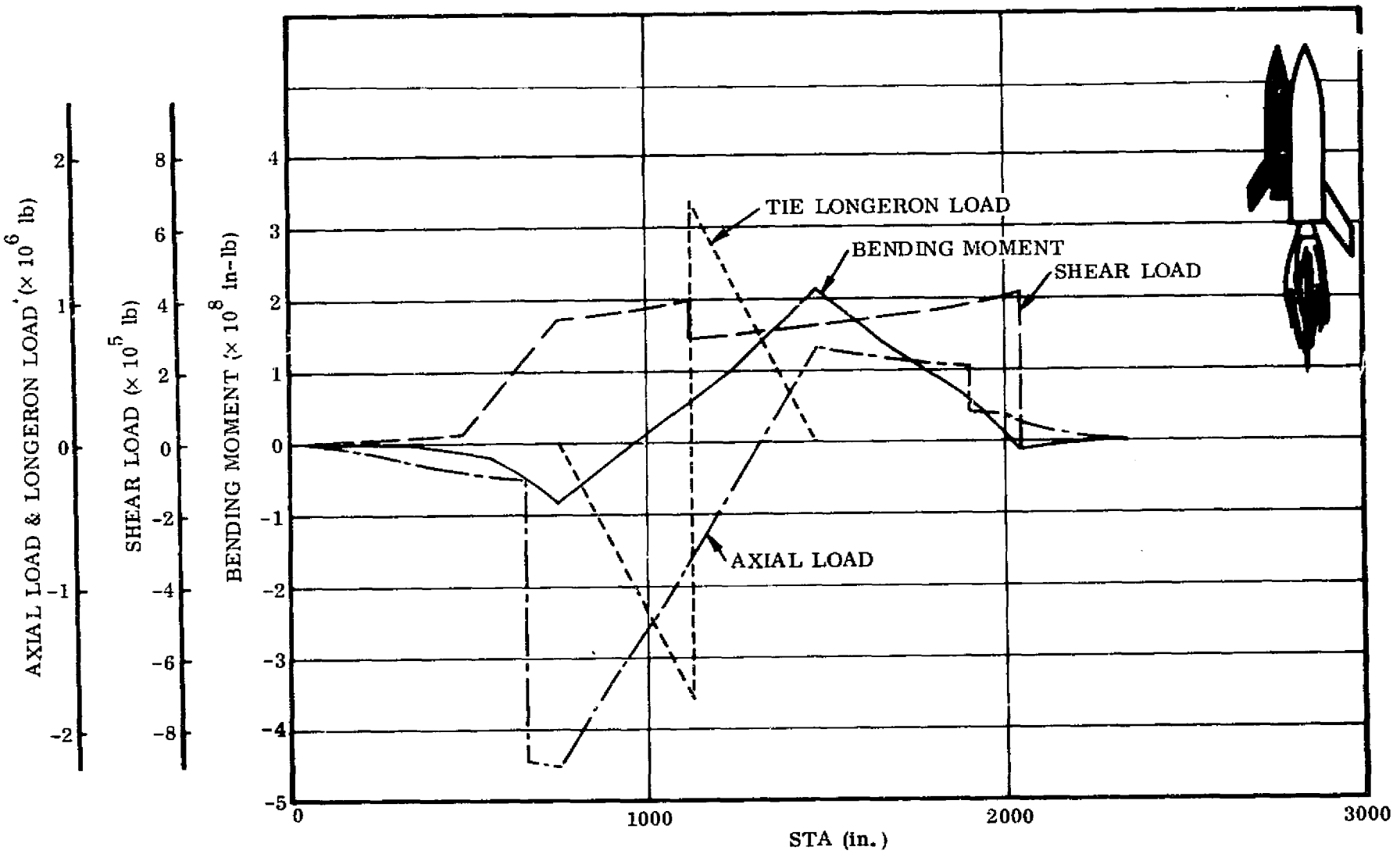

Figure 3-15. Two-Element (Nose-to-Nose) Sequential Burn 50K Lb Payload Orbiter at Booster Burnout (N_x = 4g)

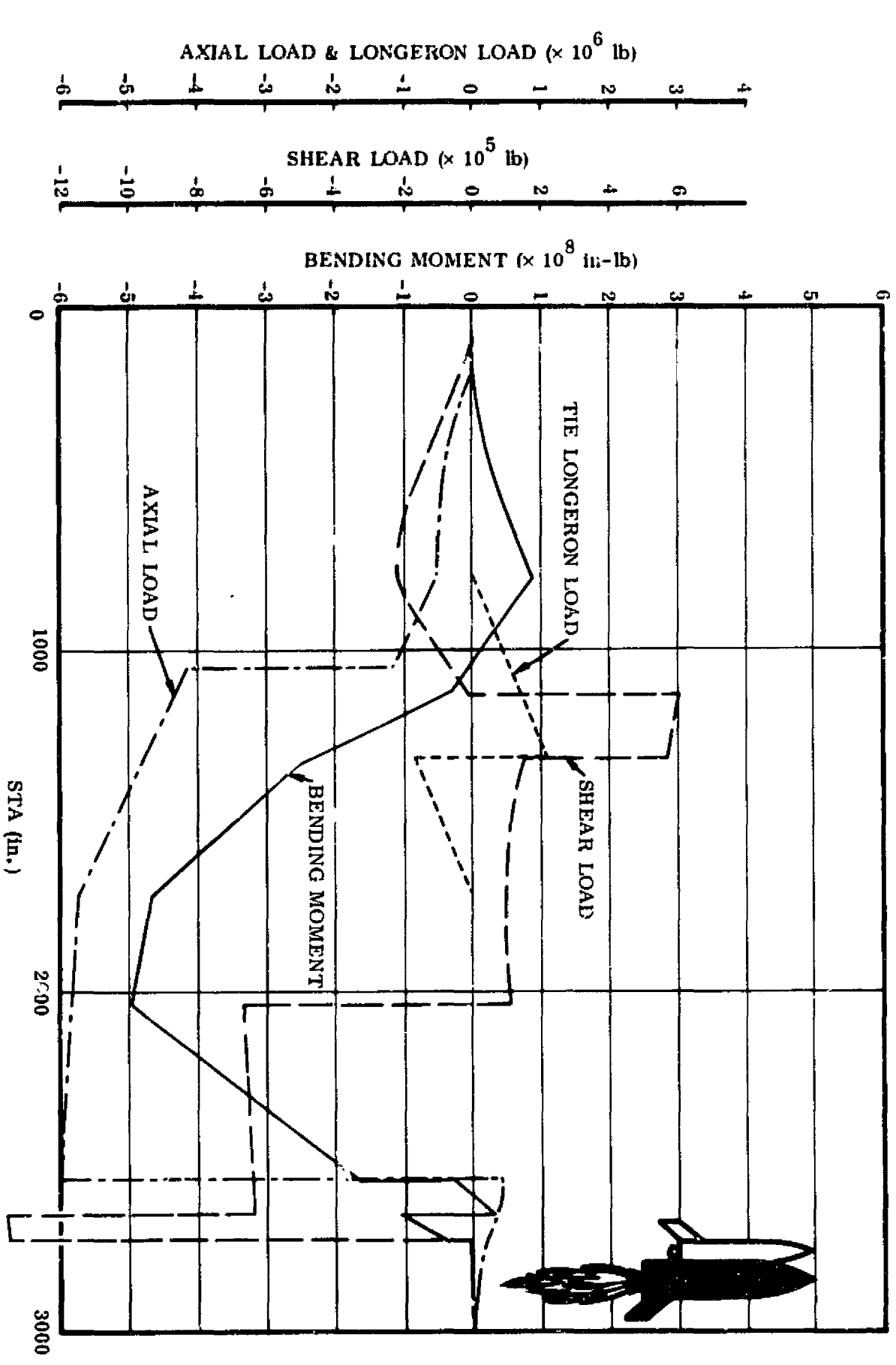

Figure 3-16. Two-Element (Nose-to-Nose) Sequential Burn 50K Lb Payload Booster at Max αq

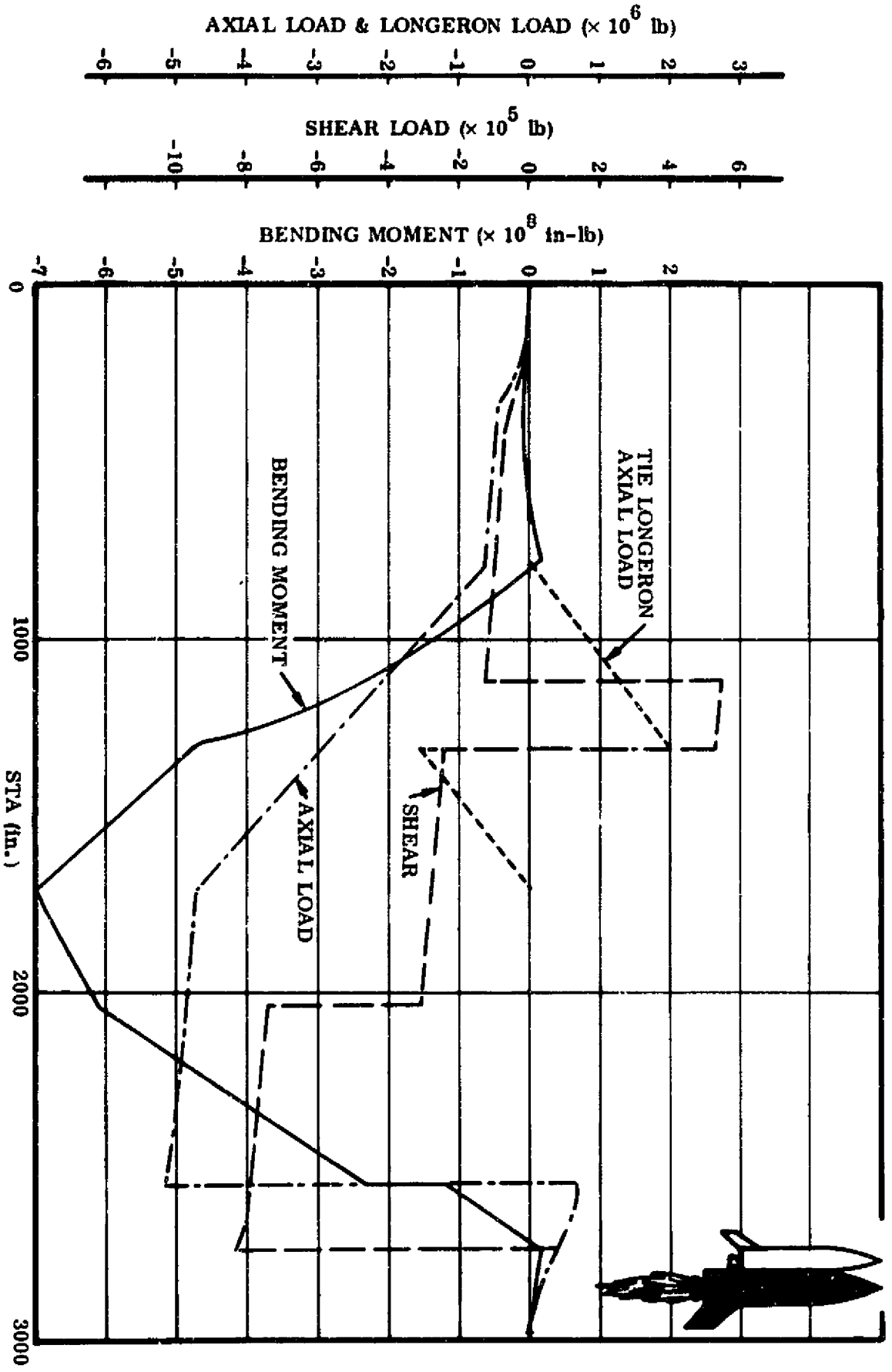

Figure 3-17. Two-Element (Nose-to-Nose) Sequential Burn 50K Lb Payload Booster at Booster Burnout (N_x = 4g)

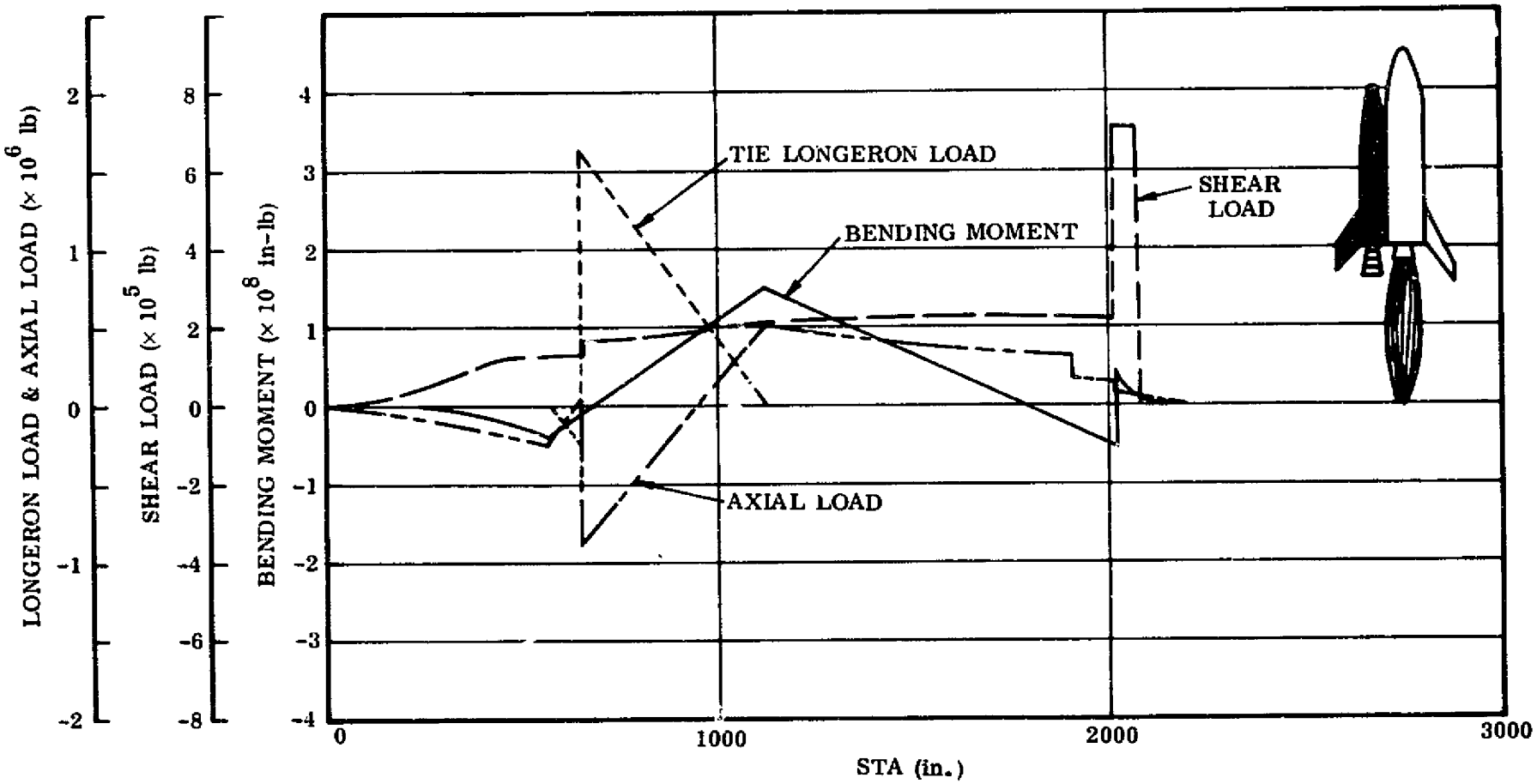

Figure 3-18. Two-Element (Tail-to-Tail) Sequential Burn 50K L[illegible] Payload Orbiter at Max α q

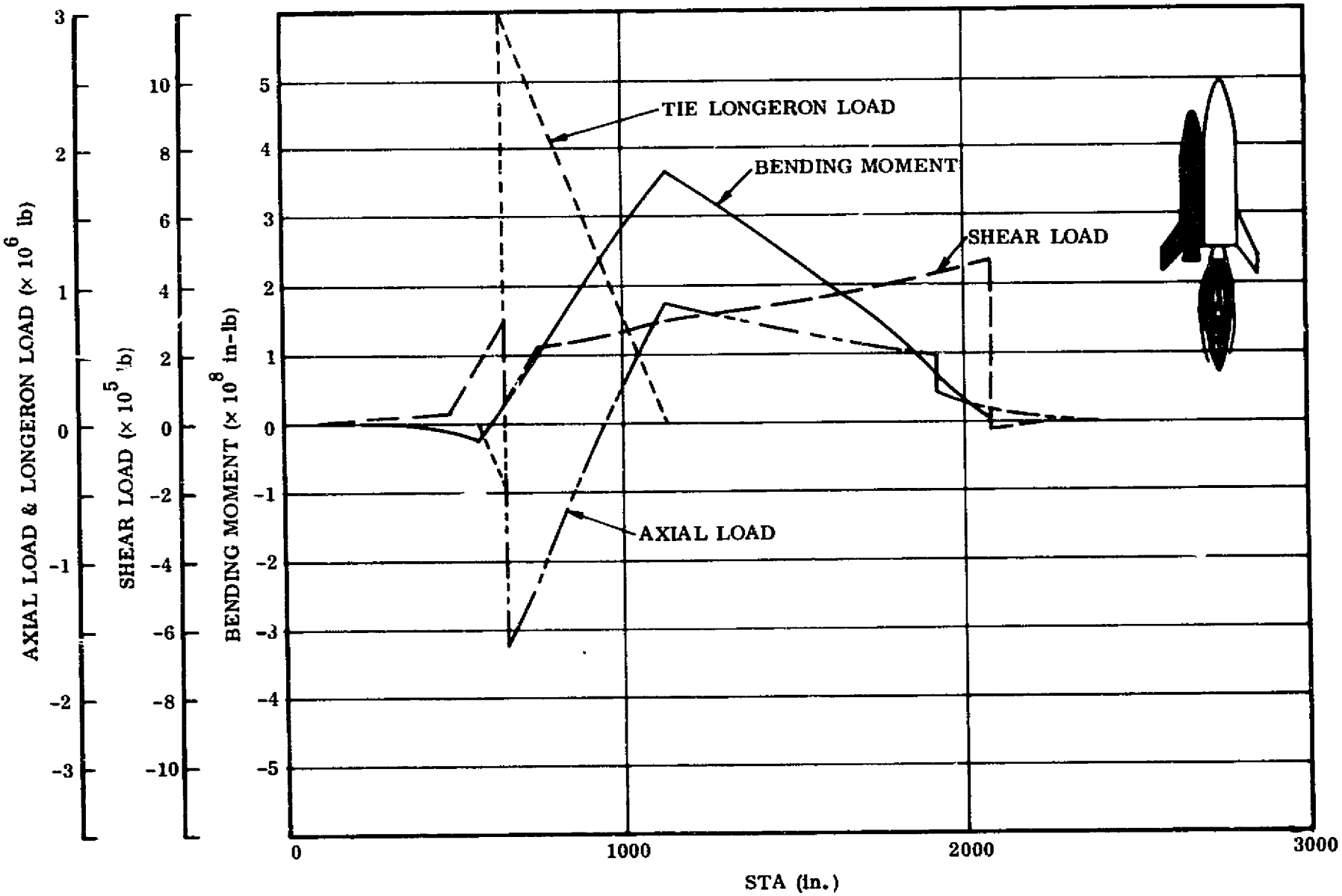

Figure 3-19. Two-Element (Tail-to-Tail) Sequential Burn 50K Lb Payload Orbiter at Booster Burnout (N_x = 4g)

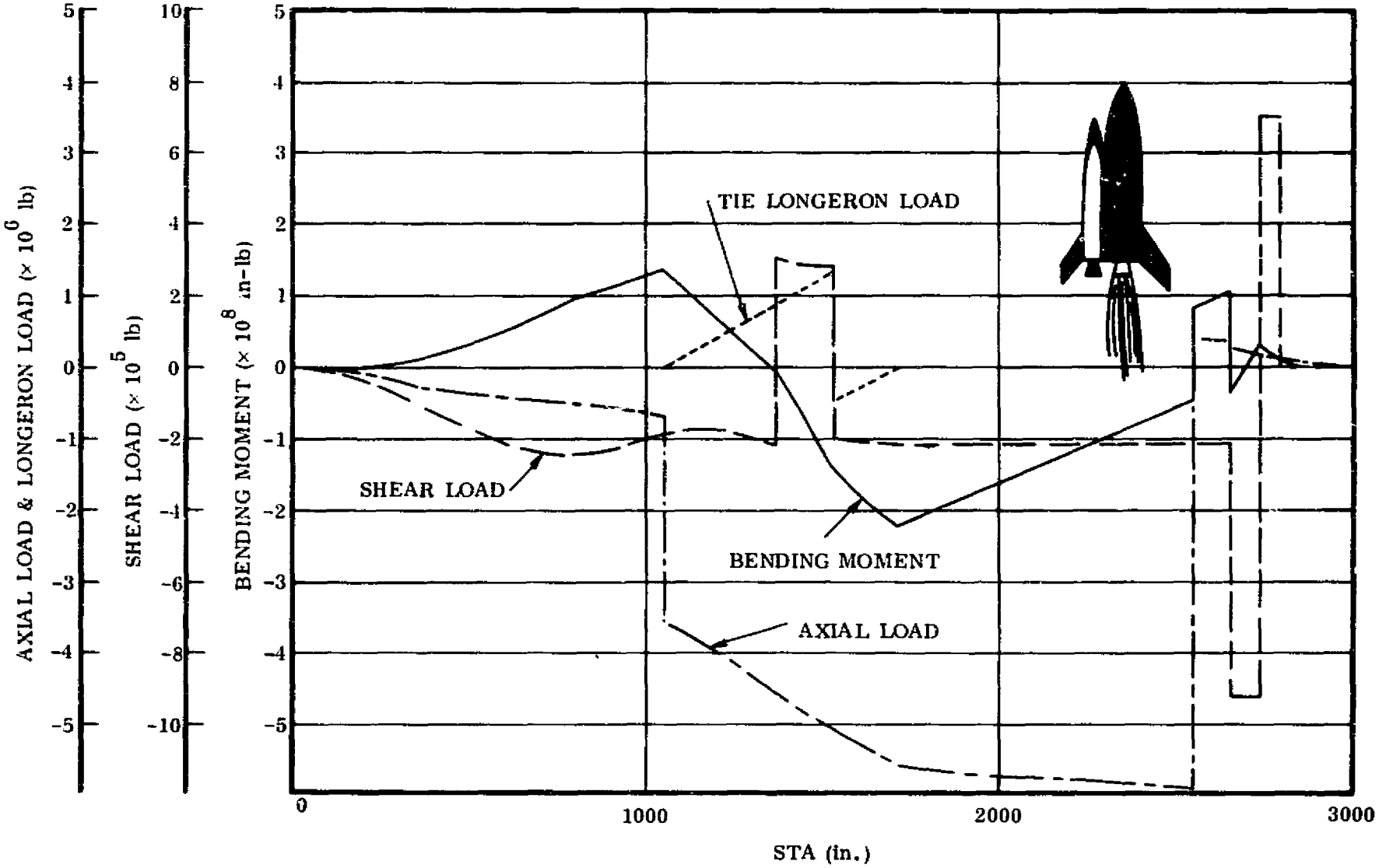

Figure 3-20. Two-Element (Tail-to-Tail) Sequential Burn 50K Lb Payload Booster at Max α q

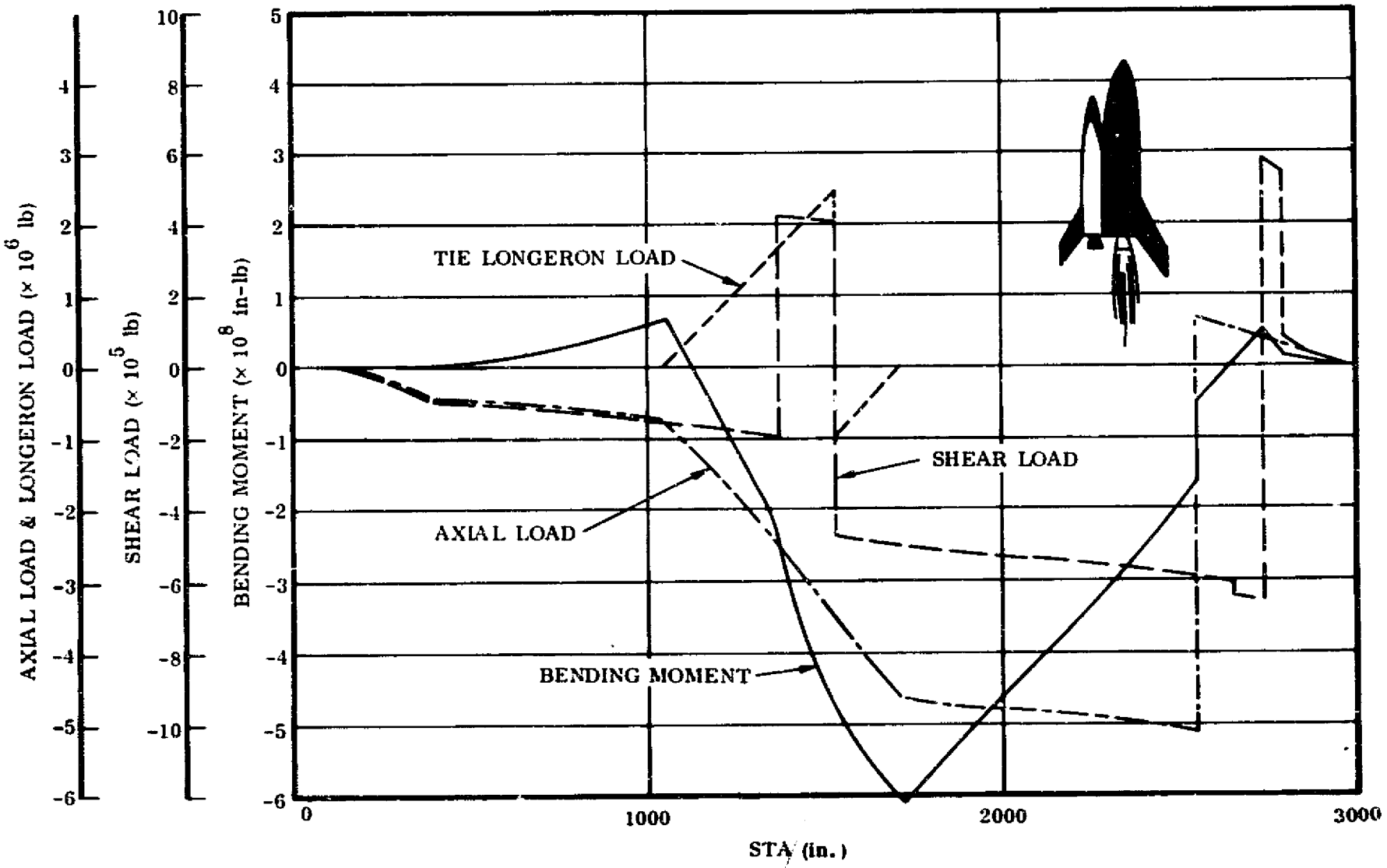

Figure 3-21. Two-Element (Tail-to-Tail) Sequential Burn 50K Lb Payload Booster at Booster Burnout (N_x = 4g)

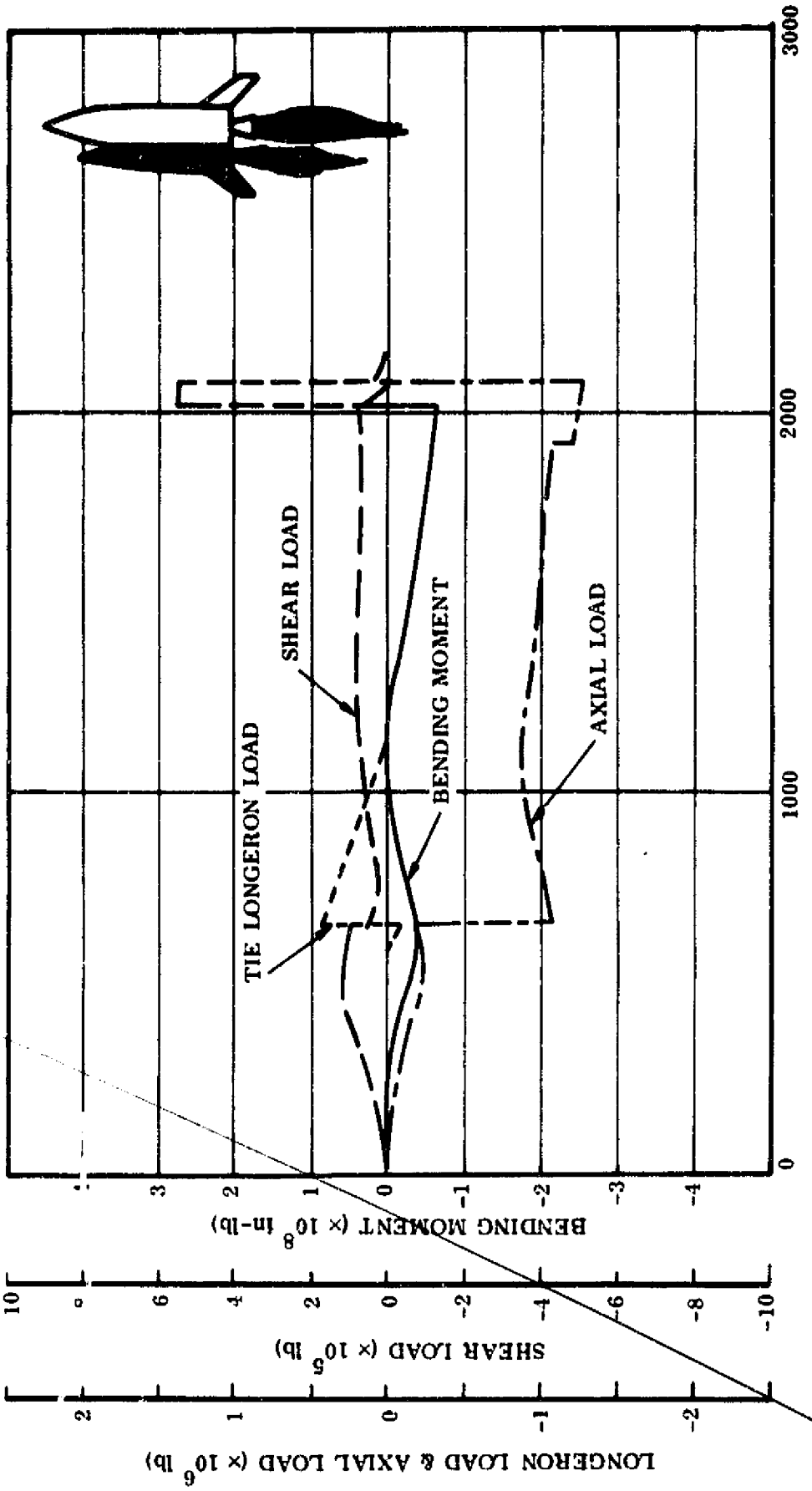

Figure 3-22. Two-Element Simultaneous Burn 50K Lb Payload Orbiter at Max αq

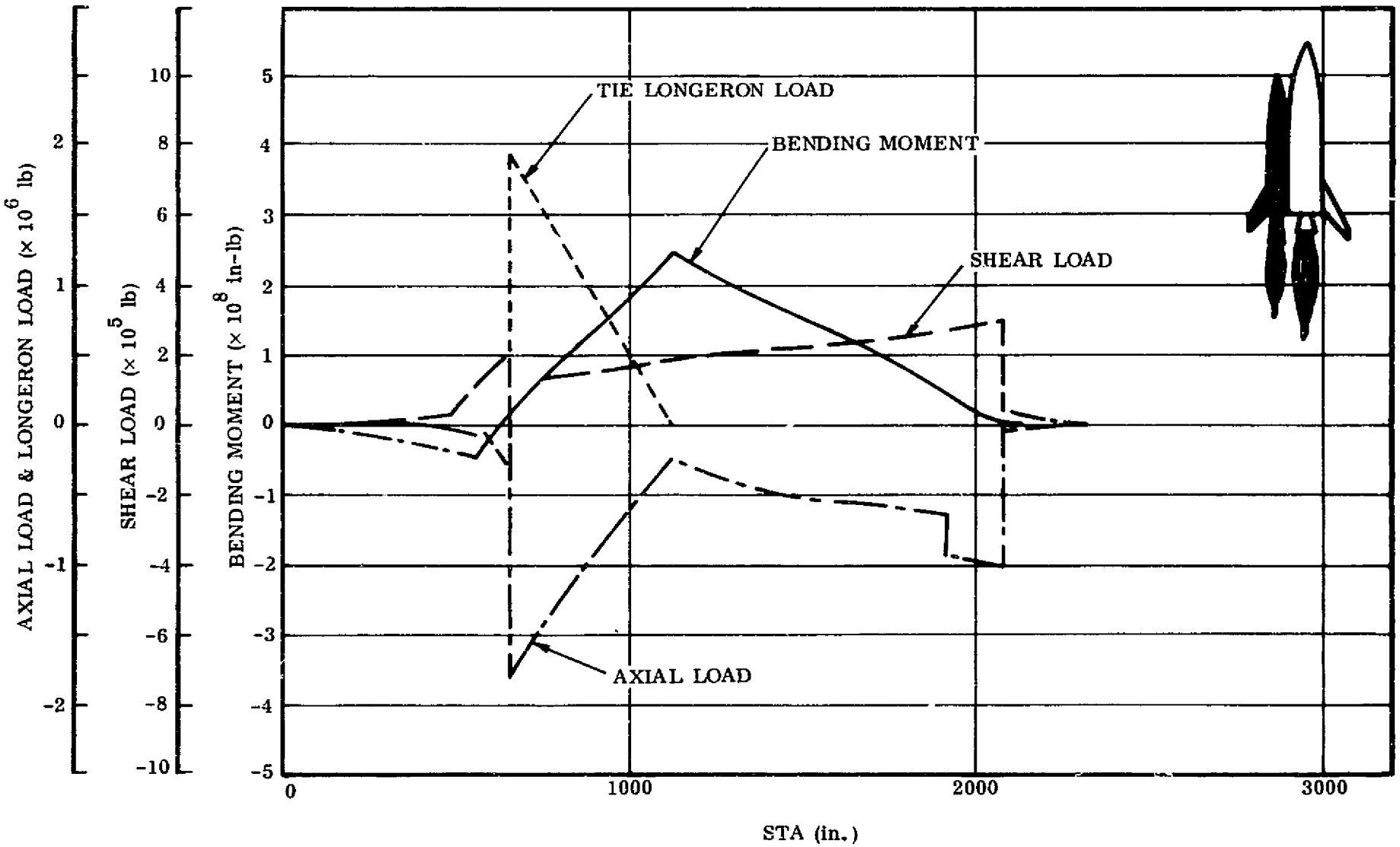

Figure 3-23. Two-Element Simultaneous Burn 50K Lb Payload Orbiter at Booster Burnout (N_x = 4g)

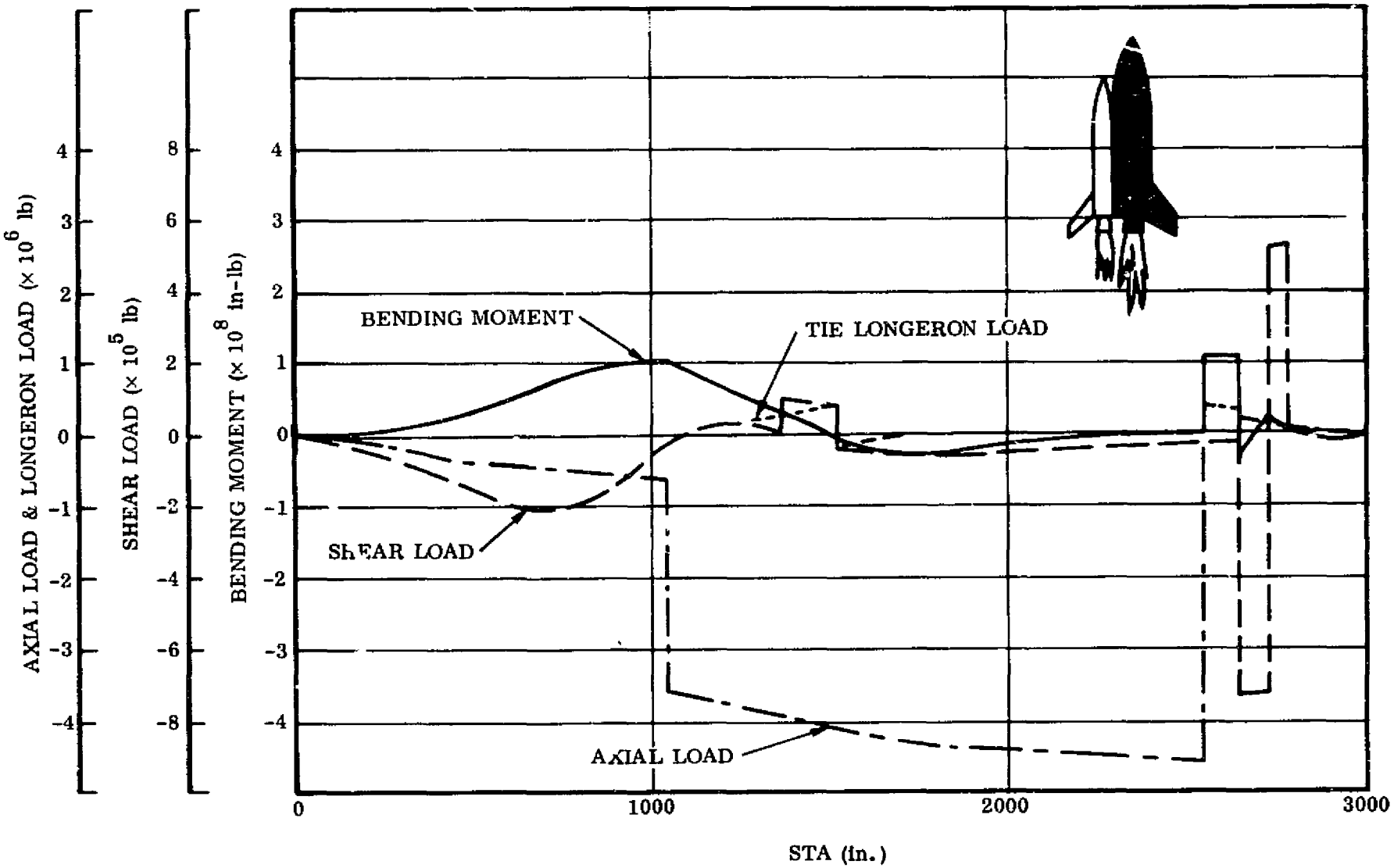

Figure 3-24. Two-Element Simultaneous Burn 50K Lb Payload Booster at Max α q

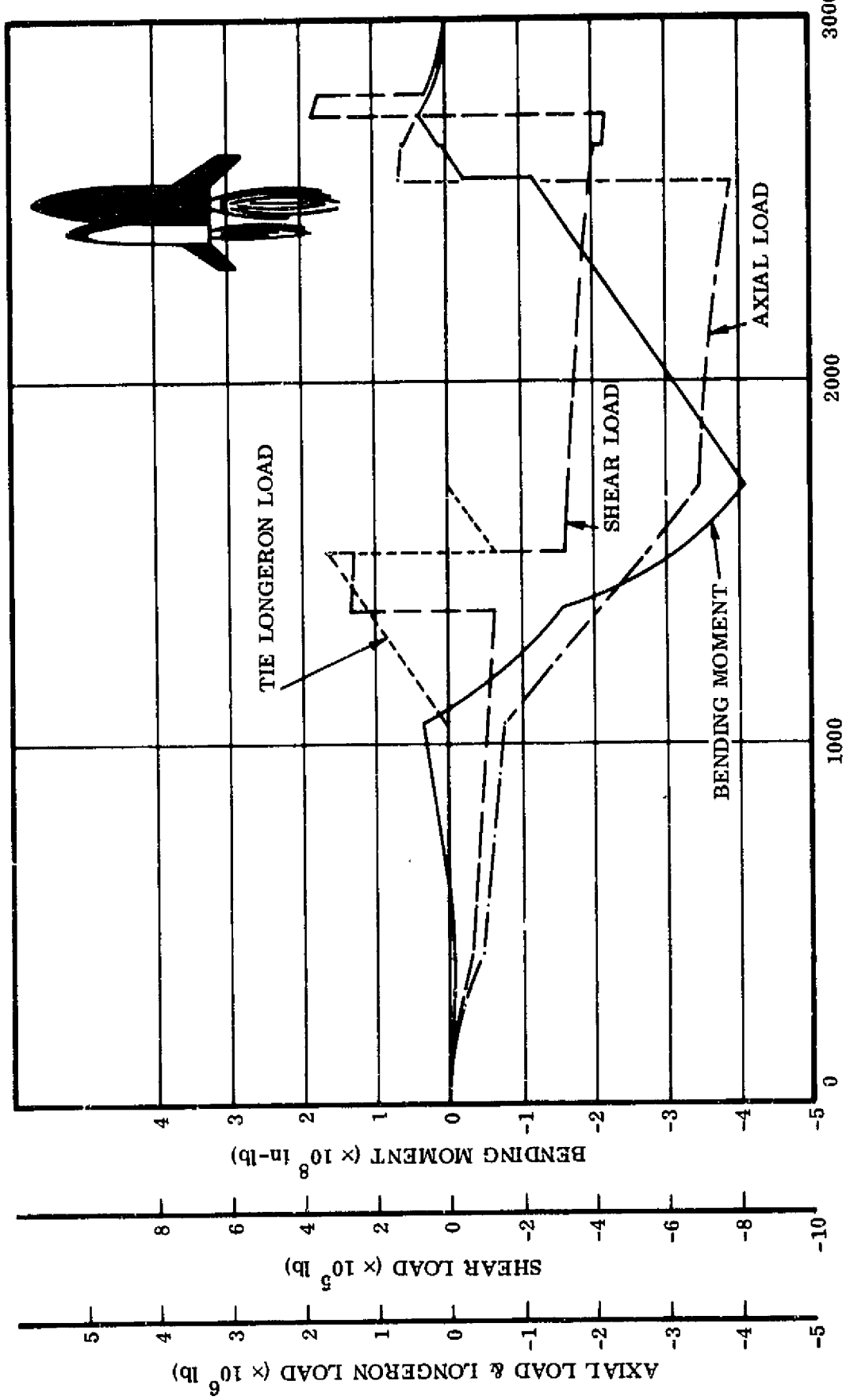

Figure 3-25. Two-Element Simultaneous Burn 50K Lb Payload Booster at Booster Burnout (N_x = 4g)

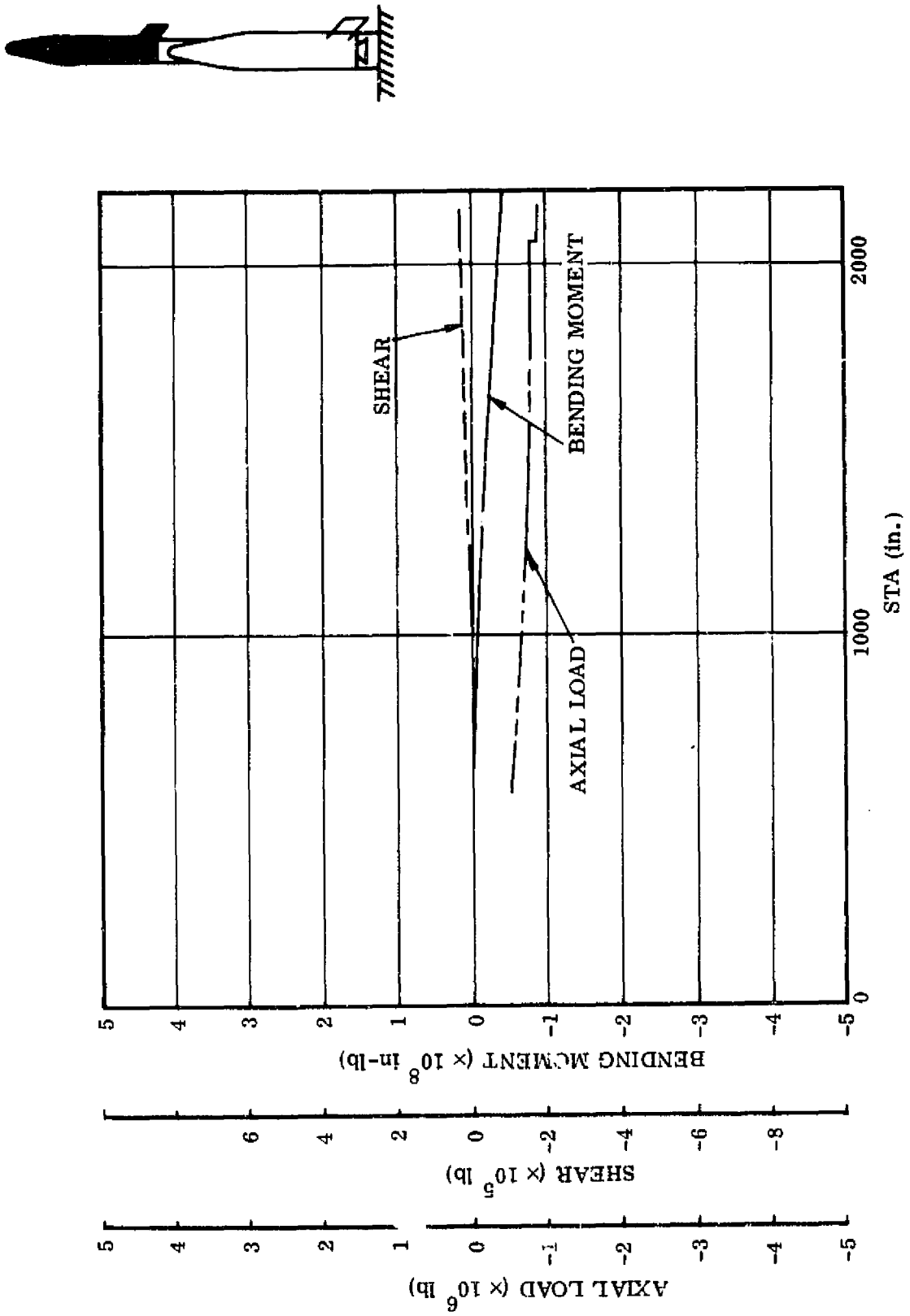

Figure 3-26. Two-Element Tandem 50K Lb Payload Orbiter Ground Wind Effects

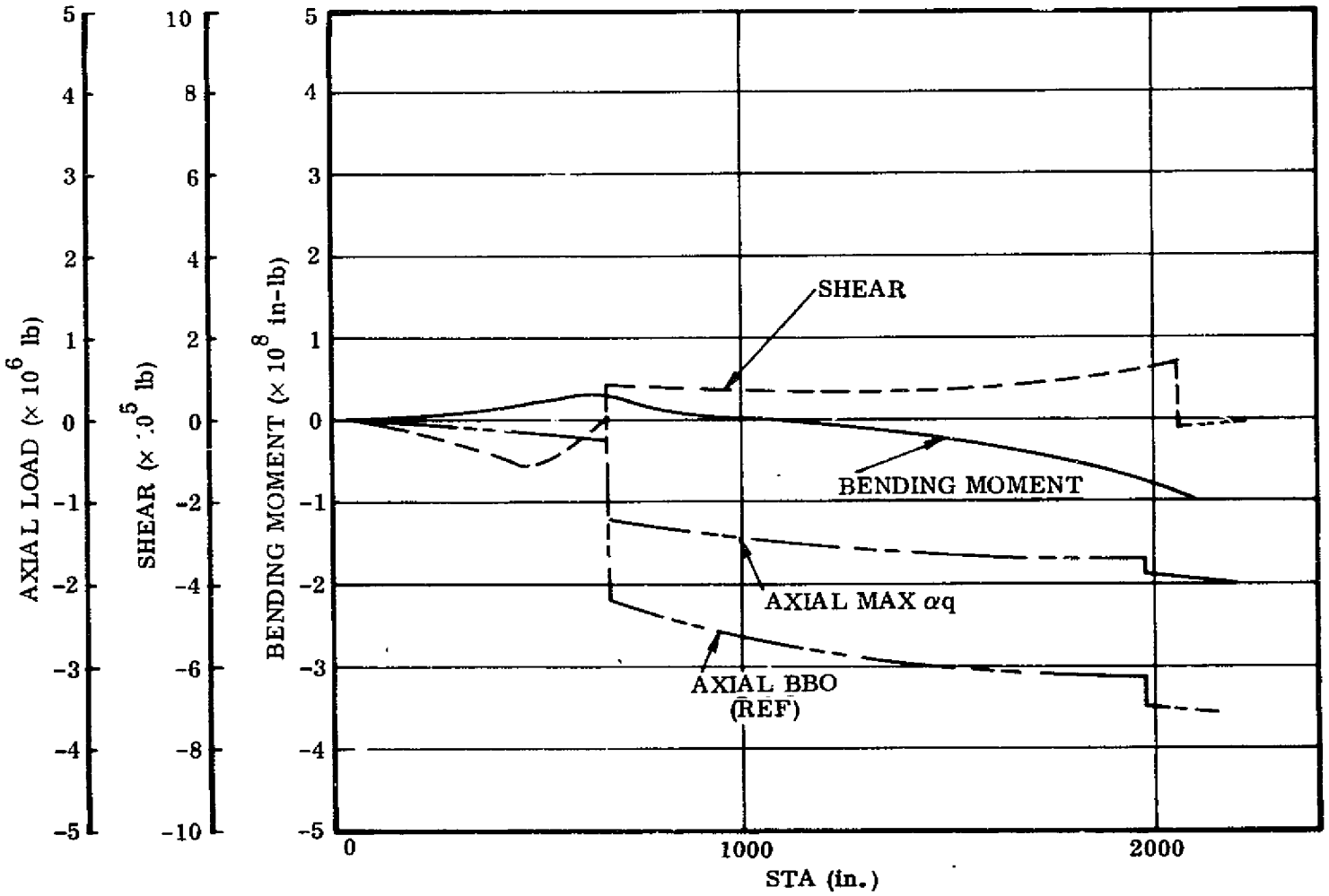

Figure 3-27. Two-Element Tandem 50K Lb Payload Orbiter at Max αq (Booster Burnout)

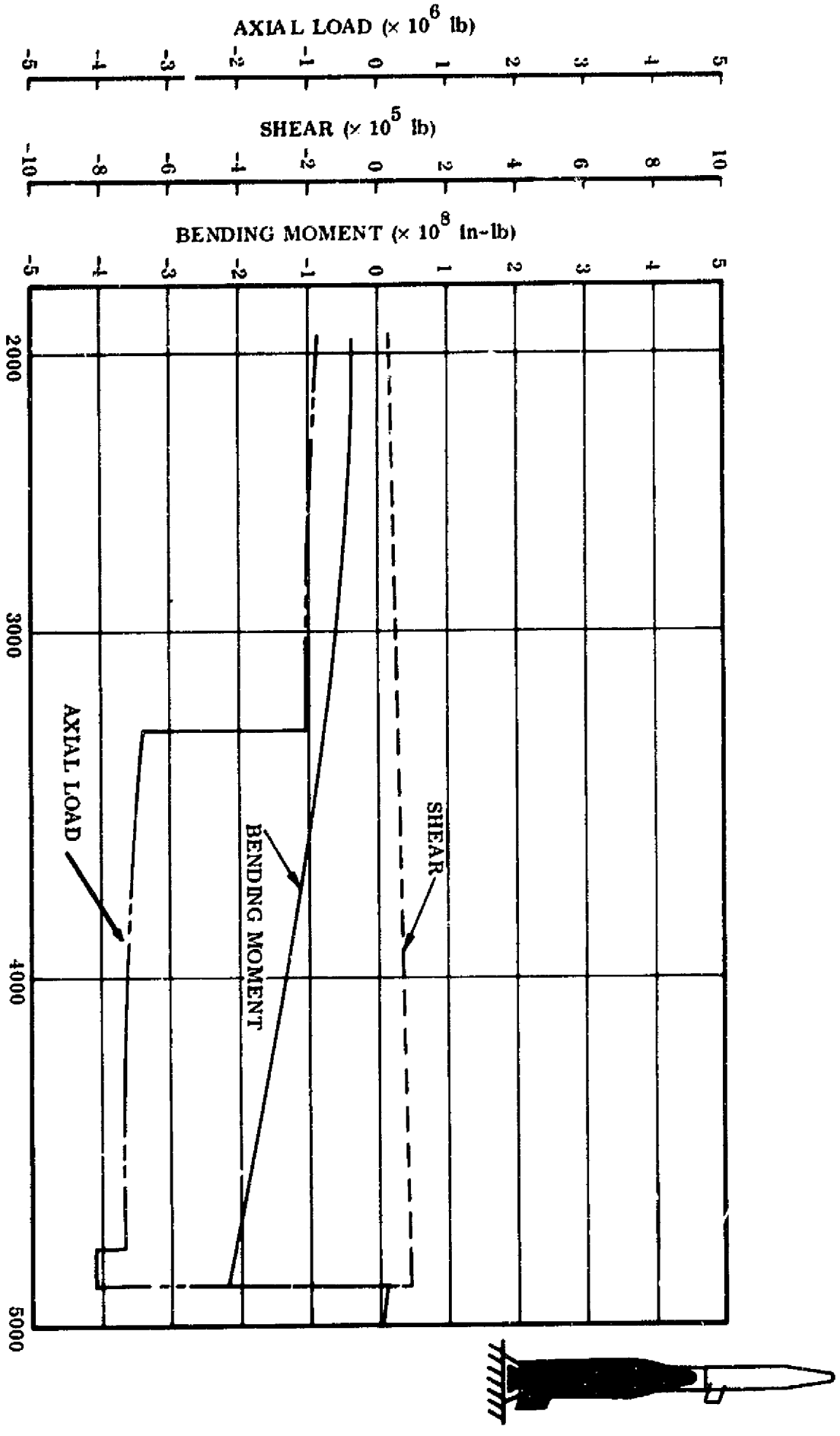

Figure 3-28 . Two-Element Tandem 50K Lb Payload Booster Ground Wind Effects

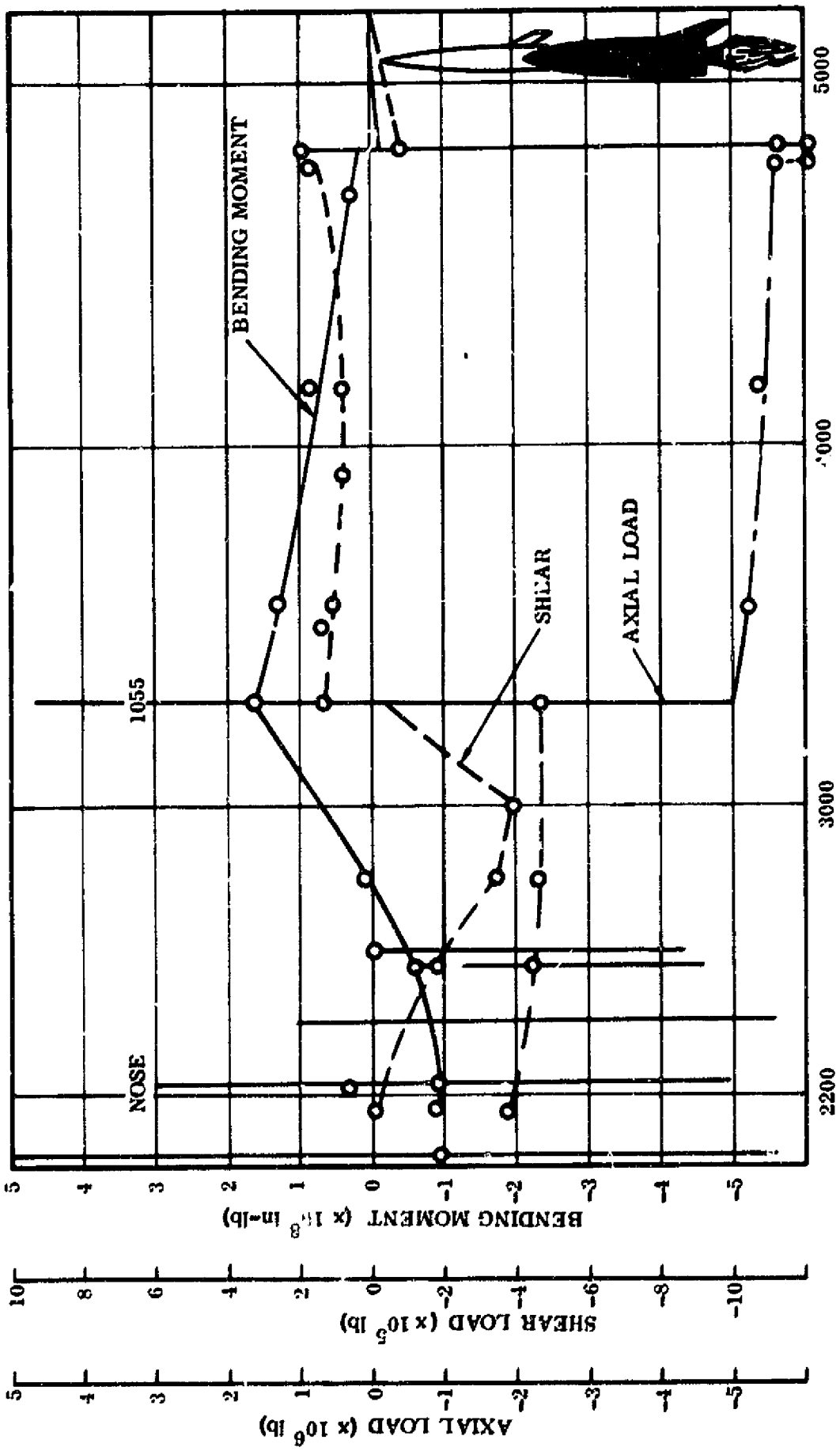

Figure 3-29. Two-Element Tandem 50K Lb Payload Booster at Max αq

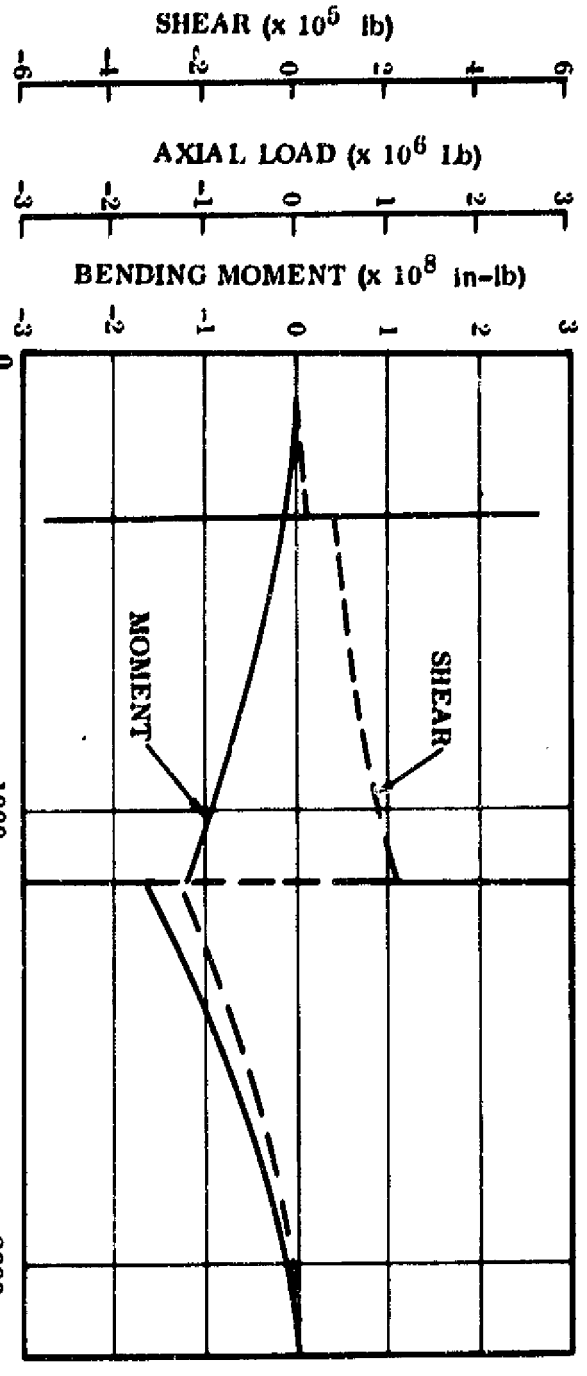

Figure 3-30. Two-Element 50K Lb Payload Orbiter at Subsonic Gust

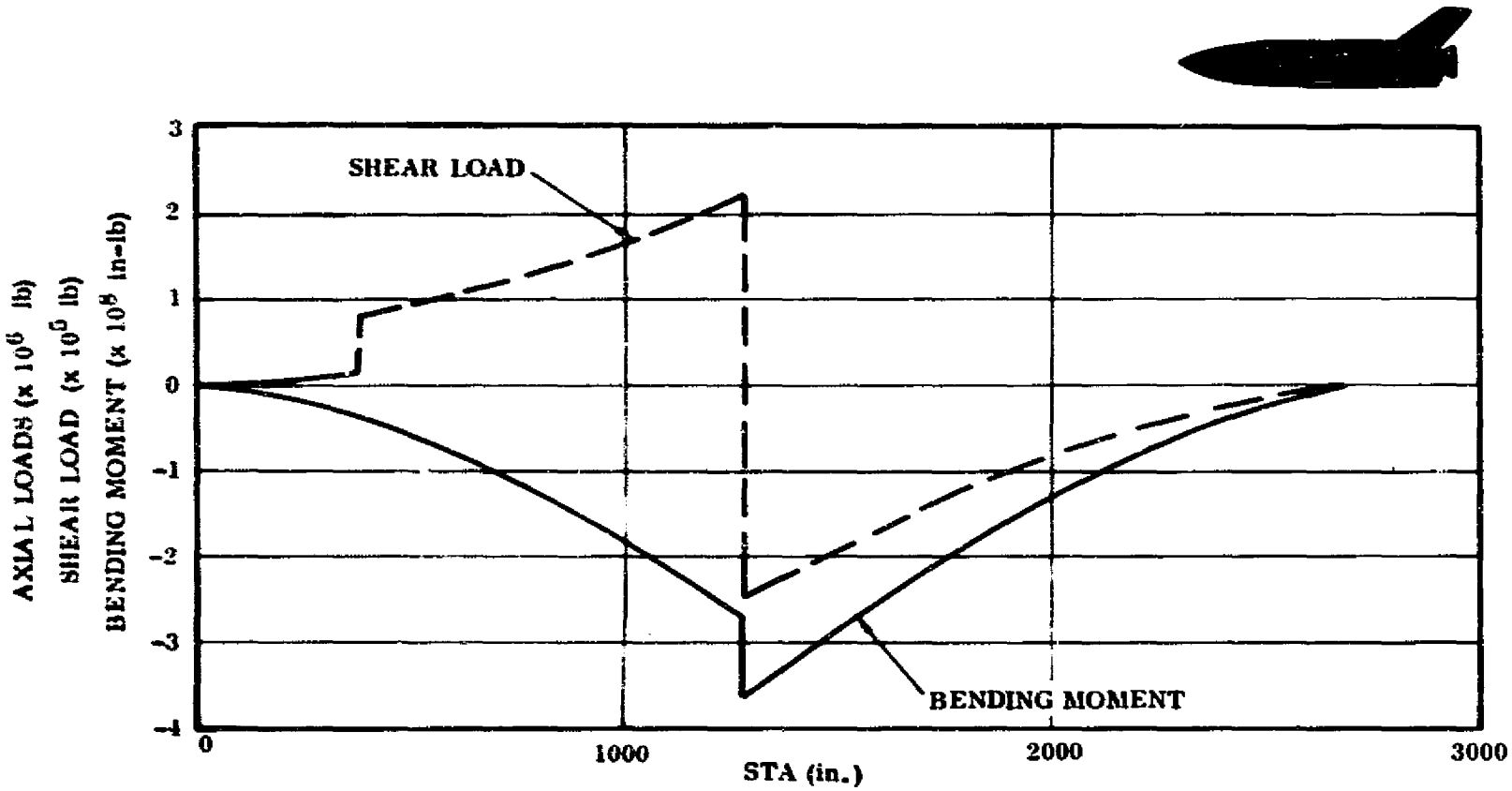

Figure 3-31. Two-Element 50K Lb Payload Booster at Subsonic Gust

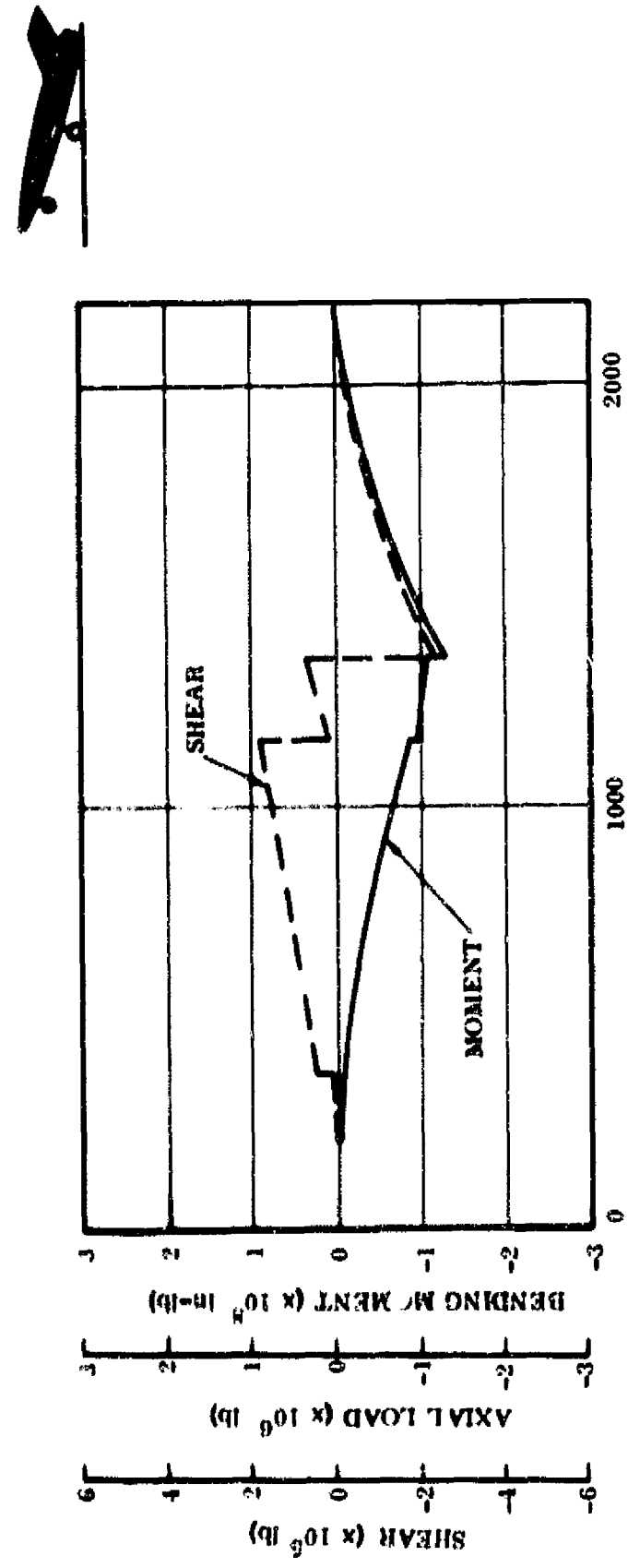

Figure 3-32. Two-Element 50K Lb Payload Orbiter Two-Point Landing

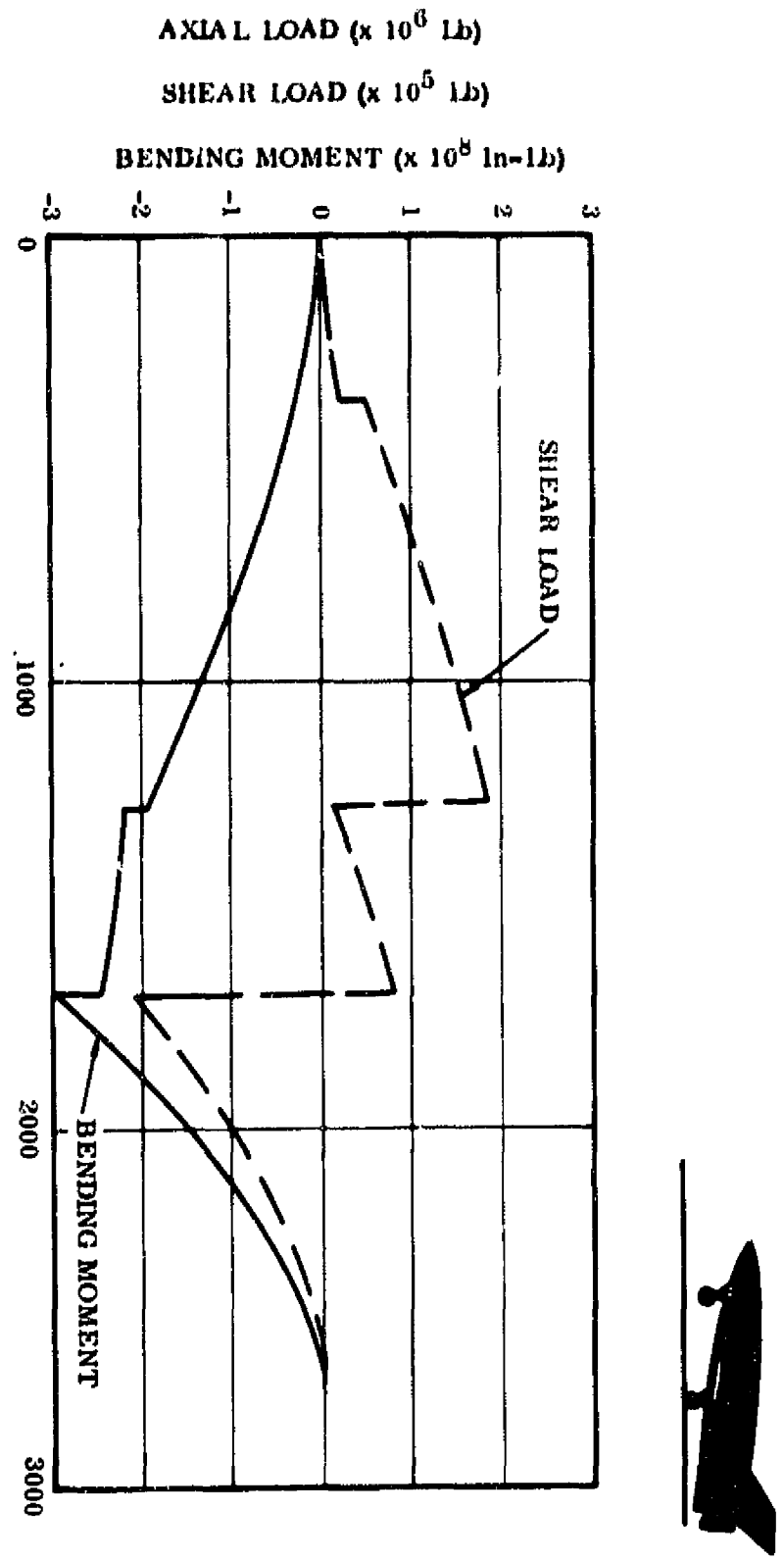

Figure 3-33. Two-Element 50K Lb Payload Booster Two-Point Landing

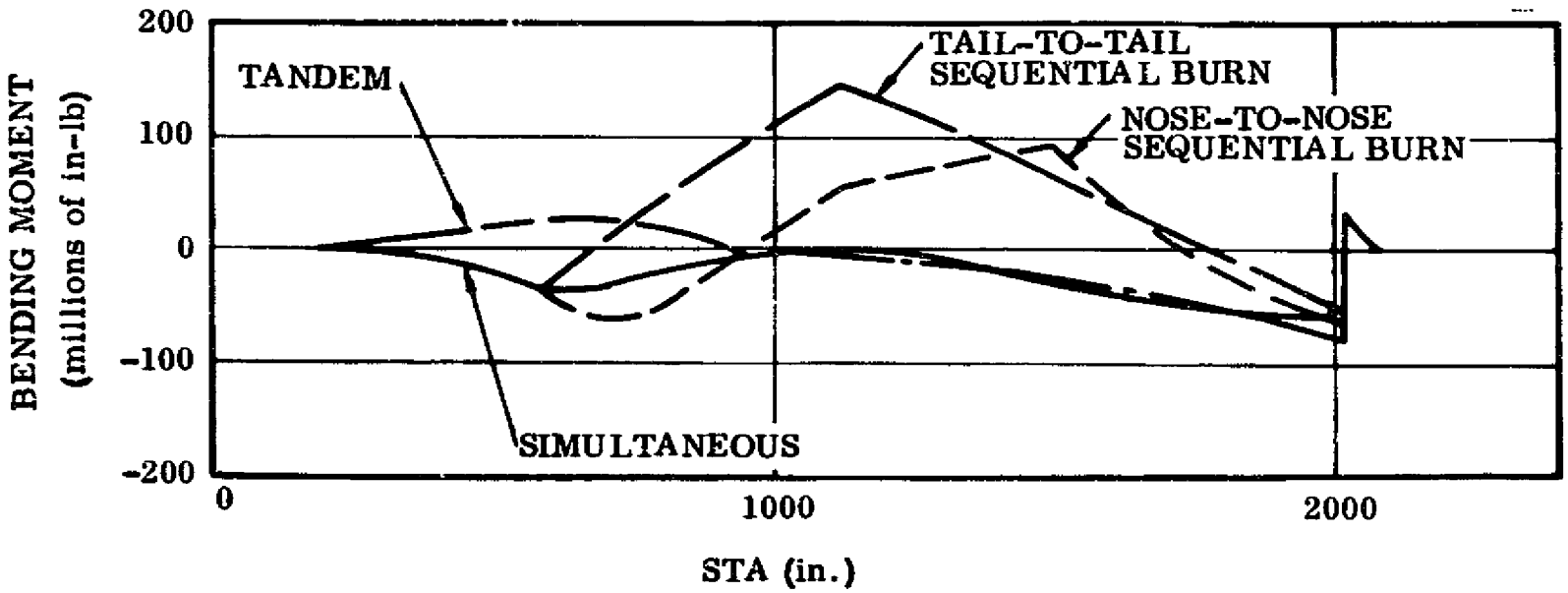

Figure 3-34. Two-Element Orbiter Bending Moments at Max αq

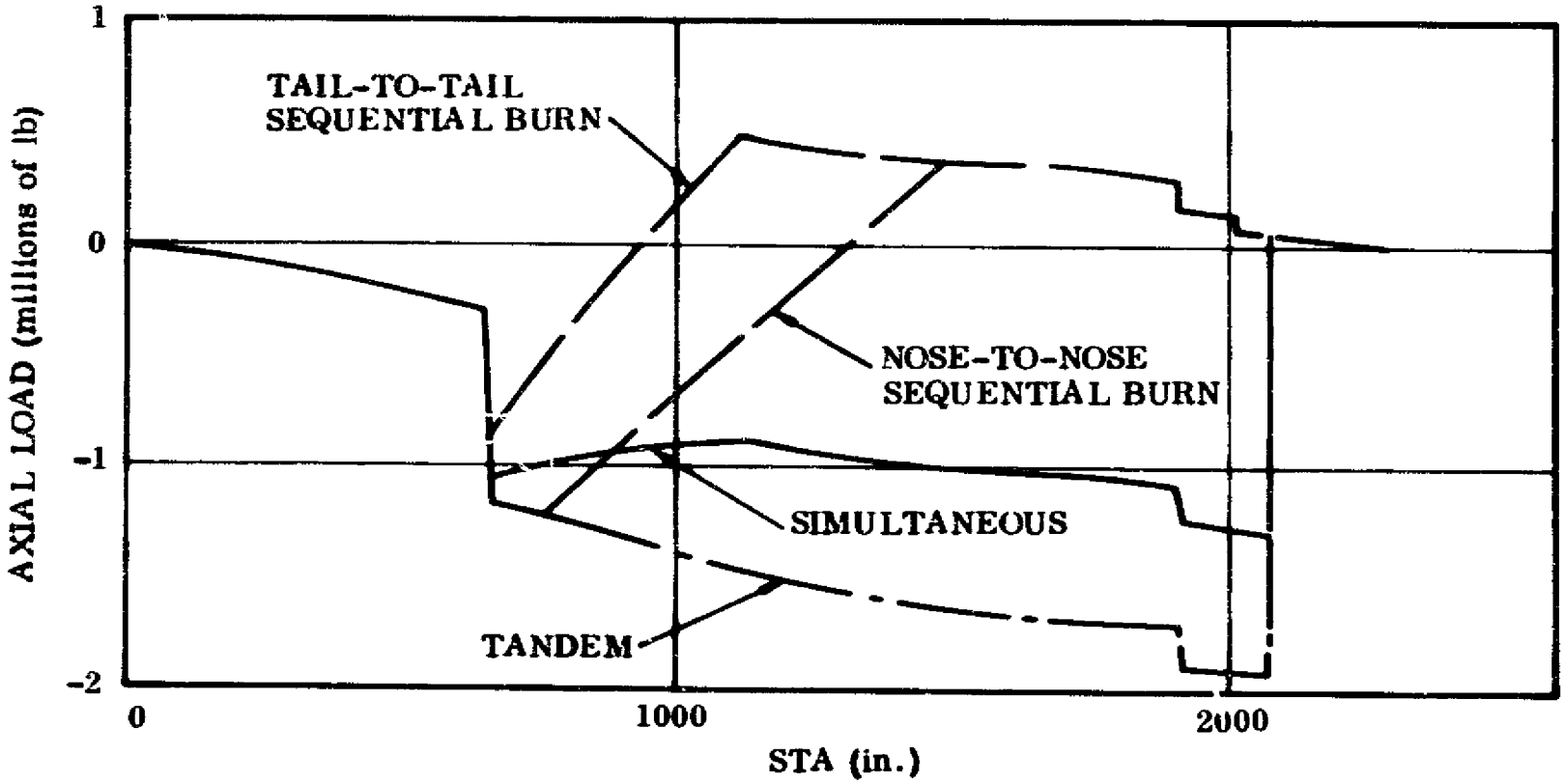

Figure 3-35. Two-Element Orbiter Axial Loads at Max αq

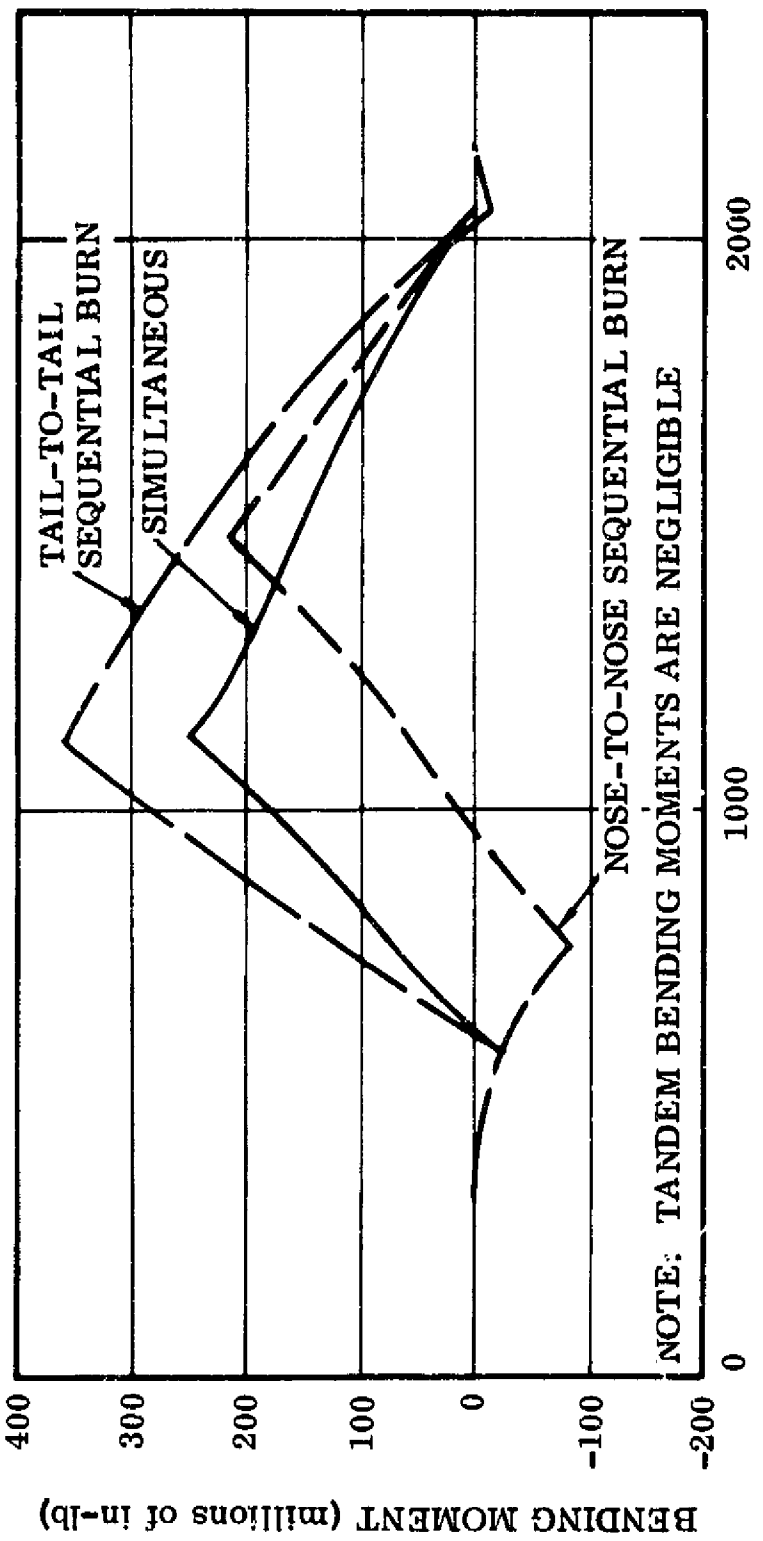

Figure 3-36. Two-Element Orbiter Bending Moments at 4g Booster Burnout

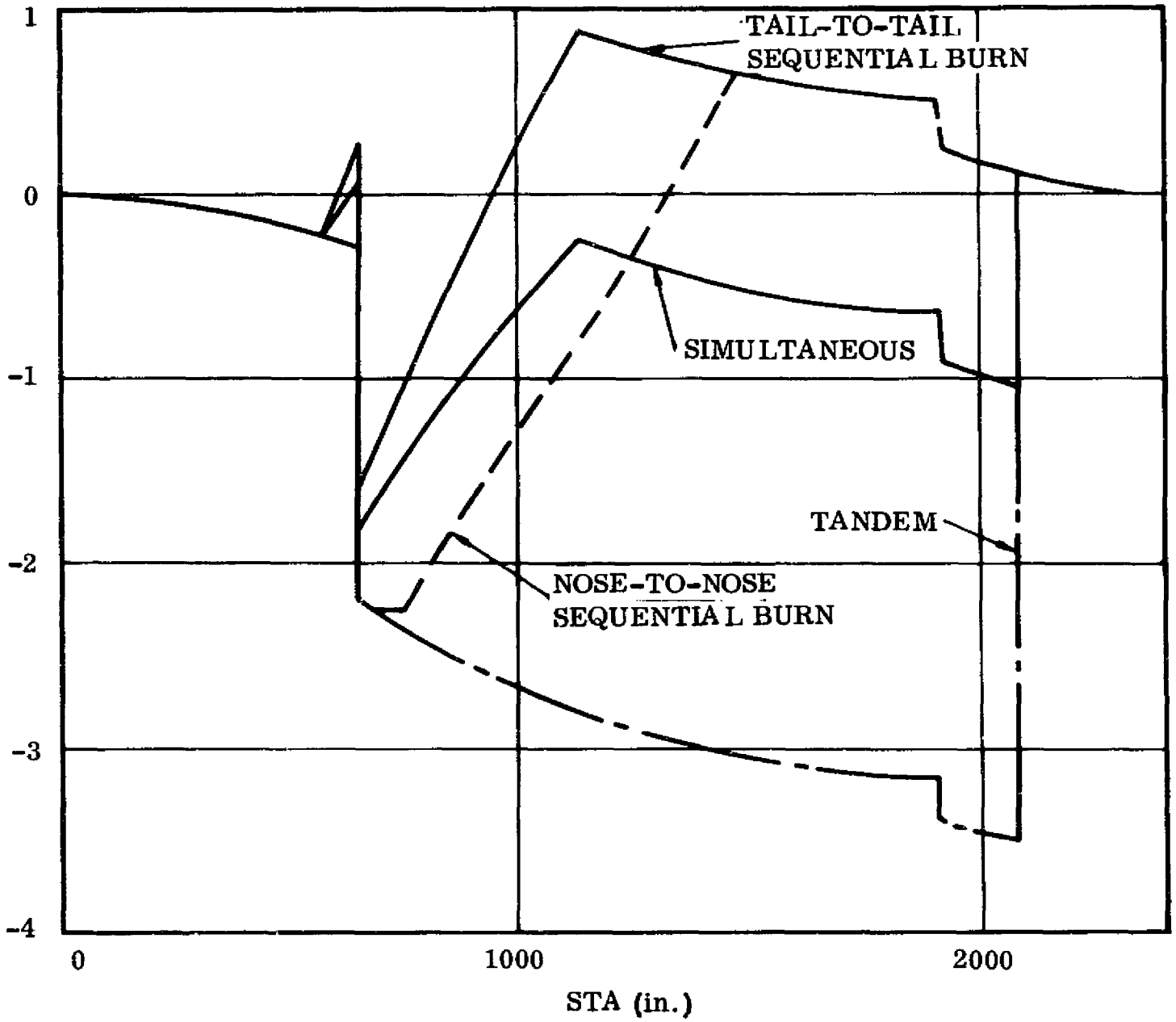

Figure 3-37. Two-Element Orbiter Axial Loads at 4g Booster Burnout

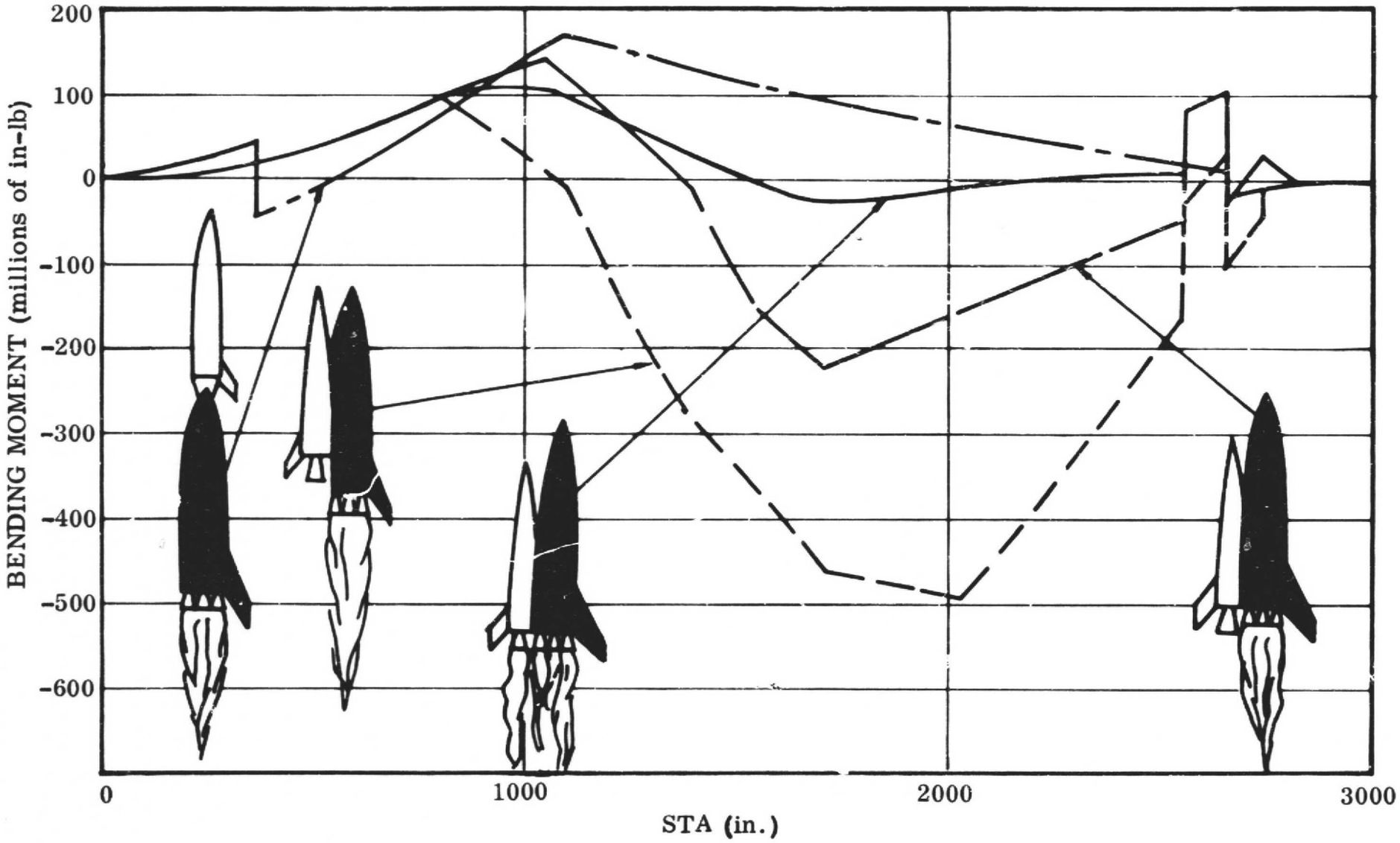

Figure 3-38. Two-Element Booster Bending Moments at Max αq

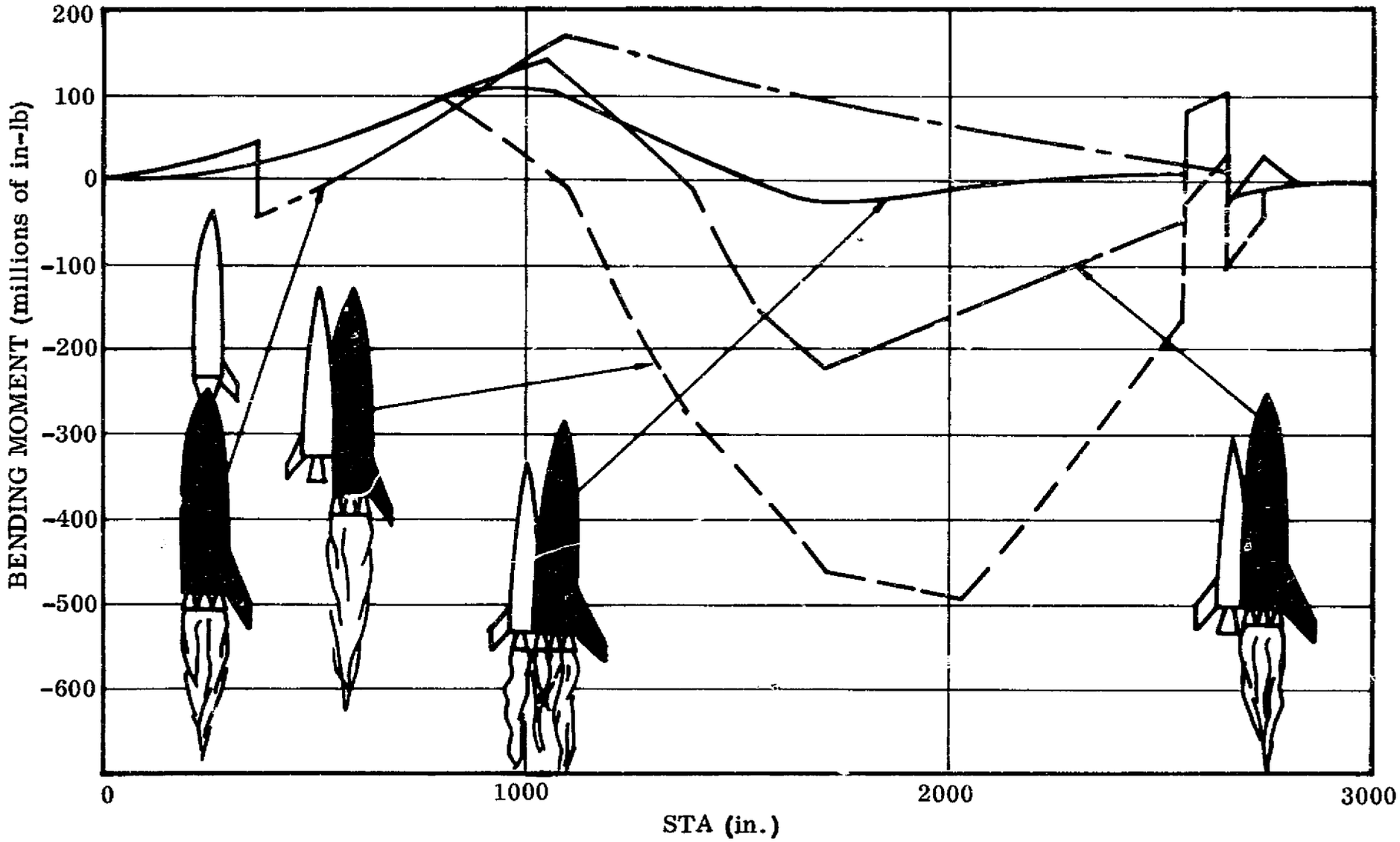

Figure 3-38. Two-Element Booster Bending Moments at Max αq

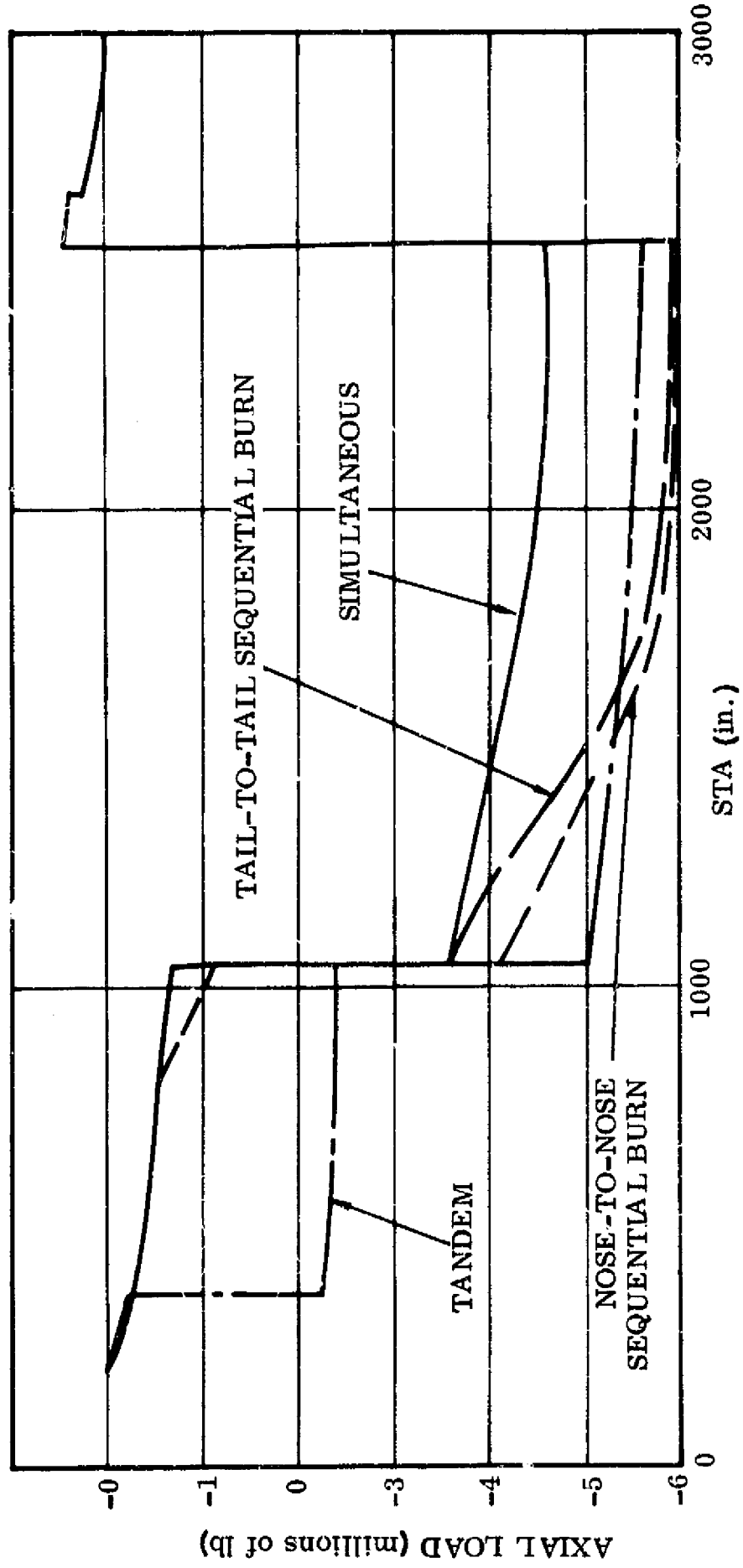

Figure 3-39. Two-Element Booster Axial Loads at Max $\bar{q}$

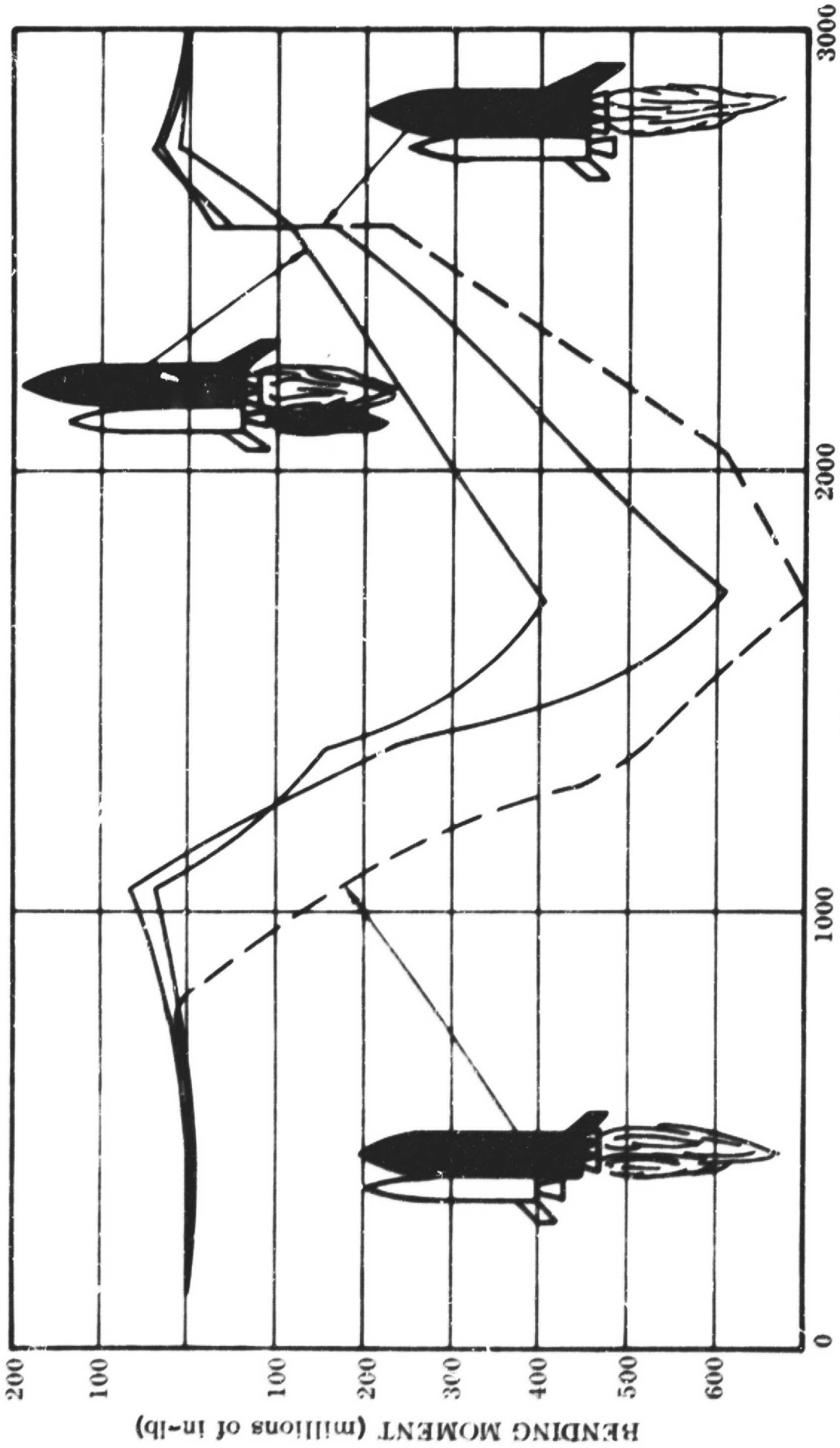

Figure 3-40. Two-Element Booster Bending Moments at 4g Booster Burnout

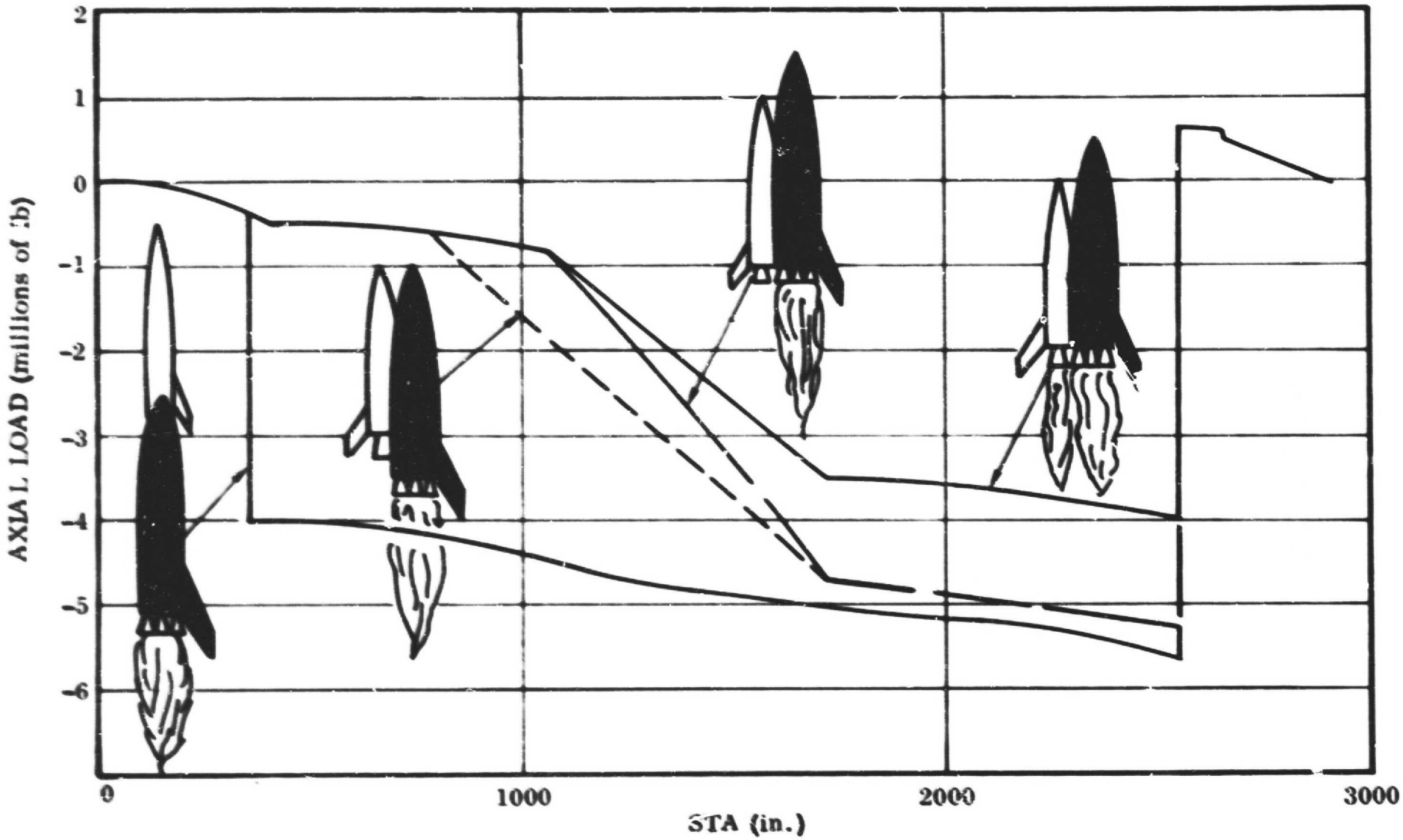

Figure 3-41. Two-Element Booster Axial Loads at 4g Booster Burnout

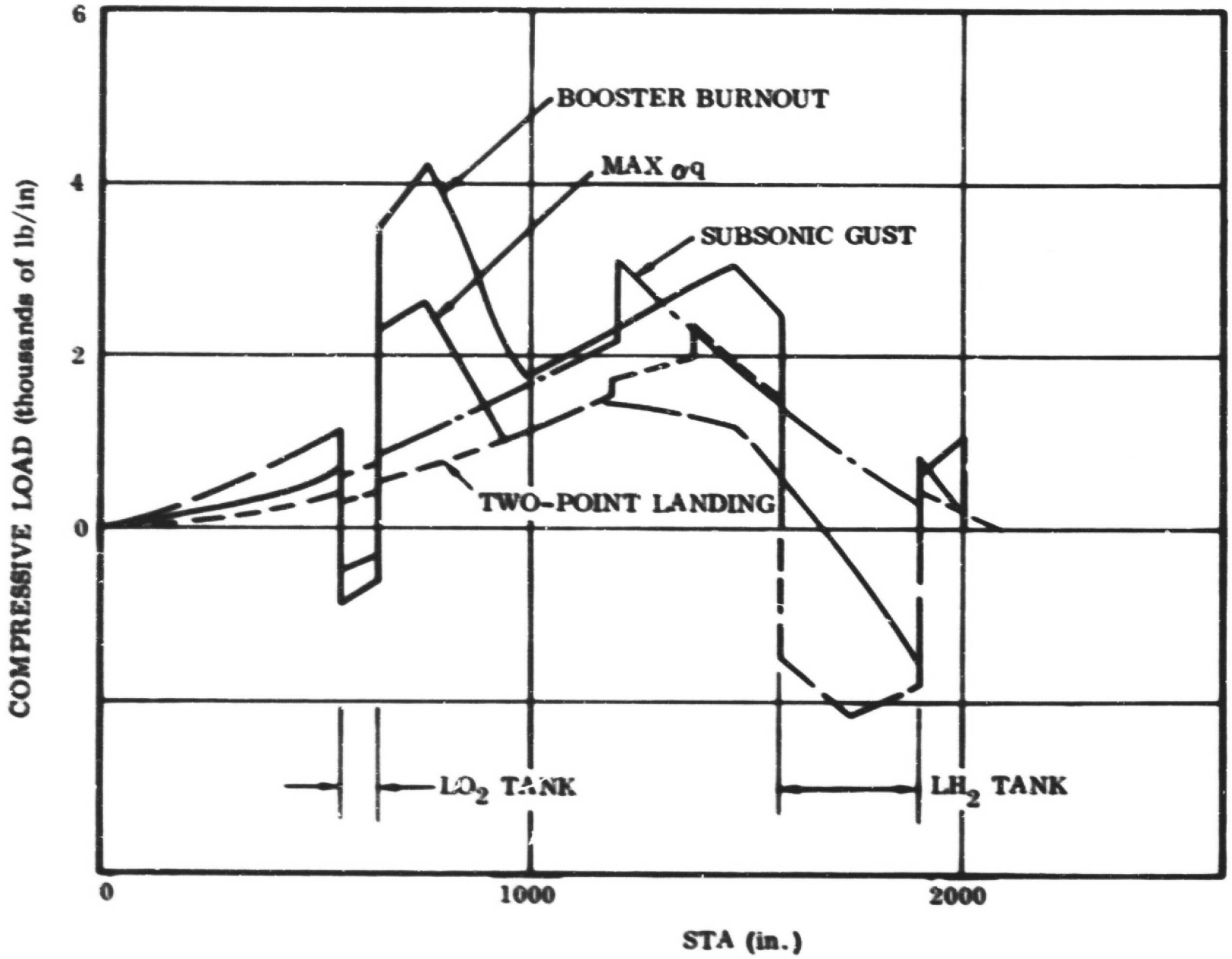

Figure 3-42. Two-Element (Nose-to-Nose) Sequential Burn 50K Lb Payload Orbiter Peak Compression Loads

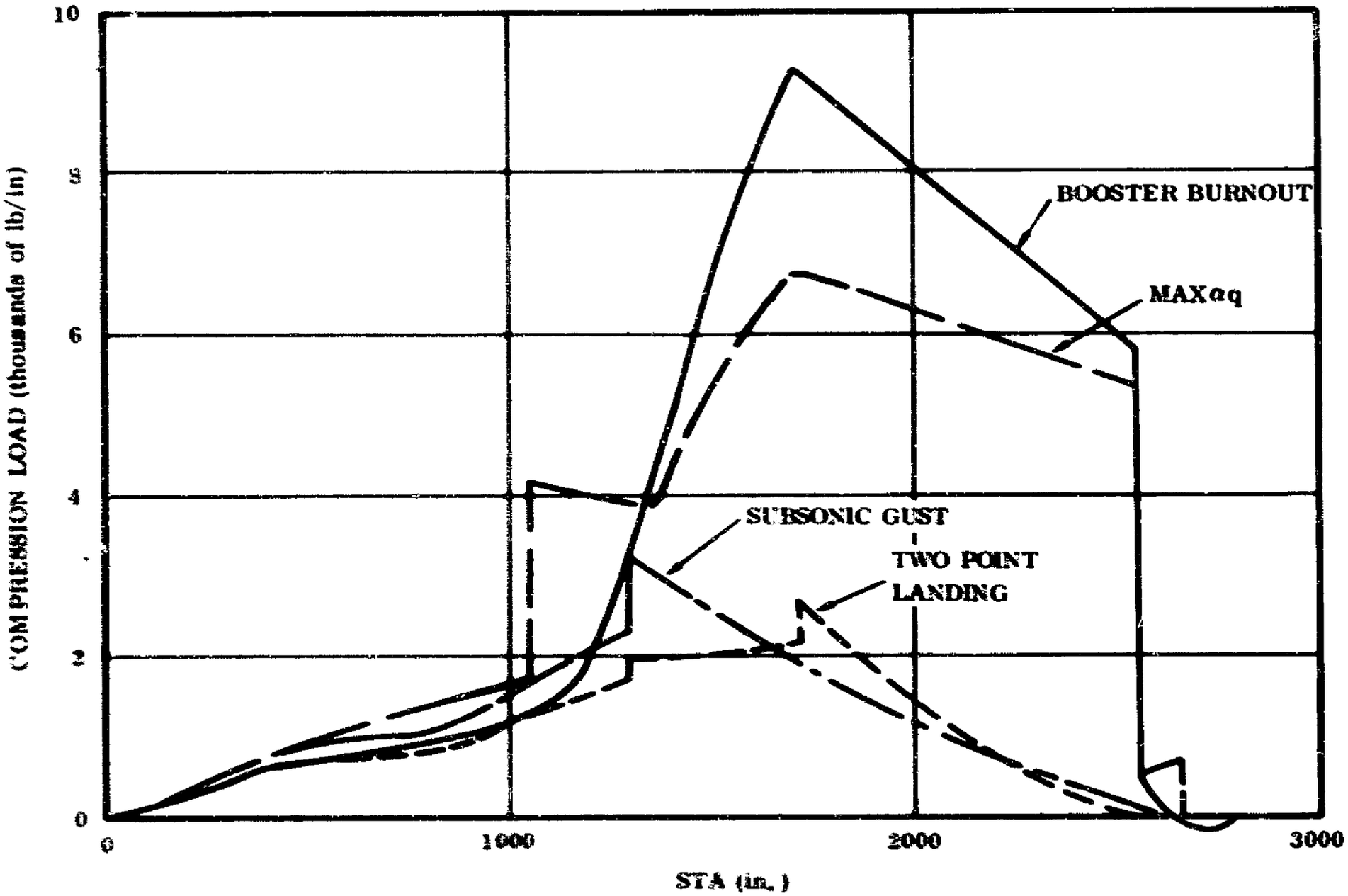

Figure 4-43. Two-Element (Nose-to-Nose) Sequential Burn 50K Lb Payload Booster Peak Compression Loads

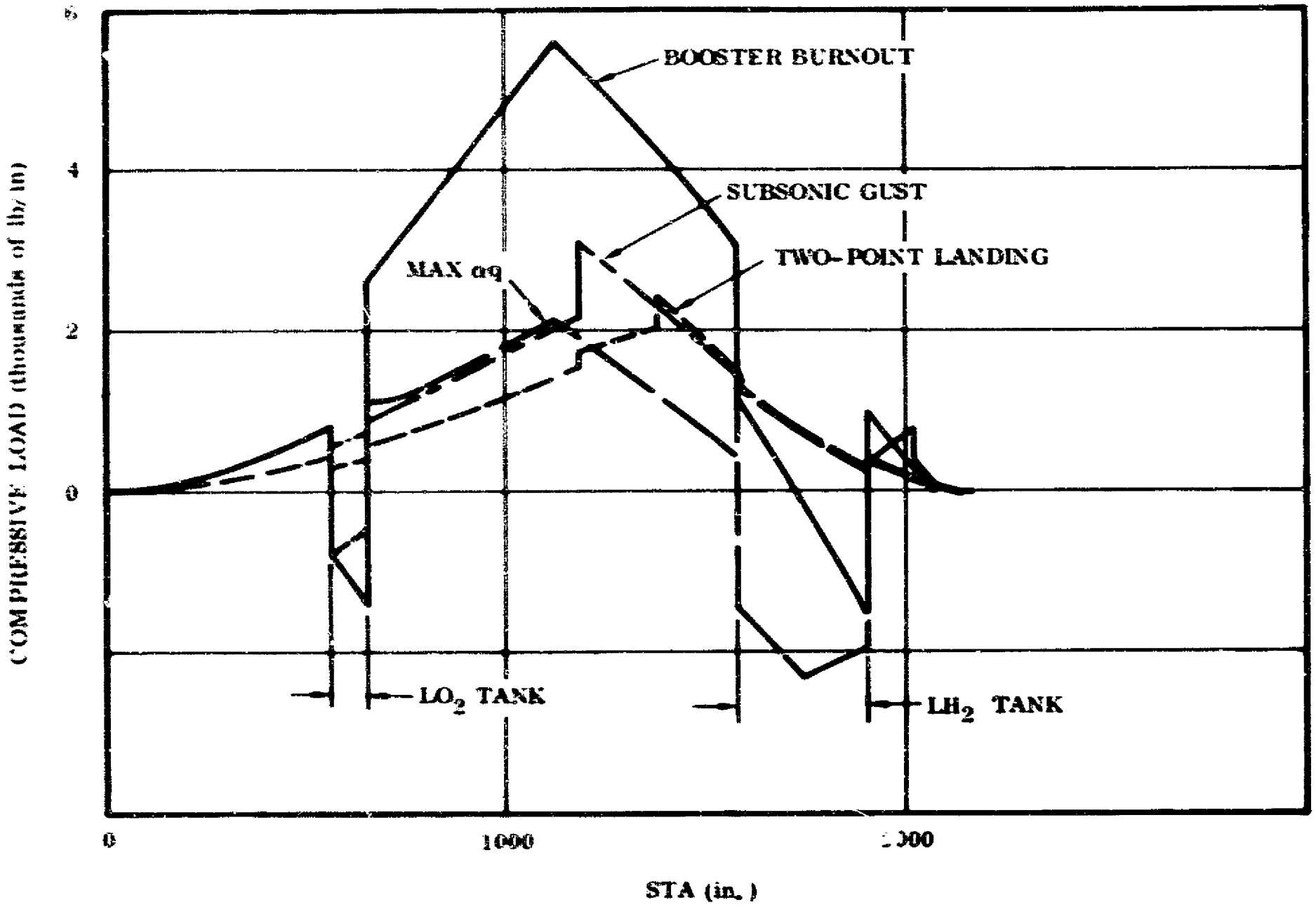

Figure 4-44. Two-Element (Tail-to-Tail) Sequential Burn 50K Lb Payload Orbiter Peak Compression Loads

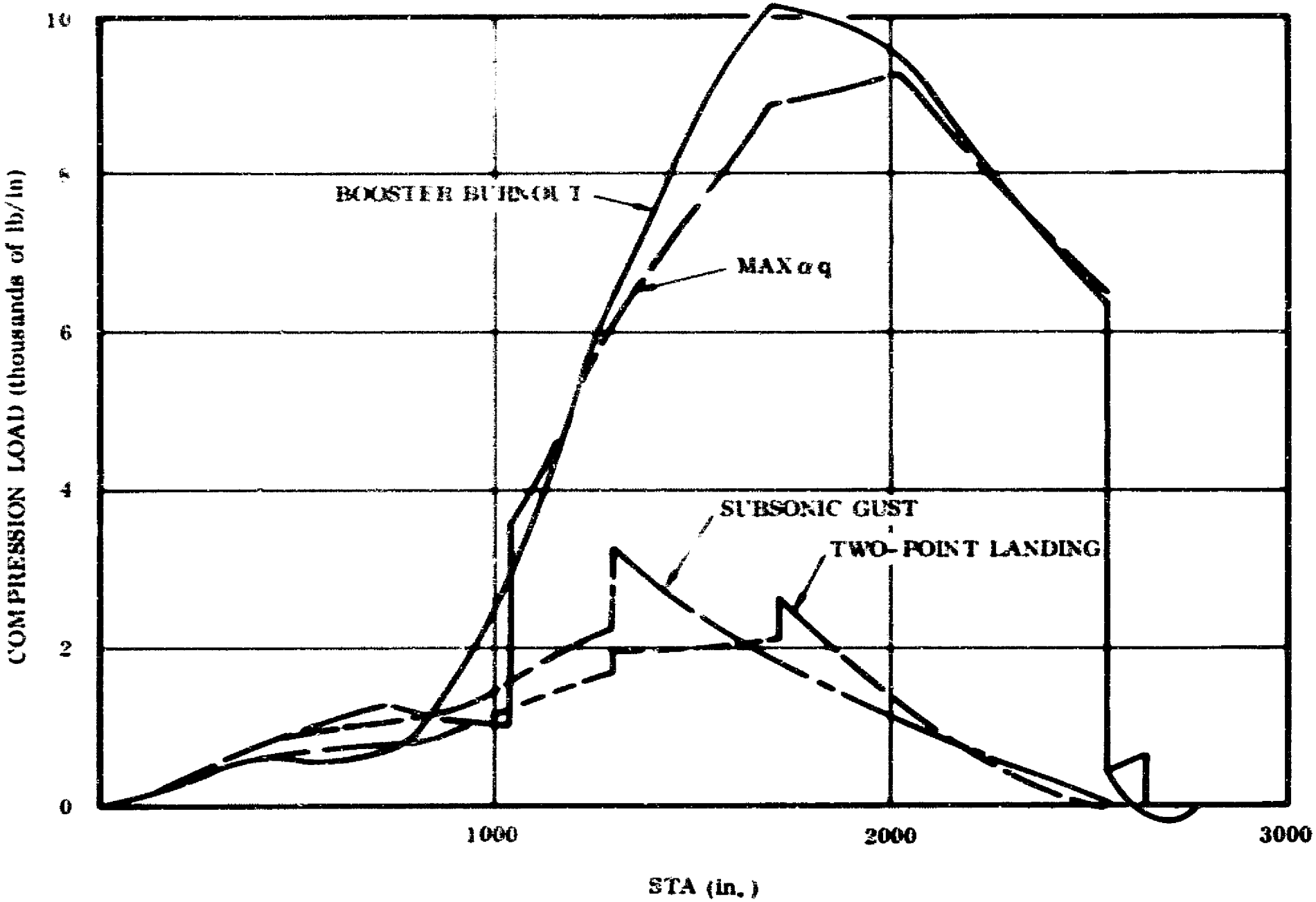

Figure 3-45. Two-Element (Tail-to-Tail) Sequential Burn 50K Lb Payload Booster Peak Compression Loads

Table 3-4. Mass Properties Summary FR-3 Two-Stage, Parallel, Sequential Burn

Condition	Weight (lb)	X - C.G.		Z-C.G.	Millions of slug - ft^2			
		Sta. (ft)	[illegible]	WL (ft)	I_{xx} - Roll	I_{yy} - Pitch	I_{zz} - Yaw	P_{xz}
Gross - Liftoff	4,267,617	88.6	36.1	99.4	12.654	344.773	334.682	-2.071
Booster								
Liftoff	3,403,092	91.5	37.3	99.5	10.929	284.979	284.949	-2.000
Max. αq (64 sec)	2,363,942	104.0	42.4	99.3	7.280	224.602	224.584	-1.350
Burnout	567,555	139.0	56.7	97.1	4.964	118.927	119.024	0.461
Entry	534,056	136.5	55.7	97.1	4.873	112.468	112.606	0.046
Flyback (Initial)	534,056	135.3	55.2	97.1	8.011	111.792	115.067	0.344
Landing	483,919	147.1	60.0	96.6	8.101	89.880	93.056	1.030
Booster Propellants	2,835,537	85.9	35.1	00.0	10.598	115.509	115.509	0
Max. αq Propellants	1,796,387	93.0	50.3	00.0	2.201	77.167	77.167	0
Flyback Propellant	50,137	23.0	9.4	00.0	0.001	0.057	0.057	0
Orbiter								
Liftoff	864,525	77.2	41.7	99.0	1.725	49.764	49.702	-0.081
Burnout	311,884	99.6	53.8	97.3	1.430	24.505	24.487	0.506
Entry (Payload in.)	259,809	102.5	55.4	98.2	1.330	22.381	22.348	0.261
Flyback (Initial)	259,809	101.2	54.7	98.2	2.060	22.041	22.738	0.375
Landing	256,698	102.5	55.4	97.9	2.137	21.569	22.187	0.361
Payload	50,000	93.0	50.3	103.0	0.044	0.488	0.488	0
Orbiter Propellants	552,641	64.4	34.8	100.0	0.247	17.653	17.653	0
Flyback Propellants	3,111	35.0	18.9	95.0	0	0.003	0.003	0

Table 3-5. Mass Properties Summary — (3A) Two-Stage, Tandem

CONDITION	WEIGHT (lb)	X — CG		Z - CG	Millions of slug - ft^2			
		Sta-(ft)	% Length	WL (ft)	I_{xx} - Roll	I_{yy} -Pitch	I_{zz} - Yaw	P_{xz}
GROSS LIFTOFF	4,192,476	234.3	54.5	99.5	9.496	1220.333	1219.783	0.483
BOOSTER								
Liftoff	3,267,047	278.6	38.7	99.6	7.297	259.612	259.333	0.322
Max αq	2,230,245	292.3	44.3	99.4	6.608	196.090	195.820	0.913
Burnout	582,655	327.2	58.5	97.6	4.369	96.302	96.107	2.420
Entry	549,934	326.7	58.3	97.3	4.273	93.868	93.752	2.550
Flyback (Initial)	549,934	325.4	57.7	97.3	7.504	93.432	96.547	2.830
Landing	499,908	329.8	59.5	98.3	7.343	90.118	93.327	2.050
Booster Propellants	2,684,392	268.4	34.6	100.0	5.286	110.839	110.839	0
Max αq Propellants	1,647,590	280.0	39.3	100.0	2.163	69.901	69.901	0
Flyback Propellants	50,026	284.0	40.9	95.0	0.024	0.021	0.065	0
ORBITER								
Liftoff	925,429	77.8	40.5	99.3	2.198	56.778	56.508	0.147
Burnout	323,771	101.4	52.8	98.0	1.397	26.741	26.496	0.617
Entry (Payload in)	269,404	106.7	55.5	99.0	1.320	24.511	24.326	0.333
Flyback (Initial)	269,404	105.2	54.7	99.0	2.299	24.080	24.873	0.477
Landing	266,178	106.3	55.3	99.0	2.302	23.555	24.340	0.368
Payload	50,000	95.0	49.4	105.0	0.044	0.488	0.488	0
Orbiter Propellants	601,658	65.1	33.9	100.0	0.775	21.425	21.426	0
Flyback Propellants	3,226	35.0	18.2	82.0	0.001	0.002	0.005	0

Table 3-6. Mass Properties Summary — FR-1

CONDITION	WEIGHT (lb)	X — CG		Z — CG	Millions of slug - ft^2			
		Sta-(ft)	% Length	WL (ft)	I_{xx} - Roll	I_{yy} - Pitch	I_{zz} - Yaw	P_{xz}
GROSS LIFTOFF	4,843,694	82.4	39.8	99.4	12.943	290.422	289.767	-3.317
BOOSTER								
Liftoff	1,719,637	82.2	39.7	99.4	4.342	97.577	97.635	-0.618
Max αq	1,098,848	93.8	45.3	99.1	3.604	71.762	71.830	-0.260
Burnout	329,052	115.5	55.8	97.0	2.357	37.160	37.288	0.399
Entry	319,044	115.3	55.7	96.9	2.351	36.005	36.129	0.423
Flyback (Initial)	319,044	114.5	55.3	97.1	3.855	34.604	36.022	0.523
Landing	298,117	118.6	57.3	97.3	3.778	32.327	33.606	0.170
Booster Propellants	1,390,586	74.7	36.1	100.0	1.155	45.056	45.056	0
Max αq Propellants	767,603	84.5	40.8	100.0	1.157	27.486	27.486	0
Flyback Propellants	20,927	54.9	26.5	88.0	0.001	0.030	0.030	0
ORBITER								
Liftoff	1,404,421	83.0	40.1	99.5	3.506	94.229	94.212	-0.273
Burnout	418,027	113.9	55.0	98.2	2.896	40.508	40.520	0.418
Entry (Payload in.)	352,221	117.0	56.5	99.0	2.489	36.254	36.191	0.124
Flyback (initial)	352,221	116.1	56.1	99.1	3.958	34.887	36.096	0.240
Landing	298,044	117.0	56.5	98.9	3.440	29.624	30.571	0.140
Payload	50,000	109.5	50.5	105.0	0.044	0.488	0.488	0
Orbiter Propellants	986,395	70.8	34.2	100.0	0.694	38.786	38.786	0
Flyback Propellants	4,177	54.9	26.5	88.0	0	0.007	0.007	0

3.5.1 GENERAL

3.5.1.1 Longitudinal Stability and Control

a. Hypersonic. When using the ruddervators (combined rudders and elevator surfaces) for pitch control, hypersonic aerodynamic prediction (HAP) runs were made to determine the effect of deflecting the ruddervator up out of the flow. The effect of moving the ruddervator hinge line forward to obtain additional hypersonic pitch control is shown in Figure 3-46.

b. Transonic. Longitudinal stability at a C_N value ot 0.10 for the basic FR-1 shape (as determined by tests conducted at the Cornell Laboratory) through the Mach number range of 0.7 to 1.3 is shown in Figure 3-47. As shown, the stability increases markedly through the transonic range. The working plots have indicated that transonic trim occurs at low C_N values.

c. Subsonic. Static longitudinal stability as determined by tests in the Convair low speed wind tunnel is shown in Figure 3-48 for the case of eliminating the boattail and showing the effect of fore-aft wing position. As shown, the vehicle is neutrally stable for a 0.55L cg position with the wing MAC at 0.54L. Somewhat greater sweep and/or aft movement of the wing pivot is required for stability.

3.5.1.2 Lateral Directional Stability and Control

a. Hypersonic. C_{n_β} versus α is shown in Figure 3-49 for two ruddervator positions — zero and 10° down. As shown, the deflected ruddervator case provides for a comfortable stability level at L/D_{max}.

Hypersonic roll control using ruddervators only was investigated using a handling qualities program. Figure 3-50 presents roll and yaw angle versus time for ruddervator deflection of 5.7 deg (each). Because of the very high moment of inertia about the yaw axis compared with that about the roll axis, the yaw introduced by using the ruddervators for roll control is very small. Figure 3-50 is for q = 30 psf, and Figure 3-51 is for a q = 260 psf. At the higher q, it is seen that the yaw is again very small, and decreases past a time of 16 seconds. This data indicates the feasibility of using the ruddervator for roll control through the speed regime where the wings are retracted. A yaw disturbance (due to gust, etc.) is counteracted by the positive C_{n_β} for the vehicle.

b. Transonic. The stability level through the transonic speed regime is seen in Figure 3-47 to increase substantially, as found in tests conducted at Cornell, over the hypersonic case. At Mach 0.95, the stability level is somewhat lower than for the subsonic case with the wing deployed as determined by tests conducted at Princeton (Reference 3-1).

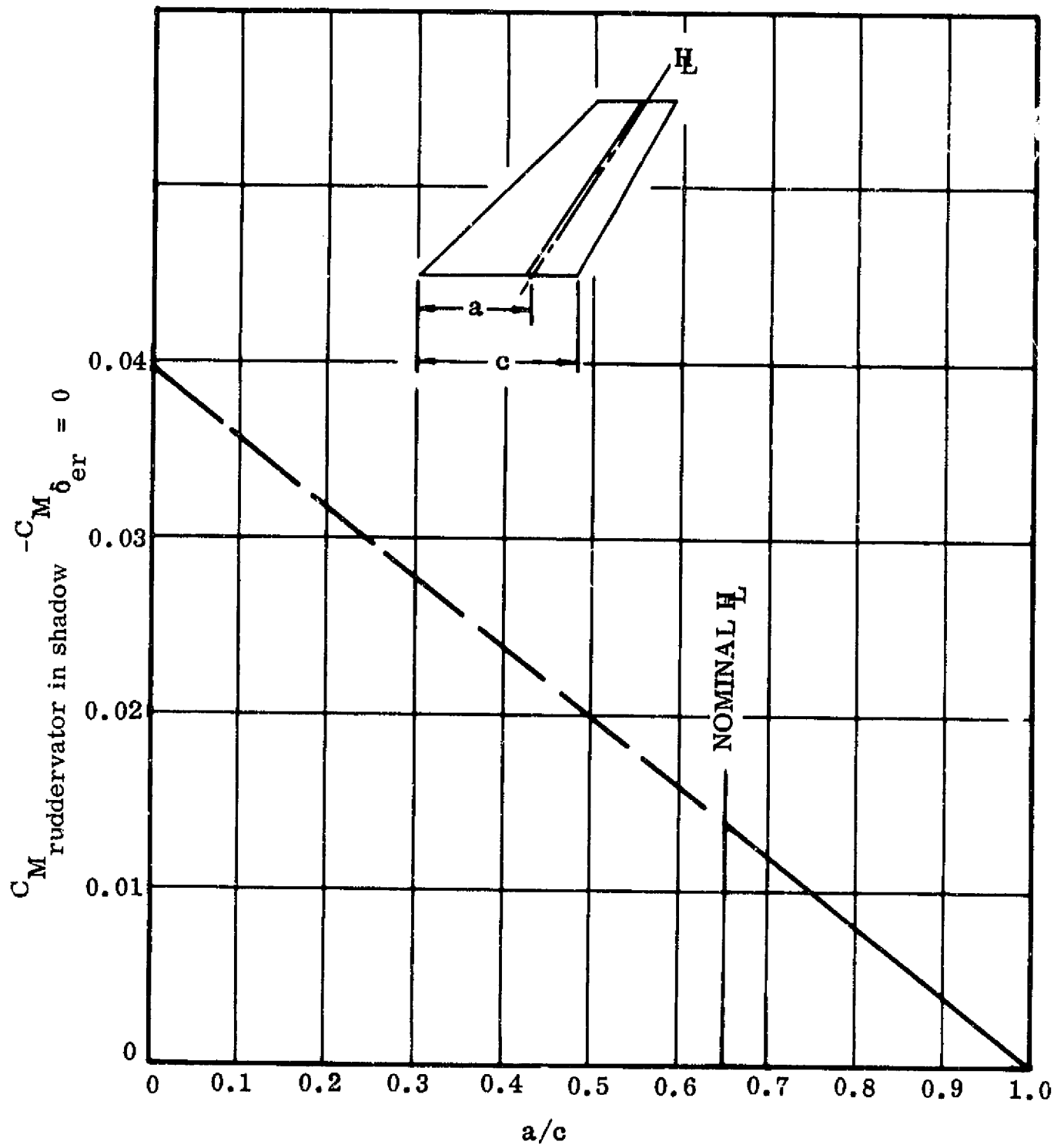

Figure 3-46. Effect of Rudde:vator Hinge Line Position

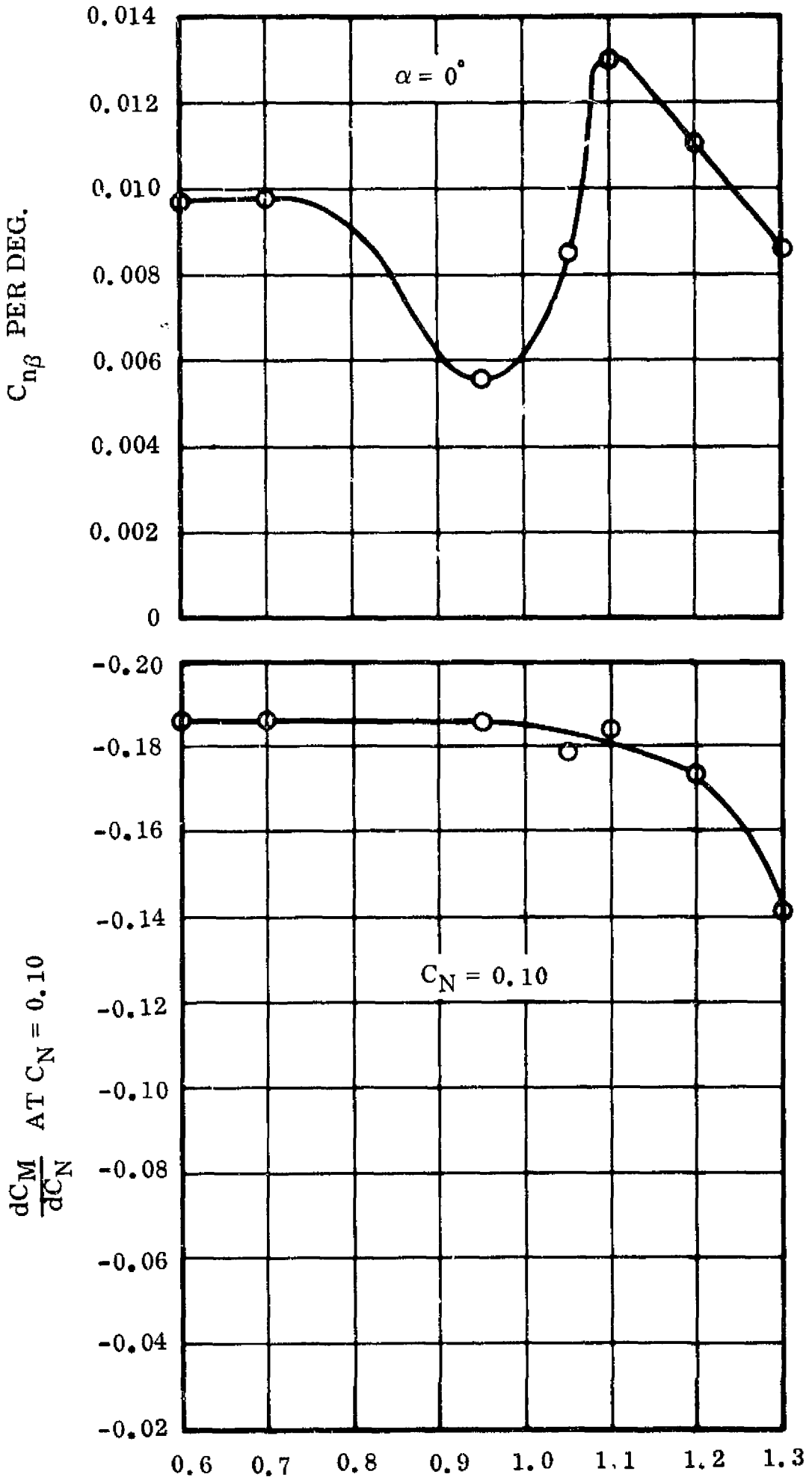

Figure 3-47. Transonic Stability

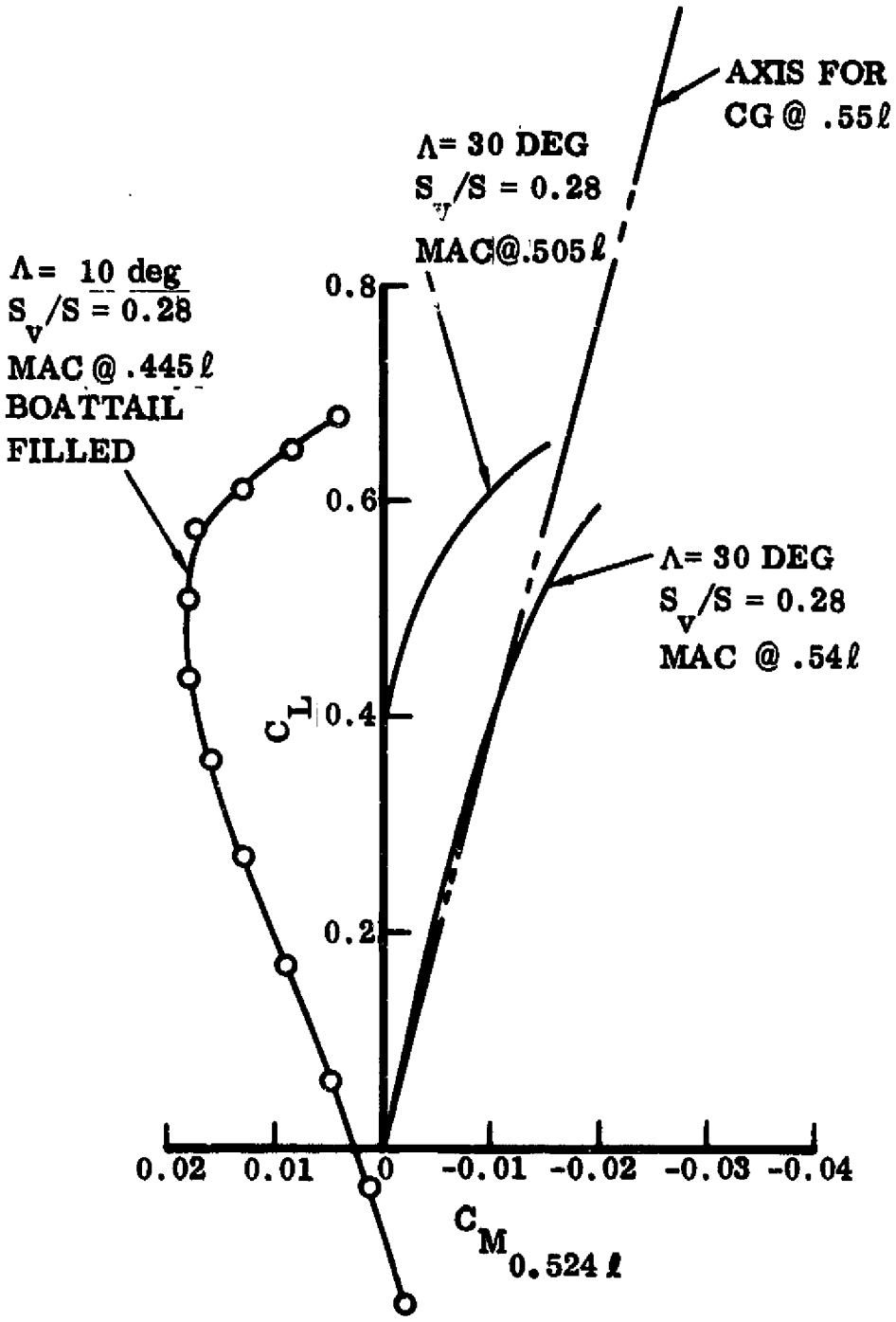

Figure 3-48. Effect of Wing Position

3

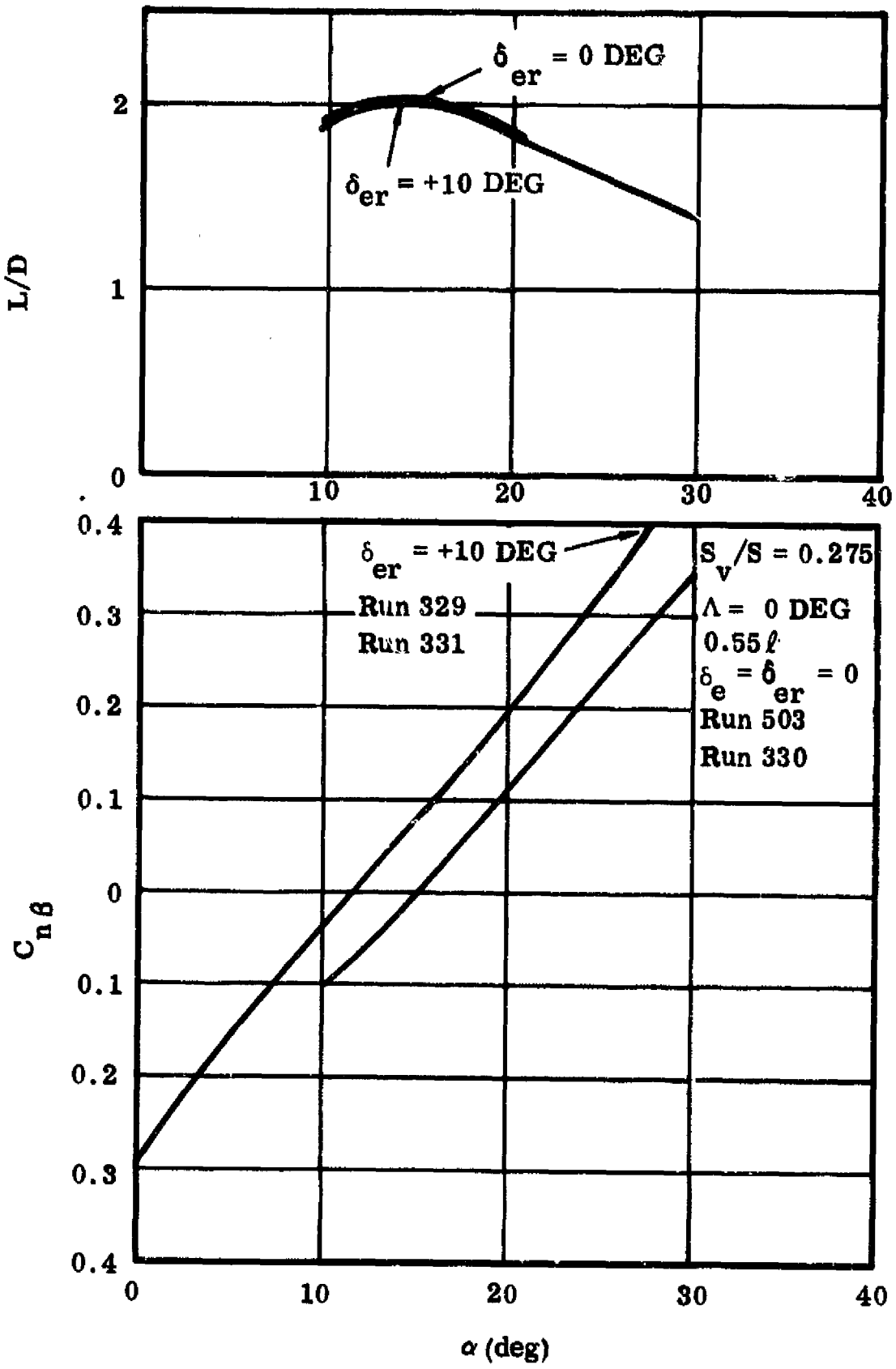

Figure 3-49. Hypersonic Directional Stability and L/D

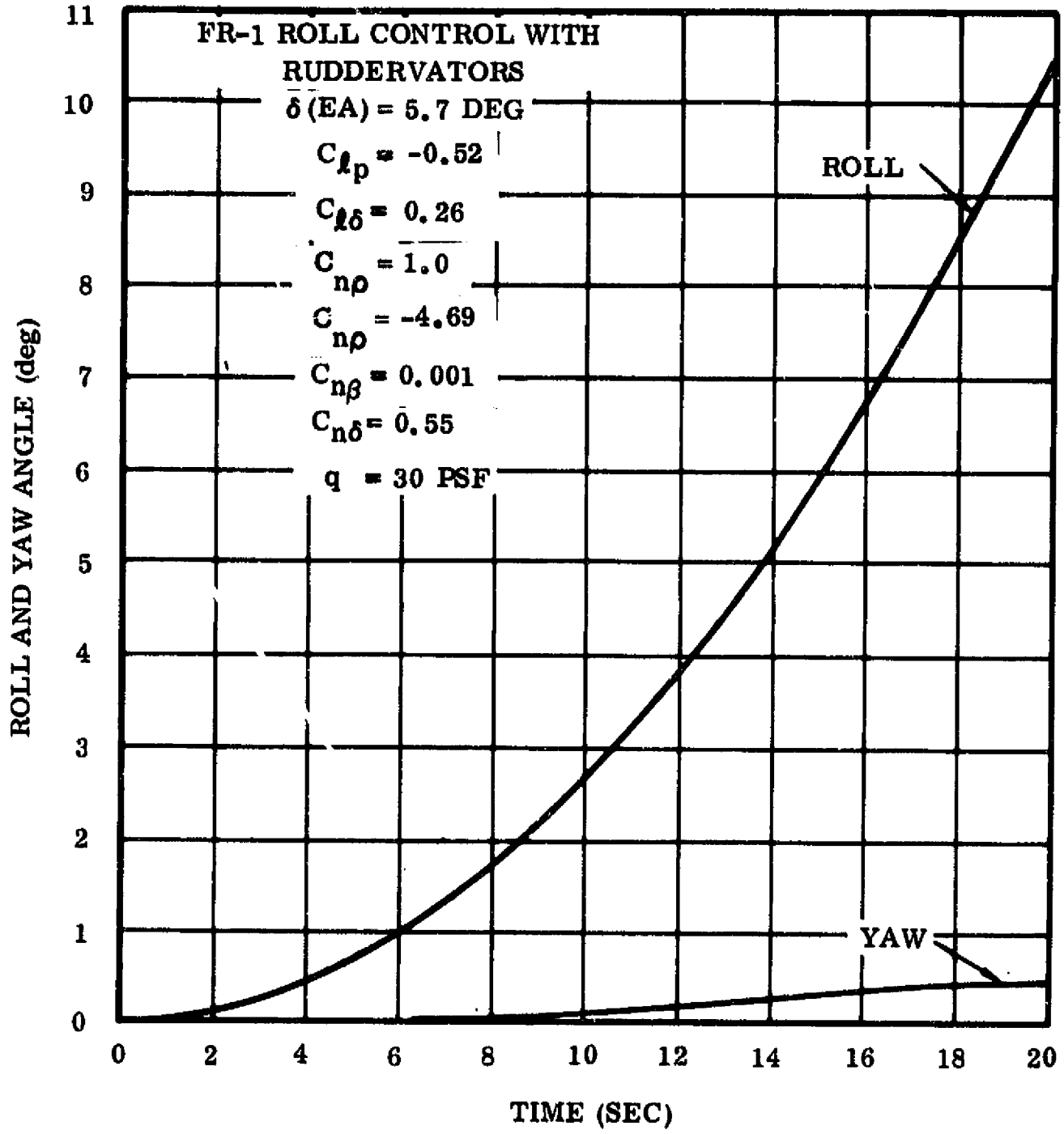

Figure 3-50. Roll and Yaw Time History Using Fuddervators Only (q = 30 psf)

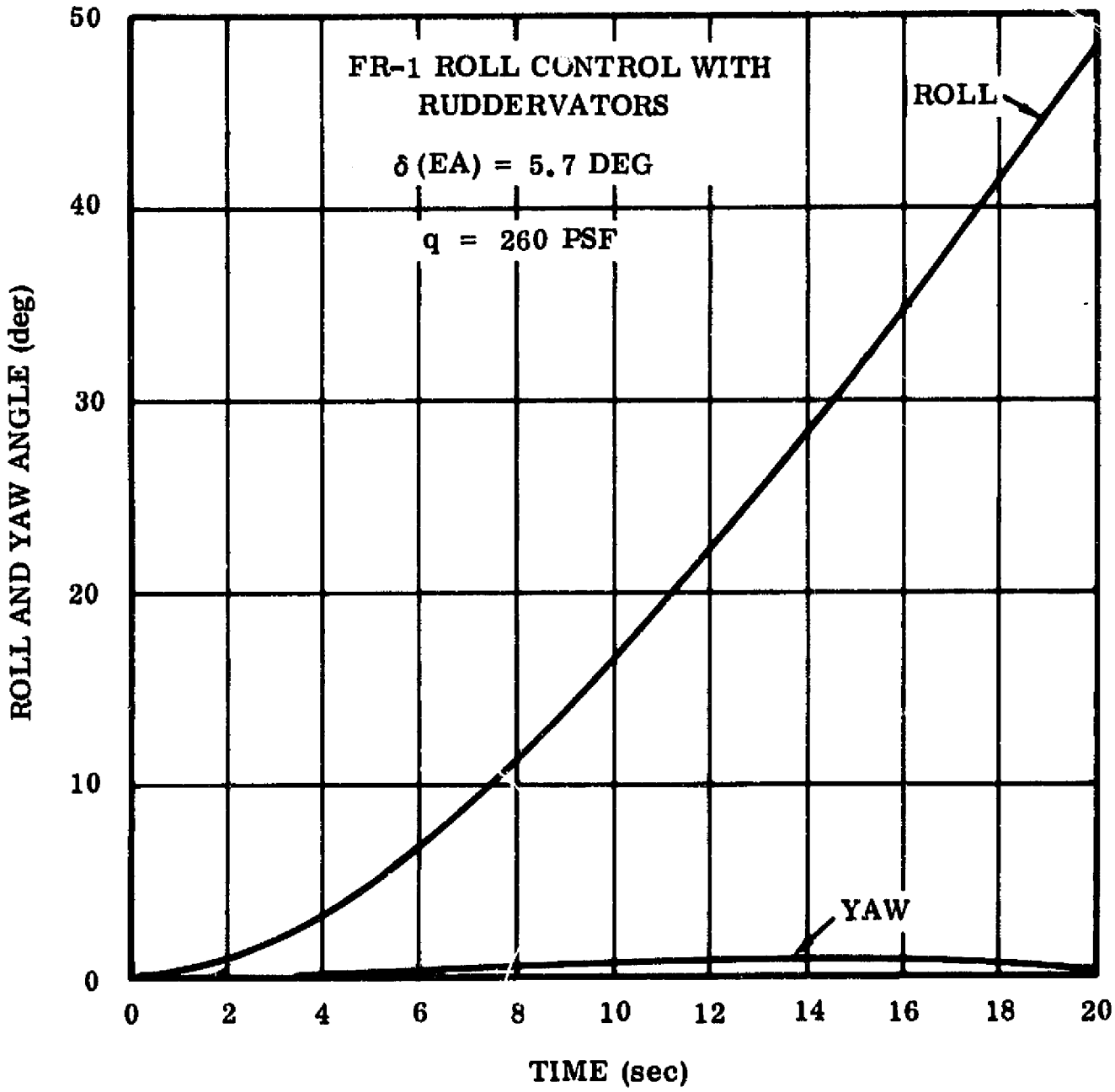

Figure 3-51. Roll and Yaw Time History Using Ruddervators Only (q = 260 psf)

c. Subsonic. Direction stability data from the Convair low speed tests was used to obtain C_{n_β} versus center of gravity position. As shown in Figure 3-52, the stability drops to zero at a cg position of 0.64L.

3.5.1.3 Cruise. The Breguet expression for range was used to develop the fuel fraction versus subsonic L/D for a range of 300 n. mi. and an SFC (specific fuel consumption) of 0.5, using a turbofan engine, for cruise speeds of from 200 knots to 320 knots. This is shown in Figure 3-53. For a representative case of a vehicle having a wing loading of 70 psf and cruising at L/D_{max} (7.0 at a C_L of 0.5 for a cruise speed at 256 knots true) at 15,000-ft altitude, the fuel fraction is 0.079.

3.5.1.4 Tail Sizing. A study was conducted to determine the effect of vehicle length on the tail size required to yield identical yaw acceleration. The resulting variation of tail area versus length is shown in Figure 3-54. The effect of changing the body sidewall angle on tail size required to maintain an identical level of yaw acceleration is shown in Figure 3-55. There is question regarding the influence of the shadowing effect of the vehicle forebody on the effectiveness of the tail. Two assumptions are shown: for the tail geometry fully shadowed by the forebody, and completely unshadowed. As shown, the required tail size is affected very little for the sidewall range of zero to about 15 deg, but as the sidewall angle increases, the required tail size is affected substantially by this shadowing effect.

3.5.1.5 Boost Drag. Drag characteristics for boost performance of the two-element vehicles, including a tandem arrangement the drag of which is of interest for general application, is shown in Figure 3-56. Three configurations are shown: simultaneous burn, sequential burn, and tandem. Data obtained from Cornell tests of a basic FR-1 shape at transonic speeds was adjusted for the effect of rocket engine operation.

3.5.1.6 Time to Ground. The time required to touchdown from what is usually considered the end of "entry" of the entry computer runs was approximated and is shown in Figure 3-57, where altitude, velocity, Mach number, and C_L are plotted versus time. These plots are based on the assumptions that Newtonian aerodynamics apply down to Mach 1.0, the wing is extended from Mach 1.0 down to Mach 0.6, and that the aerodynamic characteristics in this Mach range are lir ear with Mach number. Subsonic aerodynamics are used from Mach 0.6 to touchdown, with the vehicle flying at L/D_{max}.

3.5.2 TWO-STAGE BOOSTER

3.5.2.1 Longitudinal Stability and Control

a. Hypersonic. Longitudinal characteristics for the booster, which incorporates lower horizontal surfaces, are shown in Figure 3-58. The effects of deflecting the ruddervators down 10 deg and up out of the flow are shown in this figure.

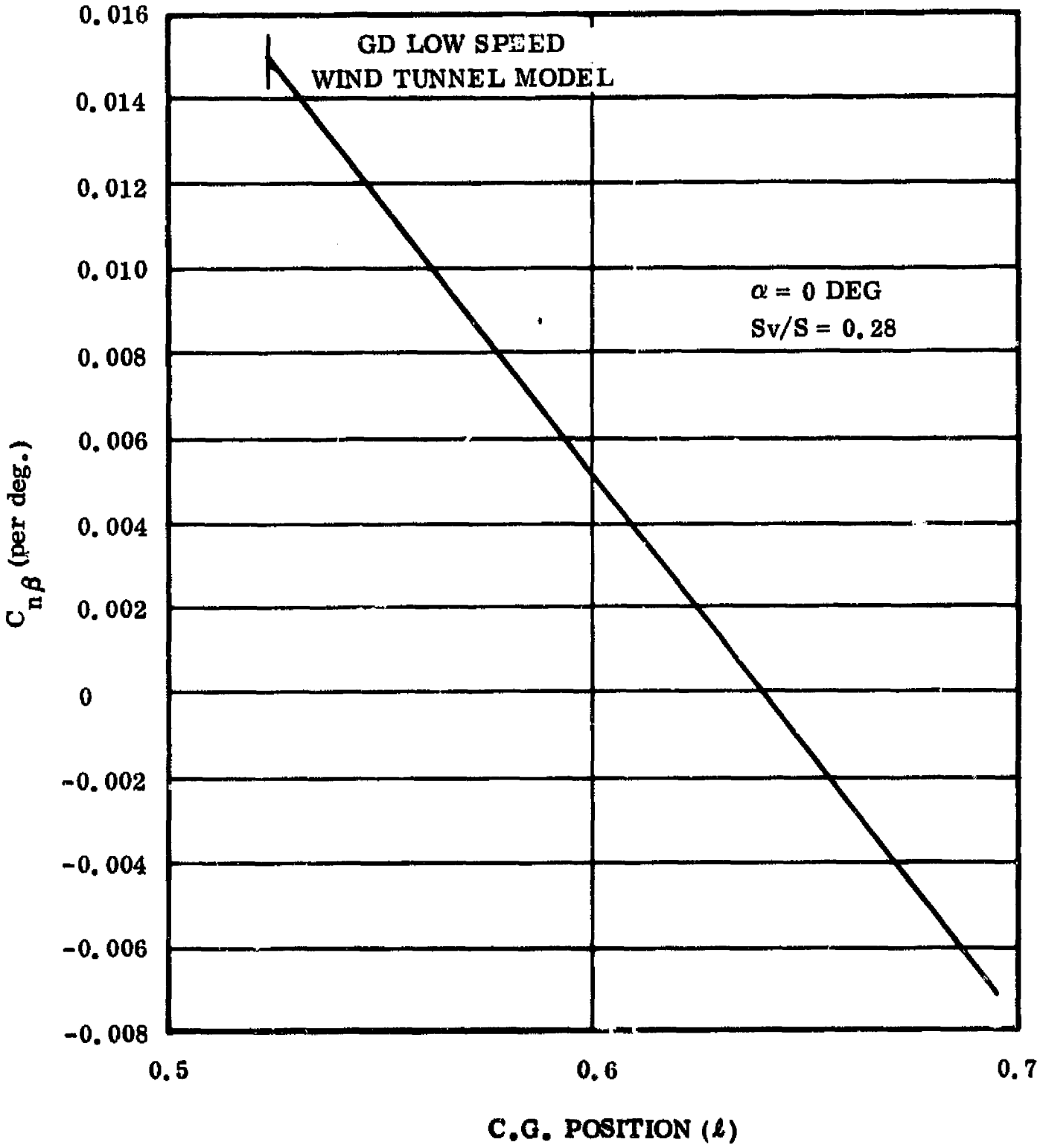

Figure 3-52. Directional Stability vs cg Position

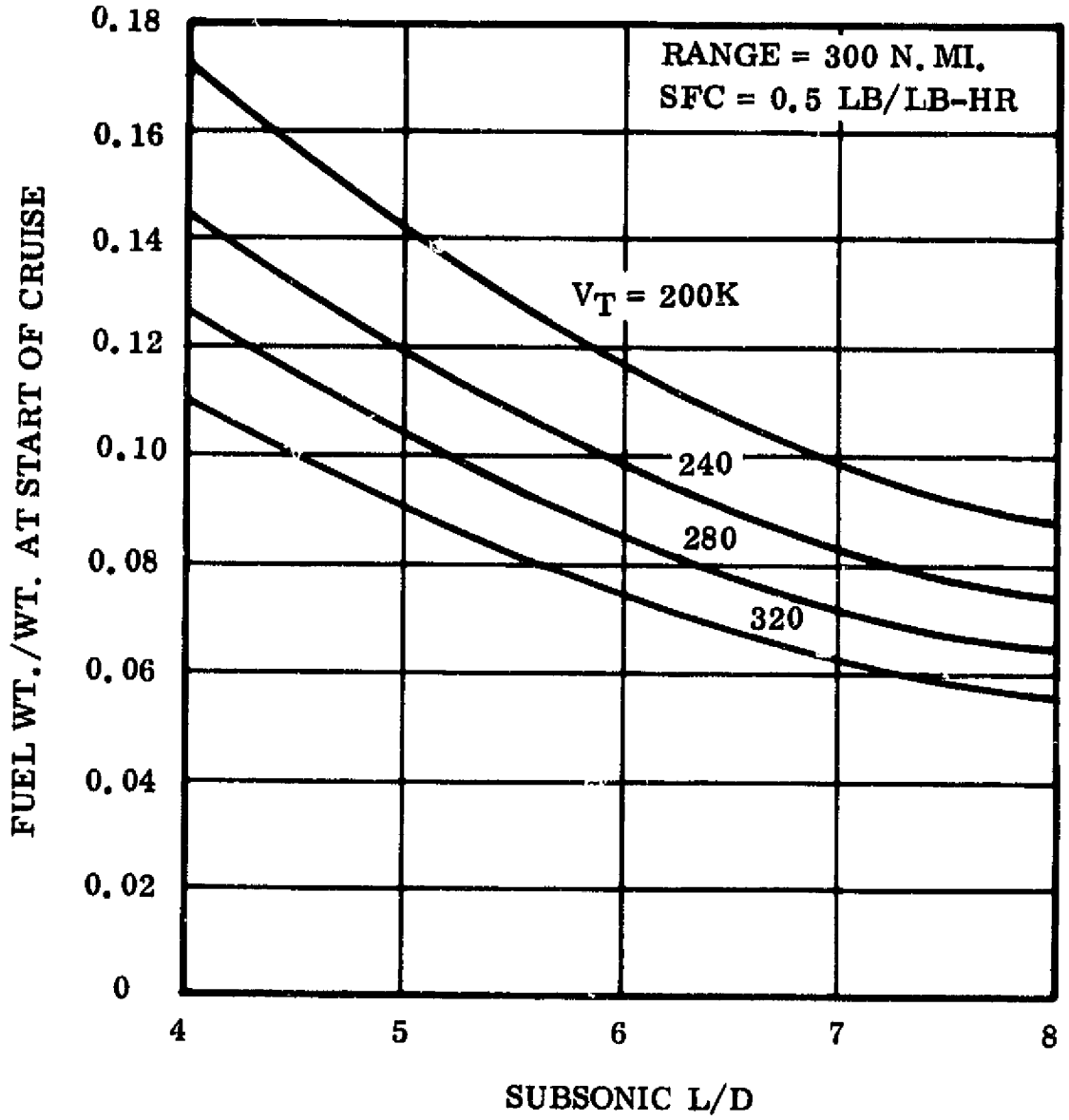

Figure 3-53. Fuel Fraction vs. L/D

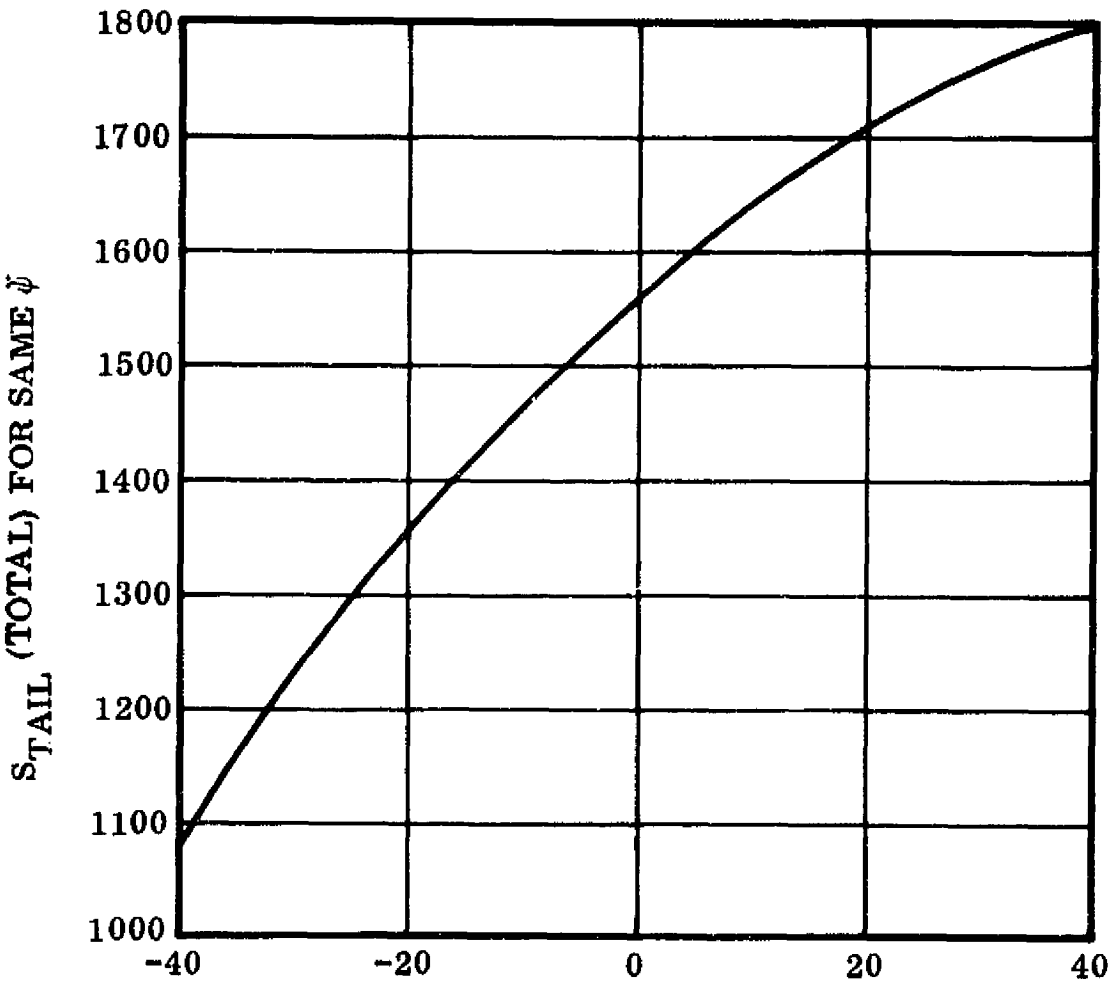

Figure 3-54. Effect of Length of Tail Area Required

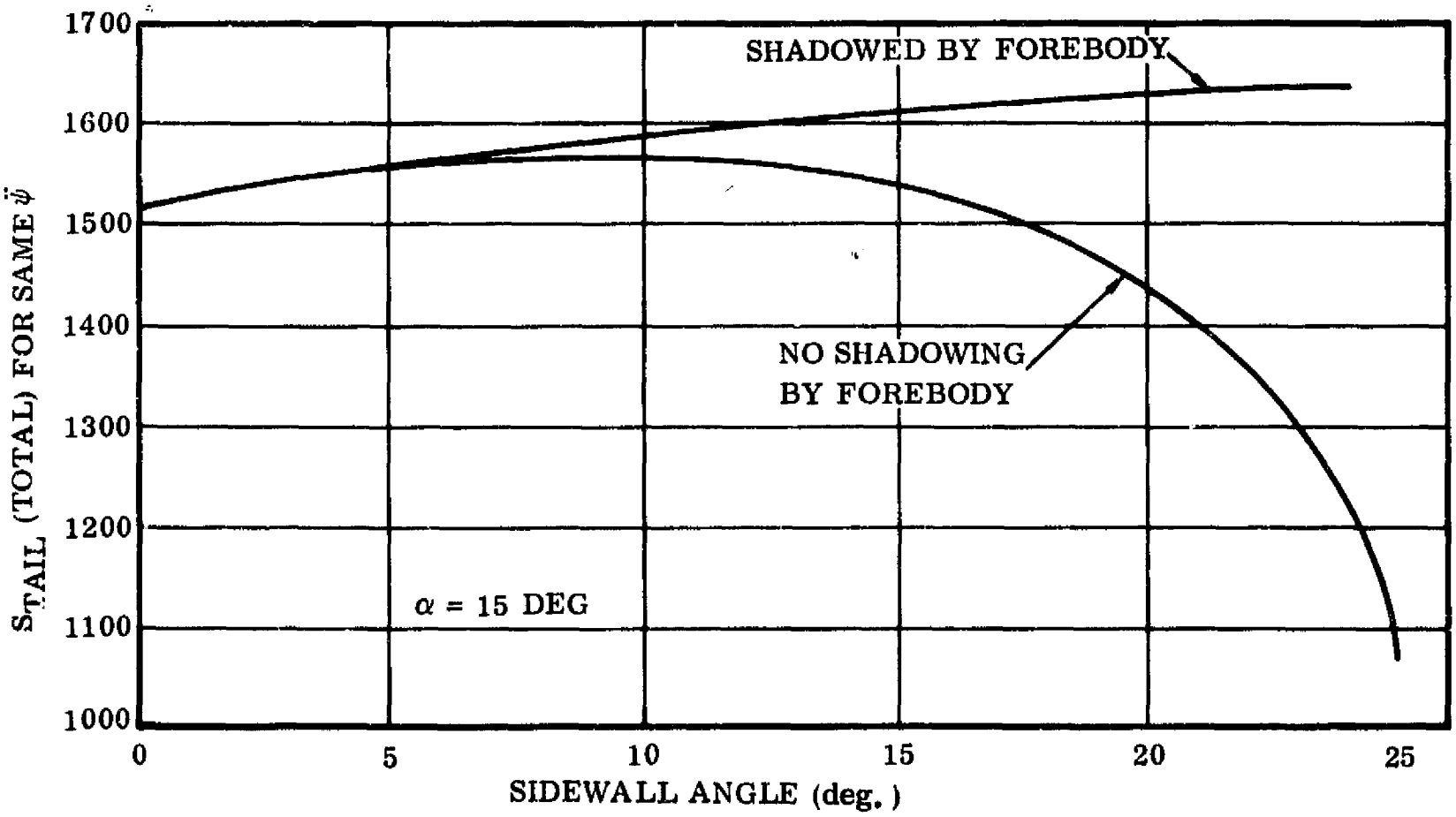

Figure 3-55. Effect of Sidewall Angle on Tail Area Required

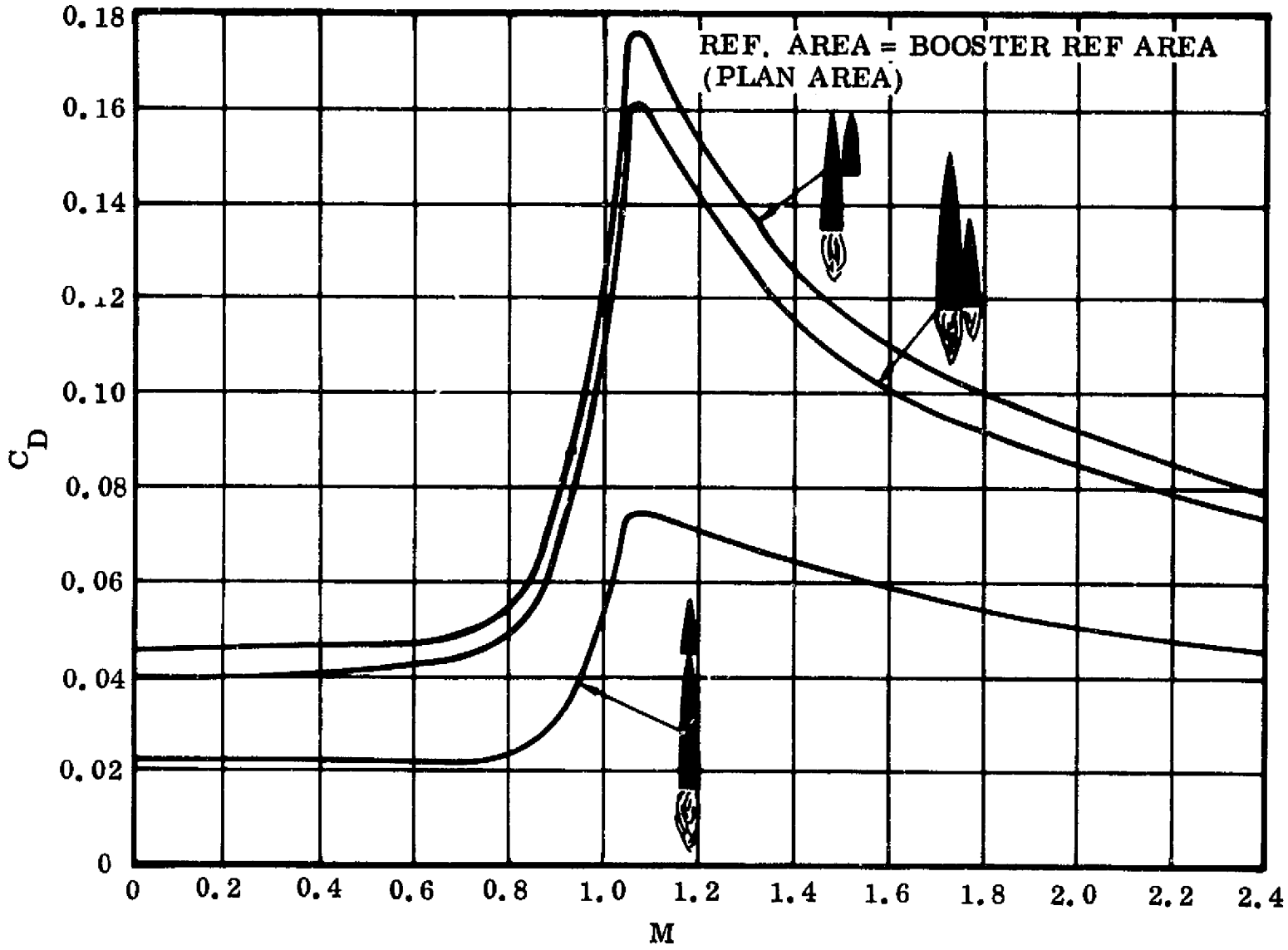

Figure 3-56. Drag Data for Boost

An axis line for a cg position of 0.583L is shown, corresponding to the current cg position for the vehicle at entry. As shown, the vehicle can be trimmed to an α of about 33 deg using the ruddervator alone. Higher values could be obtained using a hingle line farther forward than the 0.65 chord position currently shown. Also, some negative incidence would help, and would also relieve the subsonic trim situation. (The hypersonic directional stability is good at high angles of attack, and remains acceptable at the lower angles if longitudinal trimming is accomplished using ruddervators rather than the elevons.) Using 10 deg of down ruddervator, the vehicle can be trimmed down to an alpha of about 25 deg, which is as low as need be provided for in the two-stage booster. As speed is reduced below hypersonic, the transonic data indicates that the vehicle will trim at the lower angles of attack(α).

b. Transonic. (See remarks in Section 3.5.1)

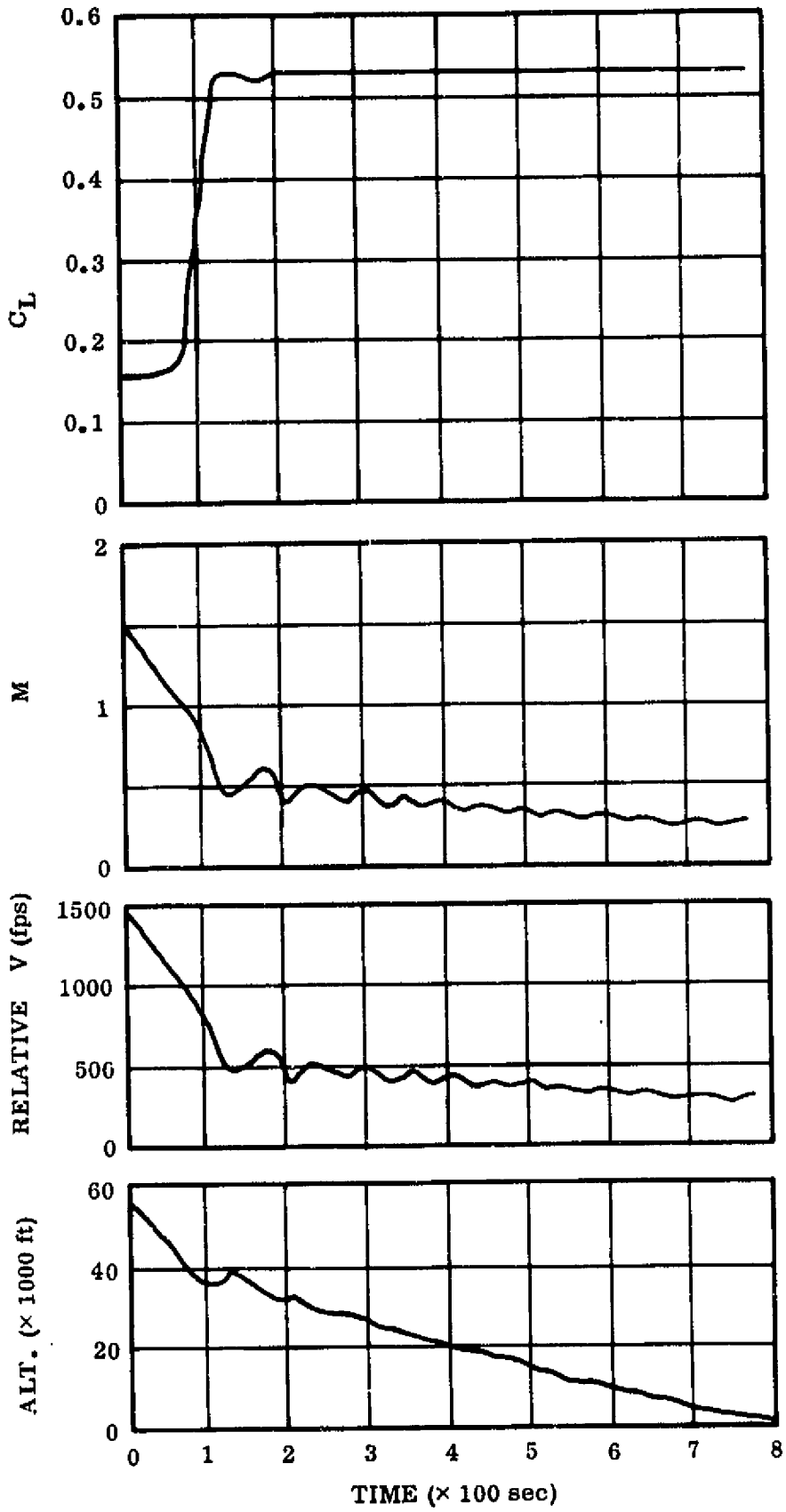

Figure 3-57. Time to Ground

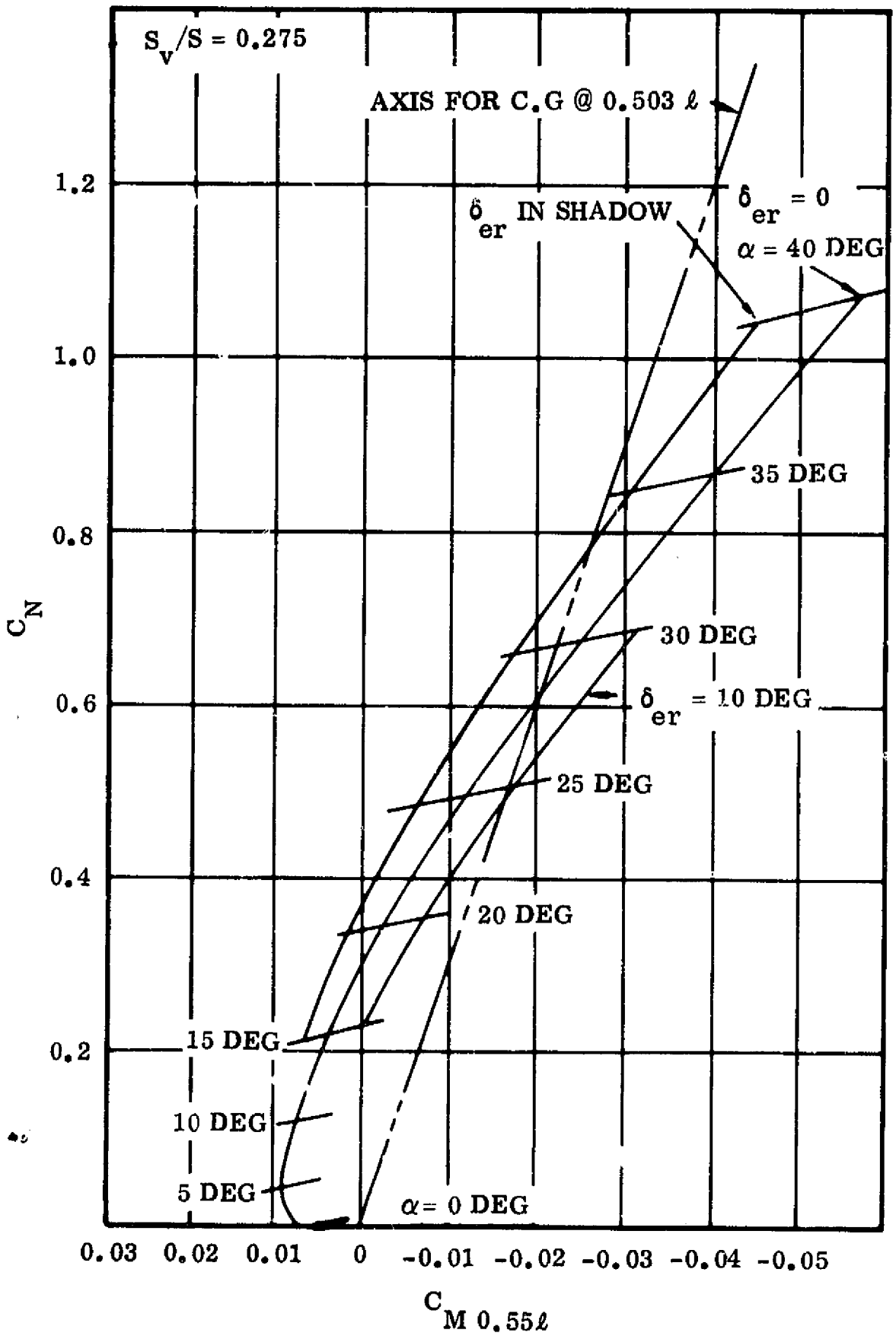

Figure 3-58. Hypersonic Longitudinal Stability and Control

c. Subsonic. The effect of adding a horizontal surface to the subsonic longitudinal characteristics of the basic vehicle was approximated by using the data obtained in the Princeton tests of Reference 3-1. It was assumed that the effectiveness of the horizontal surface is the same as that of a horizontal surface used in these tests which incorporated considerably greater leading edge sweep (75 deg compared to 45 deg) on the basis of equal horizontal area. The actual area of the horizontals is about double that of the tests, and the dC_m/dC_L is adjusted accordingly. The value taken as representative of the effect of adding the horizontals is 0.040 dC_m/dC_L.

3.5.2.2 Lateral/Directional Stability and Control

a. Hypersonic. See remarks in Section 3.5.1.

b. Transonic. See remarks in Section 3.5.1.

c. Subsonic. See remarks in Section 3.5.1.

3.5.2.3 Tail Sizing. The center of gravity for the two-element booster vehicle is substantially farther aft than for the other vehicles being examined. The landing cg is substantially farther aft than the entry cg, requiring that the longitudinal and lateral/directional characteristics be examined throughout the hypersonic, transonic, and subsonic speed regimes. This examination has revealed that the critical condition is that of static longitudinal stability for landing. In this case, it is more desirable to add lower horizontal area than to add area to the Vee tail. Figure 3-59 presents the required tail size as a function of cg position to satisfy the landing stability requirement. The dashed line indicates how the cg is affected by adding weight to the tail in the form of tail size increase. For the current case, it is seen that a tail size of 1.76 times the original area is required to provide landing stability and eliminate ballast. This added tail weight amounts to about 7,000 pounds.

3.5.2.4 Entry. Entry trajectory computer runs for booster entry following staging were made to provide data for aerodynamic heating analysis and for footprint and load factor study. The angle of attack used was 40 deg, and bank angles of 0 deg (Run 304), 30 deg (Run 305), 45 deg (Run 306, and 60 deg (Run 307) were run with these initial conditions at staging:

$C_L = 0.645$

$C_D = 0.643$

$C_{L_\alpha} = 0.01612$

W/S = 64 psf

Alt. = 187,290 ft

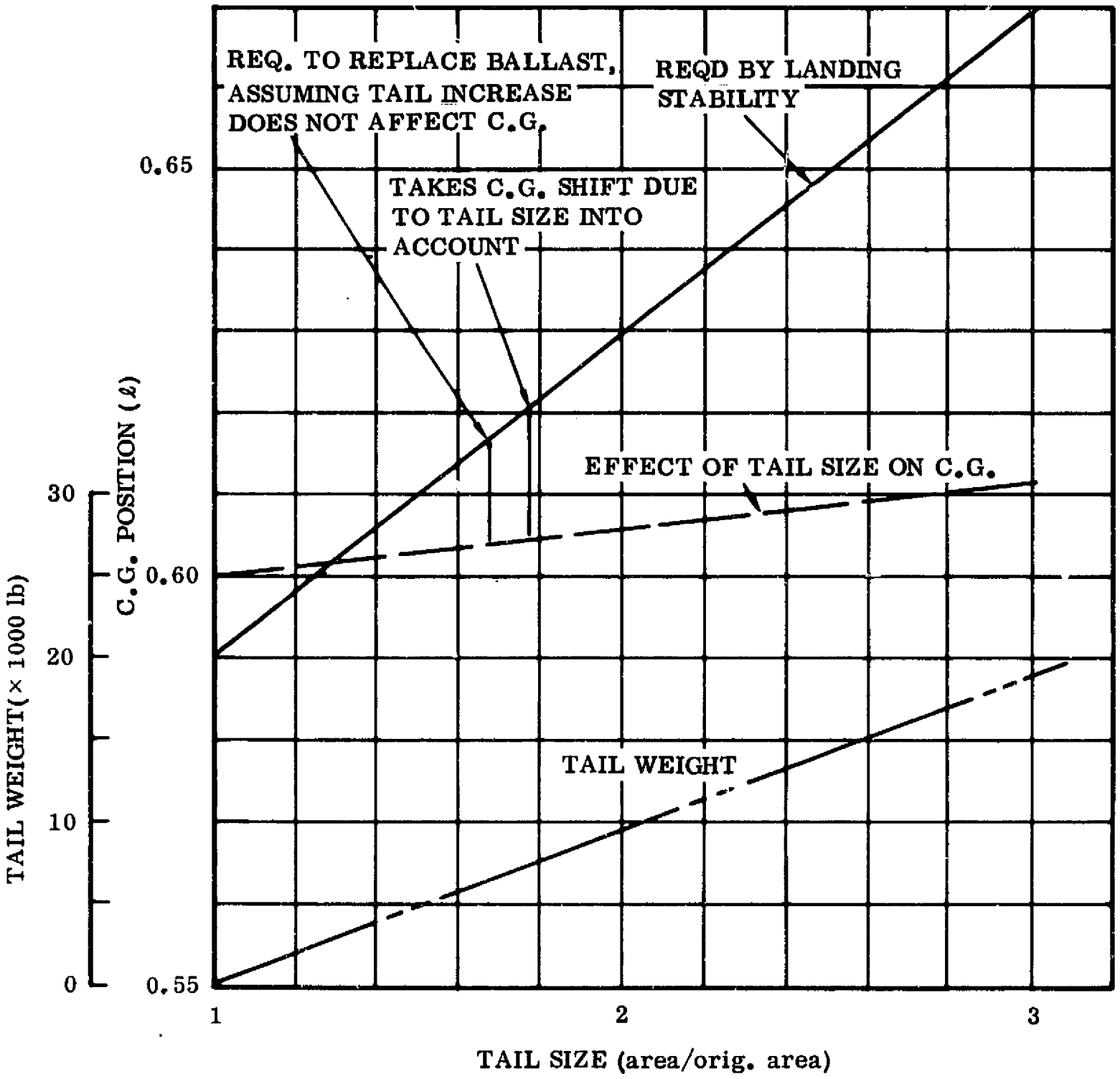

Figure 3-59. Tail Size Required vs. cg Position

V_{rel}	= 10,754 fps
γ_{rel}	= 2.89 deg
Latitude	= 29.8 deg N
Long.	= 79.2 deg W
Heading (E of S)	= 146.2 deg

Figure 3-60 presents the footprint resulting from these runs. Figure 3-61 shows the maximum values of the resultant load factor experienced during the entry, and it is seen that the limit value of 4.0 is never exceeded.

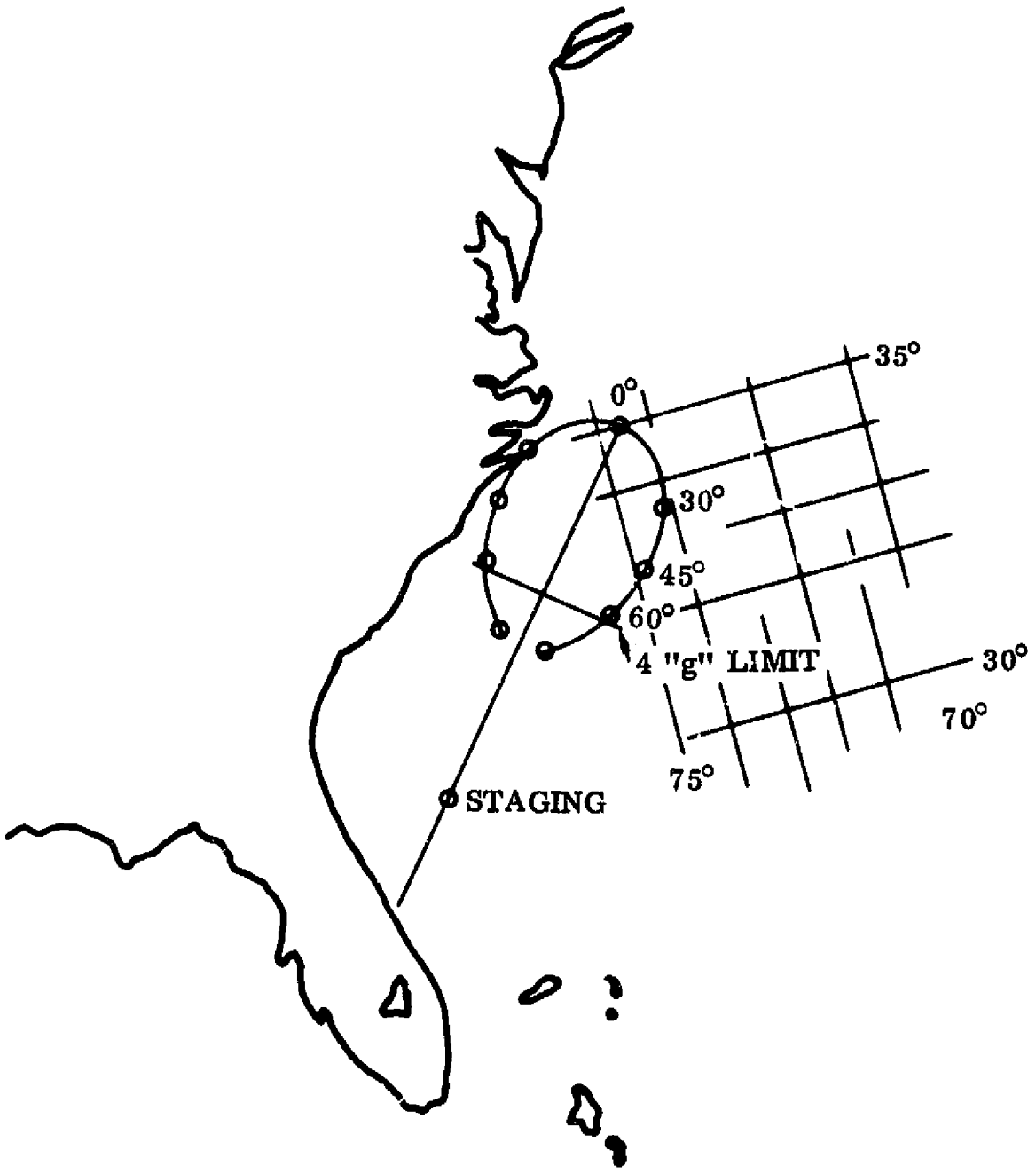

Figure 3-60. Booster Entry Footprint

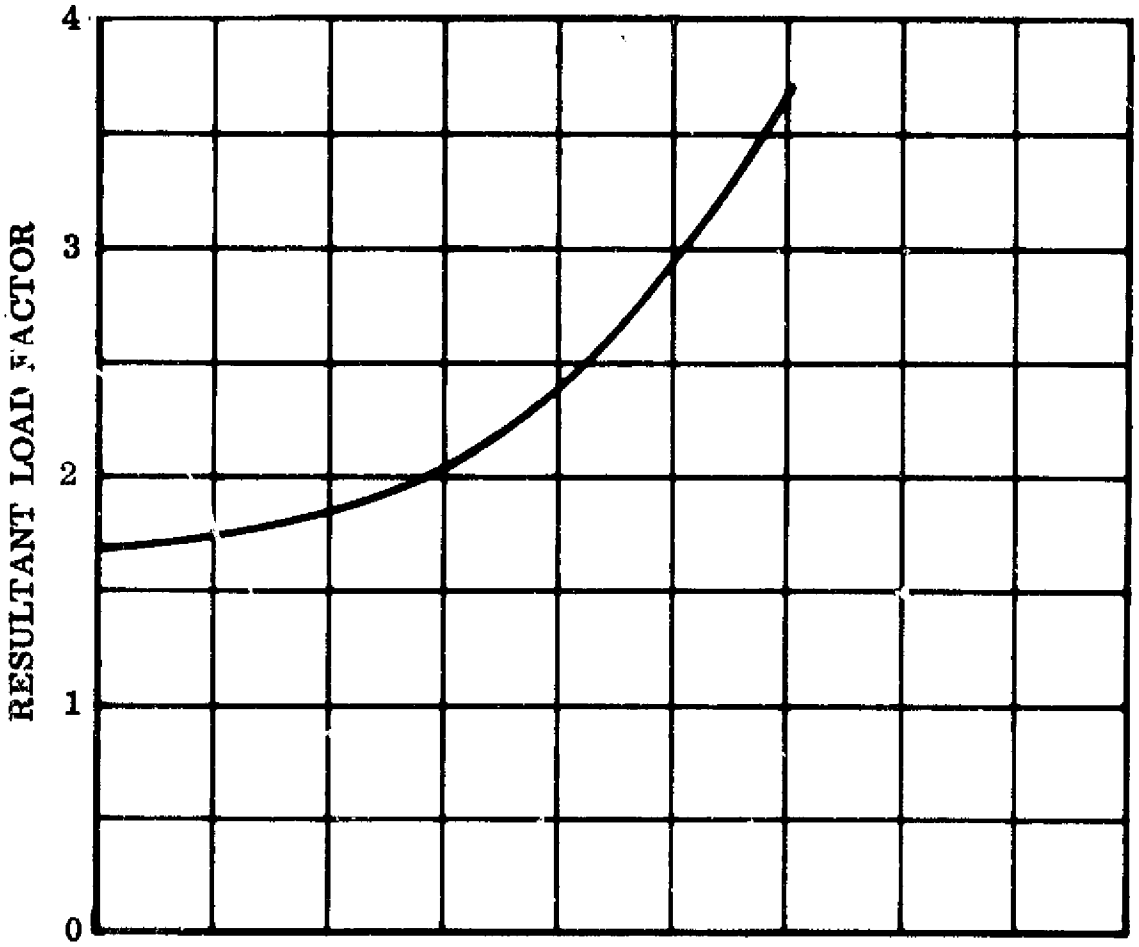

Figure 3-61. Booster Entry Load Factor

To further explore entry heating, the following runs were made for various staging dynamic pressures and for various velocities at a common dynamic pressure of 50 psf. Initial conditions were the same as above except as noted:

Run No.	321	322	323	325	326	327
Altitude, ft	185395	174641	167104	179604	191329	189526
V_{rel}, fps	10509	10569	10612	9450	11715	11328
α_{rel}, deg	2.217	1.207	0.509	3.91	1.74	1.19
q, psf	50	75	100	50	50	50

3.6 AERODYNAMIC HEATING

The aerodynamic heat transfer studies performed had two objectives: one was to establish the variation of lower surface peak temperature with entry angle (γ); the other was to establish the peak temperature of the first element of the two-element sequential burn concept as a function of staging velocity and staging dynamic pressure (q_A). Results of the first objective led to selecting an entry angle of -1.0 deg instead

of the -2.0 deg used previously because of a reduction in peak lower surface temperature with a reduction in entry angle. Results of the second objective supported the selection of a staging velocity of 11,000 fps at a dynamic pressure (q_A) of 50 lbf/ft^2.

3.6.1 METHOD OF ANALYSIS. Figure 2-16 shows the FR-1 configuration analyzed. Figure 3-62 presents the lower surface angle as a function of centerline distance. The aerodynamic heating prediction procedure used was tangent wedge dissociated flow field properties, Eckert's reference enthalpy method for laminar boundary layers, adiabatic wall reference enthalpy method for turbulent boundary layers (i^*_{aw}), and gradual transition starting at a shock layer Reynolds number of 1×10^6 and ending at 2×10^6. These methods are described in Reference 3-2. Figure 3-63 presents the corrections applied to the tangent wedge heat transfer rates to account for the angle-of-attack-induced flow divergence on the lower surface. The transitional boundary layer Reynolds number ratio of 2.0 was chosen based upon the data presented in Reference 3-3. Nose stagnation temperatures were calculated using the Detra, Kemp and Riddell (Reference 3-4) laminar stagnation heating equation. All surface radiation equilibrium temperature and insulation (radiative) sizing calculations were done with the Convair 3020 aerodynamic/structural heating program (Reference 3-2). The emissivity chosen was 0.90 except for the nose and leading edges, which were assumed to have emissivities of 0.8 and 0.85, respectively. The insulation thermal protection subsystem (TPS) thermodynamic model is shown in Figure 3-64.

Trajectories were calculated using the nominal hypersonic aerodynamic characteristics presented in Section 3.5. These aerodynamic characteristics were derived for a preliminary FR-1 design and show a maximum hypersonic L/D of 2.03. The trajectory analysis program uses empirical relations to adjust these nominal aerodynamic characteristics to account for the change in viscous effects along the trajectory.

3.6.2 ENTRY ANGLE STUDY. The configuration selected for the entry angle study was the orbital element of the FR-1, shown in Figure 2-16. This configuration was representative of all the orbital elements of the Integral Launch and Reentry Vehicle (ILRV) concepts being studied, and hence the temperature trends established apply to all concepts.

The trajectories used in the analyses for the FR-1 orbiter were numbered 113, 110, 120, and 114. Entry was from the 270-n. mi., 55-degree orbit, and all trajectories gave a nominal 800-n. mi. lateral range. The planform loading of the orbital element was 53.1 lb/ft^2. In respective trajectory number order the entry angles were -1.0, -1.5, -2.0 and -2.0 deg at 400,000 feet. Respective angles of attack were 40, 40, 35, and 30 deg. Respective bank angles were 25, 30, 20 and 0 deg. Entry velocities at 400,000 feet were 24,690, 24,450, 24,130, and 24,130 fps.

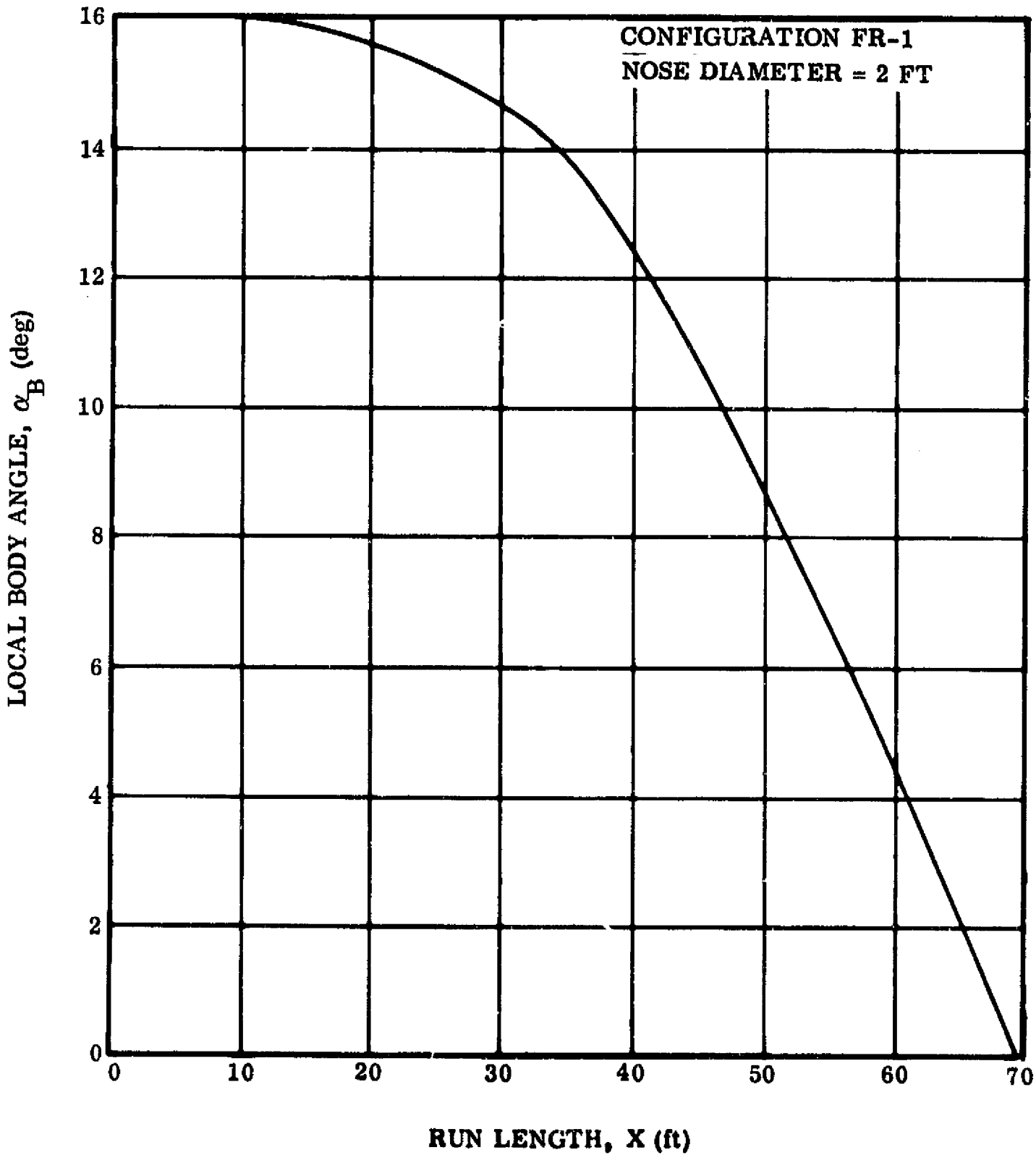

Figure 3-62. FR-1 ILRV Orbiter Lower Surface Local Body Angle Versus Distance From Nose

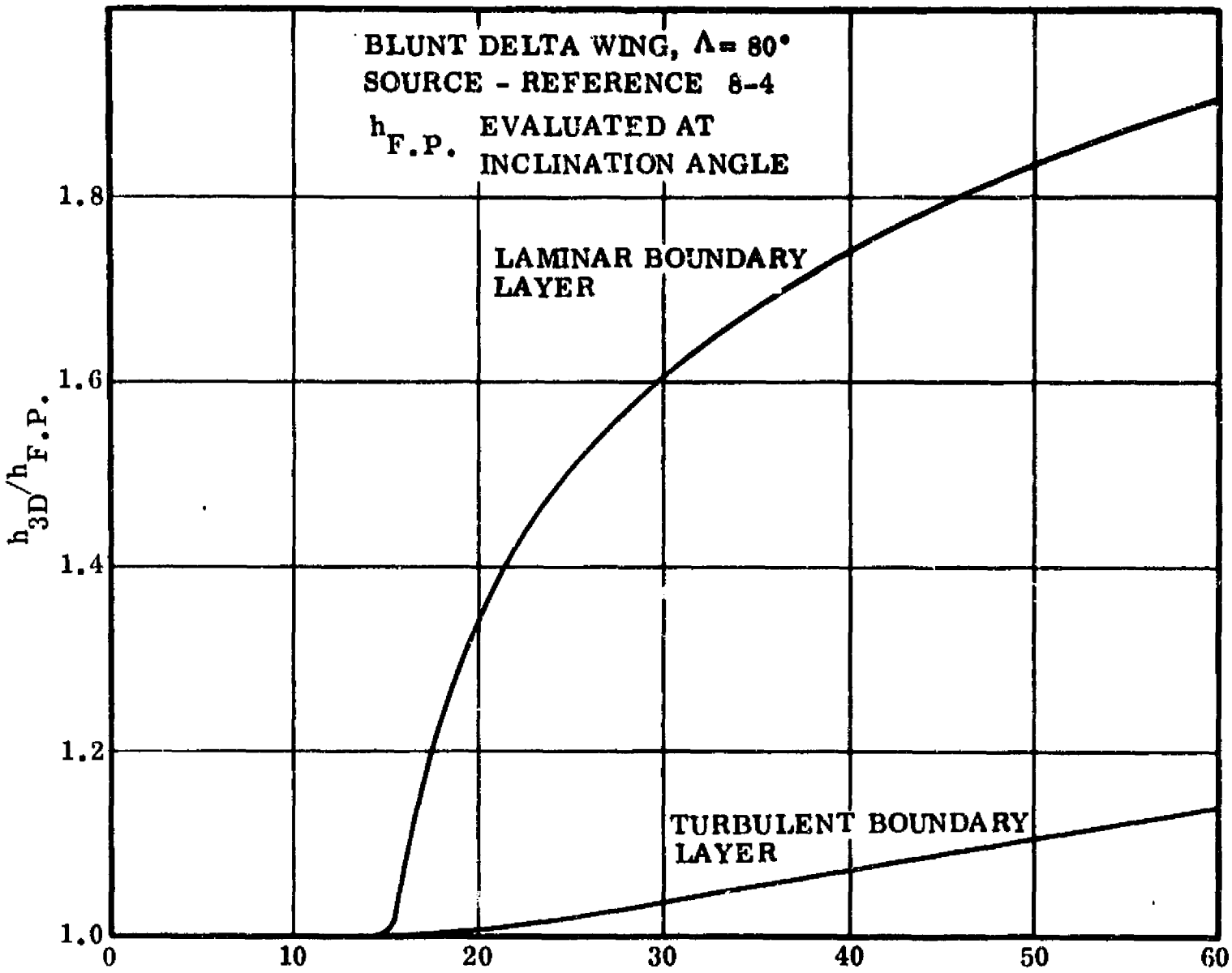

Figure 3-63. Heat Transfer Correction Due to Three-Dimensional Flow Effect on Lower Surface Centerline

Relative velocity relationships as well as altitude and relative velocity histories of the FR-1 orbiter during entry for different trajectories are presented in Figures 3-65 through 3-72. Some variation in pull-out altitudes and velocities readily can be noted.

Hot-wall heat transfer rate histories to the vehicle two-foot diameter nose and one-foot diameter fin leading edge are shown in Figure 3-73 for the -1.0 degree entry angle trajectory.

Radiation equilibrium temperature histories for the nose, lower surface, upper surface, and fin leading edge and outboard surface are plotted in Figures 3-74 through 3-80. The effect of the change in entry angle from -1.0 to -2.0 deg on the peak temperatures can be seen. In addition, the effect of the local body angle and the

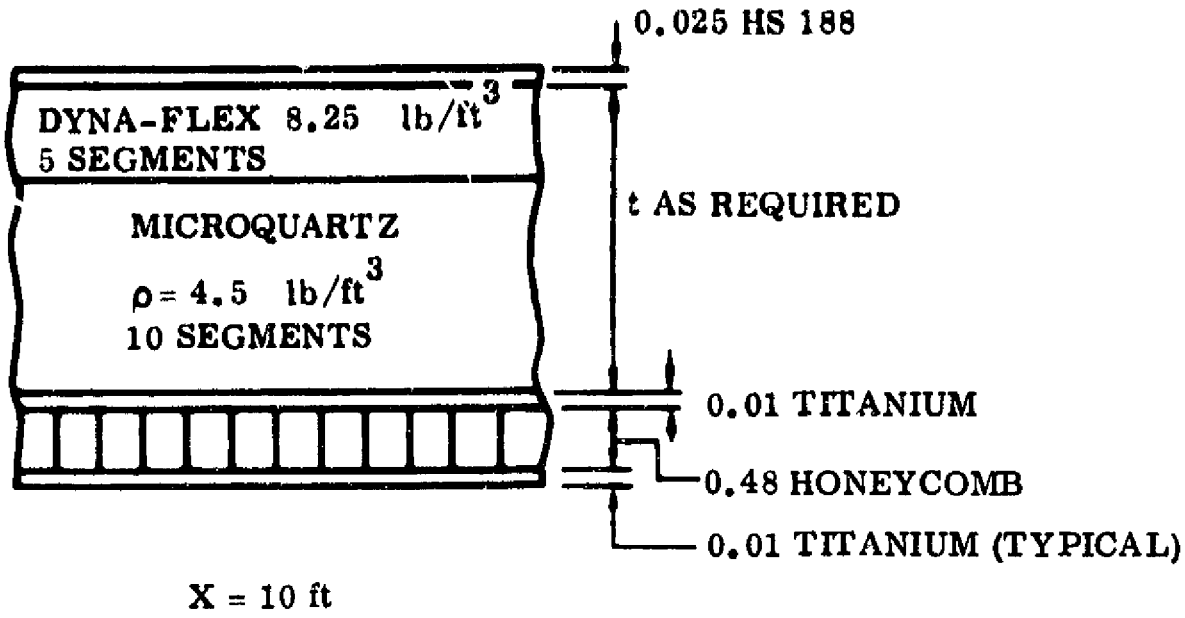

X = 10 ft

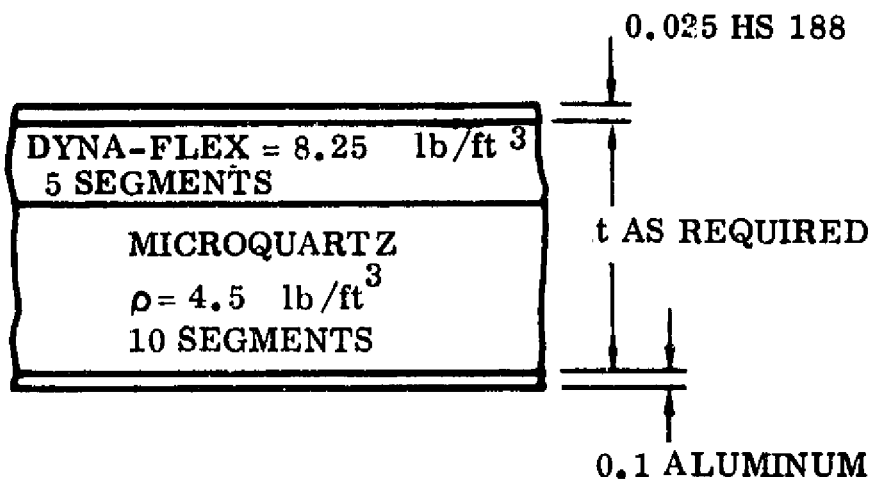

X = 60 ft

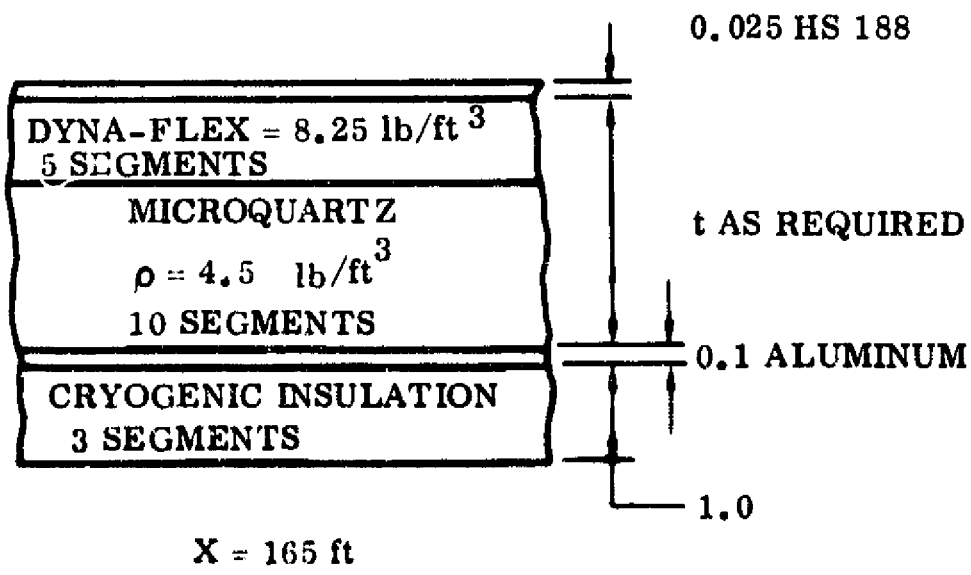

X = 165 ft

Figure 3-64. Insulation Thermodynamic Model

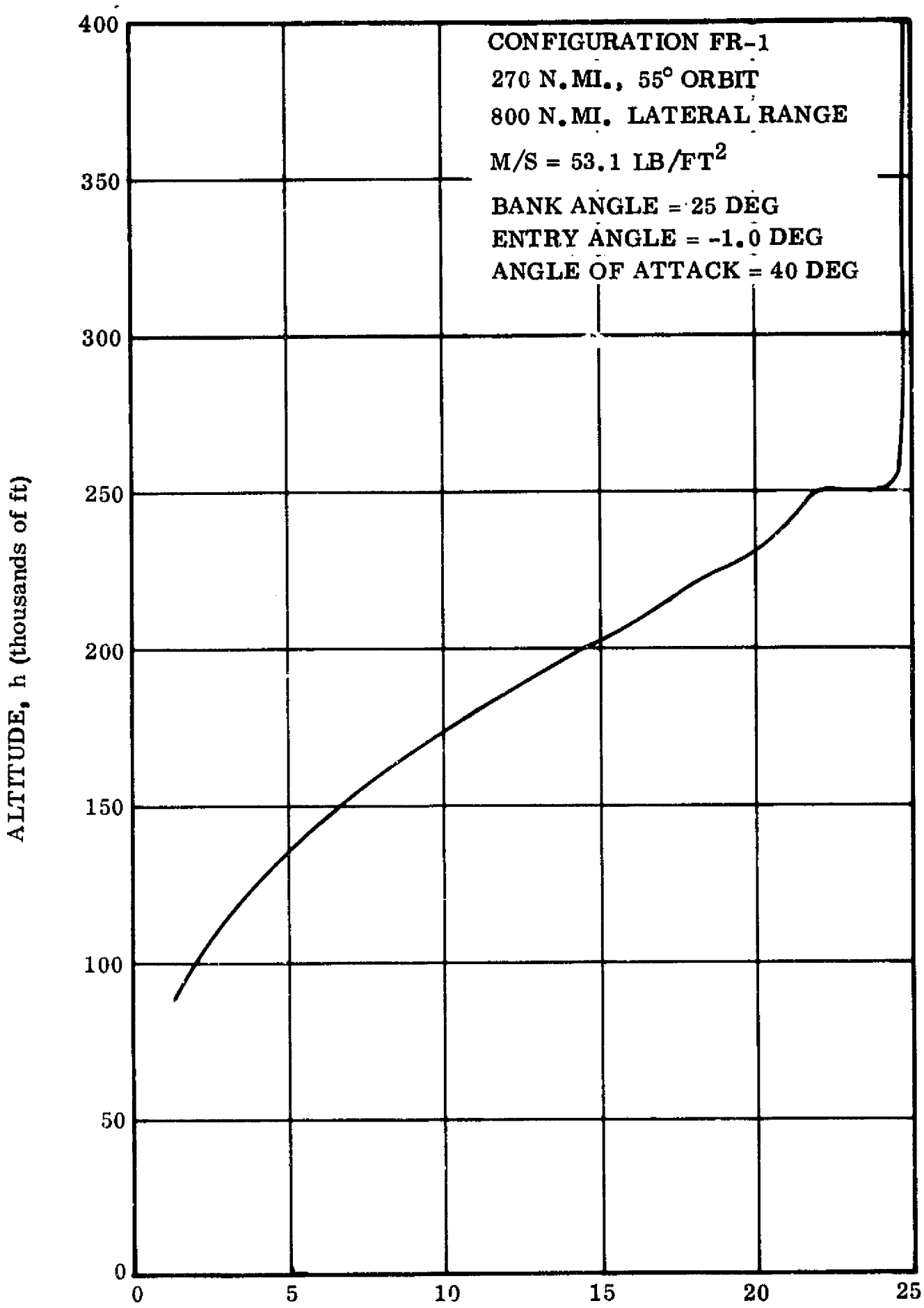

Figure 3-65. FR-1 ILRV Orbiter — Trajectory 113 — Altitude vs. Relative Velocity

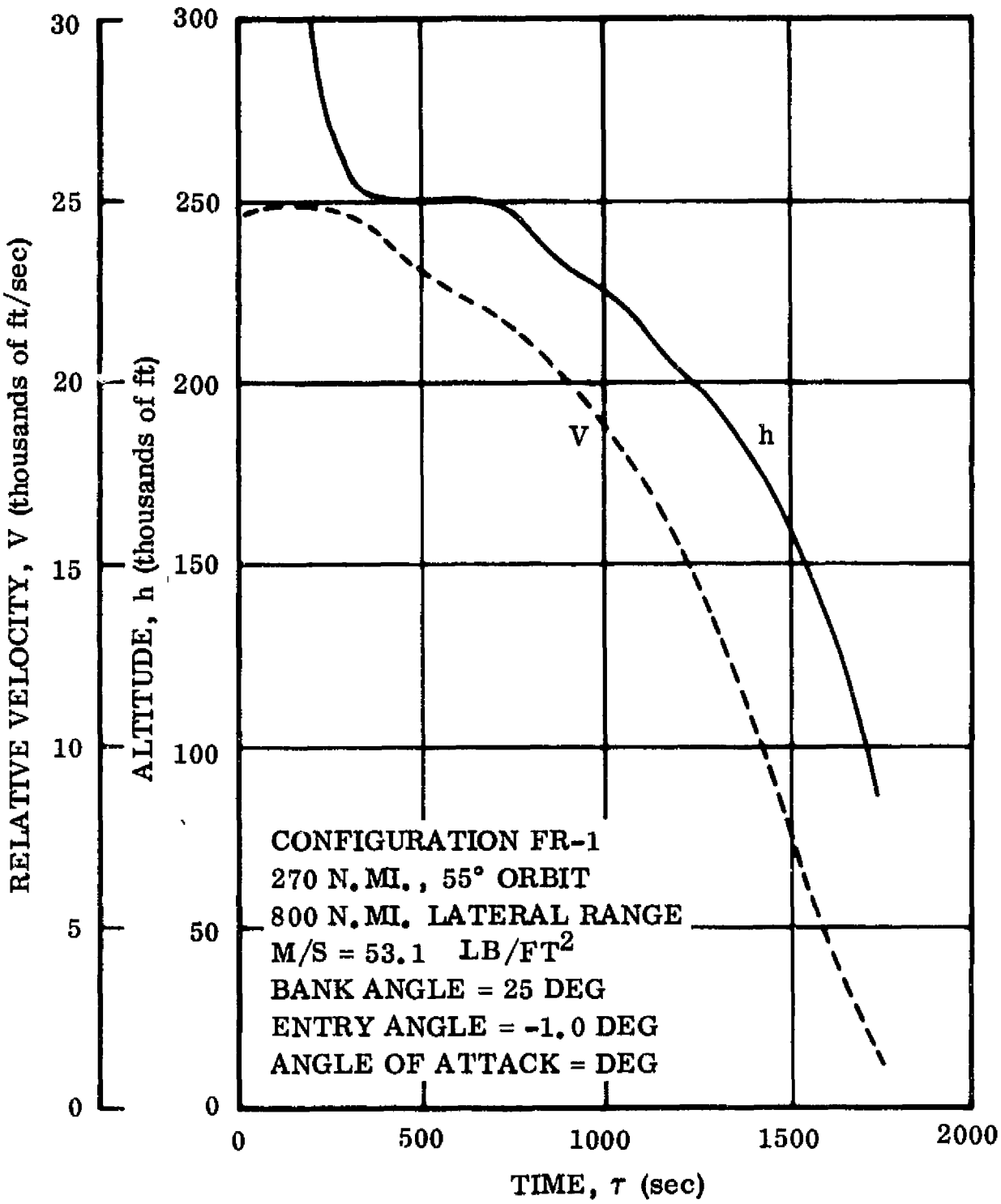

Figure 3-66. FR-1 ILRV Orbiter — Trajectory 113 — Altitude and Relative Velocity vs. Time

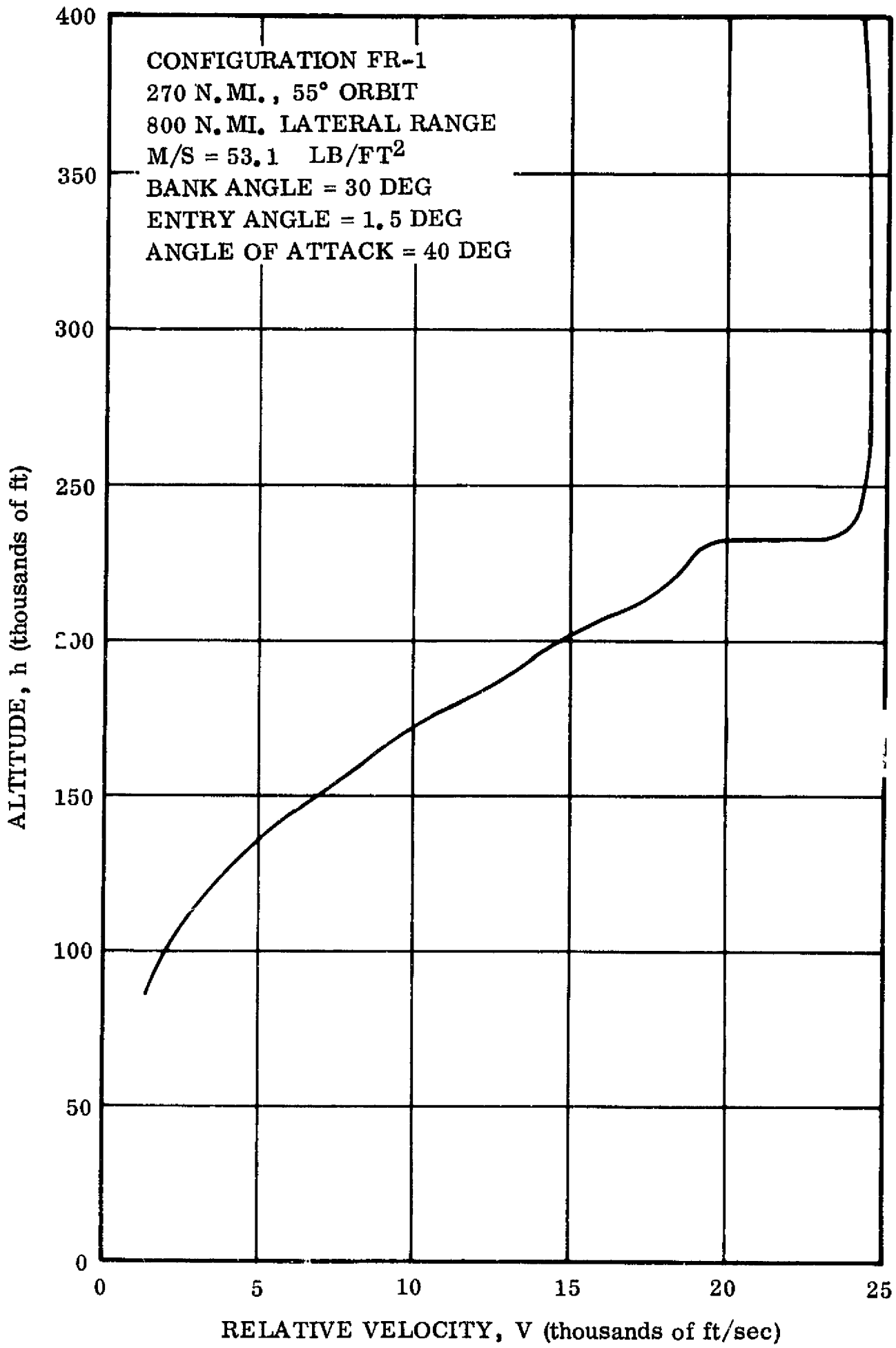

Figure 3-67. FR-1 ILRV Orbiter — Trajectory 110 — Altitude vs. Relative Velocity

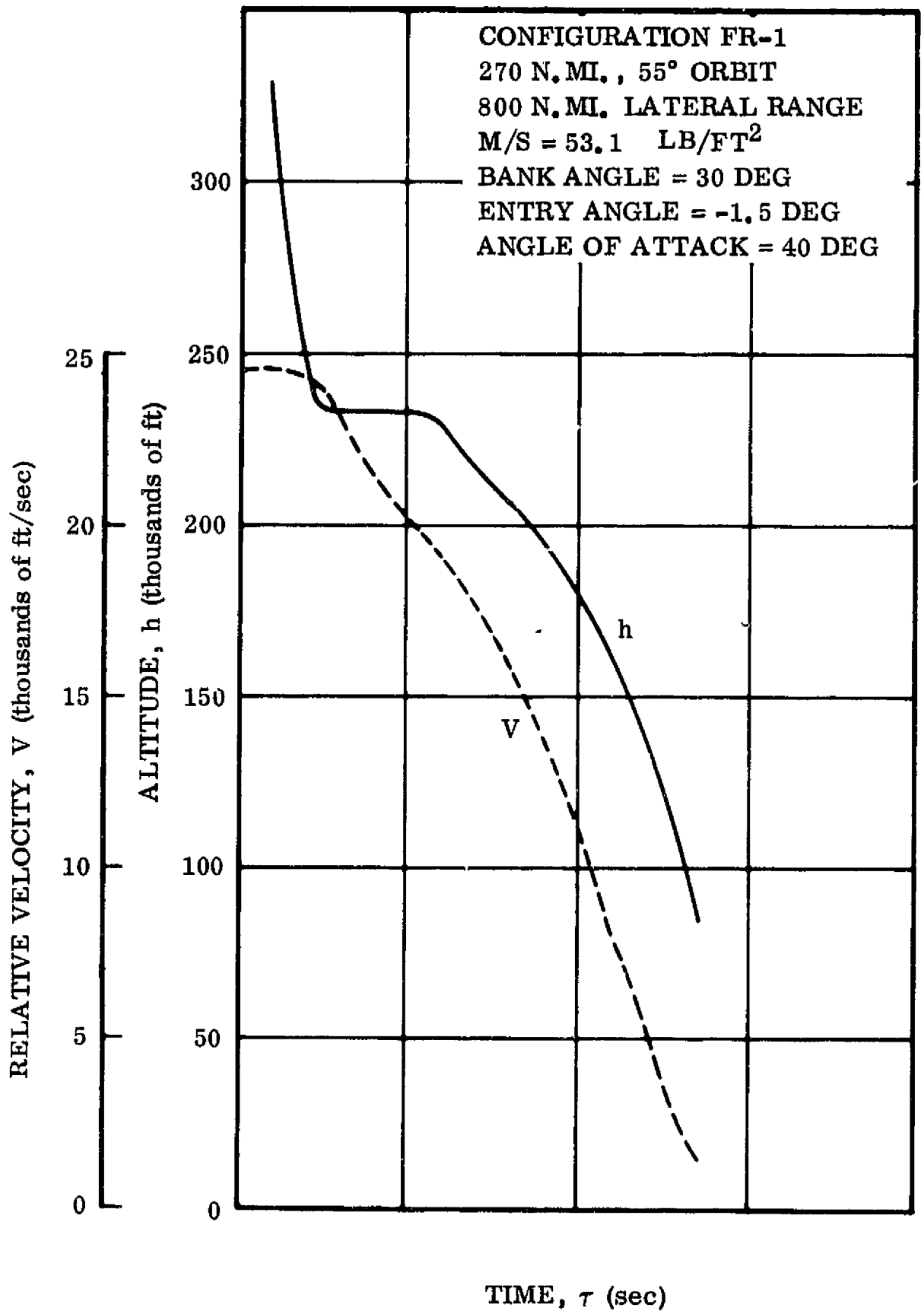

Figure 3-68. FR-1 ILRV Orbiter — Trajectory 110 — Altitude and Relative Velocity vs. Time

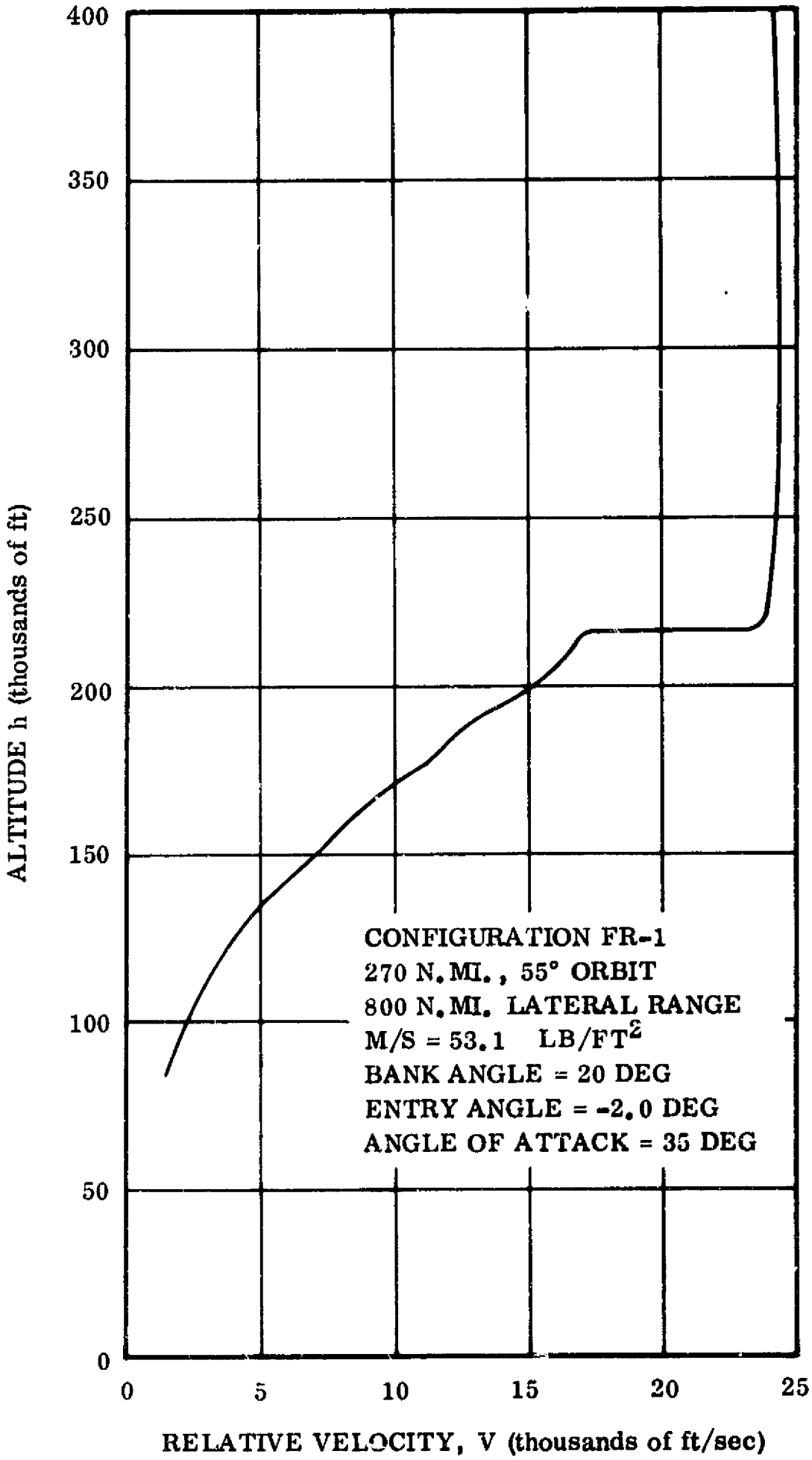

Figure 3-69. FR-1 ILRV Orbiter — Trajectory 120 — Altitude vs. Relative Velocity

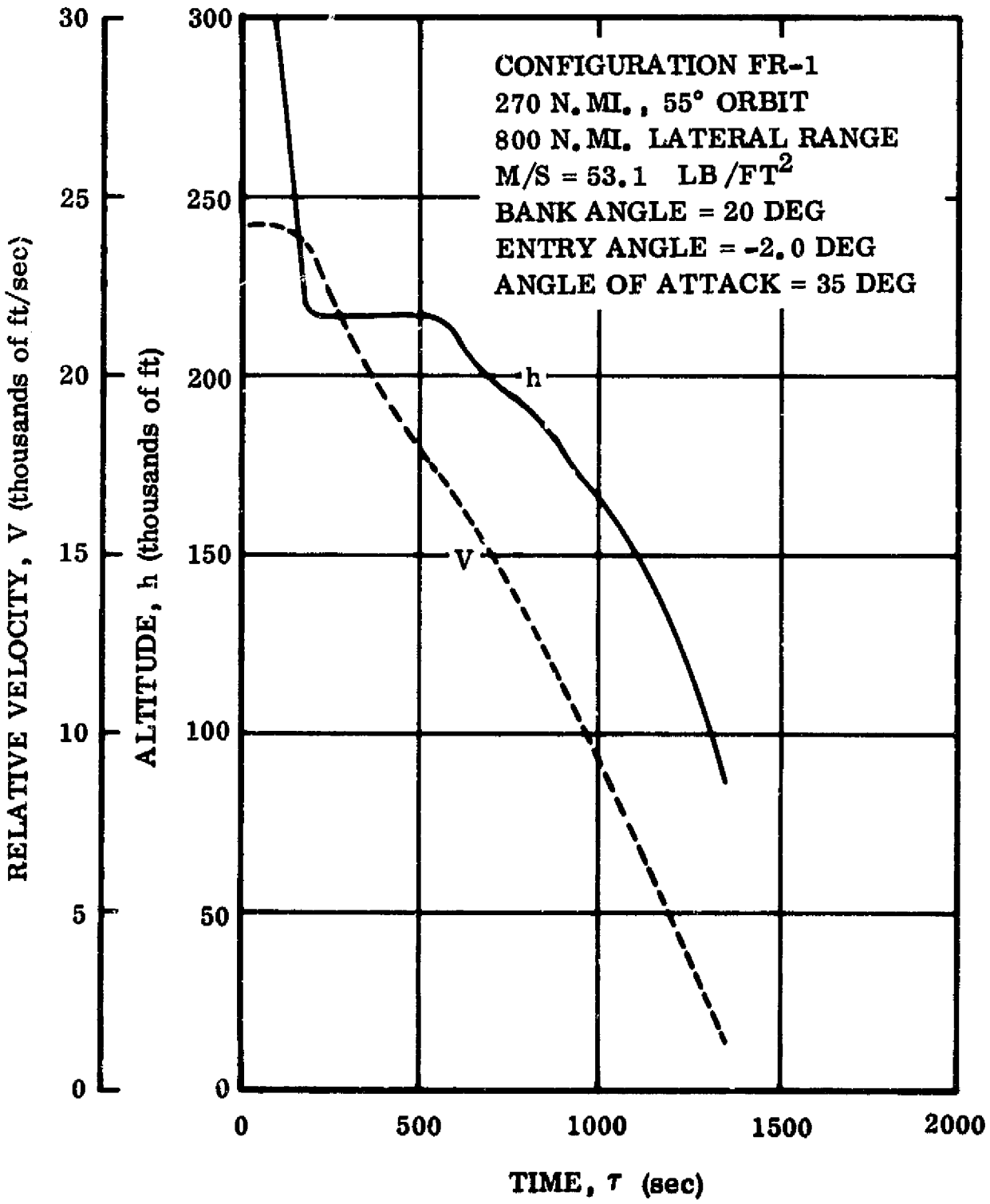

Figure 3-70. FR-1 ILRV Orbiter — Trajectory 120 — Altitude and Relative Velocity vs. Time

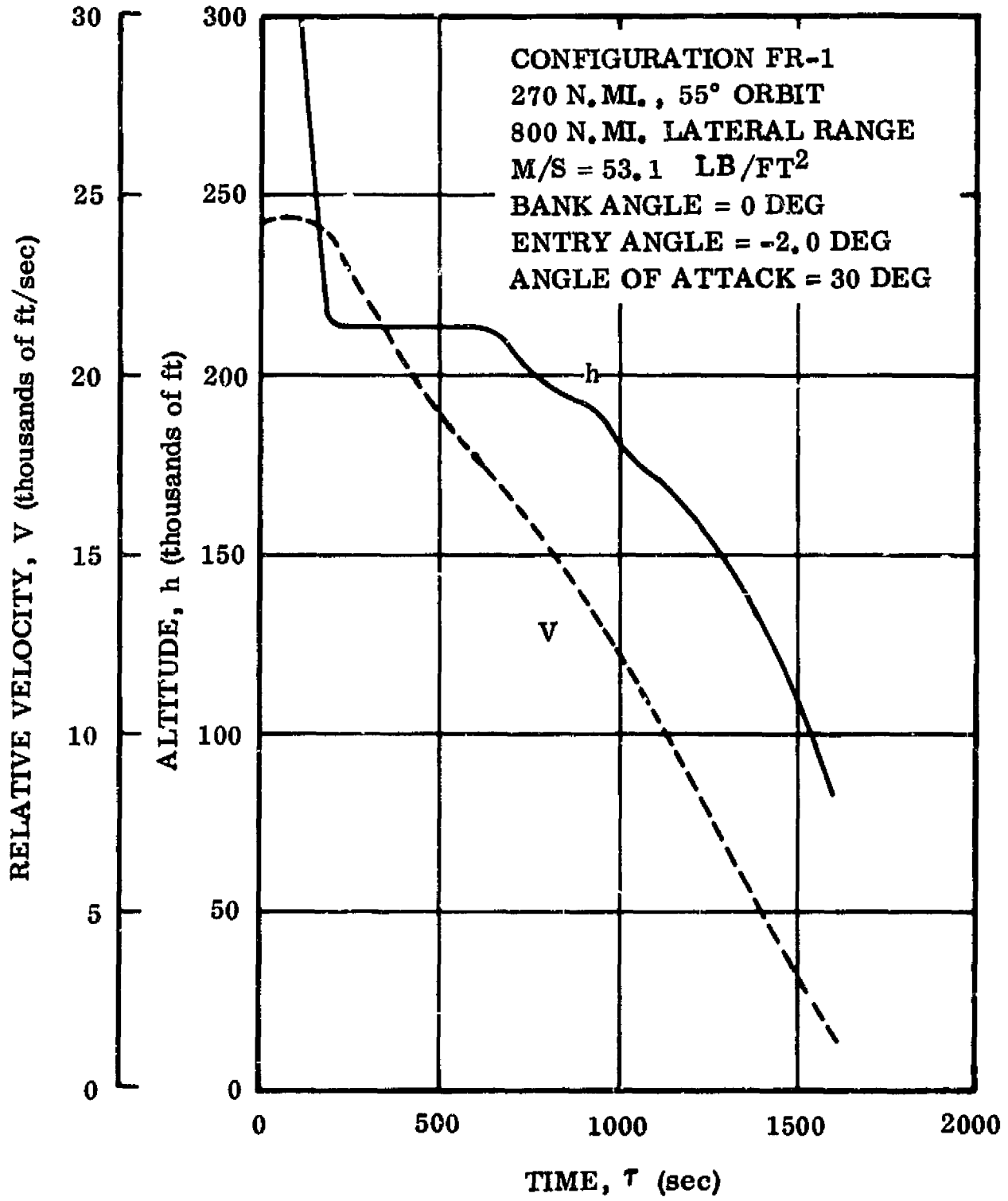

Figure 3-71. FR-1 ILRV Orbiter — Trajectory 114 — Aititude and Relative Velocity vs. Time

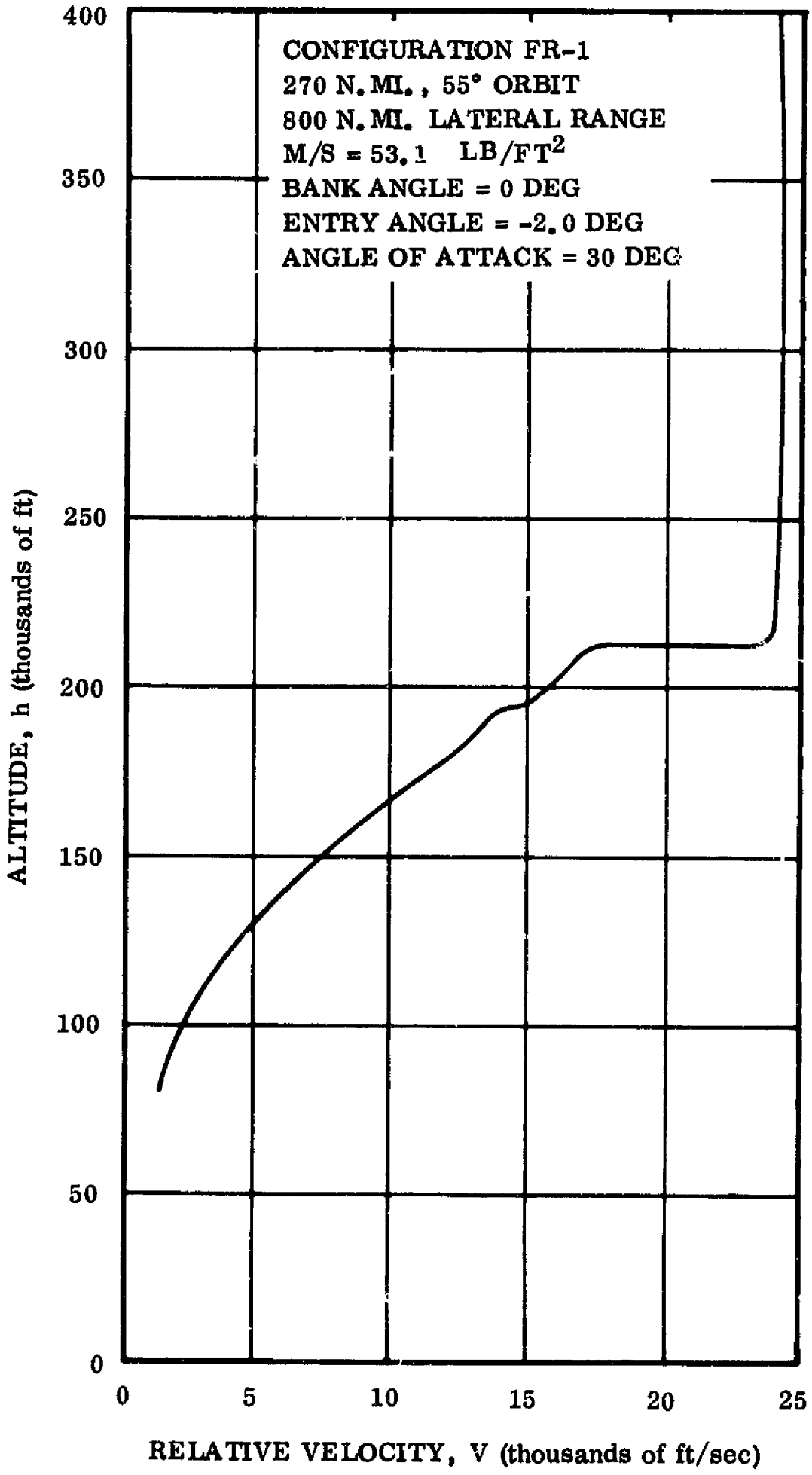

Figure 3-72. FR-1 ILRV Orbiter — Trajectory 144 — Altitude versus Relative Velocity

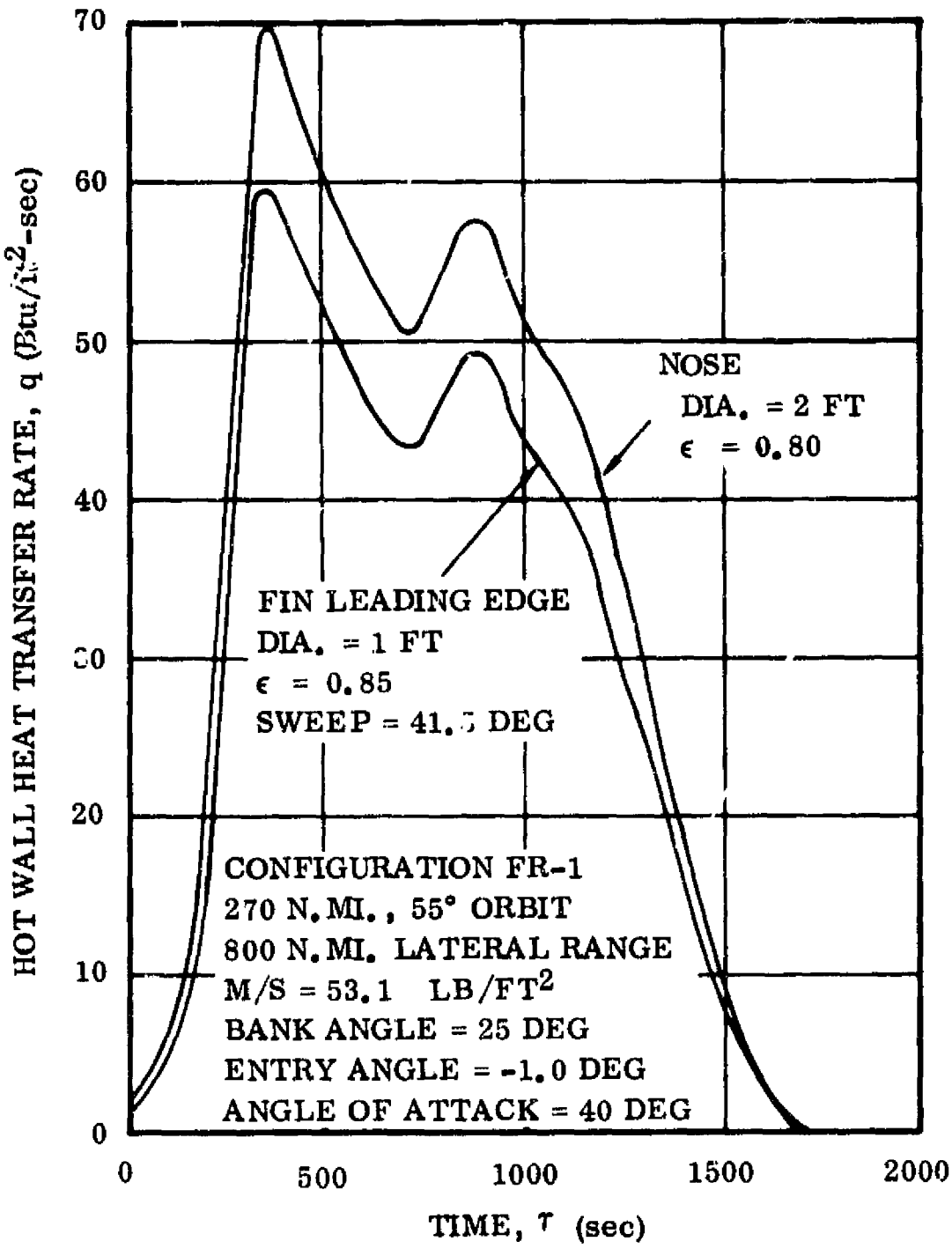

Figure 3-73. FR-1 ILRV Orbiter — Trajectory 113 — Nose and Fin Leading Edge Hot Wall Heat Transfer Rate vs. Time

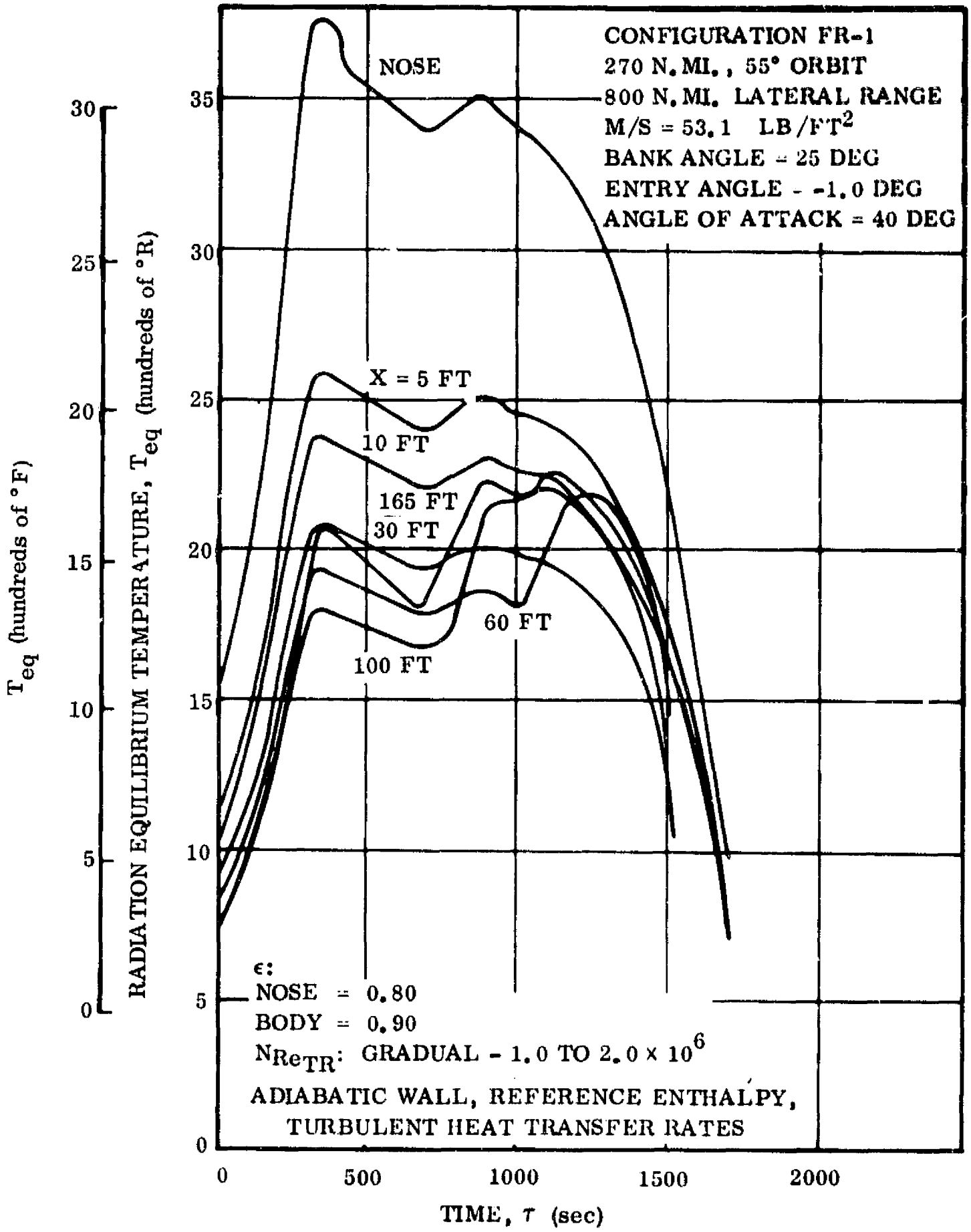

Figure 3-74. FR-1 ILRV Orbiter — Trajectory 113 — Nose and Lower Surface Temperature Histories

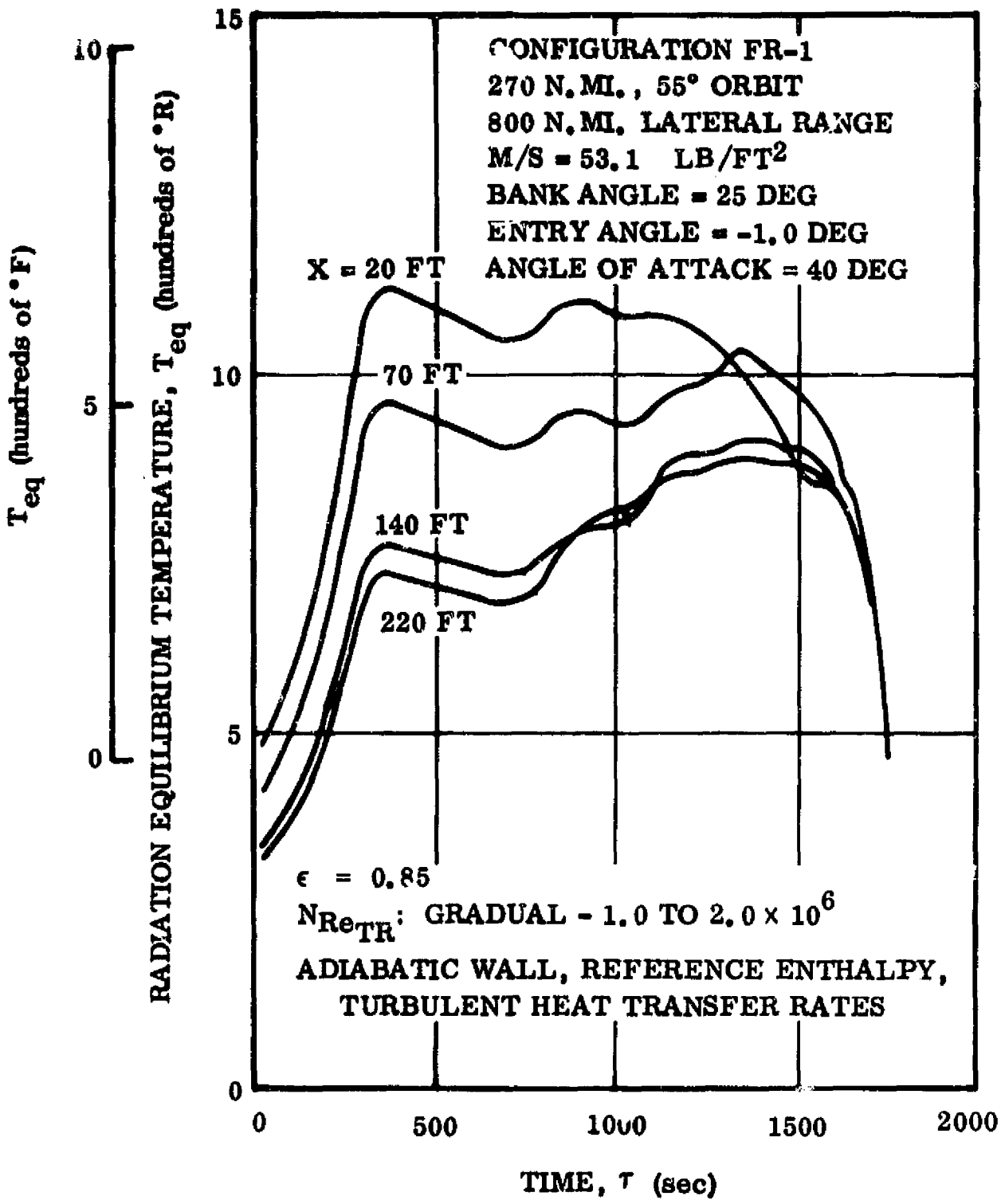

Figure 3-75. FR-1 ILRV Orbiter — Trajectory 113 — Upper Surface Temperature Histories

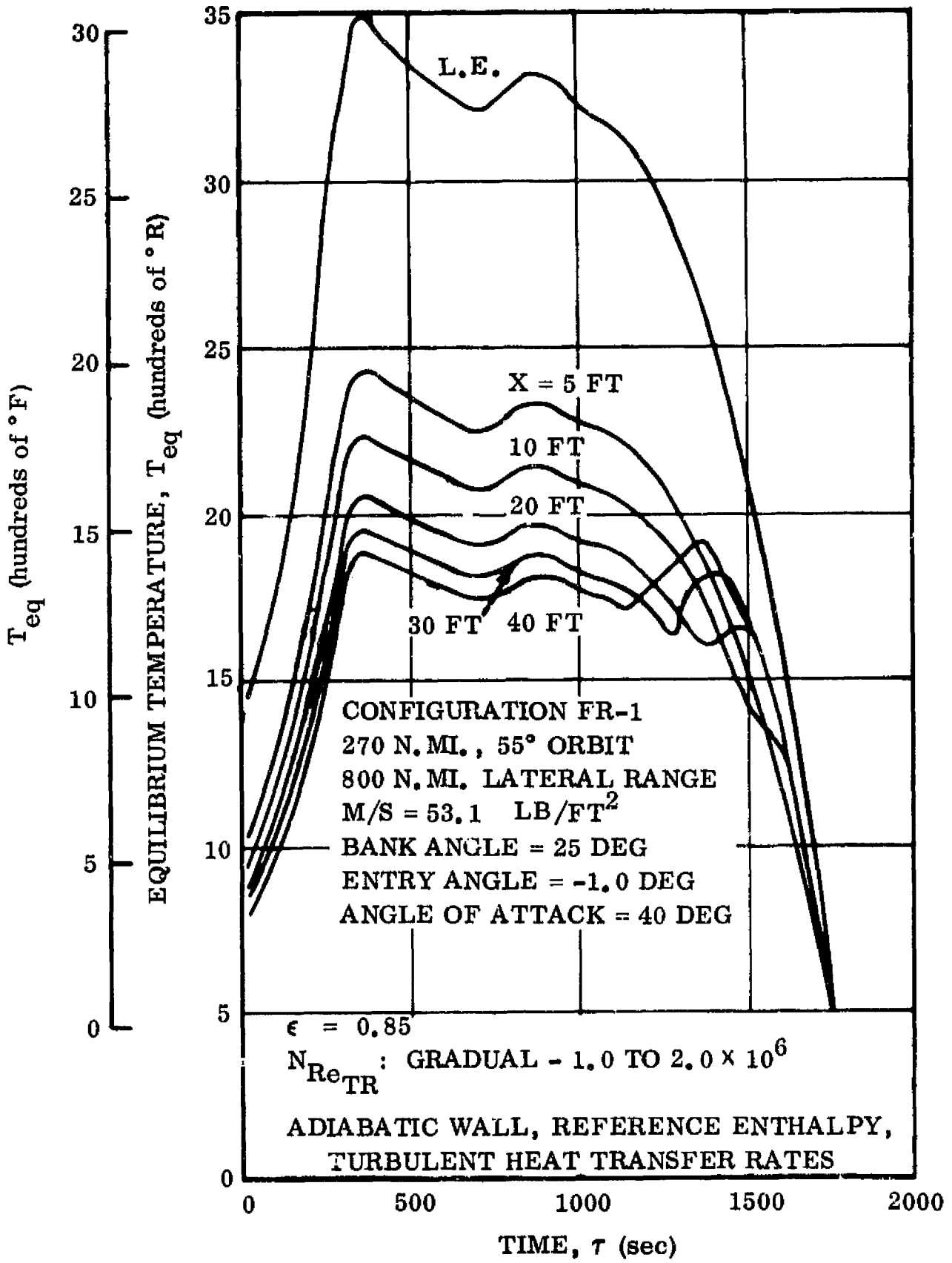

Figure 3-76. FR-1 ILRV Orbiter — Trajectory 113 — Fin Temperature Histories

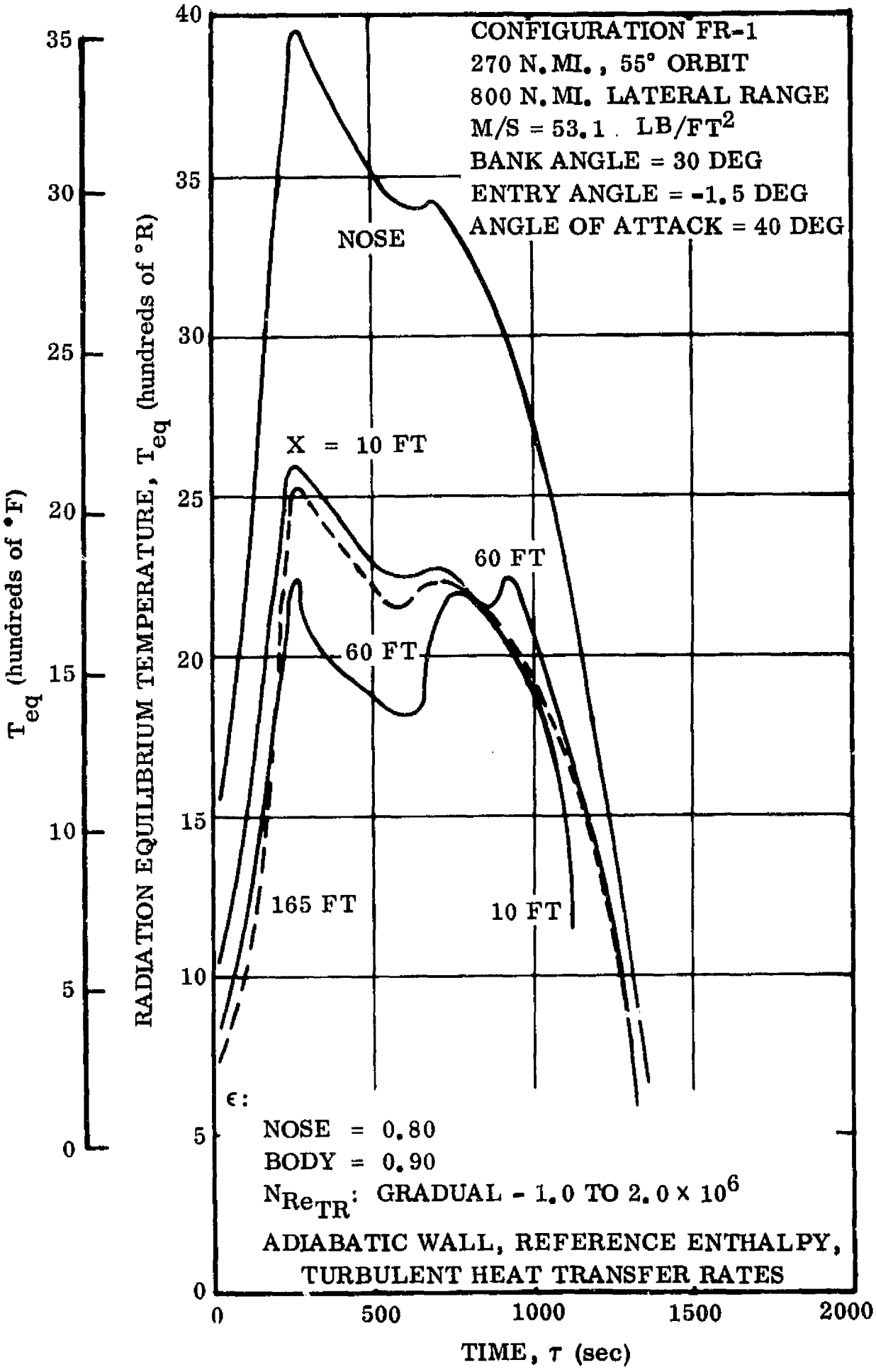

Figure 3-77. FR-1 ILRV Orbiter — Trajectory 110 — Nose and Lower Surface Temperature Histories

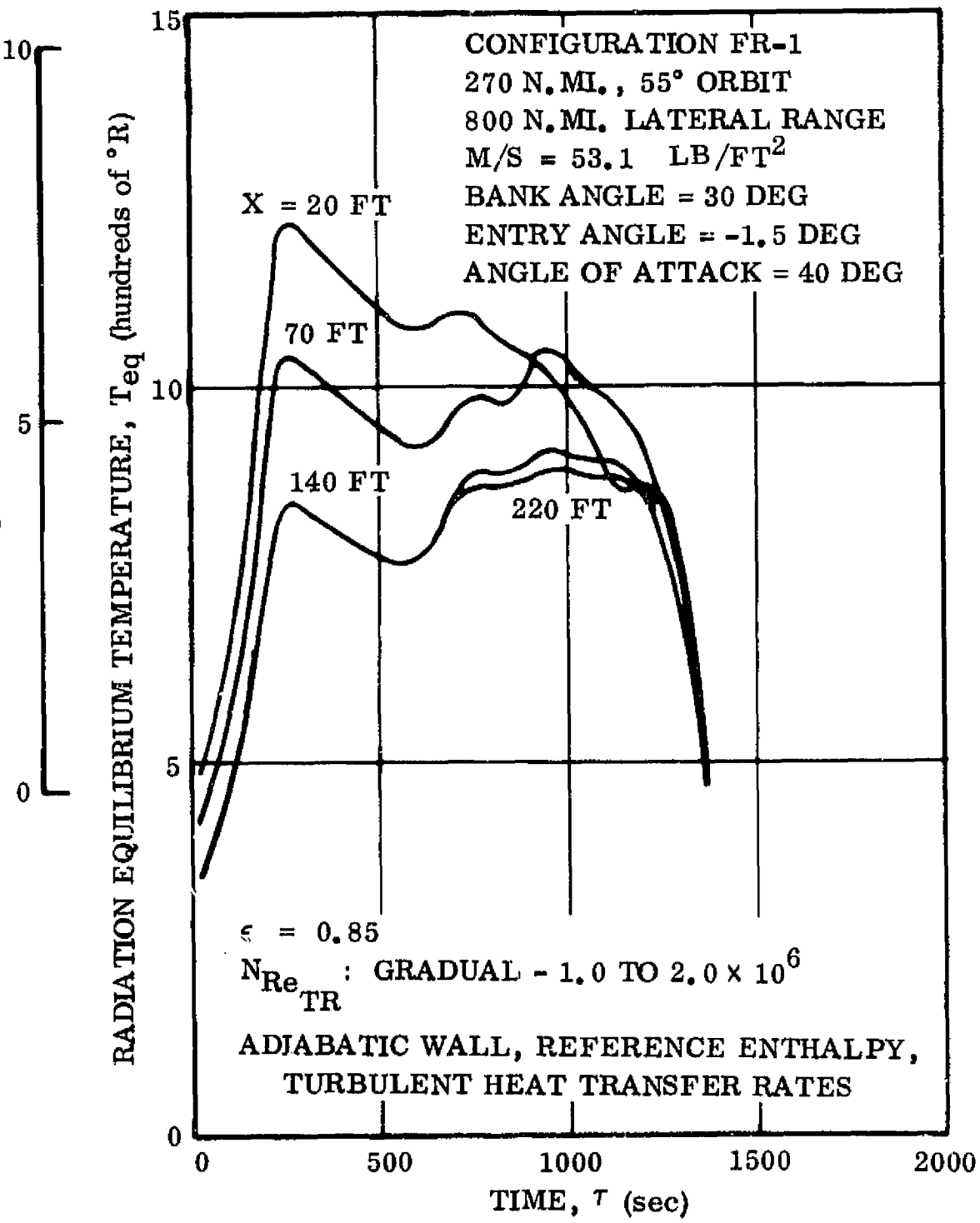

Figure 3-78. FR-1 ILRV Orbiter — Trajectory 110 — Upper Surface Temperature Histories

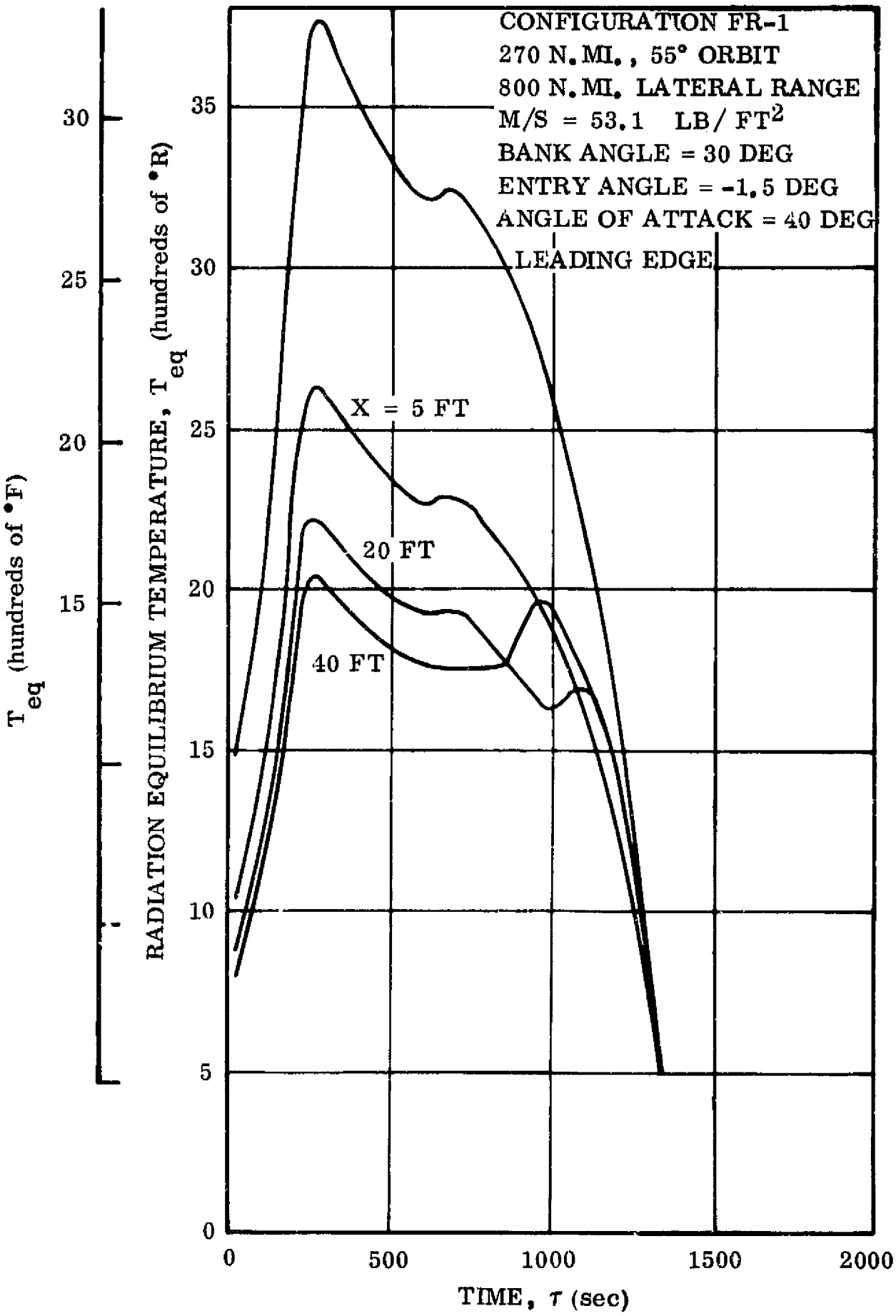

Figure 3-79. FR-1 ILRV Orbiter — Trajectory 110 — Fin Leading Edge and Surface Temperature Histories

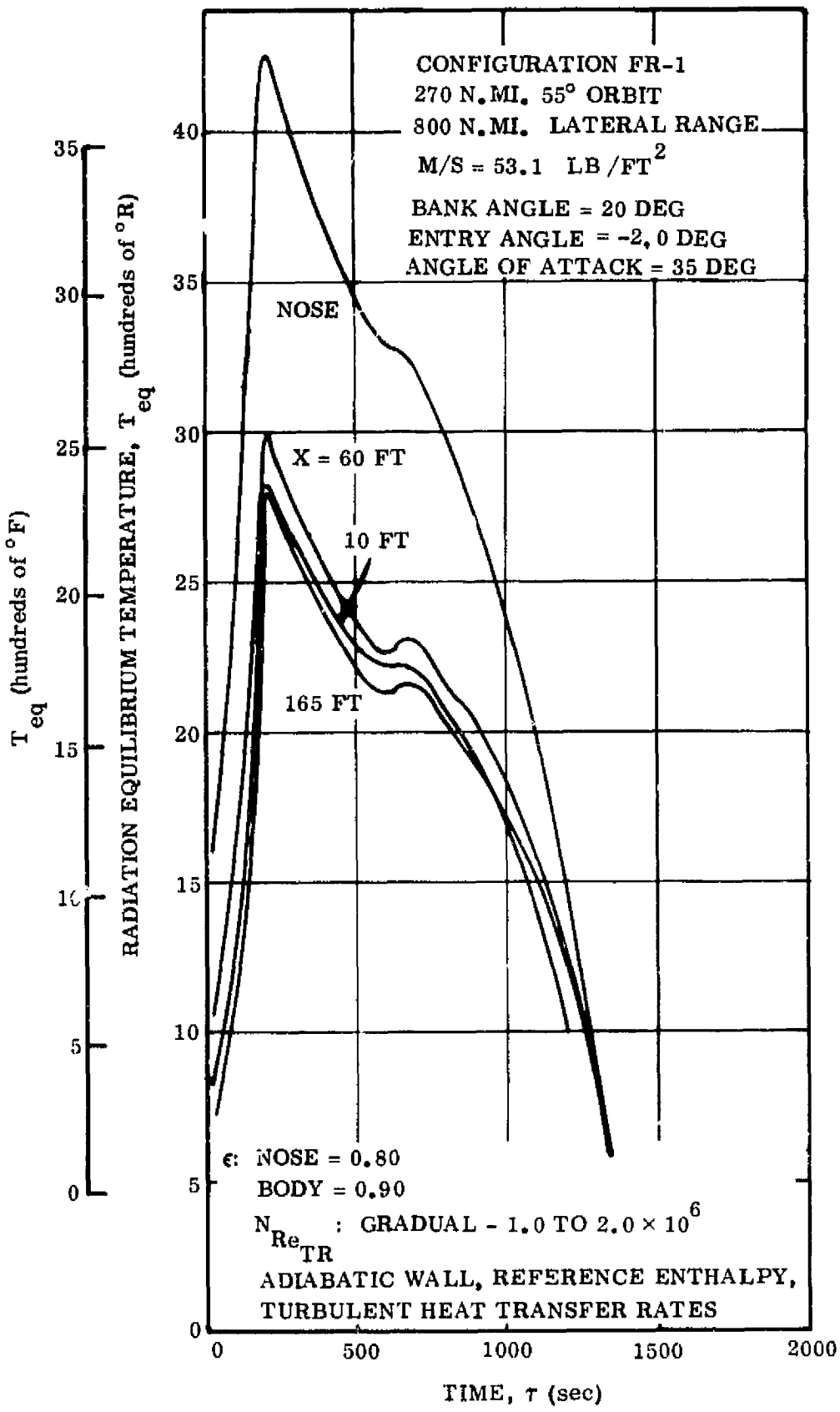

Figure 3-80. FR-1 HLRV Orbiter — Trajectory 120 — Nose and Lower Surface Temperature Histories

distance aft of the nose, X, is observed. Table 3-7 lists the maximum radiation equilibrium temperatures of the nose and lower surface for the trajectories analyzed. The entry angle effect on the peak lower surface temperatures has been plotted in Figure 3-81. This variation led to the selection of the -1.0 degree entry angle. Figure 3-82 also indicates vehicle surface materials as well as the peak temperature distribution for Trajectory 113 (-1.0 deg entry angle).

Insulation thickness requirements were based on limiting the structural temperature to 660°R (200°F) before or at a time 60 seconds after landing. The structural temperature at X = 10 feet was the value of the honeycomb inner faceplate, and at X = 60 and X = 165 feet was the value of the 0.1-inch aluminum tank wall, Figure 3-64. Figure 3-81 shows the lower surface average insulation thickness as a function of entry angle.

The results shown on Figure 3-81 all pointed toward the selection of a -1.0 deg entry angle. Hence, the remainder of the study was conducted at this entry angle.

3.6.3 STAGING CONDITION STUDY. An aerothermodynamic analysis was performed on the first element of the two-element sequential burn vehicle configuration (FR-3) shown in Figure 2-3. Figures 3-83 through 3-88 present the recovery trajectories for staging velocities of 9,450, 10,510, and 11,720 fps at a dynamic pressure of 50 psf. Similar trajectories were obtained for a staging velocity at 10,510 fps and dynamic pressures of 75 and 100 psf. Temperature/radiation equilibrium histories were calculated at various locations on the vehicle lower surface, upper surface, and fin outboard surface for the five trajectories. Figure 3-89 presents the lower surface contour. The peak temperature results are plotted on Figure 3-90 as a function of staging dynamic pressure (q_A) and staging velocity. Also shown on the curve of temperature versus q_A is the variation in gross liftoff weight (GLOW) with q_A for a thrust-to-weight ratio of 1.392. The lower surface temperature was at a minimum at q_A = 75 psf while the GLOW was a minimum at q_A = 50 psf. Since the temperature was only approximately 50° R less at q_A = 75 psf than at 50 psf, the staging q_A was selected at 50 psf to minimize the GLOW. The surface temperatures increased with staging velocity at the q_A of 50 psf. A temperature limit of 1,260°R (800°F) on the upper surface (811 titanium) limited the staging velocity to 11,000 fps. Also, the lower surface temperature was below the temperature limit of 2,260°R (1,800°F) for L605 cover panels (heat shields).

The variation of GLOW with staging velocity has been shown in Section 2 for the individual two-stage vehicles and parametrically in this section.

The resulting staging condition was then determined to be at a staging velocity of 11,000 fps and a staging dynamic pressure of 50 psf. Figure 3-91 presents the peak temperature distribution for a staging velocity of 10,510 fps and q_A = 50 psf. This is representative of the selected staging condition and results in 811 titanium upper surface and L605 lower surface cover panels for the outer skin. Sizing of an

Table 3-7. ILRV Orbiter Maximum Radiation Equilibrium Temperatures for the Nose and Lower Surface

Trajectory (800 n. mi. Lateral Range)					
Distance	113	110	120	114	105
Aft of	$\alpha = 40^{o}$	40^{o}	35^{o}	30^{o}	20^{o}
Nose,	$\Psi = -25^{o}$	-30^{o}	-20^{o}	0^{o}	0^{o}
X (ft)	$\gamma = -1.0^{o}$	-1.5^{o}	-2.0^{o}	-2.0^{o}	-1.5^{o}
	Temperatures In Degrees Fahrenheit				
5	2125	2355	2610	2680	2610
10	1910	2130	2360	2422	2400
20	1720	1920	2140	2190	2125
30	1620	1810	2010	2280	2200
40	1560	1740	2340	2560	2410
60	1665	1780	2530	2540	2280
100	1790	2110	2400	2370	2050
165	1750	2070	2335	2310	1995
Nose	3204	3499	3788	3876	3908

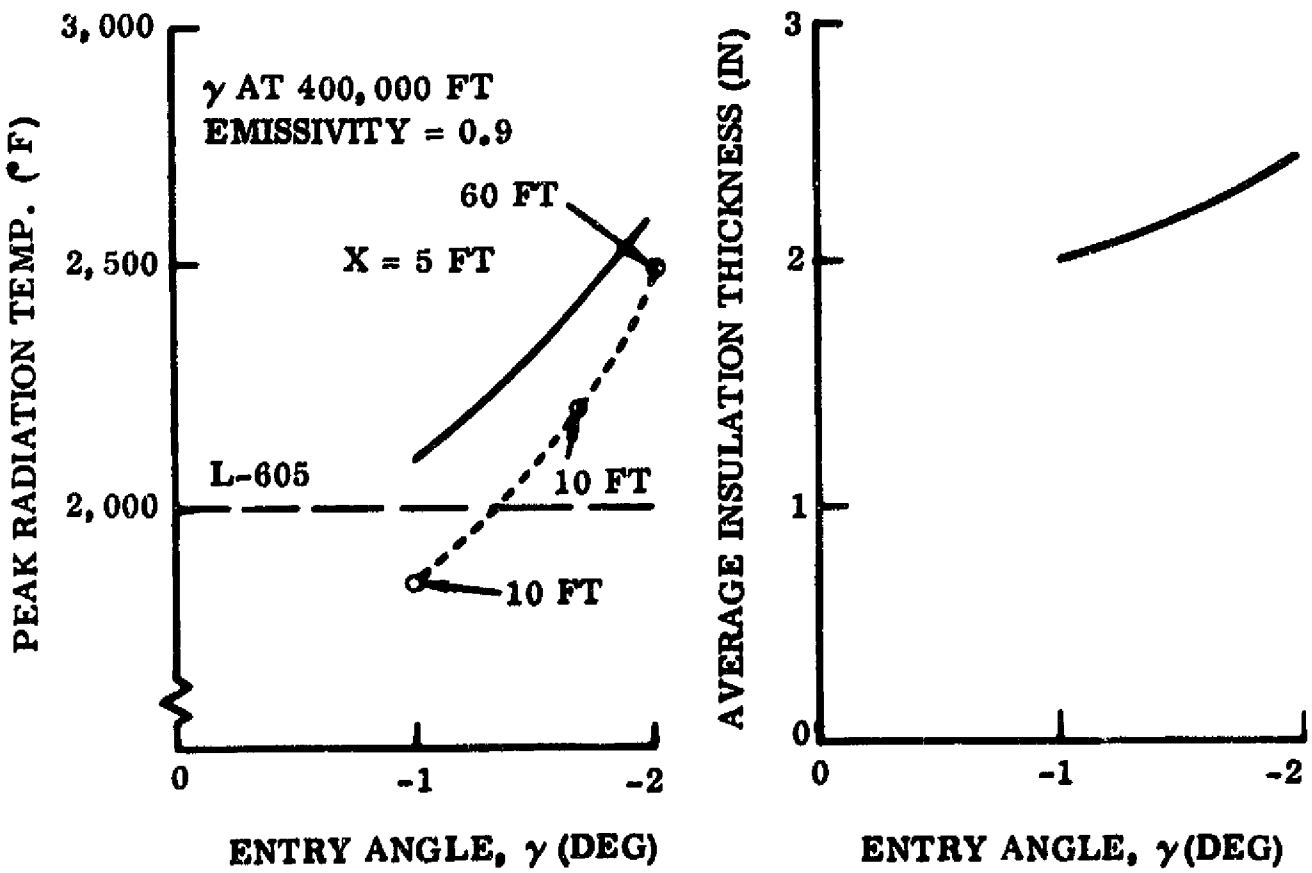

Figure 3-81. FR-1 ILRV Orbiter — Temperature and Insulation Thickness vs. Entry Angle — Lower Surface

insulation system composed of the cover panels and a Microquartz blanket indicated that 0.7 inch of insulation at X = 10 feet, and approximately 0.125 inch in the propellant tank area on the lower surface would maintain a 660°R (200°F) peak structural temperature. The upper surface would require 0.15 inch at X = 10 feet and no insulation in the propellant tank areas to maintain 660°R (200°F) or lower structural temperature peak.

3.7 PROPULSION

All propulsion data used in the two-stage vehicle studies is contained in Volume VI, which gives detail performance, configuration, and weight data for the high chamber pressure bell engine. All vehicles studied were assumed to have an increased thrust rating at liftoff. The basis for the liftoff rating is the actual maximum thrust capability for the engine, which has a design mixture ratio (MR) band of 5.0 to 7.0 with maximum thrust at MR = 6.4. This is discussed in detail in Section 2.5 of Reference 3-5.

In base-area-limited configurations, area ratios used were the maximum that would fit into available space, with a minimum of one-foot clearance between nozzle exits. Where space available was sufficient, a maximum area ratio of 150 was used. Resulting I_{sp} values are given in the synthesis summary for each vehicle.

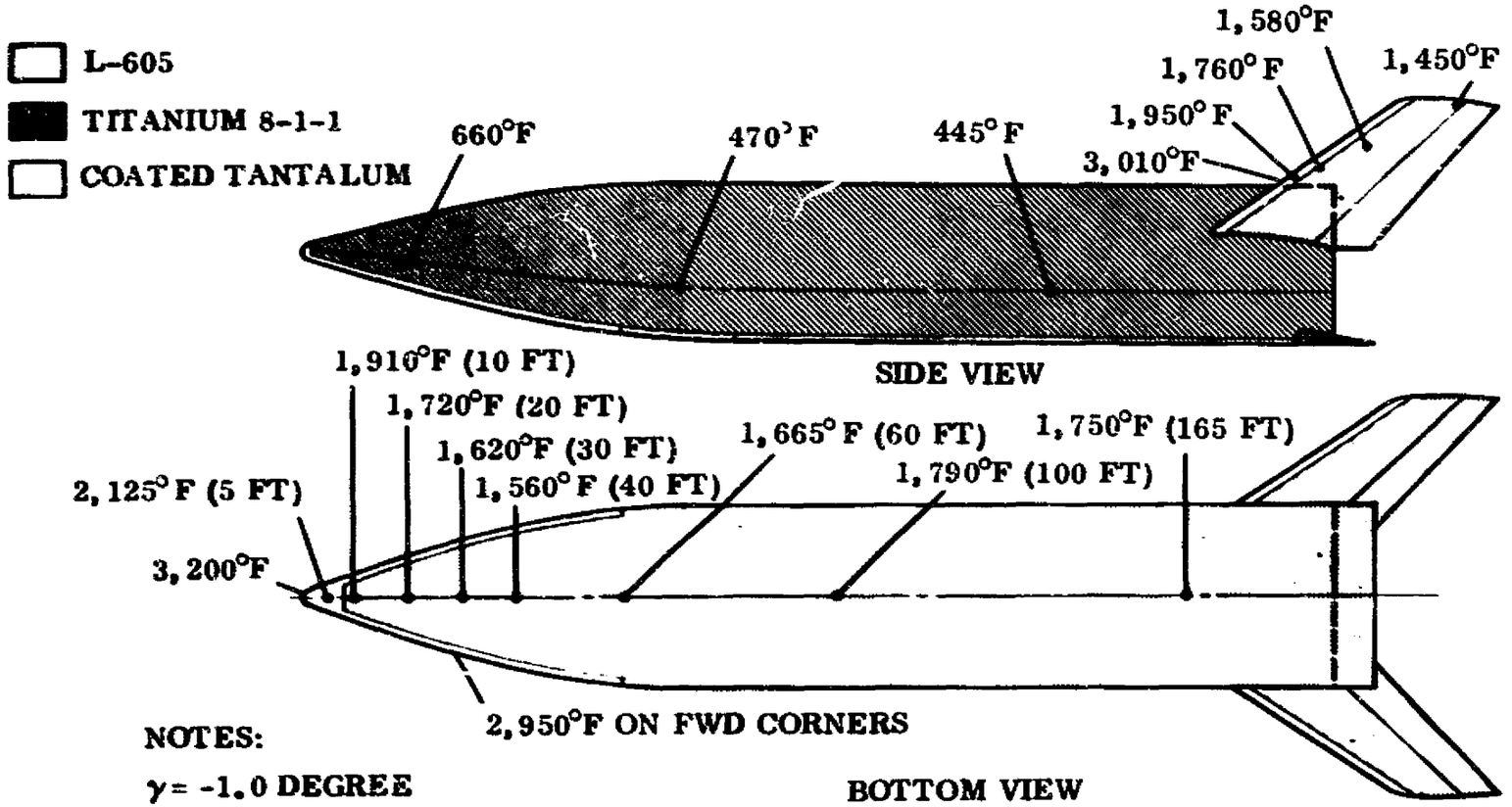

Figure 3-82. FR-1 ILRV Orbiter — Surface Materials and Peak Entry Temperature Distribution — Trajectory 113

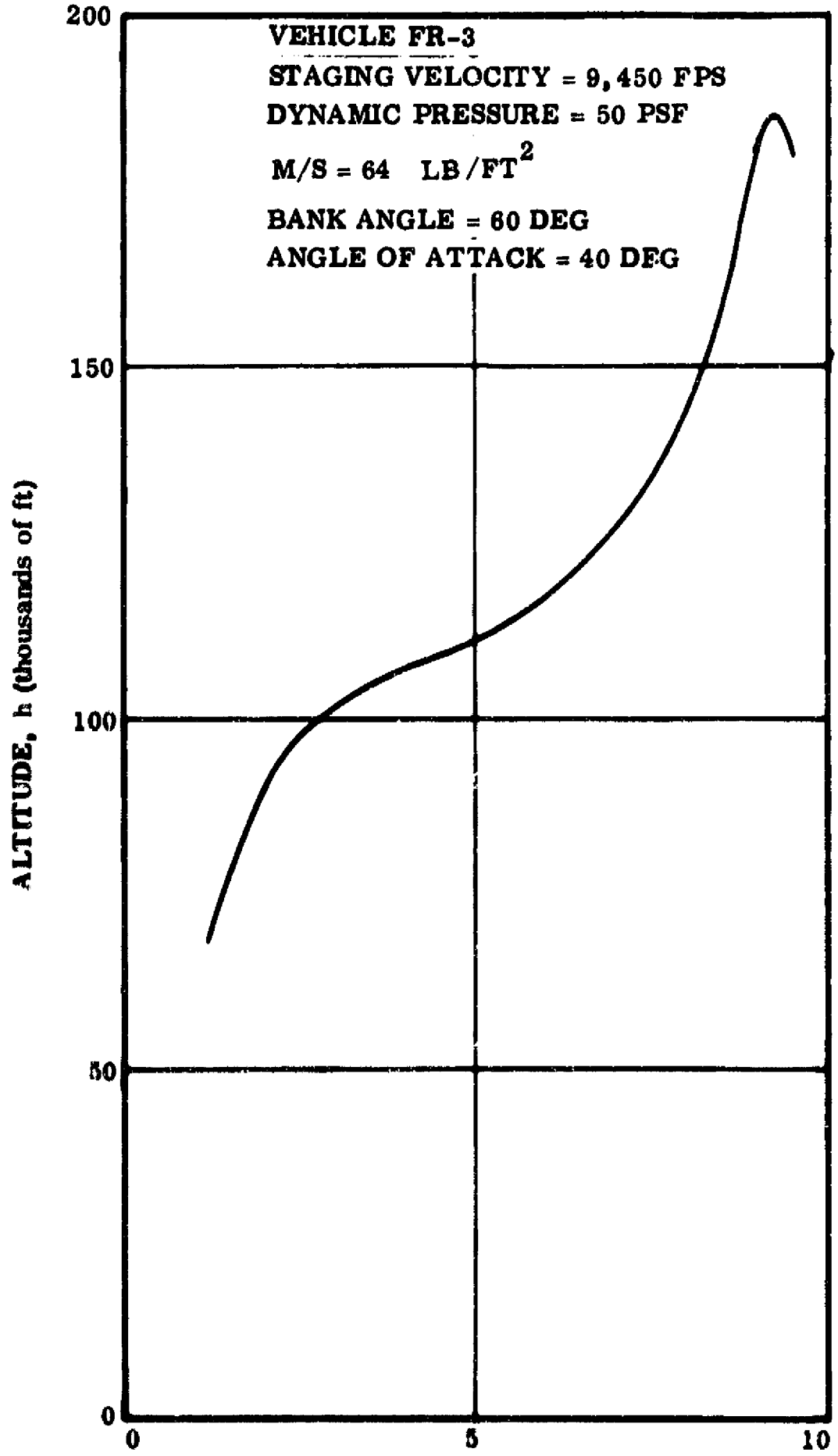

Figure 3-83. Two-Element ILRV, First Element — Trajectory 325 — Altitude versus Relative Velocity

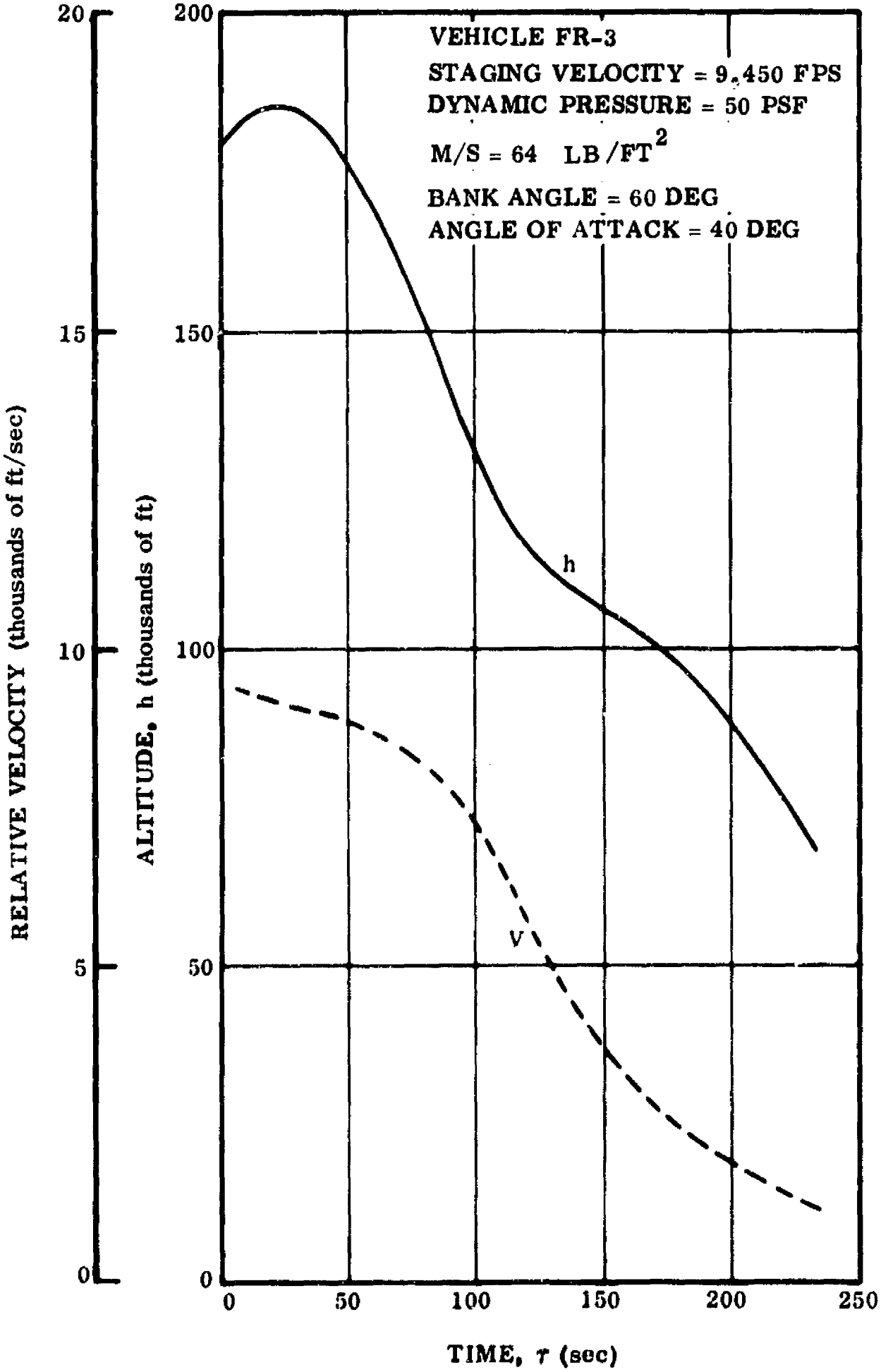

Figure 3-84. Two-Element ILRV, First Element — Trajectory 325 — Altitude and Relative Velocity versus Time

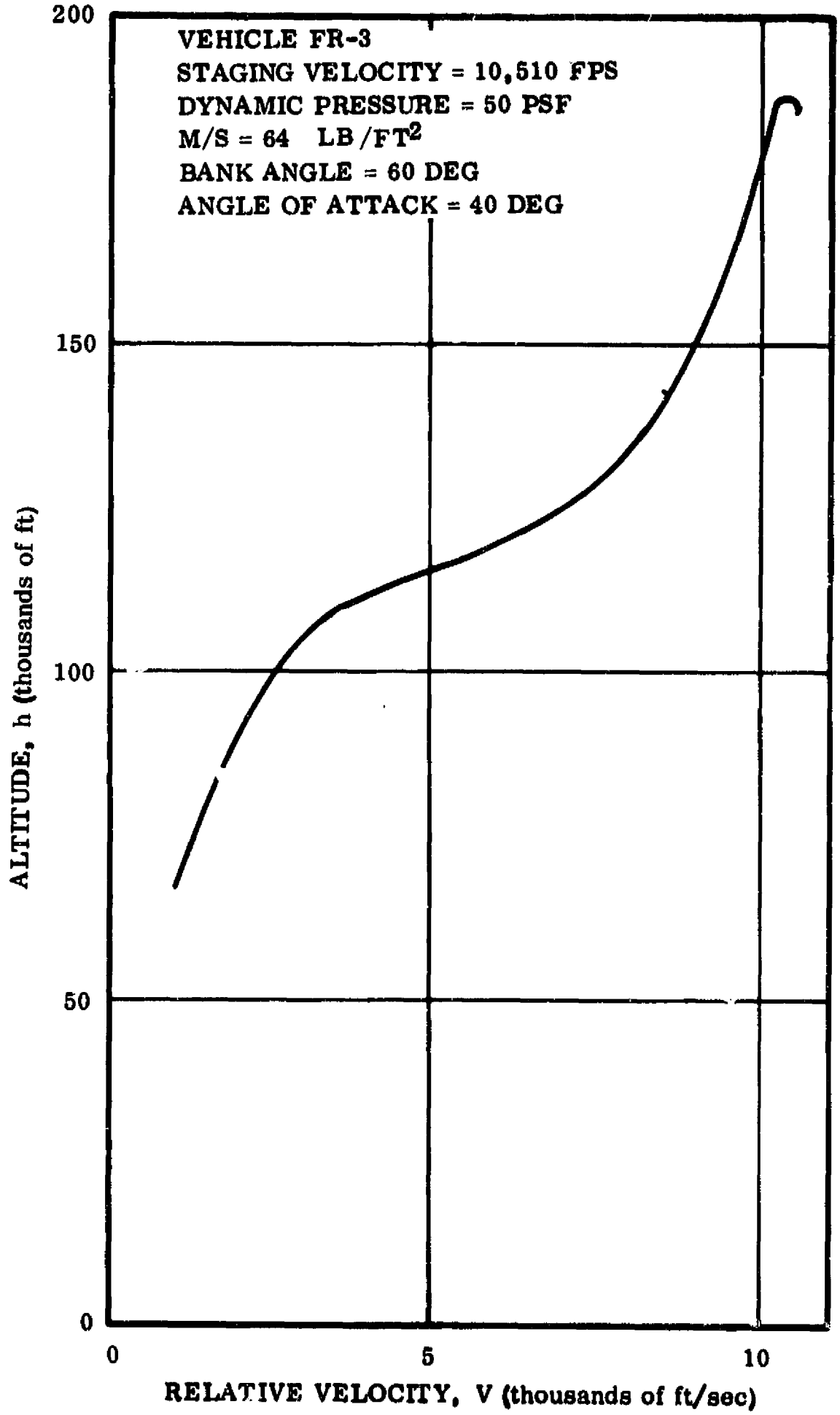

Figure 3-85. Two-Element ILRV, First Element — Trajectory 321 — Altitude versus Relative Velocity

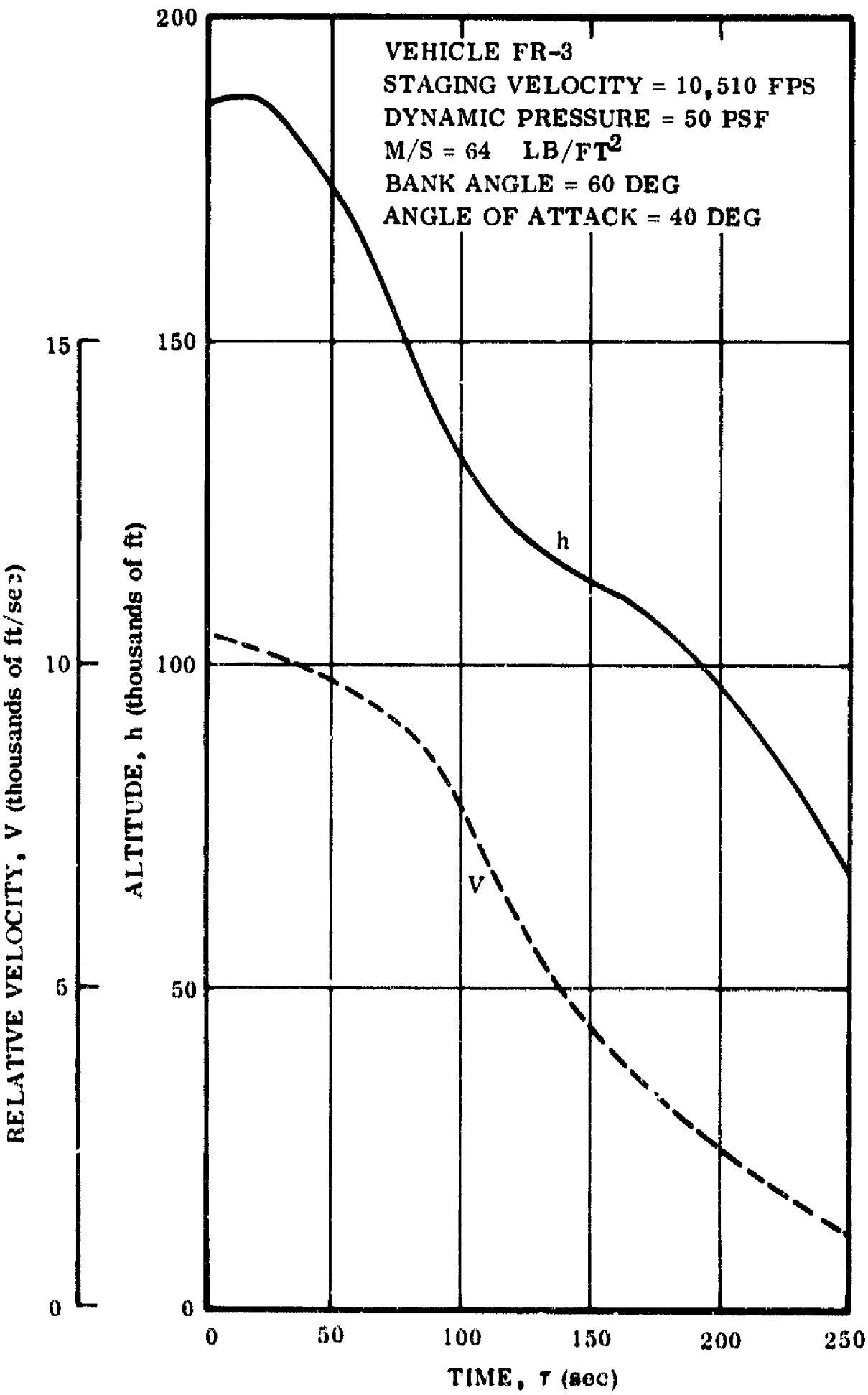

Figure 3-86. Two Element ILRV, First Element — Trajectory 321 — Altitude and Relative Velocity versus Time

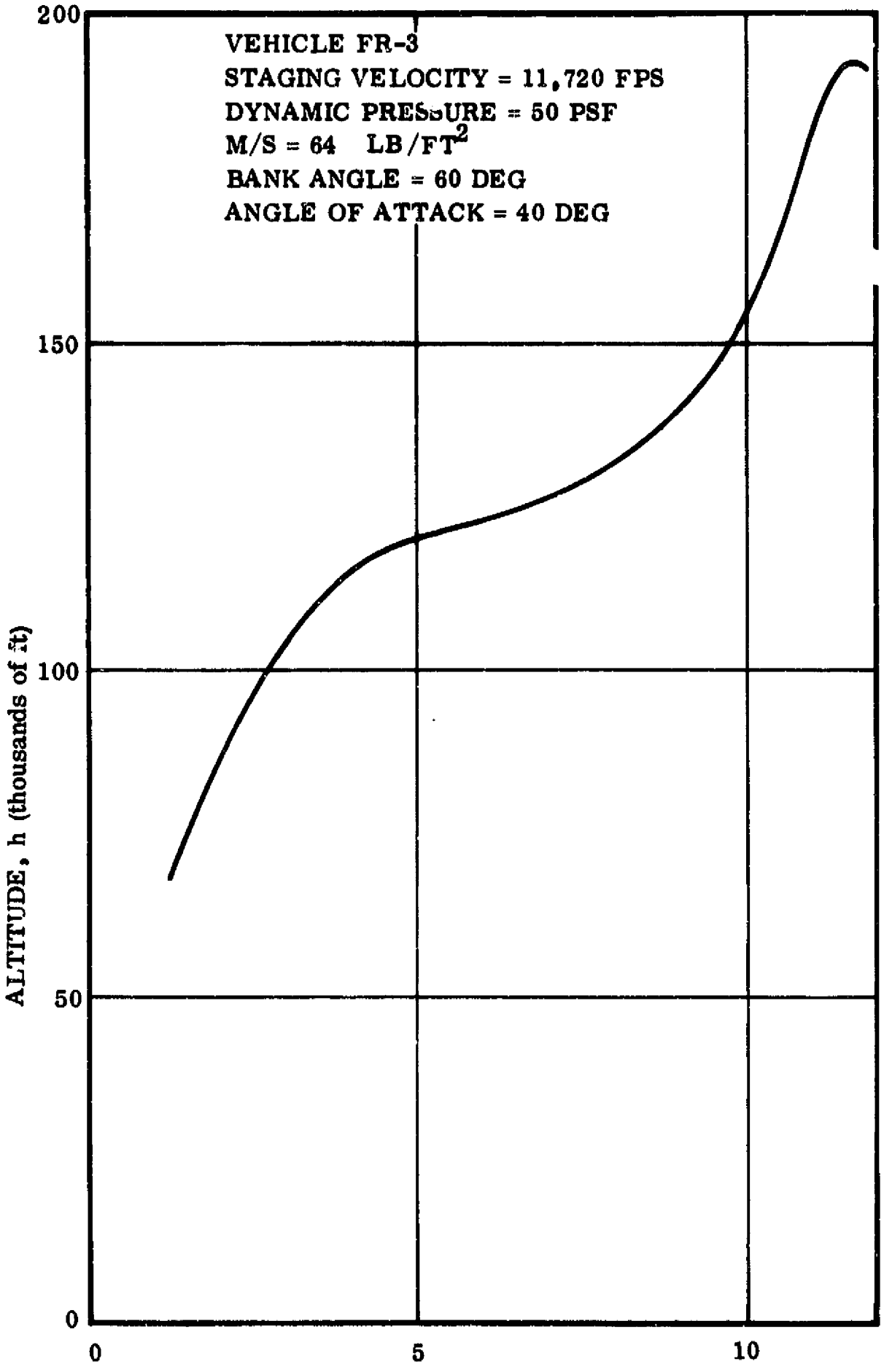

Figure 3-87. Two Element ILRV, First Element — Trajectory 326 — Altitude versus Relative Velocity

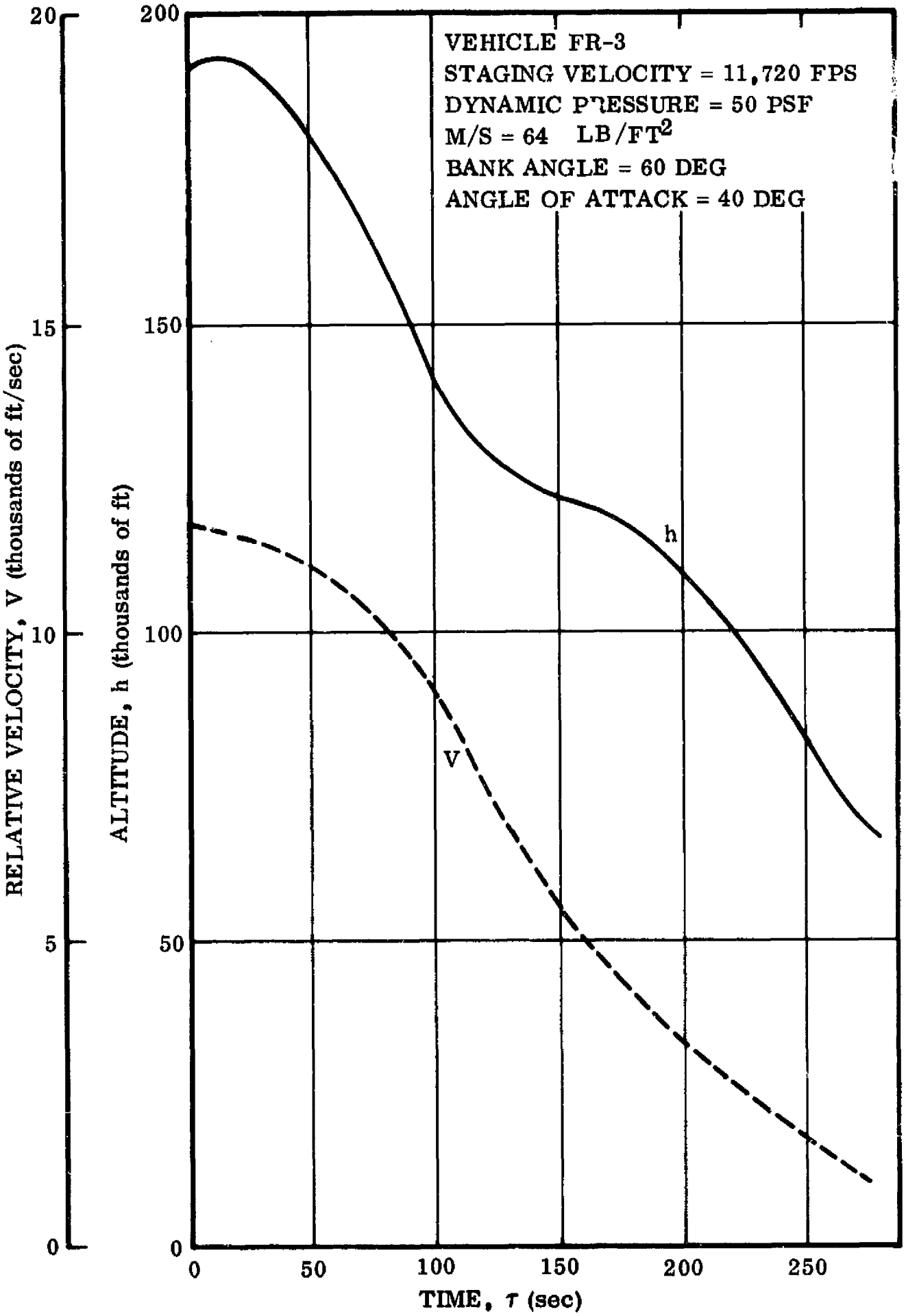

Figure 3-88. Two-Element ILRV, First Element — Trajectory 326 — Altitude and Relative Velocity versus Time

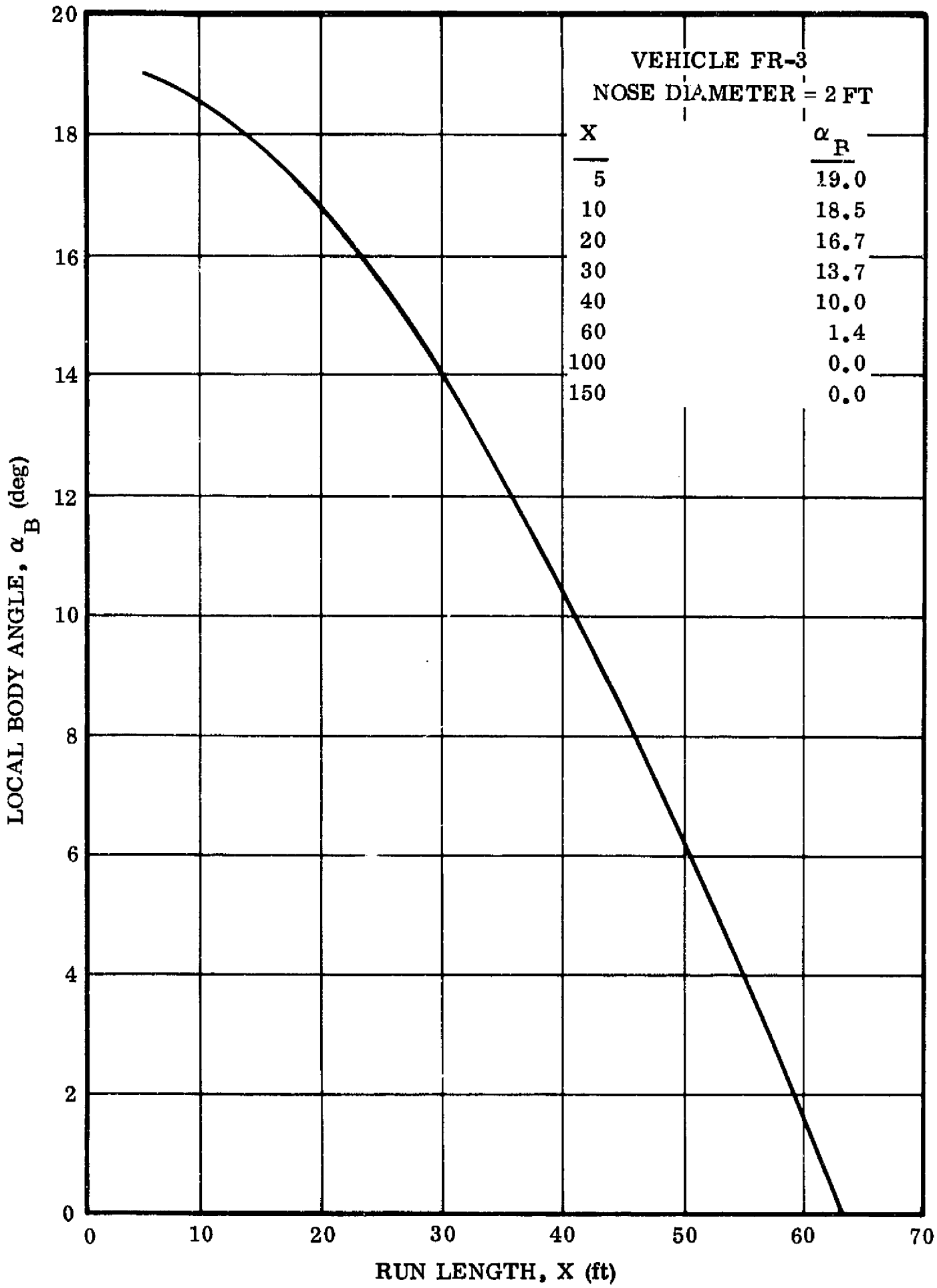

Figure 3-89. Two-Element ILRV, First Element — Lower Surface Local Body Angle versus Distance from Nose

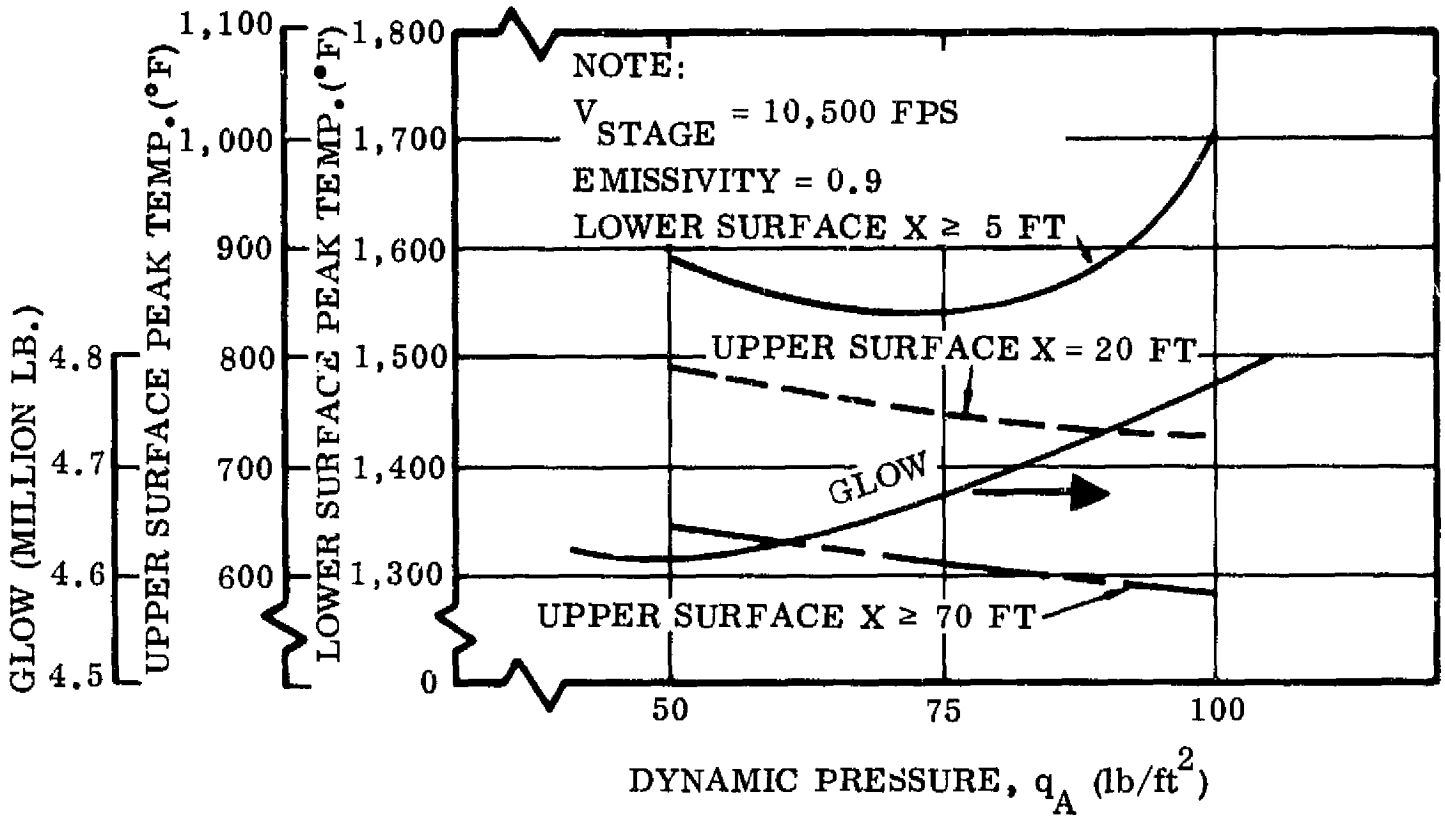

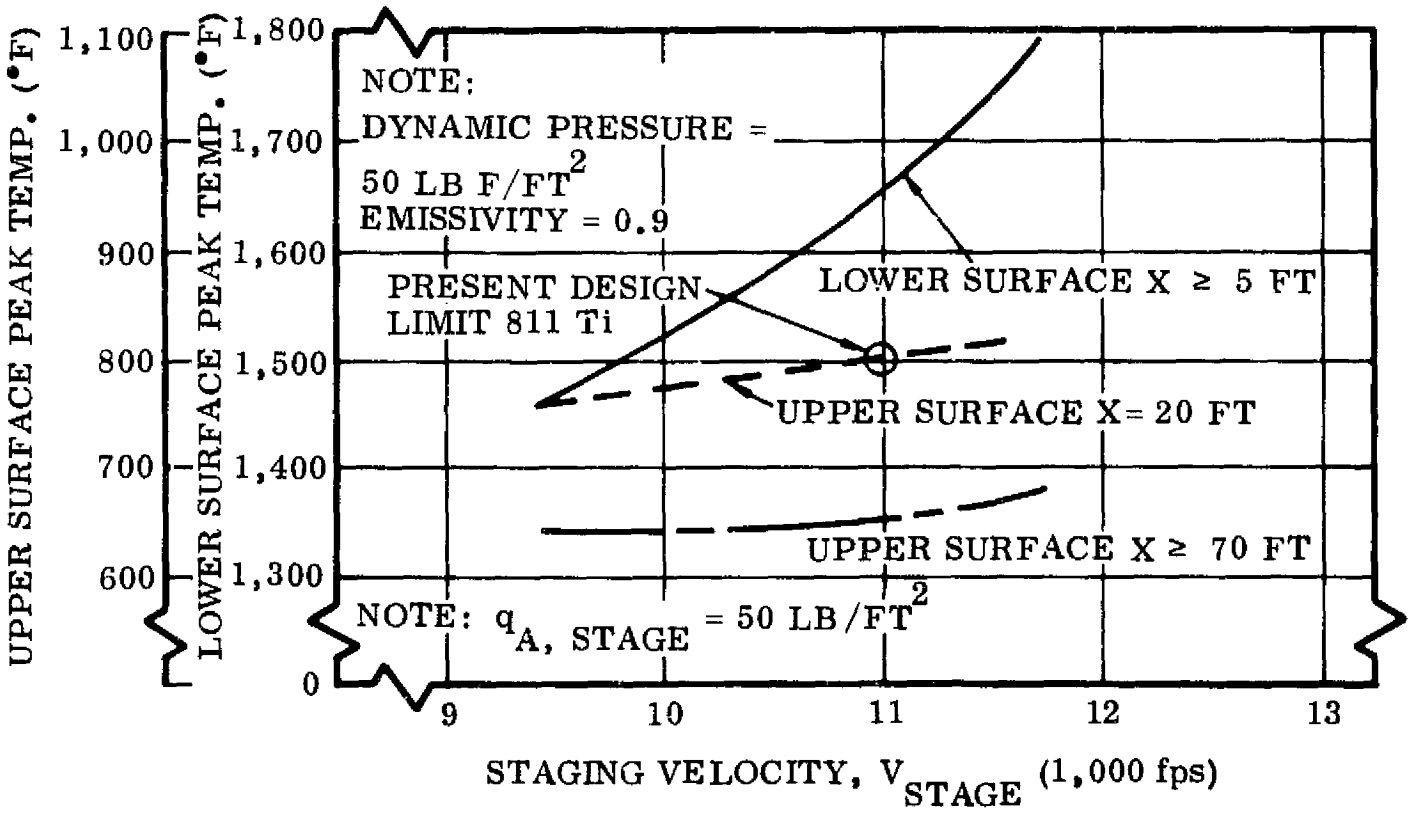

Figure 3-90. Configuration FR-3 Surface Temperatures for Various Staging Conditions

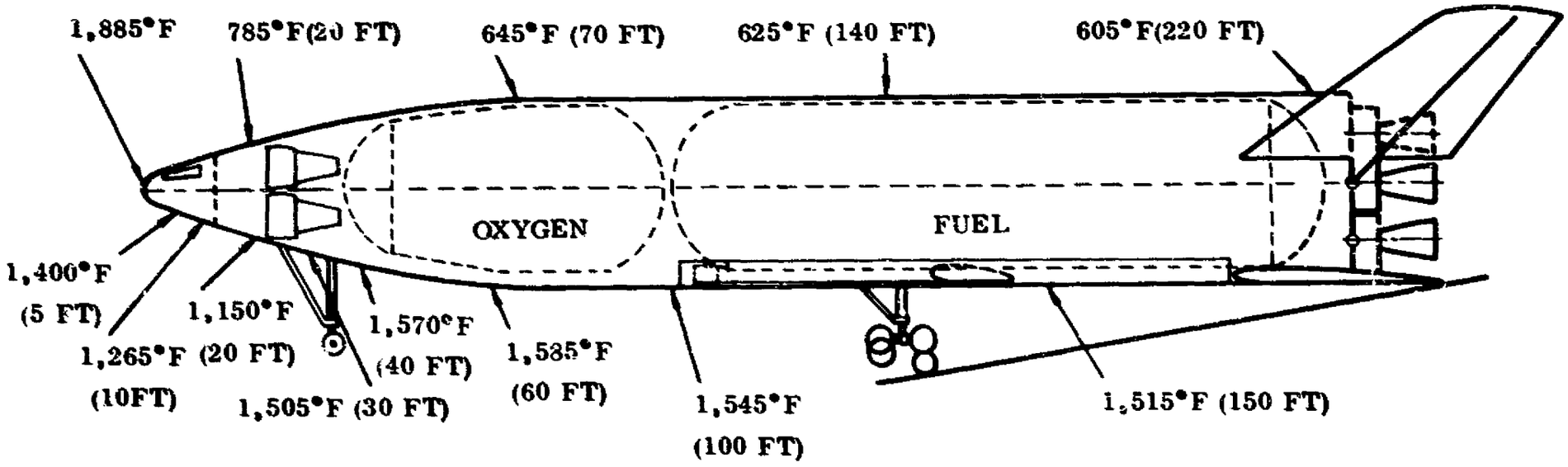

Figure 3-91. Two-Element ILRV, First Element — Configuration FR-3 — Radiation Equilibrium Temperatures

3.8 TWO-STAGE VEHICLE STRUCTURE

For the purpose of this initial study, thermostructural concepts for the two-stage vehicles were selected on the basis of previous work accomplished at Convair. These concepts utilize nonintegral propellant tankage for the boost element.

The concept selected as most appropriate for the orbital element (shown in Figure 3-92) features a fully thermally protected primary structure insulated to a peak structural temperature of 200°F. The body structure is essentially a "cylindrical" semi-monocoque of aluminum alloy into which the propellant tanks are integrated in a manner similar to that proven on expendable vehicles. The liquid hydrogen tank uses an internal insulation system to minimize boiloff and to prevent cryopumping. The body primary structure is isolated from the aerothermal environment by a system of large, slip-jointed cover panels overlaying fibrous insulation. Typical cover panel materials are coated tantalum on the nose cap and leading edges, L605 cobalt alloy on the windward surface, and titanium on the sides and upper surface. The deployable wing is housed inside the thermal protection subsystem during entry and is protected to a peak temperature of 200°F. The wing structure utilizes a two-spar torsion/bending box with stringer-stiffened wide column skins. A similar structure is also used for the stabilizer which is protected by an insulation/cover panel thermal protection system. The elevons feature a thermally protected box structure.

The more moderate temperatures applicable to the boost element permit a lighter and simplified thermostructural concept. This is illustrated in Figure 3-93. The primary structure of the body is a hot load-carrying structure insulated by cover panels and insulation on the nose and lower surface only. The lower-surface cover panels are type 718 Nickel alloy. A semi-monocoque, corrugation-stiffened, frame-supported shell structure of titanium alloy is proposed. Propellant tanks are nonintegral, ring-stiffened shells of 718 Nickel alloy. Support from the primary structure is accomplished by a system of straps and links which transmit inertia loads and accommodate thermal displacements. The deployable wing is stowed above the lower-surface thermal protection subsystem during entry and is protected to a peak structural temperature of 800°F. The wing employs a two-spar torsion/bending box, as in the orbiter. The structural material is titanium. In addition to the lower-surface thermal protection subsystem, insulation is required inside the hot structure for the personnel compartment and for critical subsystems, etc. The stabilizers use hot structures. Thermostructural design criteria are shown in Table 3-8.

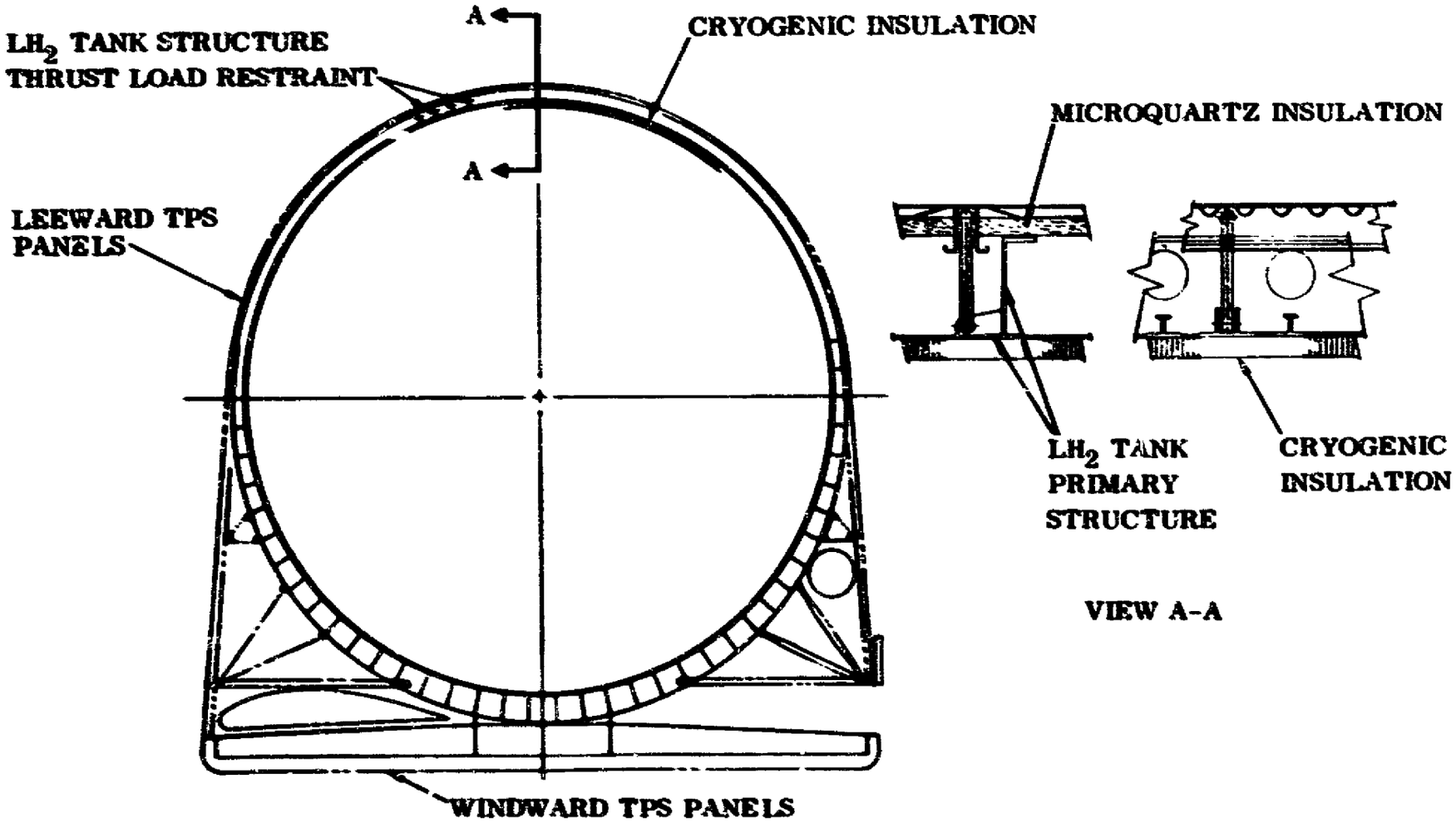

Figure 3-92. Typical Orbiter Structure

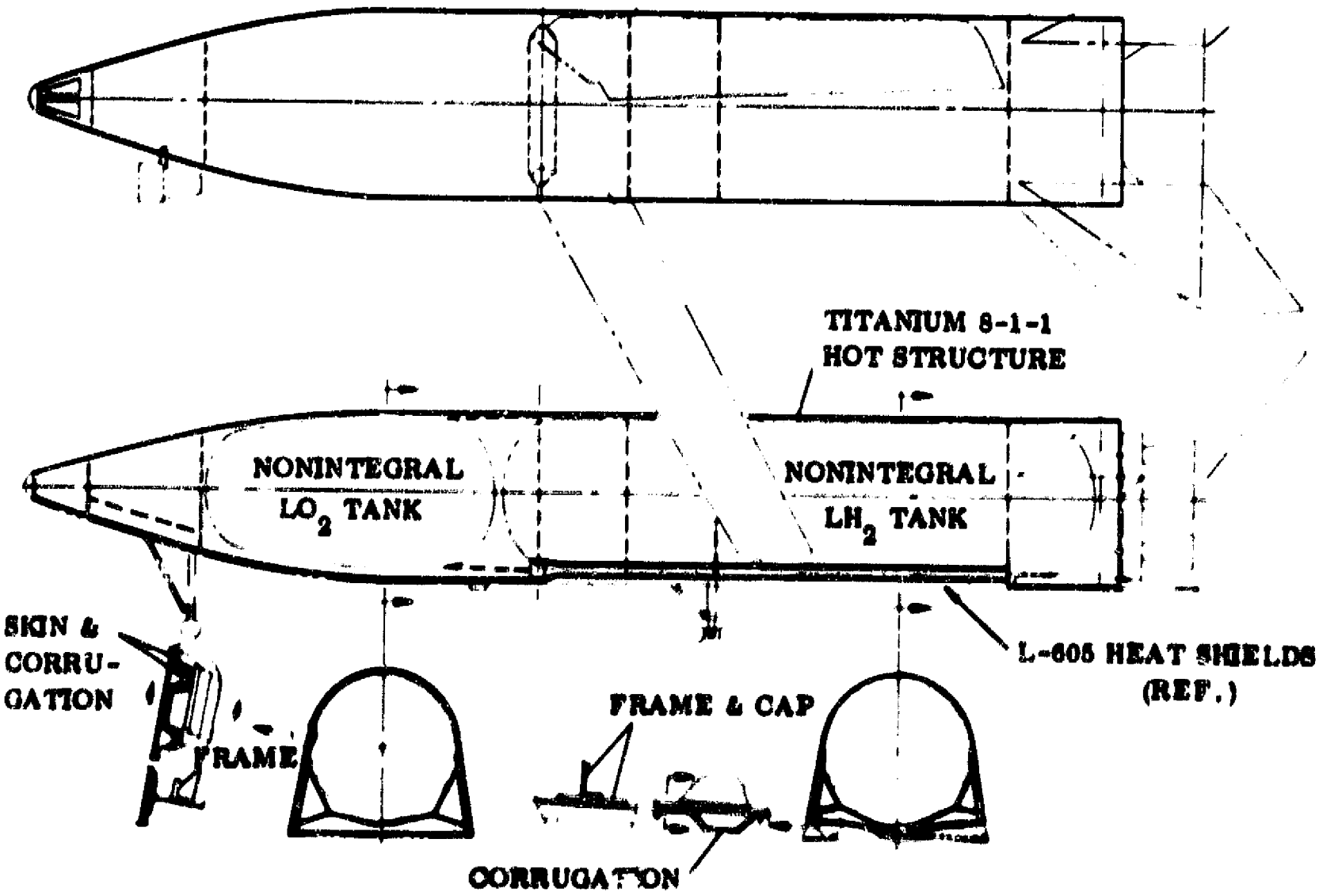

Figure 3-93. Two-Element Booster Structural Concept

3.9 VEHICLE SPECTRUM COMPARISON

Figure 3-94 compares the six baseline vehicles defined in Section 2. As noted, the three-element systems have elements of identical size and shape. The two-element vehicles are optimized for minimum weight and have larger booster elements. The FR-1 and FR-2 vehicles use propellant crossfeed.

Figure 3-95 summarizes the vehicle weights and lists engine quantities, thrust, volumes and vehicle length.

Figure 3-96 shows comparative sizes of contemporary vehicles, Saturn V for on-pad comparison and C5A and 707 airplanes for ground movement facility studies.

Table 3-8. Thermostructural Design Criteria

Maximum Launch Winds:	99% Probability
Maximum Longitudinal Accelerations:	4g Limit
Factors of Safety	
Aerodynamic & Associated Inertia Loads	1.40
Thrust & Associated Inertia Loads	1.25
Personnel Compartment Pressures	2.00
Reusable Propellant Tank Pressures	1.50
Material Temperature Constraints	
	Normal Entry Temperature Range (°F)
Titanium	- to 800
Inconel 718	800 to 1,200
Rene' 41	1,200 to 1,400
L605	1,400 to 1,900
TD Ni-C	1,800 to 2,200
Columbium	2,200 to 2,500
Tantalum	2,500 to 3,100

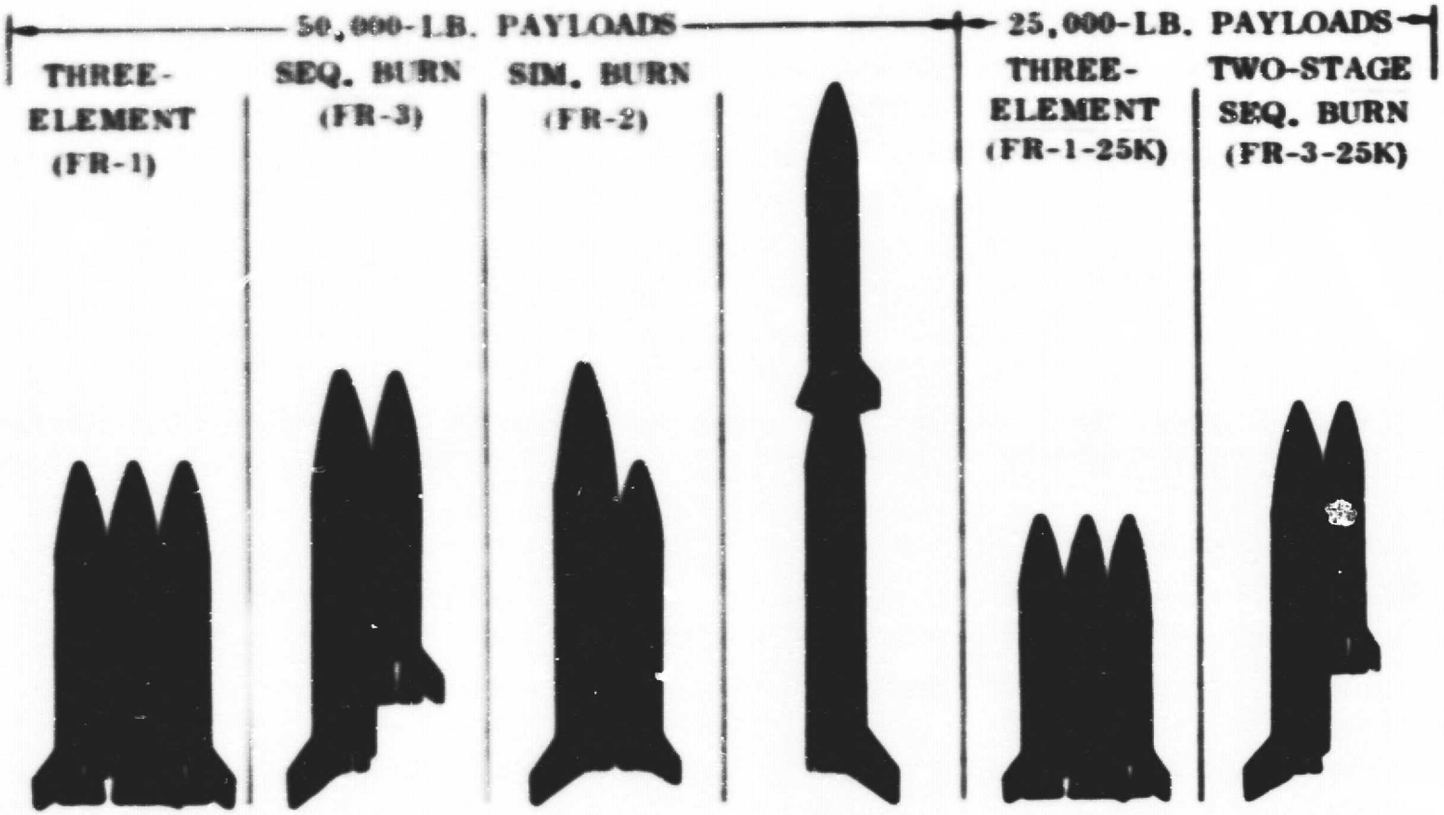

LIFTOFF WT. (10^6 LB.)	4.53	4.00	3.53	3.86	2.81	2.76
THRUST/ENG. (10^6 LB.)	1.070	0.710	0.497	0.681	0.670	0.488
COMMON AERO SHAPE	YES	NO	NO	NO	YES	NO
CROSS-FEED	YES	NO	YES	NO	YES	NO

Figure 3-94. Vehicle Spectrum Comparison

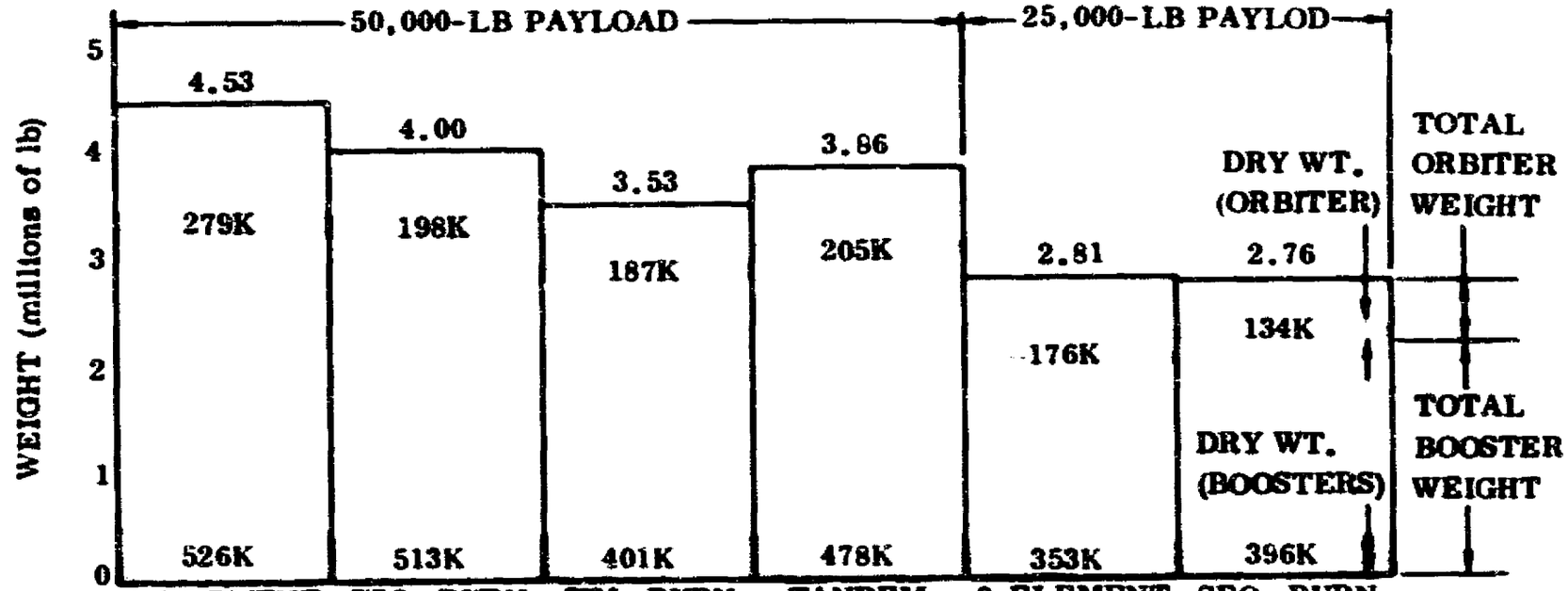

ENGINES	2-2-2	8-2	8-2	8-2	2-2-2	8-2
VAC. THRUST ENG. (10^6 lb)	1.07	0.71	0.457	0.681	0.67	0.488
VOLUMES (10^3 ft^3)	117	193/74.3	174/72.7	188/76.7	66.5	165/44.6
VEHICLE LENGTH (ft)	203	240/174	232/173	238/176	162	227/142

Figure 3-95. Summary of Vehicle Characteristics

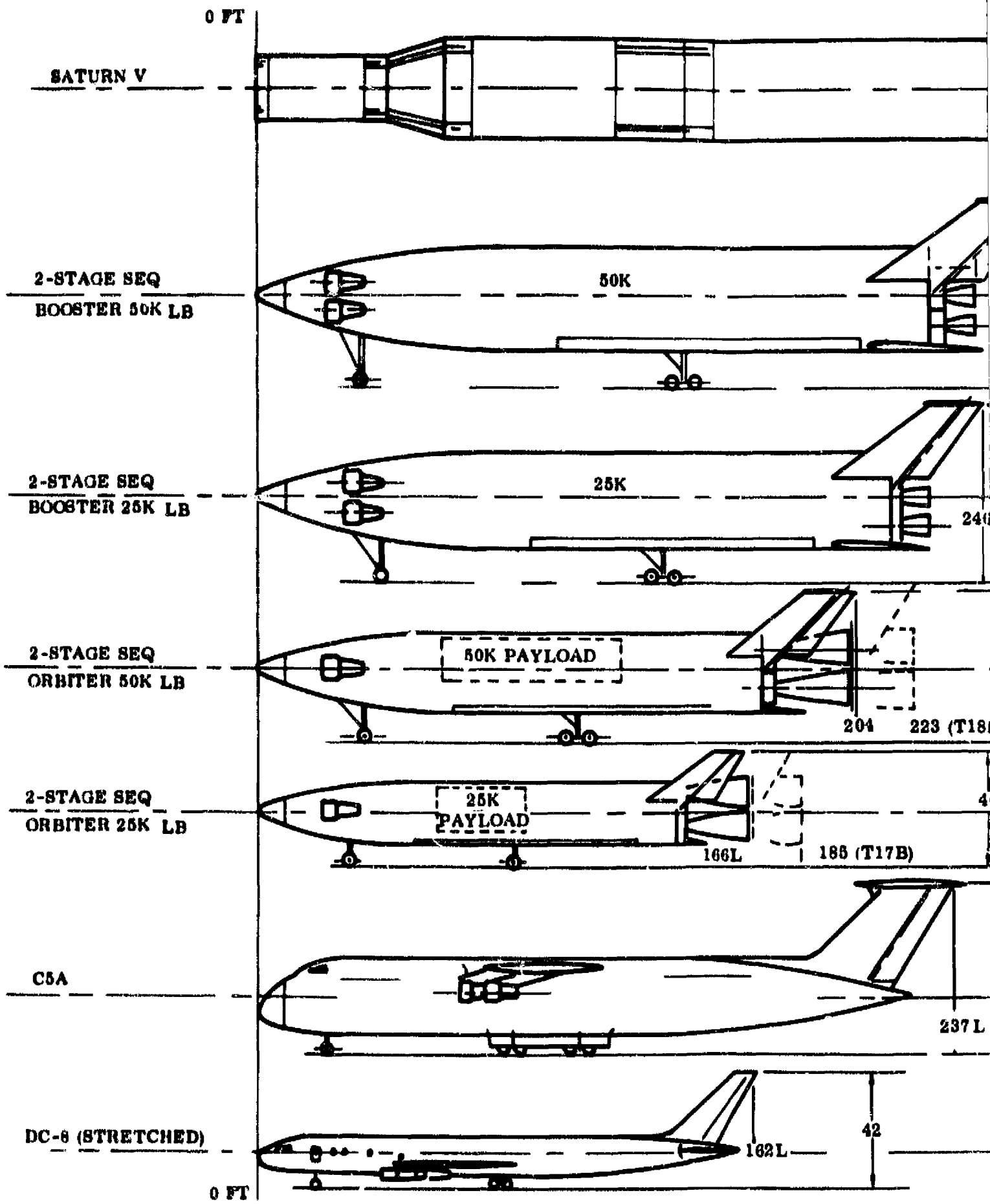

FOLDOUT FRAME

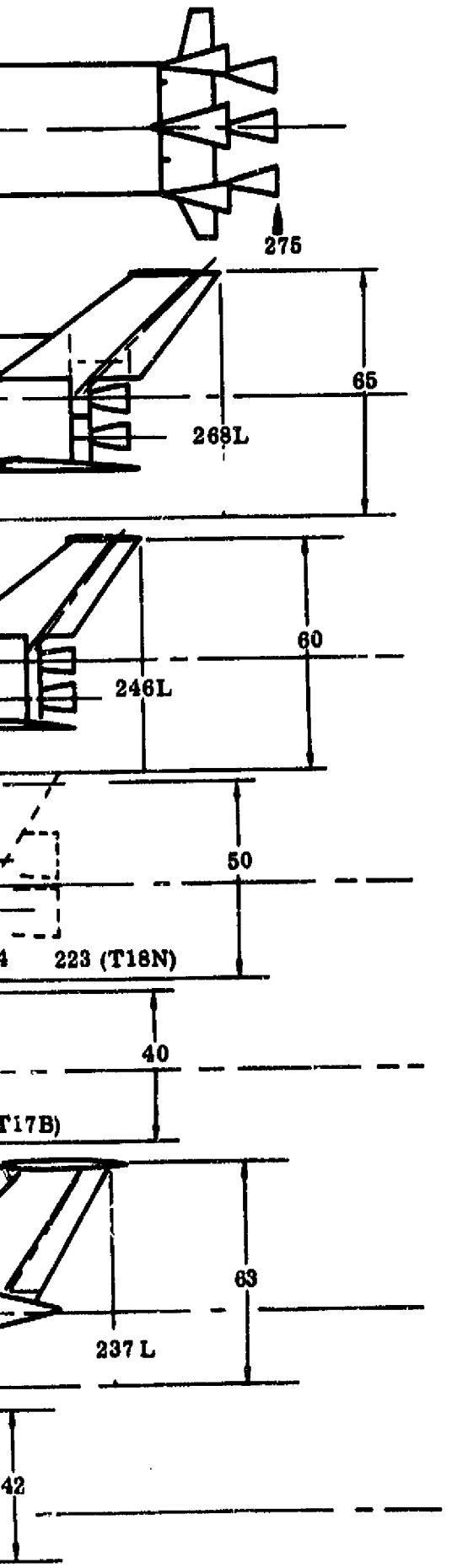

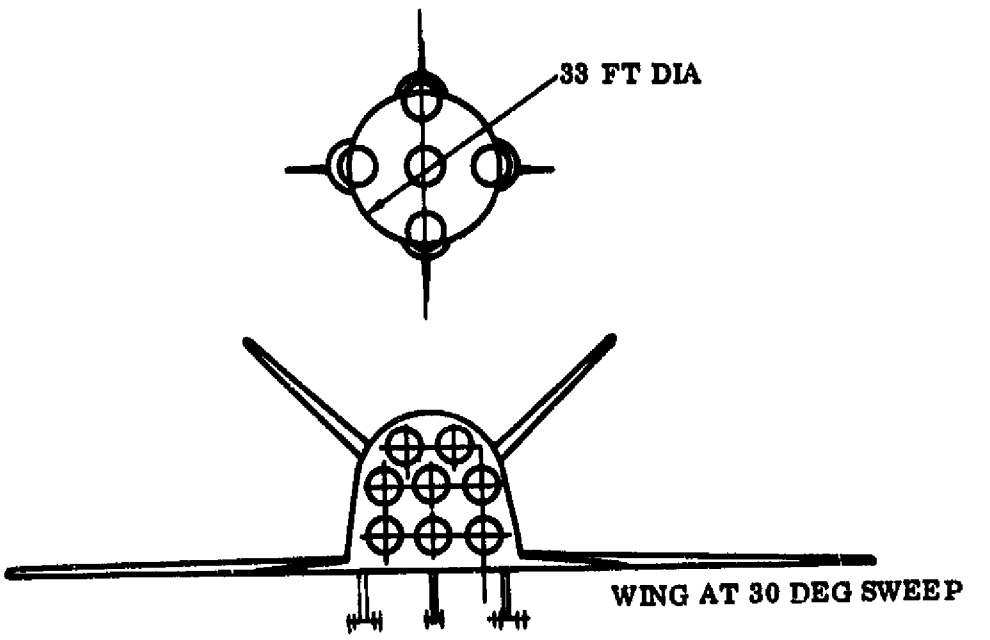

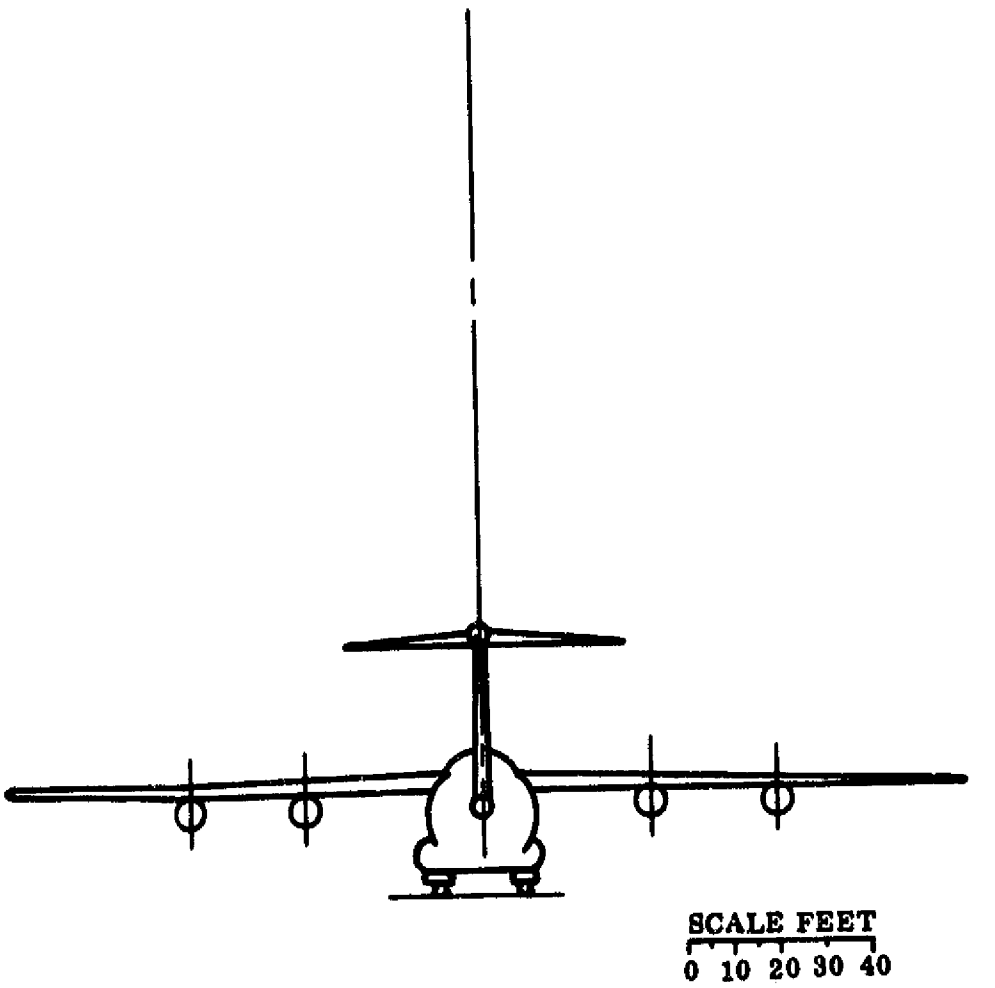

FOLDOUT FRAME 2

Figure 3-96. Contemporary Vehicle Size Comparison

3.10 REFERENCES

3-1 K. S. Coward, Subsonic Longitudinal and Lateral/Directional Characteristics of a Number of Tail and Body Configurations of a Triamese (FR-1) Vehicle as Tested in the Princeton Wind Tunnel, TN-69-AE-03, Convair division of General Dynamics, 15 March 1969.

3-2 R. S. Scullen, A Description of the Revised Aerodynamic/Structural Heating and Radiation Equilibrium Temperature Computer Program 3020, GDC-ERR-1366, Convair division of General Dynamics, December 1968.

3-3 M. Masaki and J. Yakura, Transitional Boundary Layer Analysis of Lifting Reentry Vehicles, AIAA Paper 58-1155, December 1968.

3-4 R. W. Detra, N. H. Kemp, and F. R. Riddell, "Addendum to Heat Transfer to Satellite Vehicles Reentering the Atmosphere," Jet Propulsion, December 1957, pp. 1256-1257.

3-5 Preliminary Tradeoffs and Requirements for Boost, Maneuver, and Reaction Control Propulsion Systems, GDC-DCB69-024, Convair division of General Dynamics, 29 July 1969 (Confidential — Title Unclassified).

SECTION 4

FR-1 BASELINE

This section documents the 50K pound payload (FR-1) baseline vehicle developed toward the end of the study. This is an updated version of the FR-1 vehicle shown in Paragraph 2.7 and incorporates off-the-shelf flyback engines.

4.1 BASELINE ELEMENT CONFIGURATION

Layout of the final FR-1 configuration is shown in Figure 4-1. Orbiter and booster elements are identical in size and shape. Each is powered by two LO_2/H_2 rocket engines for liftoff, with three fanjet engines for flyback in the booster and two landing engines in the orbiter. The overall vehicle length to the fin tips is 225 feet. The fuselage is 35 feet wide and 30 feet high, with a 12-degree side slope angle. The exposed wing area of 1760 square feet is 28% of the planform area.

The wing is located in the extended position by matching the 1/4 chord of the exposed mean average chord (MAC) with the 55% balance point of the fuselage planform. The exposed area for the two fins is 1809 square feet. The fins are located with the lower surfaces at a 45-degree angle above the horizontal. They are placed high on the aft fuselage while retaining clearance from the adjacent vehicle. Front and rear fin spars are located to attach directly to the heavy thrust structure. A more efficient internal arrangement has been accomplished in the orbital vehicle by using the space below the 15- by 60-foot payload for stowage of 7500 cu ft of main hydrogen fuel. This reduces the length of the main hydrogen tank, thereby reducing vehicle length. This area is replaced in the booster by a large LO_2/H_2 tank with a common bulkhead. (This tank also includes the 7500 cu ft of hydrogen carried in the orbiter bay.) This arrangement provides maximum commonality between orbiter and booster by merely replacing the orbiter payload bay doors with frames and skin on the booster. Two super-insulated maneuvering oxygen tanks are located in the aft bay, forward of the wing pivot bulkhead and isolated from the hydrogen tanks by the lower payload bay structure.

Location of major components and compartments is identical for the orbital and booster elements.

a. The nose from station 0 to station 14 contains space for two side-by-side pilots, and navigation/communication equipment.

b. Stations 14 to 21 contain subsystem components such as fuel cells, hydraulic power units, reservoirs, accumulators, and environmental control subsystem components.

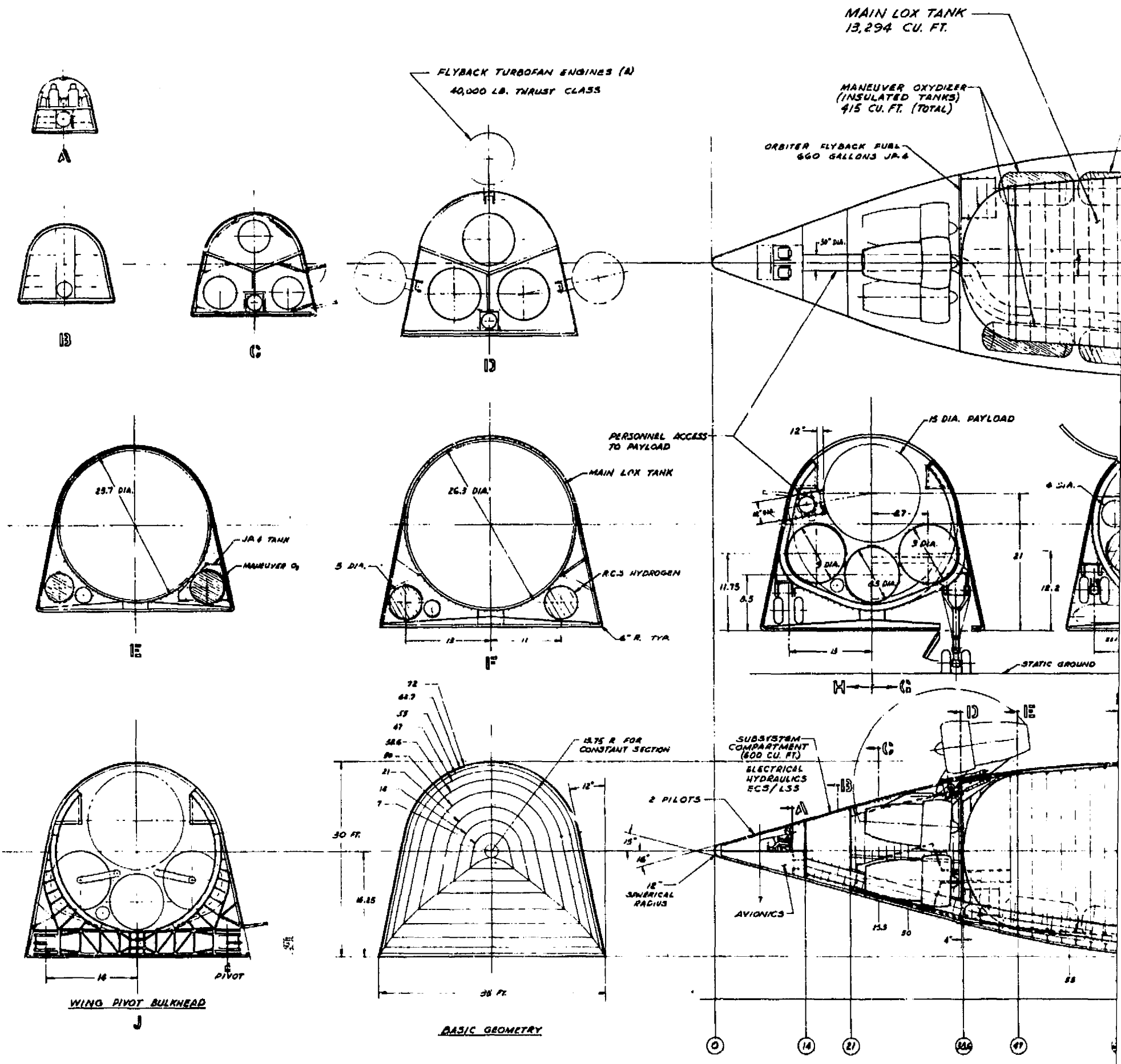

Figure 4-1. FR-1 Element

FOLDOUT FRAME \

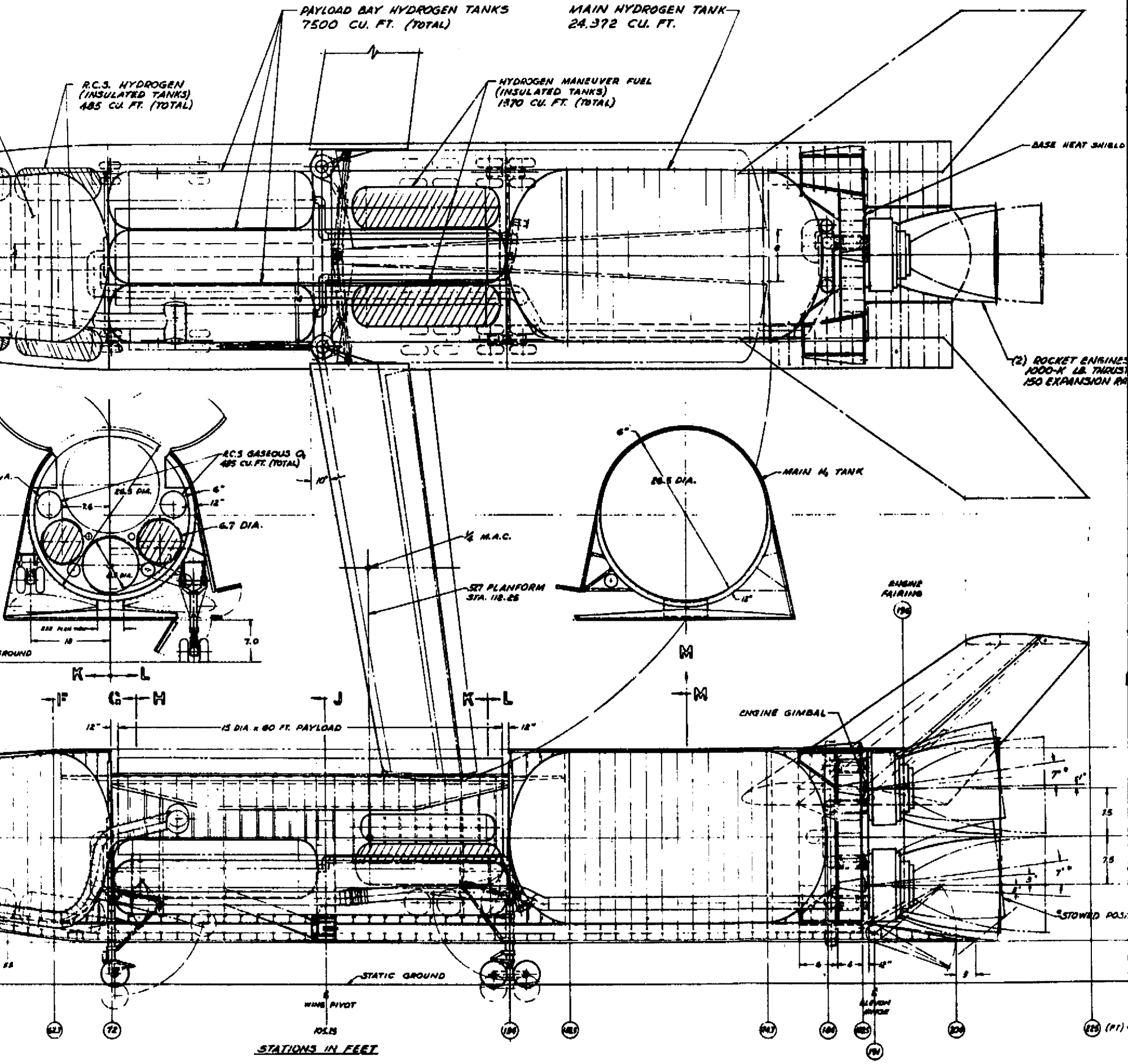

FOLDOUT FRAME 2

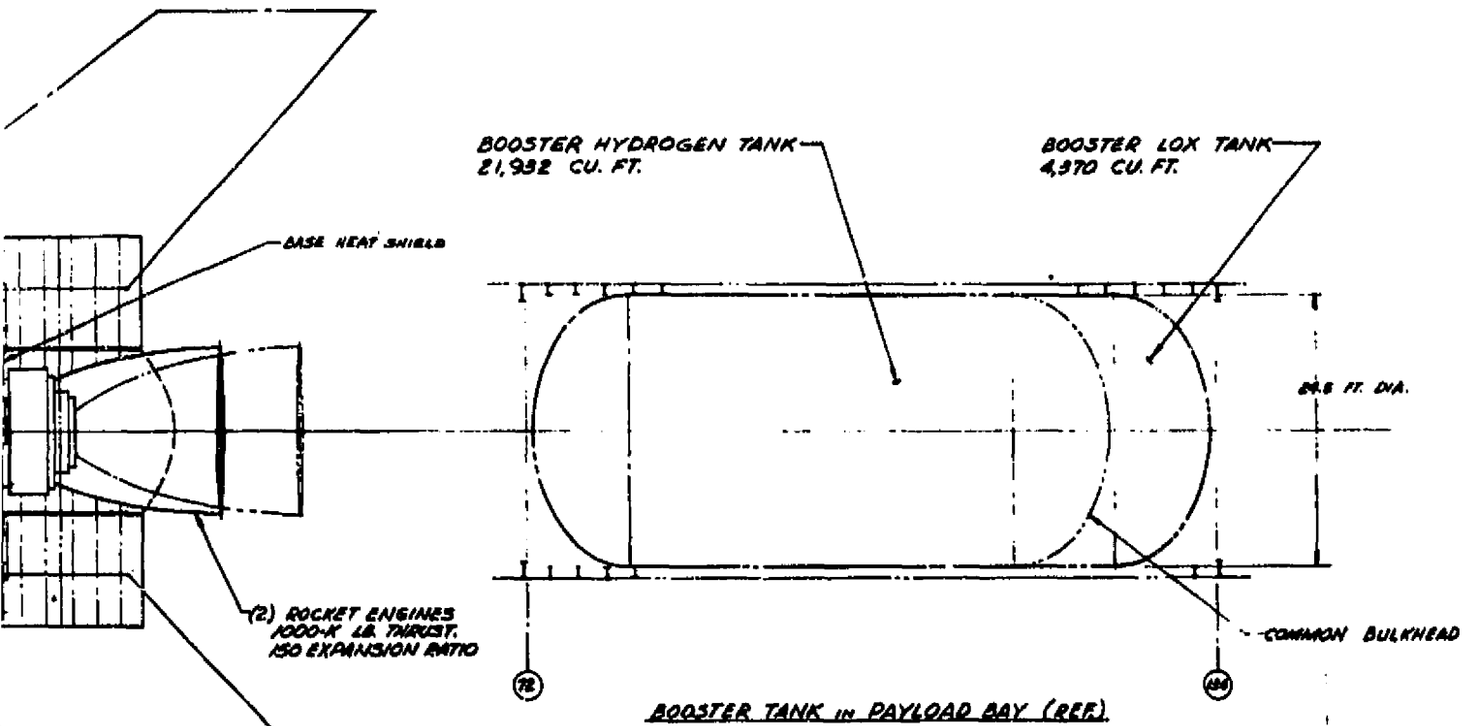

BOOSTER TANK IN PAYLOAD BAY (REF.)
FR-1 CONCEPT ONLY

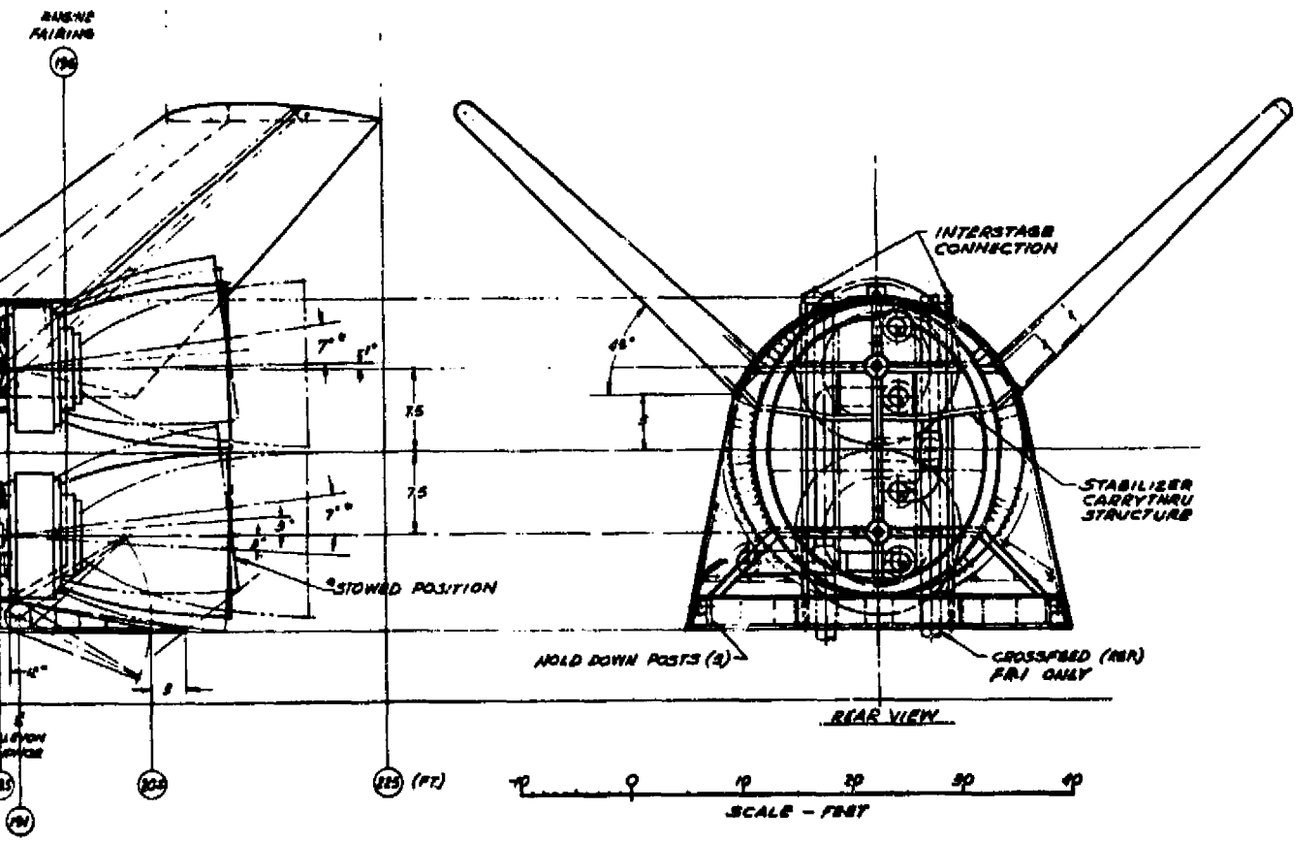

FOLDOUT FRAME 8

FOLDOUT FRAME 3

c. The engine compartment between stations 21 and 38.3 provides space for stowage of the three fanjet flyback engines. They are extended to the flying position by a simple double acting system (similar to a wing-fold mechanism). Doors will be closed after the engines are extended to retain a clean aerodynamic surface.

d. The main LO_2 tank is located between stations 38.3 and 72 and forms an integral part of the structure.

e. The compartment between stations 72 and 134 contains the payload in the orbiter and additional propellants in the booster as discussed previously. This compartment also contains the wing pivot bulkhead and the landing gear attachment and stowage space. These items will be located outside the lower circular frames and skin thereby providing good structural continuity through this compartment.

f. The main hydrogen tank is located between stations 134 and 184 and forms an integral part of the structure.

g. The thrust structure extends from the hydrogen tank aft to station 190.5 and provides support for the two rocket engines. This structure also supports the fin spars, the vehicle separation mechanism, and the pad support fittings.

4.2 ELEMENT ARRANGEMENT

Figure 4-2 shows the 50K pound payload (FR-1) vehicle in the launch configuration. Separate views also show the orbiter element and the booster element before mating. Basic technical data is also listed on the drawing. The vehicle lines drawing is documented in Figure 4-3.

4.3 (FR-1) SYNTHESIS

The latest synthesis program output for the 50K pound payload FR-1 system is shown in summary in Table 4-1. This vehicle includes updated wing structural considerations resulting in higher weight than the FR-1 in Paragraph 2.7, and it also includes off-the-shelf flyback engines; namely, Rolls Royce RB-211 type turbofans in the 50K pound sea-level static-thrust category. The synthesis runs represent an iteration with the layouts of Figures 4-1 and 4-2 so that the dimensions will not match precisely as is usual during this interim design development phase. Table 4-2 shows the summary weight statement for this vehicle. Sensitivity of the 50K pound payload FR-1 vehicle is shown below. The two-stage sensitivities are also shown for comparison.

	FR-1	Two-Stage
$\frac{\Delta \text{ Gross Liftoff Weight}}{\Delta \text{ Pounds Inert in Orbiter}}$	31.8 lb/lb	26.6 lb/lb
$\frac{\Delta \text{ Gross Liftoff Weight}}{\Delta \text{ Pounds Inert in Each Booster}}$	9.0 lb/lb	4.82 lb/lb

	FR-1	Two-Stage
$\frac{\Delta \text{Gross Liftoff Weight}}{\Delta V \text{ Maneuver or Reserve}}$	600 lb/fps	485 lb/fps
$\frac{\Delta \text{Gross Liftoff Weight}}{\Delta I_{SP_{vac}}}$	42,700 lb/sec of I_{SP}	

DATA:		WING (EXPOSED)	STABILIZER (HALF WING, EXPOSED)	ELEVONS (TOTAL)
SPAN	FT.	127.50	38.26	20
AREA	SQ. FT.	1760	304.5	280
CHORD ROOT	FT.	15.53	22	13
TIP	FT.	12.25	19.2	13
ASPECT RATIO		9.25	1.375	—
TAPER RATIO		.80	.60	.40
SWEEP L.E.		10°	45°	—
AIRFOIL ROOT		4481	4412 MOD.	—
TIP		4418	4410 MOD.	—
M.A.C.	FT.	13.9	86	—
INCIDENCE	DEG.	6°	0°	—
DIHEDRAL	DEG.	0°	45°	—

BODY — WIDTH 35 FT. HEIGHT 30 FT. LENGTH 218 FT.
PLAN AREA 6675 SQ. FT.

FLAPS - AREA INCREASING, FULL SPAN, 25% CHORD
SPOILERS - 25% SPAN 10% CHORD
RUDDERS — 35% CHORD

ENGINES — BOOST - (2) PER ELEMENT, VAC THRUST 1,160,000# EA.
EXPANSION RATIO 150
FLYBACK (3) PER ELEMENT, S.L. THRUST 40,000# EACH.
GROWTH T-34 TURBOFANS OR EQUIV.

PAYLOAD — 50,000 POUNDS 15 FT. DIA. BY 60 FT. LONG

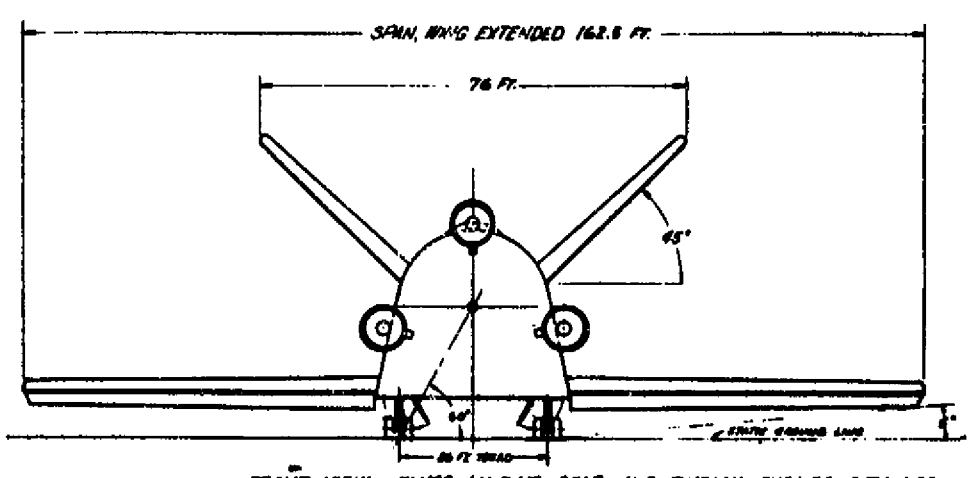

FRONT VIEW - WINGS, LANDING GEAR, AND FLYBACK ENGINES EXTENDED

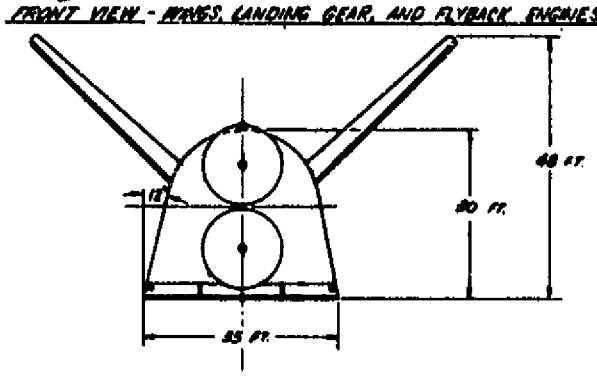

REAR VIEW - RE-ENTRY CONFIGURATION

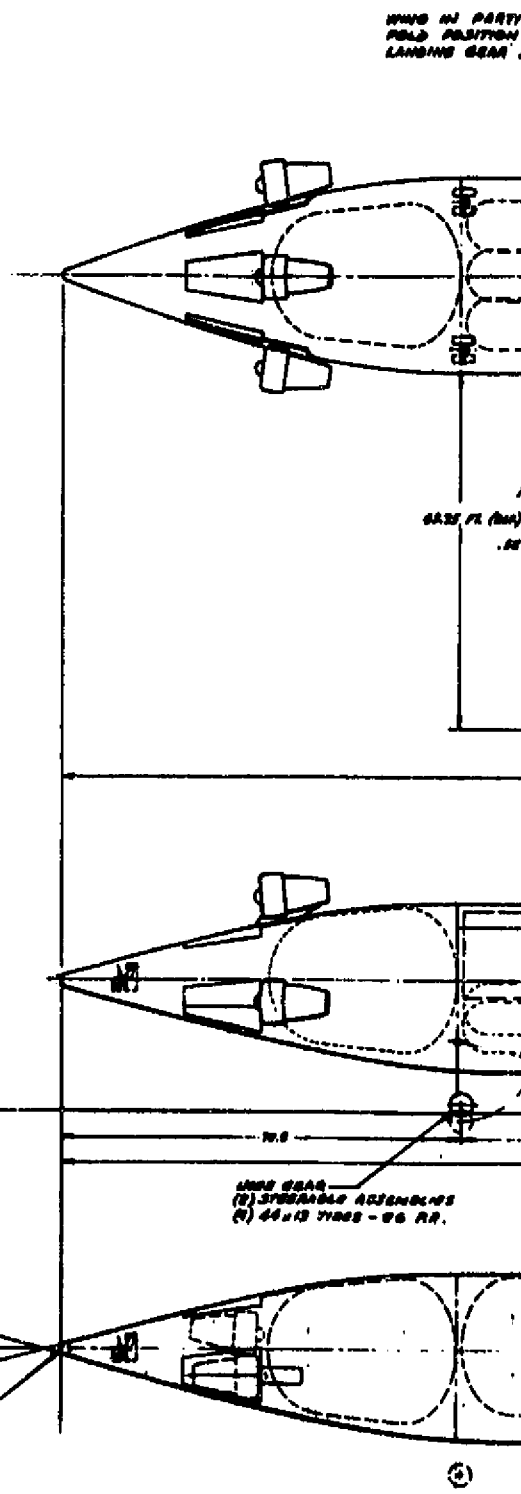

FOLDOUT FRAME

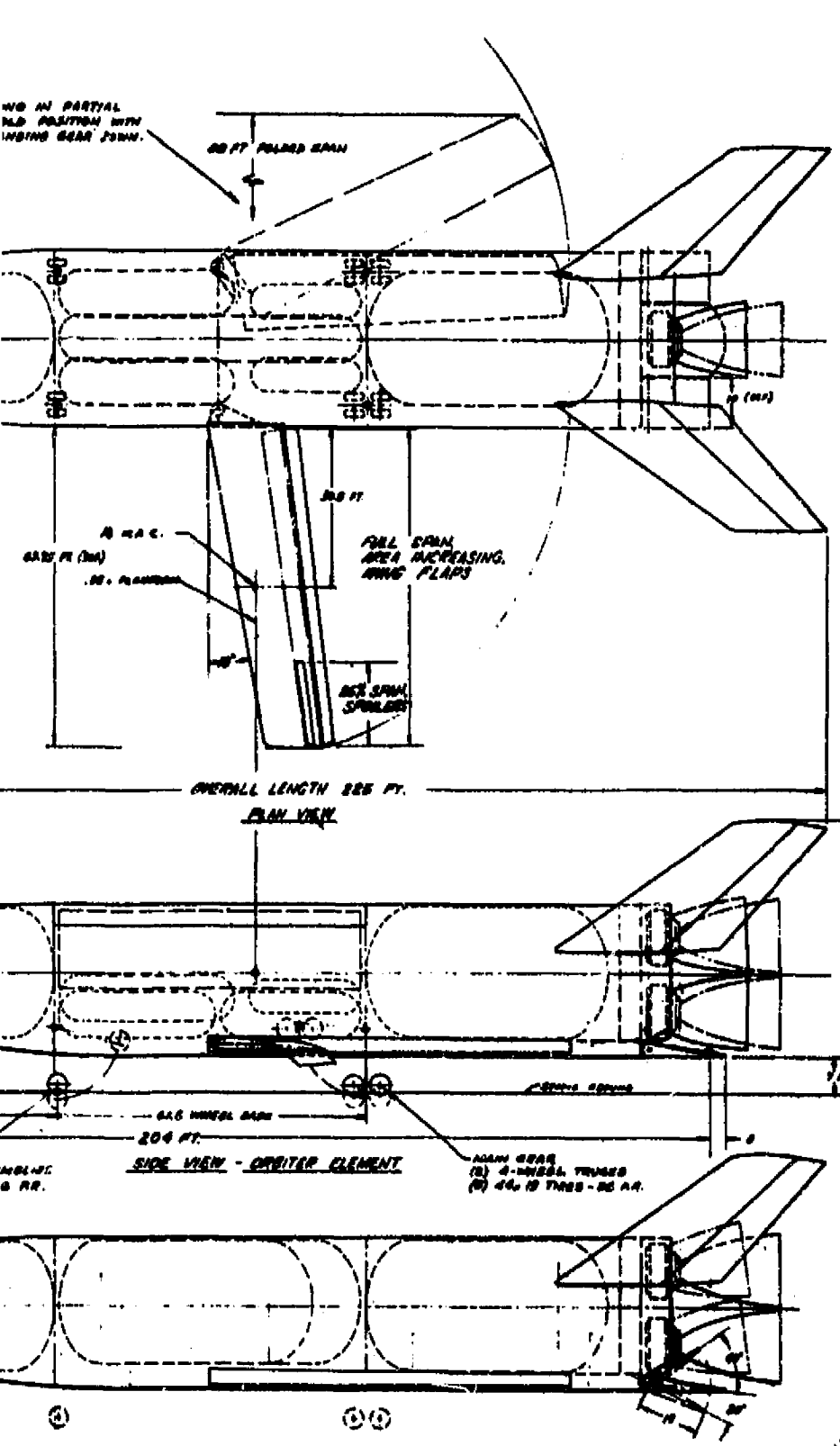

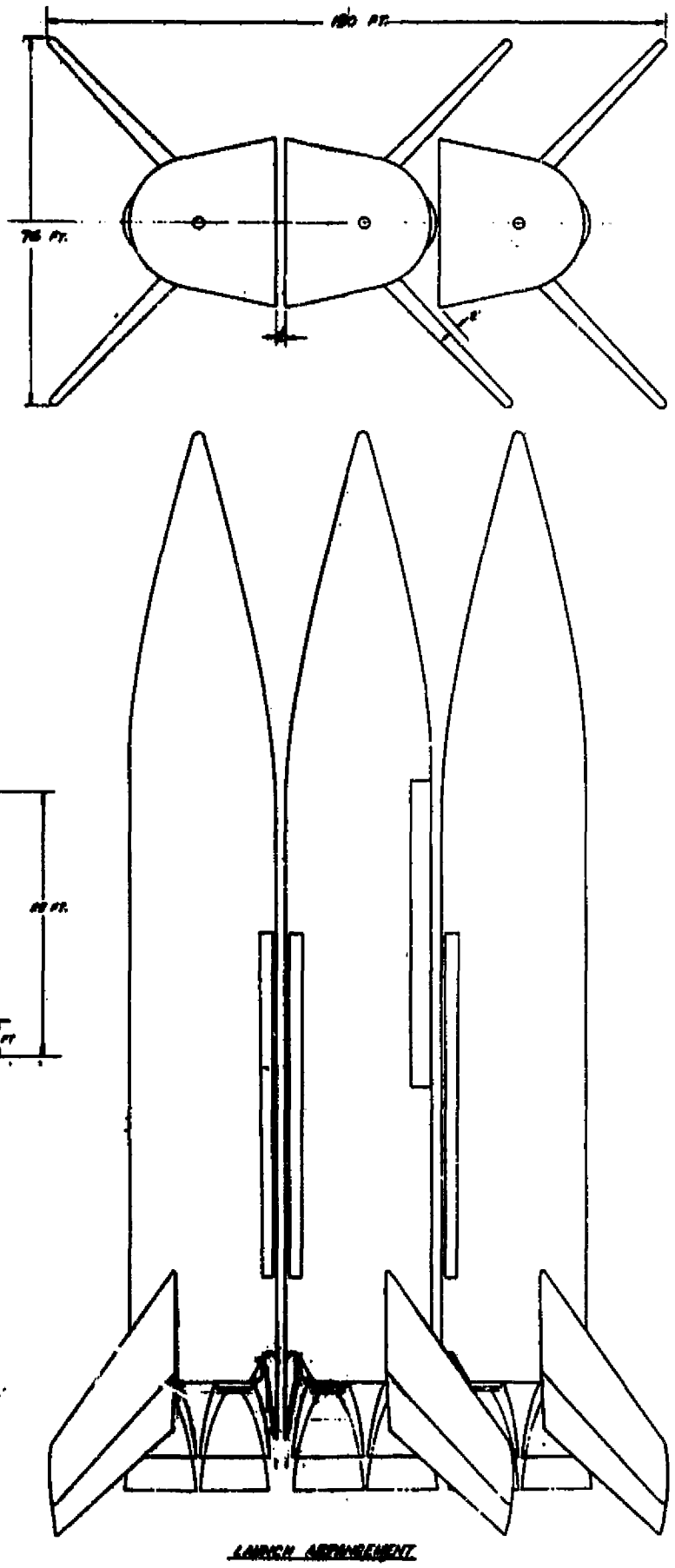

Figure 4-2. General Arrangement — FR-1 Vehicle

FOLDOUT FRAME 2

LINES DATA

BASE LINE LENGTH (POINTED NOSE TO AFT END OF ELEVON LOWER SURFACE) = 100 %

NOSE RADIUS - CONSTANT	1 FT.
BODY L.E. RADIUS - CONSTANT	.5 FT.
SIDE SLOPE - CONSTANT	12°
NOSE TOP ℄ SLOPE - CONSTANT	16°
NOSE BOTTOM ℄ SLOPE - CONSTANT	15°
ALL BODY TOP RADII CENTER ON BODY ℄	

BODY:

WIDTH			17%
HEIGHT			14.56%
CONSTANT CROSS-SECTION STARTS			36.1 %
CONSTANT SECTION TOP RADIUS			6.65 %
TOP ℄ COORDINATES.			
STRAIGHT 16° SLOPE TO			11.5 %
STA	14 %	ORD	+ 3.38 %
	18 %		+ 4.91 %
	22 %		+ 5.65 %
	26 %		+ 6.17 %
	30 %		+ 6.48 %
BOTTOM ℄ COORDINATES			
STRAIGHT 15° SLOPE TO			19.87 %
STA	22 %		- 5.86 %
	26 %		- 6.75 %
	30 %		- 7.44 %
END OF CONSTANT SECTION AT			93 %

V-TAIL CHARACTERISTICS

SWEEP L.E. TRUE	45°
ROLL OUT	45°
L.E. RADIUS - CONSTANT	.5 FT.
ROOT CHORD	15.45%
TIP CHORD	9.28 %
SEMI SPAN - TRUE	17.04%
LOCATE 60% ROOT CHORD AT	93%
ASPECT RATIO	1.375
TAPER RATIO	.60
AIRFOIL ROOT	4412 MOD.
TIP	4410 MOD.
TIP CROSS-SECTION	HALF-ROUND
BOTTOM SURFACE ∥ FUSELAGE ℄	
VERTICAL PLANE INTERSECT AT	-3.62%
INCIDENCE (FLAT BOTTOM)	0°

WING CHARACTERISTICS

SWEEP L.E.	10°
ASPECT RATIO	9.25
TAPER RATIO	.80
ROOT CHORD	7.42 %
TIP CHORD	5.92 %
SEMI SPAN	30.8%
MAC. LOCATION (WING OR BODY)	14.88%
QUARTER CHORD M.A.C. AT	35.5%
M.A.C.	6.72 %
AIRFOIL ROOT	4421
TIP	4418
DIHEDRAL (WING EXTENDED)	0°
INCIDENCE (CHORD PLANE)	
WING FULLY EXTENDED	+ 6°
WING ROOT T.E. LOCATED	
ABOVE FUSELAGE BOTTOM	
A CONSTANT	.75 FT.

EXPOSED AREA OF V-TAIL - DEFINED AS TRUE AREA OF FLAT BOTTOM SURFACE FROM INTERSECTION WITH CONSTANT FUSELAGE CROSS-SECTION TO TIP, EXCLUDING TIP FAIRING

EXPOSED AREA OF WING - DEFINED AS AREA OUTBOARD OF FUSELAGE MAXIMUM THEORETICAL WIDTH WITH WING FULLY EXTENDED (L.E. SWEPT 10°)

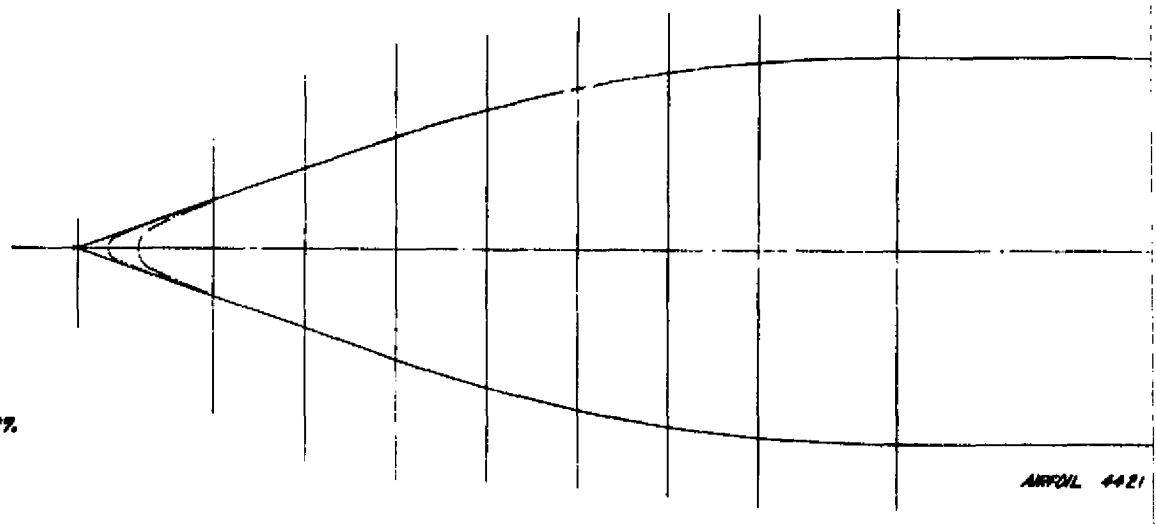

PLANFORM AREA (SQ.FT.) = 14.75% REF. LENGTH (FT.) x 100 % REF LENGTH (FT.)
WING AREA (EXPOSED, SQ. FT.) = 28 % PLAN AREA
V-TAIL AREA (EXPOSED, TRUE, SQ.FT.) 28.75% PLAN AREA
BODY WETTED AREA = 3.0℄ TIMES PLAN AREA
BODY TOTAL VOLUME = PLAN AREA TIMES 10.1 % REF LENGTH IN FEET.

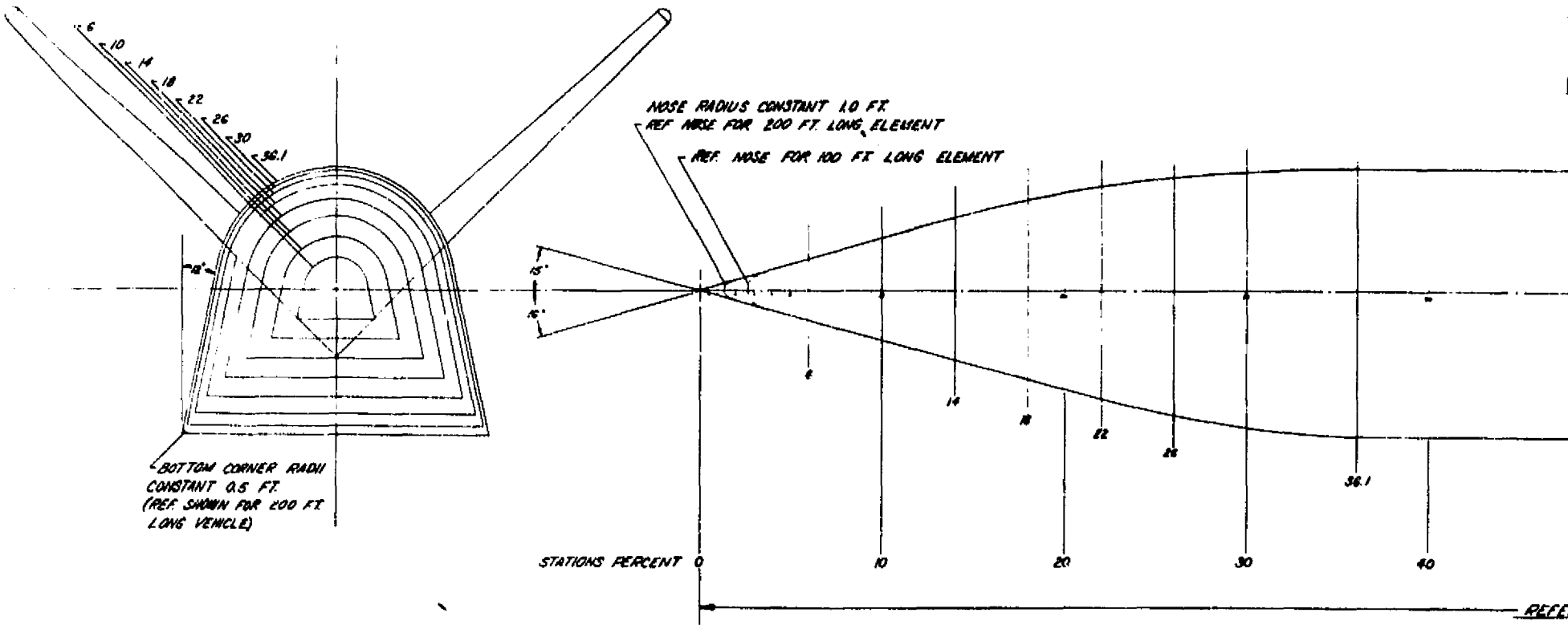

Figure 4-3. Vehicle Lines

FOLDOUT FRAME

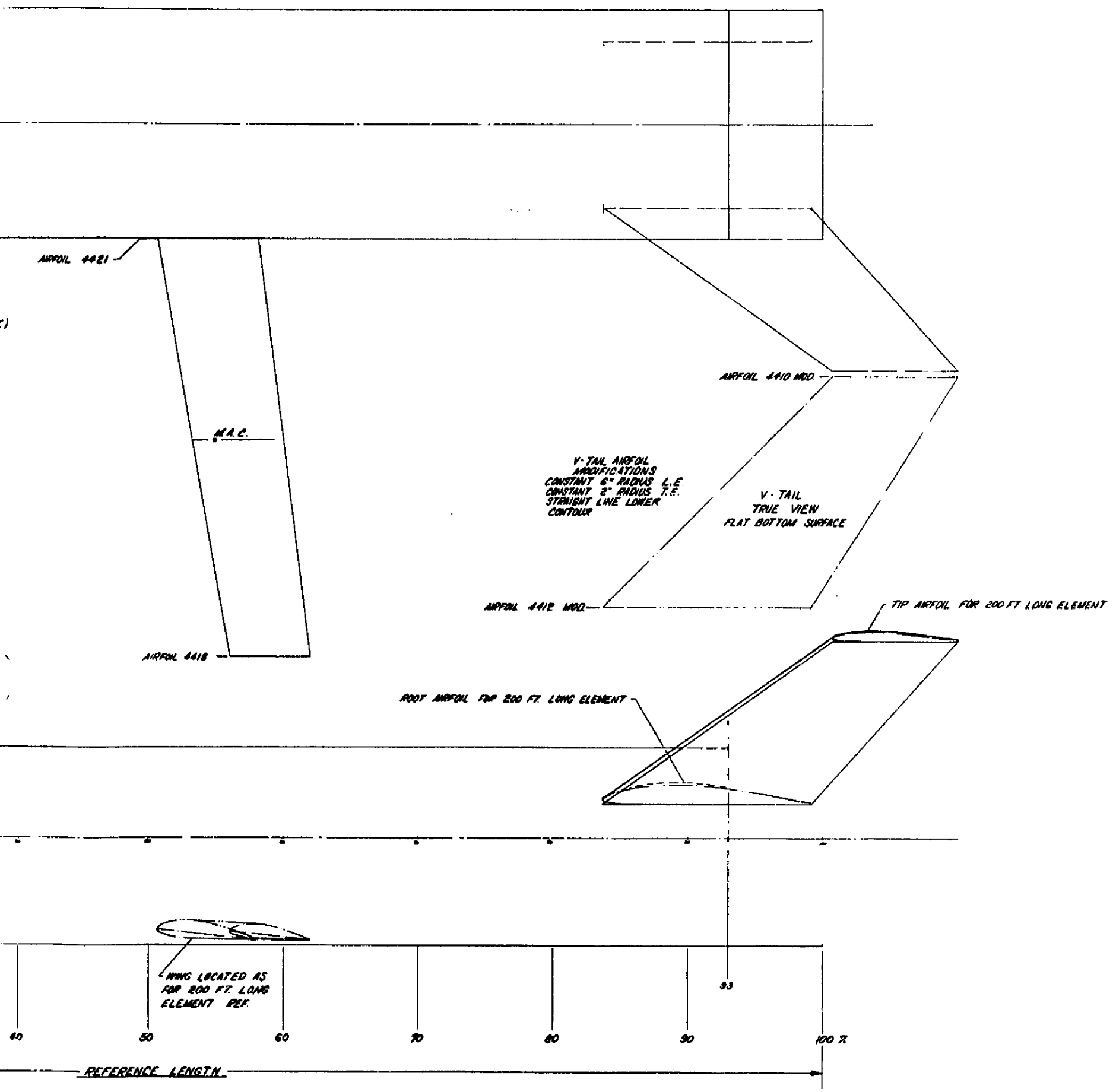

FOLDOUT FRAME 2

Table 4-1. FR-1 Synthesis Summary

	BOOSTER ELEMENT	ORBITER	VEHICLE
WEIGHT			
FUEL	187917	123299	
OXIDIZER	1202669	863096	
PROPELLANT	1390586	986395	
FLYBACK FUEL	20927	4177	
PAYLOAD		50000	
STRUCTURE	270197	270113	810507
CONTINGENCY	27020	27011	
OTHER	10907	66725	
TOTAL	1719637	1404421	4843694
IN ORBIT		424546	
RETURN CONDITION	329053	409961	
ENTRY	319313	353695	
LANDING	298123	348042	
VOLUME			
FUEL	46695	26640	
OXIDIZER	17813	12779	
PROPELLANT	64508	39419	
PAYLOAD		10638	
OTHER	59373	73839	
TOTAL	123881	123896	
GEOMETRY			
LENGTH	206.8	206.8	
BODY WETTED AREA	18727.3	18728.9	
BODY PLANFORM AREA	6047.1	6047.6	
ENTRY PLANFORM LOADING	52.8	58.5	
PROPULSION			
THRUST-TO-WEIGHT		1.63542	1.39273
NO. OF ENGINES	2	2	
THRUST PER ENGINE (SL)	1124400 UPRATED		
THRUST PER ENGINE (VAC)	O/F = 6.4 1148411 NOMINAL		
SPECIFIC IMPULSE (SL)	391.3	383.0 O/F = 7.0	391.2
SPECIFIC IMPULSE (VAC)	455.6	451.7	455.6
TRAJECTORY			
MASS RATIO		3.30749	2.34843
MAXIMUM DYNAMIC PRESSURE			611.7
STAGING DYNAMIC PRESSURE			50
STAGING VELOCITY (RELATIVE)			8096
STAGING ALTITUDE			171148
STAGING FLIGHT PATH ANGLE (RELATIVE)			8.534
INJECTION VELOCITY (INERTIAL)		25897	
INJECTION ALTITUDE		260008	
INJECTION FLIGHT PATH ANGLE (INERTIAL)		.000	
INJECTION INCLINATION		54.92	
FLYBACK RANGE	224.9		

Table 4-2. FR-1 Vehicle Summary Weight

SPACECRAFT SUMMARY WEIGHT STATEMENT

CONFIGURATION: FR-1 | BY: | DATE:

CODE	SYSTEM	ITEM OR MODULE A	B	C	D	E	F	SPACECRAFT M	U
1.0	AERODYNAMIC SURFACES	44396						48359	
2.0	BODY STRUCTURE	89176						96623	
3.0	INDUCED ENVIR PROT	52283						56381	
4.0	LNCH RECOV & DKG	17119						17449	
5.0	MAIN PROPULSION	80621						59893	
6.0	ORIENT CONTROL SEP & ULL	9057						11756	
7.0	PRIME POWER SOURCE	613						2092	
8.0	POWER CONV & DISTR	2742						2852	
9.0	GUIDANCE & NAVIGATION	220						310	
10.0	INSTRUMENTATION	220						275	
11.0	COMMUNICATION	220						242	
12.0	ENVIRONMENTAL CONTROL	330						616	
13.0	(RESERVED)								
14.0	PERSONNEL PROVISIONS								
15.0	CREW STA CONTRL & PAN	220						275	
16.0	RANGE SAFETY & ABORT								
SUBTOTALS (DRY WEIGHT)		297217						297123	
17.0	PERSONNEL	900						920	
18.0	CARGO							50000	
19.0	ORDNANCE								
20.0	BALLAST								
21.0	RESID PROP & SERV ITEMS	9740						8064	
SUBTOTALS (INERT WEIGHT)		10640						58984	
22.0	RES PROP & SERV ITEMS								
23.0	INFLIGHT LOSSES	21194						15417	
24.0	THRUST DECAY PROPELLANT								
25.0	FULL THRUST PROPELLANT	1390586						1032897	
26.0	THRUST PROP BUILDUP								
27.0	PRE-IGNITION LOSSES								
TOTALS (GROSS WEIGHT) (LB)		1719637						1404421	
DESIGN ENVELOPE VOLUME (FT^3)		123881						123896	
PRESSURIZED VOLUME (FT^3)									
DESIGN ENVEL SURF AREA (FT^2)		18727						18729	
PRESSURIZED SURF AREA (FT^2)									
DESIGN q, MAX (LB/FT^2)		612						612	
DESIGN ε, MAX		4						4	
DESIGN POWER, MAX (KW)									
DESIGN NO. MEN/DAYS		3/.1						2/7	

DESIGNATIONS:

CODE, SYSTEM: REF. MIL-M-38310A OR SP-6004

ITEM OR MODULE

A - Booster

B

C

D

E

F

SPACECRAFT

M MANNED LAUNCH - Orbiter

U UNMANNED LAUNCH

NOTES & SKETCHES:

Thrust decay propellants are included in residual weights.

Tanks are over-sized to account for thrust build-up and pre-ignition losses.

MSC Form 1523 (Jul 69)

SECTION 5

CROSSFEED VERSUS NO CROSSFEED

5.1 VEHICLE CONSIDERATIONS

With many of the parallel staged vehicle configurations being considered for space shuttle, it is possible and from some standpoints desirable to burn all engines of both booster and orbiter at launch. Operation of all engines at full thrust throughout boost phase is possible if crossfeed plumbing is provided to permit operation of the orbiter engines on propellants supplied from the booster. If all engines operate at full thrust during boost phase, the following advantages are obtained:

a. Since the orbiter engines provide part of the required thrust, the thrust required by the booster is reduced, reducing either the size or number of booster engines. The reduction in engine weight improves vehicle performance. Depending on the specific vehicle configuration, use of a higher expansion ratio or a reduction in size of aerodynamic fairings required for nozzle protection may be possible, further improving performance.

b. Loads on the connections between elements are reduced, since the orbiter, instead of being carried up inert to the maximum boost phase acceleration (generally 3g), is being accelerated by its own engines (generally at about 1.5g). This could reduce interconnection loads by up to 50 percent, depending on design criteria for orbiter engine-out. This reduction in weight could improve vehicle performance.

c. All main engines operate from launch, eliminating the requirement for in-flight start of the orbiter engines. This is somewhat more important for space shuttle than for past rocket vehicles because of intact abort requirement (no separate escape system for crew or passengers). Complete failure of the orbiter engines to operate results in the loss of vehicle and crew.

d. Balance of booster vehicles is improved because of the reduction in engine weight.

Addition of subsystems required for propellant crossfeed capability in the space shuttle produces a number of disadvantages:

a. Hardware to interconnect the main propellant systems of the booster and orbiter must be added. At the minimum, a main propellant crossfeed incorporating a retracting, non-spilling disconnect 10 to 20 inches in diameter is required for each propellant. For additional safety, valves to back up the disconnect, recirculation systems, and purge systems may be required.

b. Heat shield doors — for some vehicle designs, the crossfeed plumbing must penetrate the heat shield, requiring doors and related opening/closing mechanisms. Failure of a door could result in loss of a vehicle.

c. Additional staging functions — at staging, orbiter propellant flow must be phased from booster tanks to orbiter tanks, crossfeed lines disconnected and retracted, and heat shield doors closed. Timing of these functions is critical and may impose some performance penalties.

d. Increased development requirements — component development programs are required for crossfeed hardware. An all-up system static firing test stand coupling the orbiter and the booster may be required.

e. Feed system transients — pressure transients at booster engine shutdown and at staging may affect operation of the orbiter engine.

Because of the significant disadvantages associated with crossfeed, a study was made to determine the performance of comparable vehicles with and without crossfeed.

5.2 PERFORMANCE COMPARISON

The crossfeed comparison study was made on three-element vehicles. Those with crossfeed were designated FR-1, and those without crossfeed were designated FR-4. The procedure used for the study was to synthesize vehicles with and without crossfeed for identical missions, as defined in Table 5-1, on the Convair space shuttle synthesis program, incorporating a fixed weight penalty for the crossfeed plumbing, residuals, and heat shield doors. Estimated weight penalties generated by NASA MSFC and Convair were considered. Initially, the weight penalites used were based on a 4-4-4 configuration using 500, 000-pound thrust Bell engines for both the FR-1 and FR-4 configurations. Performance data generated is shown in Table 5-2 and Figure 5-1. Two major conclusions were drawn from these data.

a. For a given configuration (for example, a 5-3-5 engine arrangement) use of crossfeed reduces launch weight between 8 and 11 percent.

b. There are different optimum engine arrangements for FR-1 and FR-4, and use of these optimum configurations minimizes performance differences. FR-1 and FR-4 vehicle performance was found to be a strong function of initial orbiter F/W ratio. For equal volume vehicles with common orbiter and booster engines, orbiter F/W is uniquely determined by the engine arrangement (i.e., relative number of engines in orbiter and boosters). For the FR-4, orbiter thrust/weight is substantially higher with a given engine arrangement than FR-1. For vehicles of equal weight with a 5-3-5 engine arrangement, FR-4 orbiter thrust is 30 percent of launch thrust (3/5+5), while for FR-1 it is only 23 percent (3/5+5+3). Consequently, initial orbiter F/W is about 30 percent higher. To equalize orbiter F/W ratios, the number of orbiter engines divided by the total number of engines operating at liftoff should be approximately the same.

Because of the importance of the engine arrangement in a proper evaluation of crossfeed, the weight penalties for crossfeed were reassessed with more nearly optimum

Table 5-1. Mission Requirements for Crossfeed Study

Payload	50,000 pounds
Launch Site	ETR
Orbit	55-degree inclination
On-orbit ΔV	1800 fps
ACS ΔV	200 fps
Launch Thrust/Weight Ratio	1.47
Maximum F/W Ratio	3
Staging Dynamic Pressure	50 psf
Injection Altitude	45 n.mi.

engine arrangements. Propellant feed system designs were developed for the 6-3-6 FR-4 and the 5-3-5 FR-1 vehicles described in Table 5-2. These designs are shown in Figures 5-2 and 5-3. Two crossfeed arrangements are shown, one with "full" manifolding that allows flow of propellant completely across the vehicle from one booster to the other, and one with "partial" manifolding that provides the minimum connections required for feeding the orbiter engines. The latter arrangement has the same operational disadvantages as the no-crossfeed case in that booster-engine-out results in a buildup of cg asymmetry because of unequal booster propellant consumption.

The propellant system weight differences between the no crossfeed 6-3-6 arrangement and the two crossfeed arrangements were then determined. These differences are summarized in Table 5-3. Orbiter feed system weights are substantially increased because of added disconnects, shutoff valves, TPS doors, and residuals in the added ducting. Booster feed system weights are almost unchanged with full manifolding and reduced 1000 pounds with partial manifolding. The reason for this reduction is not obvious on inspection of the feed system layout. However, when it is considered that each FR-4 booster has six engines of 631,000-pound thrust, while the FR-1 has only five engines of 543,000-pound thrust, each with required plumbing and residuals, the reasons become apparent.

Figure 5-4 was then developed, using the crossfeed weight penalties given in Table 5-3. Gross liftoff weight (GLOW) for FR-4 no crossfeed vehicles and FR-1 crossfeed vehicles with full and partial manifolds are shown as a function of orbiter F/W ratio. Engine arrangements that result in the parametric F/W values are indicated. Evaluation of the abort capabilities of these configurations with orbiter engine-out, discussed in Paragraph 3.2.2 of Volume IV, shows that the 5-3-5 FR-1 is the lightest satisfactory configuration. The 8-3-8 FR-4 configuration is satisfactory, since orbiter engine loss affects only the orbiter solo phase, and not the boost phase of flight.

Table 5-2. Crossfeed Comparison, 50K Pound Payload Vehicle, Various Engine Arrangements

	No Crossfeed	No Crossfeed	No Crossfeed	Crossfeed NASA ΔWT(1)	Crossfeed GDC ΔWT(1)	Crossfeed NASA ΔWT(1)	Crossfeed GDC ΔWT(1)
Engine Arrangement	5-3-5	6-3-6	5-2-5	5-3-5	5-3-5	5-4-5	5-4-5
Liftoff Weight — lb	5,389,086	5,154,182	4,991,800	5,020,753	4,889,577	5,231,583	5,098,682
Booster Sea Level Thrust/Engine — lb	792,496	631,436	734,185	557,256	542,696	550,960	536,964
Orbiter Vacuum Thrust/Engine — lb	934,898	744,898	866,109	666,079	648,676	658,553	641,824
Orbiter I_{SP}, S.L./VAC	-/453.0	-/453.0	/453	378.5/456	378.5/456	378.5/456	378.5/456
Booster I_{SP}, S.L./VAC	384.0/446.0	384.0/446.0	384/446.5	381.5/451.5	381.5/451.5	381.5/451.5	381.5/451.5
Booster Engine Weight — lb	41,328	40,087	38,460	30,720	29,979	30,400	29,687
Orbiter Engine Weight — lb	25,653	20,725	15,912	18,887	18,451	24,919	24,334
Orbiter F/W @ Staging	1.975	1.651	1.327[2]	1.5	1.5	1.88583	1.88795
Liftoff Weight Change — lb	REFERENCE	-234,904	398,000	-368,333	-499,509	-157,000	-209,404

(1) Added weights for crossfeed are as follows:

	NASA	Convair
Orbiter	6412	2845
Booster (2)	6652	7028

(2) This orbiter F/W ratio is below the minimum required for "once around" abort in event of one orbiter engine failure (1.54 minimum with a total of 2 engines).

Note: Liftoff F/W for all vehicles is 1.47.

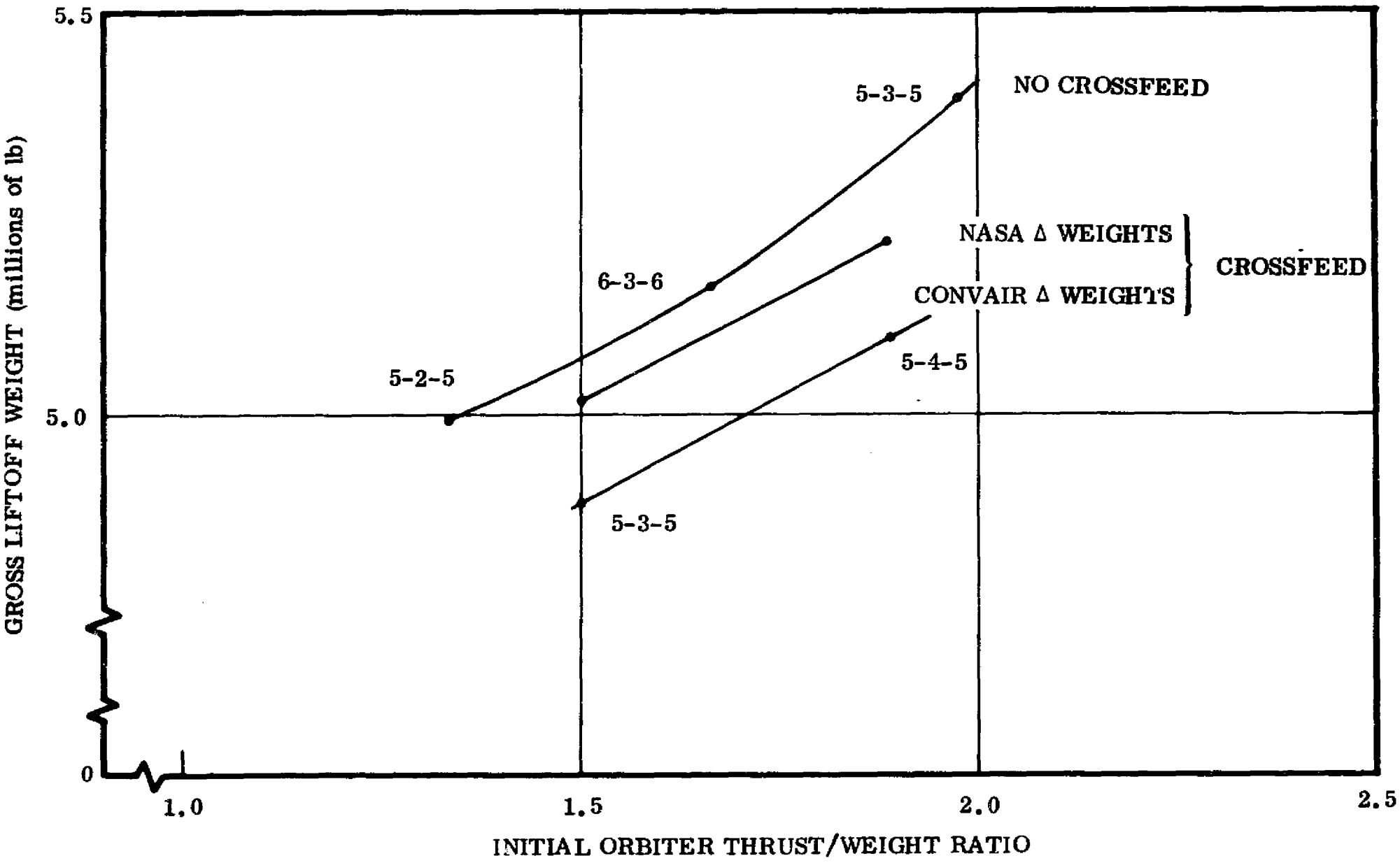

Figure 5-1. Launch Weight Comparisions for FR-1 and FR-4 Vehicles

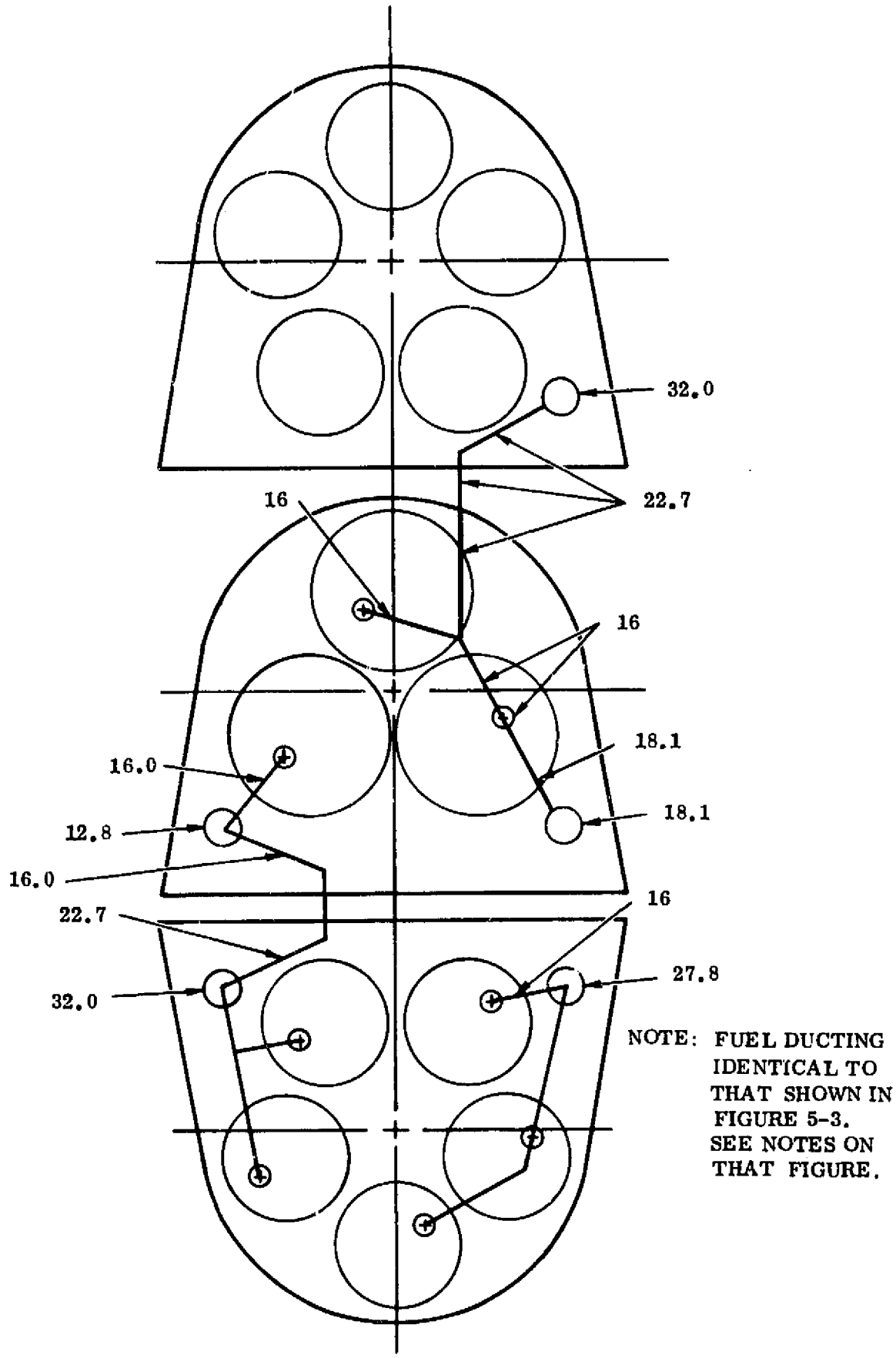

Figure 5-2. FR-1 Propellant Feed Duct Routing, Partial Manifolding

FR-4

6-3-6 CONFIGURATION

NO CROSSFEED

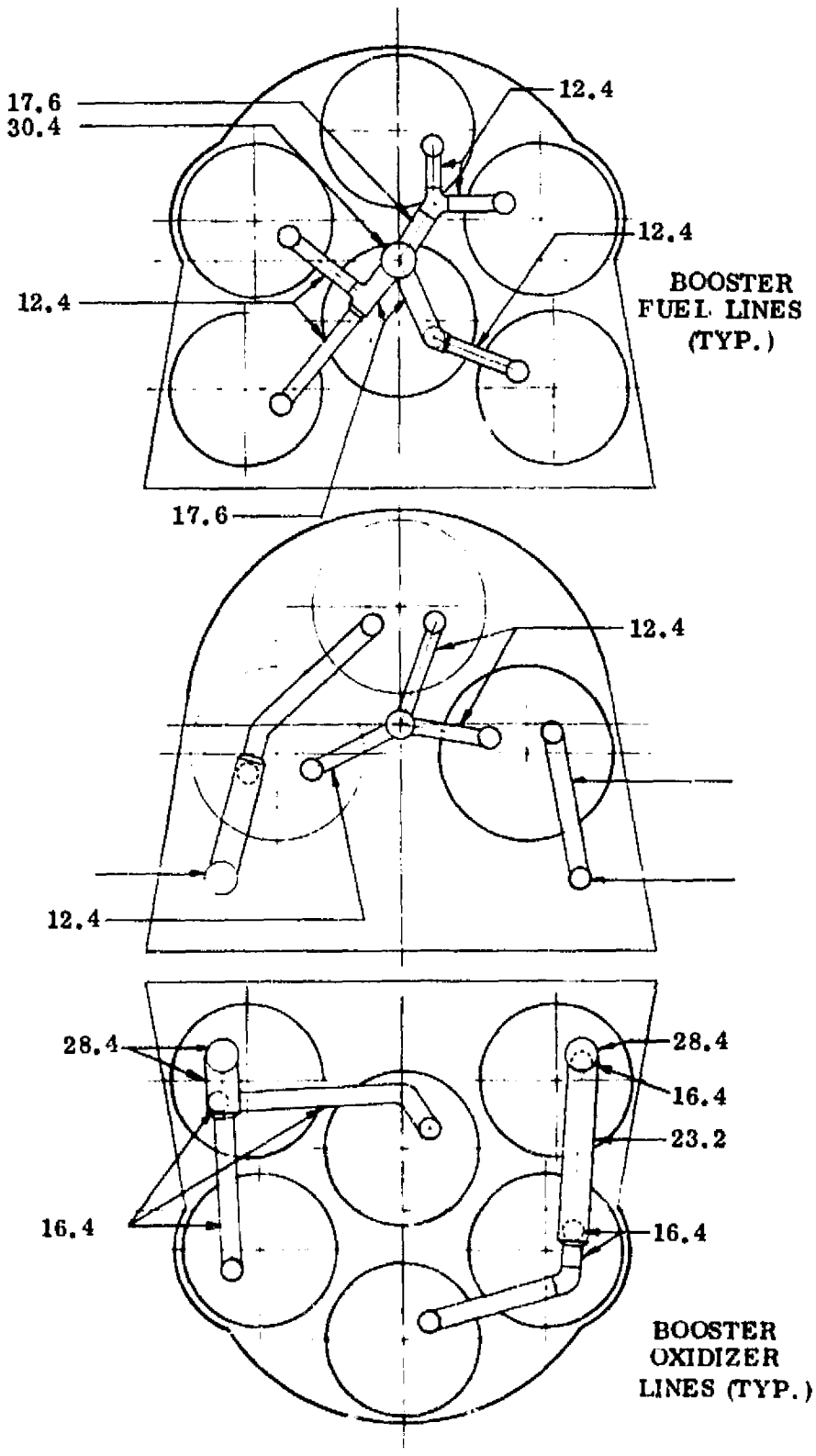

FOLDOUT FRAME

NOTE: 1. NUMBERS REFER TO LINE DIAMETER SIZED FOR MAXIMUM FLOW ACCELERATION OF 0.004 LB/SEC^2-LB. PER ENGINE.
2. ALL DIMENSIONS IN INCHES.

FR-1
5-3-5 CONFIGURATION WITH
CROSSFEED AND FULL MANIFOLDING

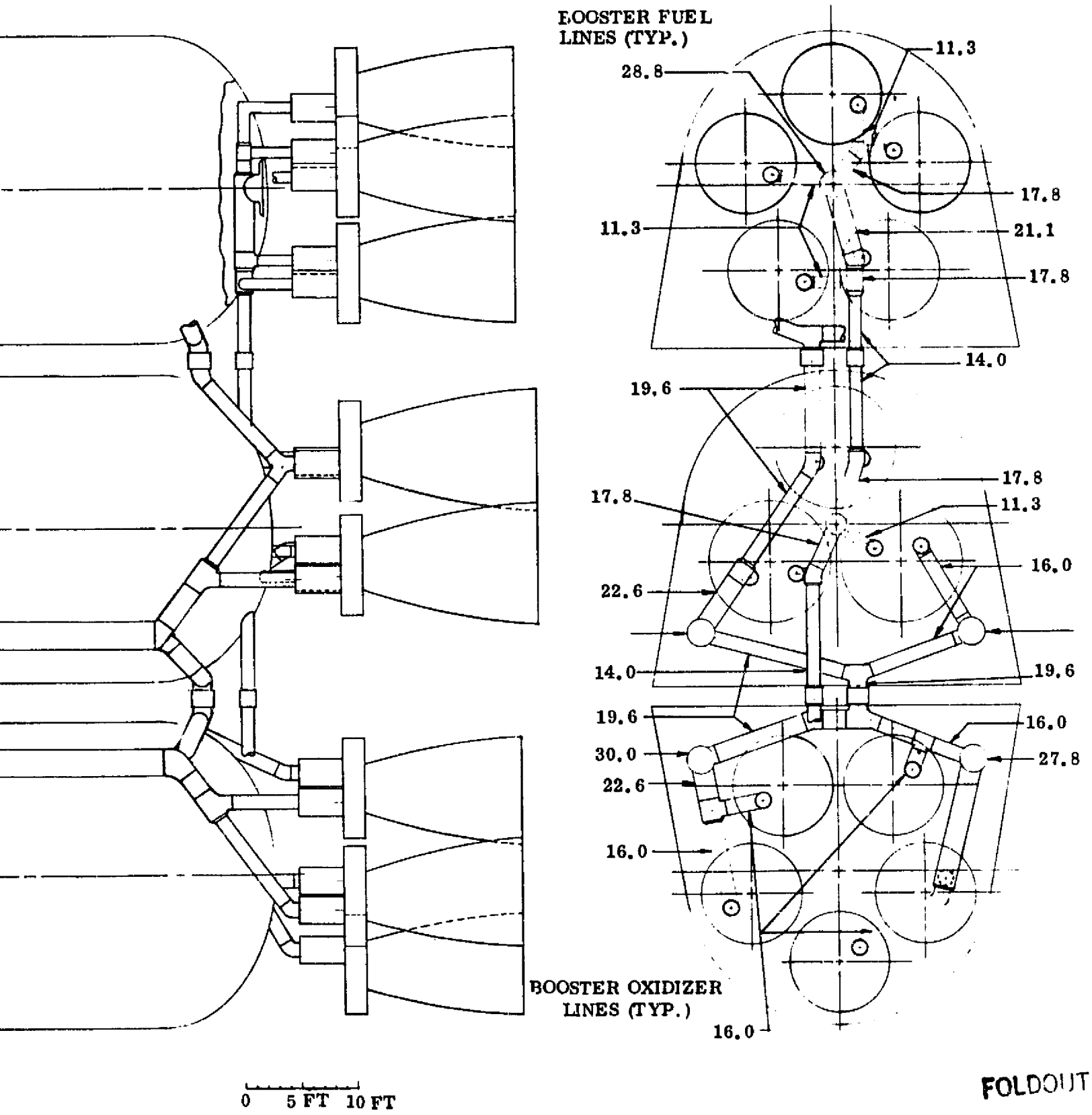

FOLDOUT FRAME

Figure 5-3. Propellant Feed Duct Routing, FR-1 and FR-4 Vehicles

Table 5-3. Propellant Feed System Weight Differences 5-3-5 FR-1 Compared With 6-3-6 FR-4, 50,000-Pound Payload

FULL MANIFOLDING	LO_2 SYSTEM (pounds)	LH_2 SYSTEM (pounds)	TOTAL (pounds)
Orbiter	6980	1148	8128
Booster (each)	510	-437	73
PARTIAL MANIFOLDING			
Orbiter	5820	1148	6968
Booster (each)	-560	-437	-997

NOTE: Plus weight values mean crossfeed system weights heavier, and minus values mean crossfeed system weight lighter.

5.3 SUMMARY

The following conclusions may be drawn from the data presented in Figure 5-4.

a. For a given vehicle configuration, use of crossfeed reduces vehicle launch weight 6 to 9 percent. This can be seen by comparing 5-3-5 configurations weighing approximately 5.39 million pounds without and 4.9 to 5.02 million pounds with crossfeed. For a "common" element vehicle, therefore, performance improvement is substantial.

b. For vehicles optimized for either crossfeed or no crossfeed differences in launch weight are minor, the exact differences depending on relative detail weight differences, pro and con, for crossfeed. This can be seen by comparing the 8-3-8 configuration at 4.82 million pounds and the 5-3-5 FR-1 at 4.9 to 5.02 million pounds.

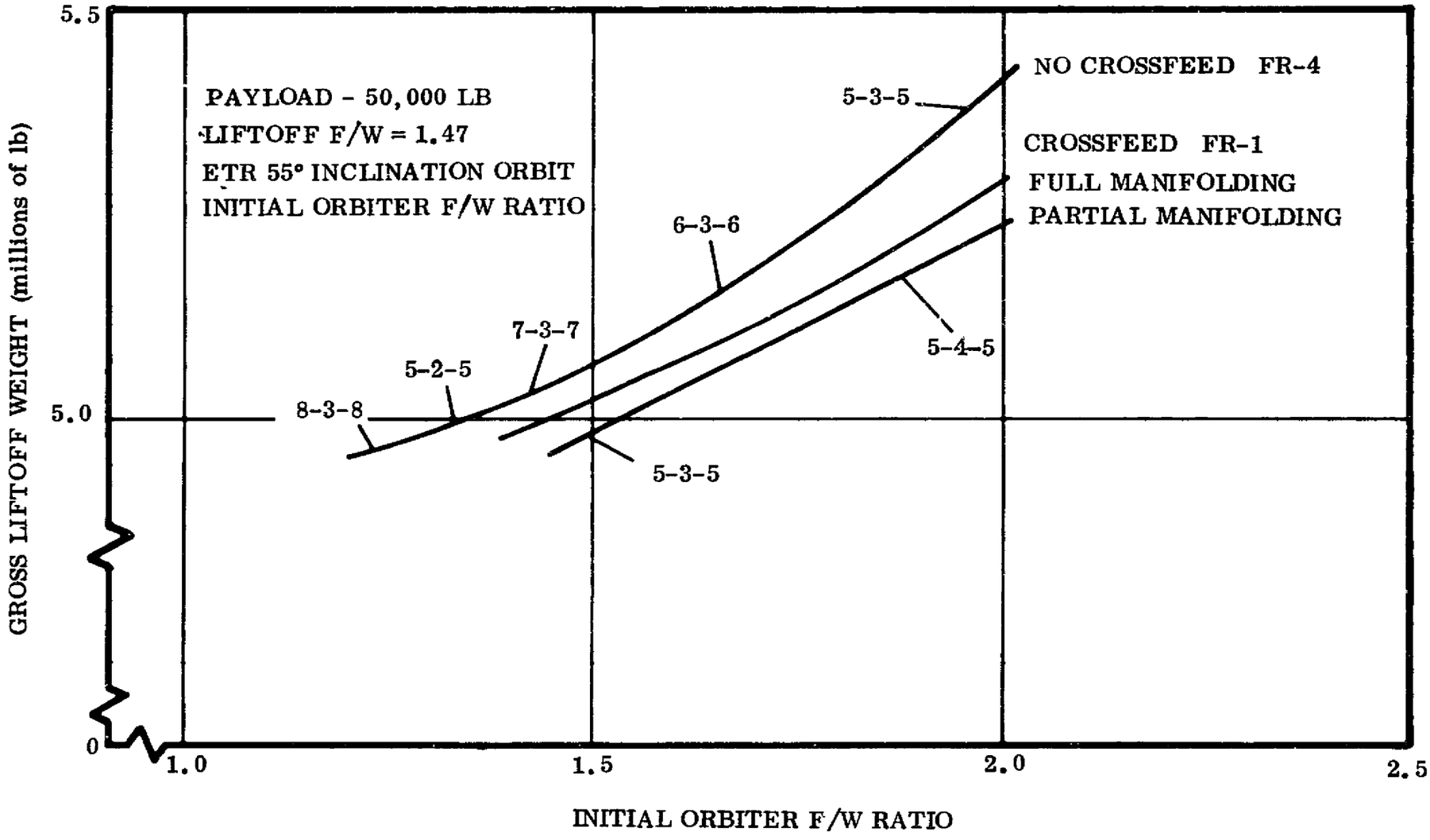

Figure 5-4. Launch Weight Comparison for FR-1 and FR-4 Vehicles

SECTION 6

FIXED-WING AND DEPLOYABLE-WING VERSIONS OF THE TWO-STAGE SEQUENTIAL-BURN SPACE SHUTTLE

6.1 FIXED-WING-CONFIGURATION DESIGN

A preliminary design study was made to evaluate a fixed-wing ILRV configuration. The fixed-wing configuration for the study was a conversion of the current FR-3 deployable-wing design. Figures 6-1, 6-2, and 6-3 show the FR-3 orbiter, booster, and launch configuration respectively.

As the fixed-wing design was to be a conversion of the existing FR-3 deployable-wing design and is inherently less complex, a list was made of the differences between them. The list is shown in Table 6-1. This list was used to ensure that the synthesis program inputs were changed to reflect the differences between the designs.

Initial configurations based on the FR-3 deployable-wing design were made and used as a model for studying the aerodynamics, dynamics, loads, thermodynamics, and structural aspects of a fixed-wing design. Some of the decisions made during the initial design phase were to use a wing area equal to the current deployable-wing design. The wing was subject to geometric growth as the design was iterated on the synthesis program as was done for the deployable-wing design. The wing shape is the same as an MSC fixed-wing design. A launch configuration similar to the FR-3 design was used throughout the study. This configuration was a nose-to-nose arrangement and is shown on the fixed-wing design, Figure 6-4. This arrangement (as stated before) is similar to the FR-3 design; consequently, comparison between the two are on the same basis. As launch shear winds are assumed to be from any direction, the positioning of wings to reduce maximum αq loads was not considered. The bottom-to-bottom arrangement gives a more symmetrical body cross-section and reduces the discontinuities between the boost and orbit elements. Flat mating surfaces appear to simplify structural attachment. A single vertical tail proportioned from the MSC design was used.

As can be seen from Figure 6-4, the plan and end view shows a complex arrangement of wing and tail surfaces in the launch configuration. The effects of shock flow, particularly during transonic boost flight, and shock impingement, during entry for the separate booster and orbiter elements, are difficult to evaluate, and considerable wind-tunnel testing is needed to bring their effects into an evaluation. These effects were not considered in this study.

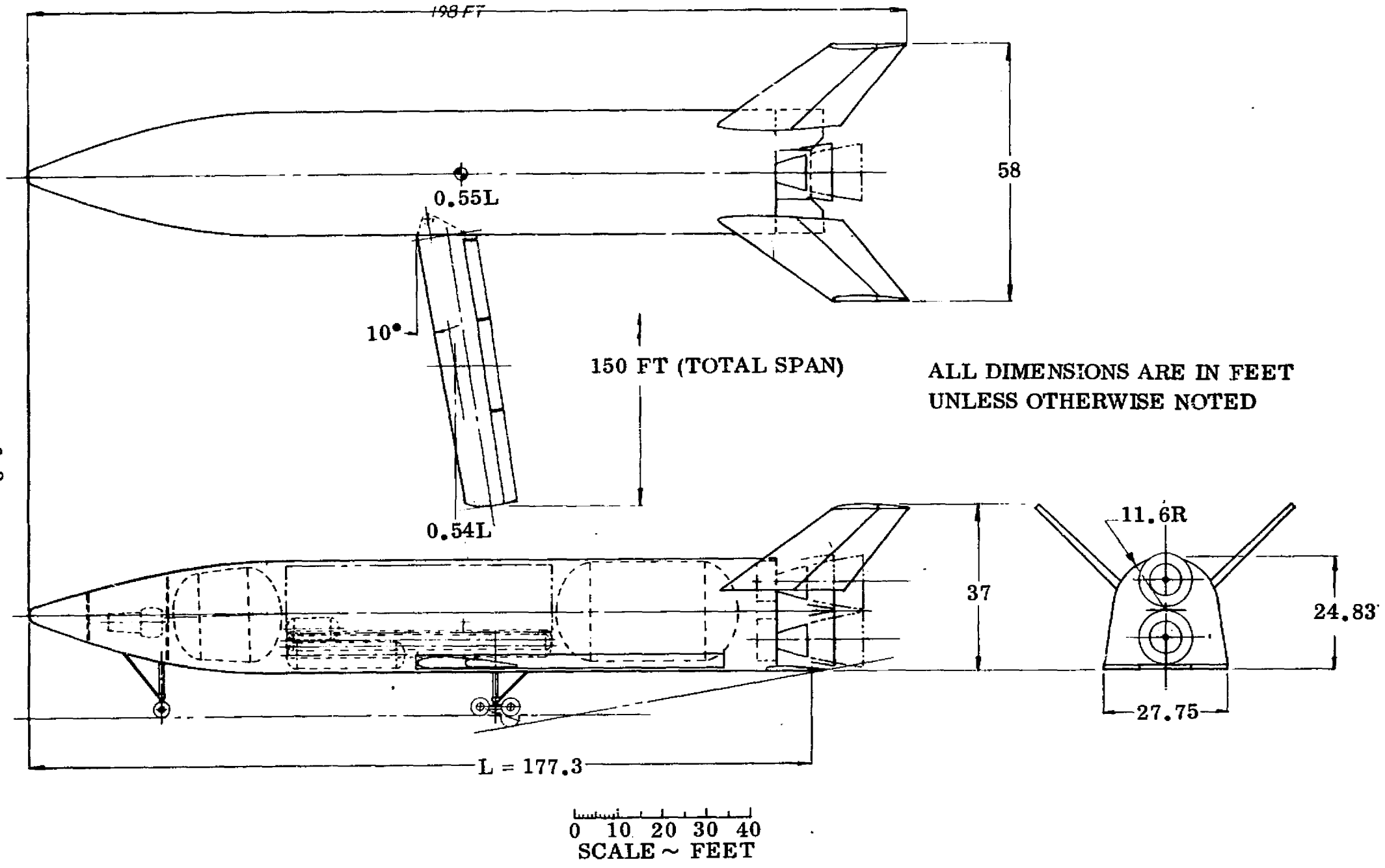

ALL DIMENSIONS ARE IN FEET
UNLESS OTHERWISE NOTED

Figure 6-1. FR-3 Two-Element Sequential-Burn Orbiter

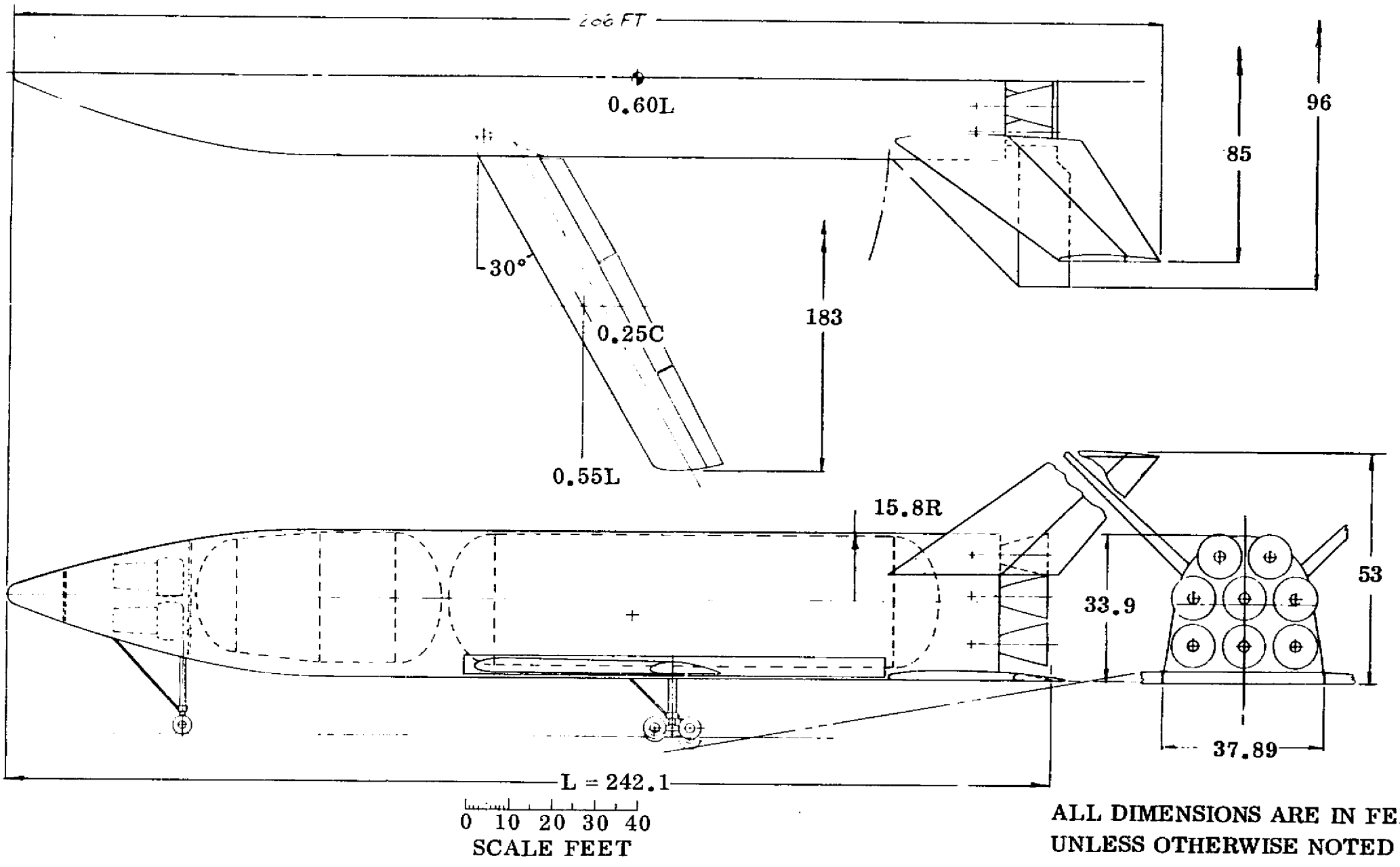

Figure 6-2. FR-3 Two-Element Sequential-Burn Booster

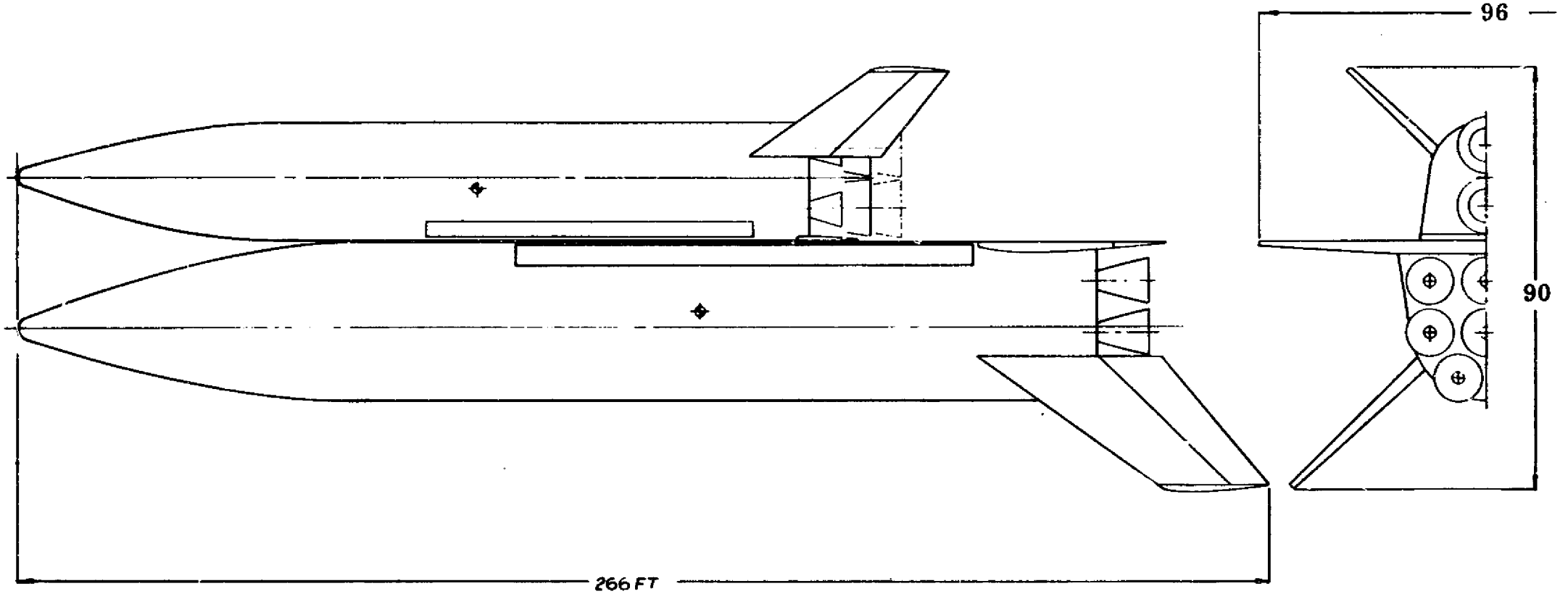

Figure 6-3. FR-3 Two-Element Sequential-Burn Launch Configuration

Table 6-1. Fixed- and Deployable-Wing Variations

	FIXED WING		DEPLOYABLE WING	
	ORBITER	BOOSTER	ORBITER	BOOSTER
BODY				
GEOMETRY	X	-	-	-
WING PIVOT FRAME	X	X	-	-
MAIN LANDING GEAR INSTALLATION	X	X	-	-
WING DOORS	X	X	-	-
WING				
GEOMETRY	X	X	-	-
PIVOT	X	X	-	-
ACTUATOR ATTACHMENTS	X	X	-	-
LEADING EDGE	X	X	-	-
TRAILING EDGE	X	X	-	-
FLAPS	X	X	-	-
SPOILERS	X	X	-	-
WING TIPS	X	X	-	-
CARRY THROUGH STRUCTURE	-	-	X	X
STRUCTURAL BOX	X	X	-	-
HORIZONTAL TAIL				
GEOMETRY	X	X	-	-
VERTICAL TAIL				
GEOMETRY	X	X	-	-
ACTUATION				
DOORS	X	X	-	-
WINGS	X	X	-	-
LANDING GEAR				
GEOMETRY	X	X	-	-
THERMAL PROTECTION SYSTEM				
COVER PANELS	X	X	-	-
INSULATION	X	X	-	-
BOOST DRAG	X	X	-	-
LOADS	X	X	-	-

X = VARIATION

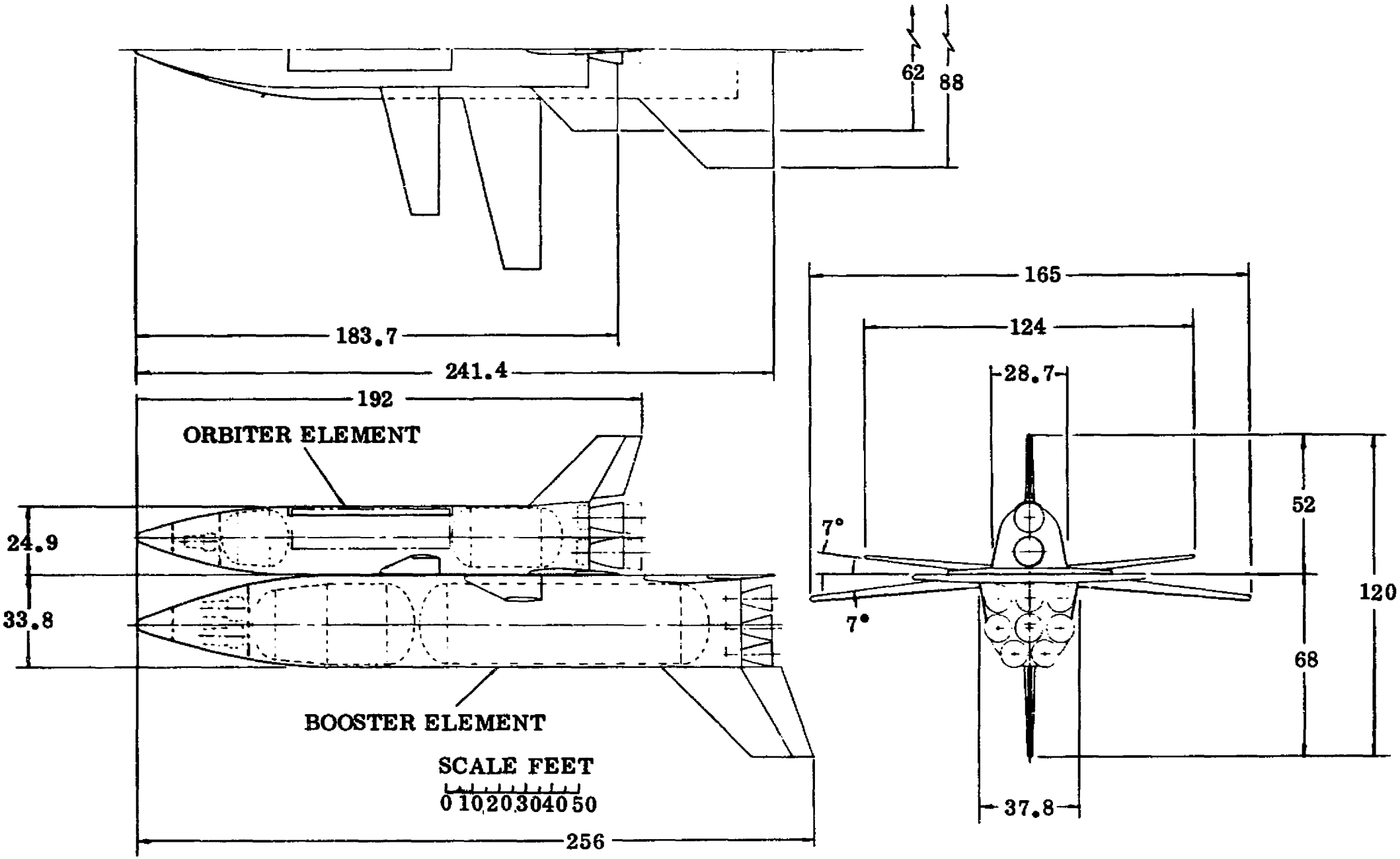

ALL DIMENSIONS ARE IN FEET
UNLESS OTHERWISE NOTED

Figure 6-4. Fixed-Wing, Two-Element, Sequential-Burn Configuration

Figure 6-5 shows typical cross-sections of a deployable-wing and fixed-wing design. For the fixed-wing orbiter-element design a 9-inch slice (to eliminate wing storage volume) was taken from the lower surface to yield an improved volume utilization factor on the synthesis program.

6.2 AERODYNAMICS

The aerodynamic characteristics of the fixed-wing FR-3 configuration for both the launch and entry phases of flight were analyzed. Figures 6-6 through 6-9 present the results of these analyses.

The launch configuration aerodynamics are presented in Figure 6-6. Axial force, normal force gradient, and center-of-pressure location are presented over the launch Mach number range. Also shown for comparison are the launch characteristics of the FR-3 (deployable-wing) configuration. The data was derived from recent tests of 3- and 2-body launch configurations conducted by Convair in the Cornell Aeronautical Laboratory 8-foot transonic wind tunnel. The contributions of the wings were derived using the methods of Reference 6-1. The data of Figure 6-6 indicates the wing contributions add substantial launch drag, double the normal force gradient and, for the nose-to-nose launch configuration, decrease the longitudinal stability (although the total moment at a given angle of attack and Mach number is increased).

Figures 6-7 and 6-8 present the fixed-wing orbiter hypersonic entry aerodynamics, for angles of attack from 20 to 60 degrees. Also shown for comparison are the characteristics of the deployable-wing orbiter. These characteristics were analyzed by using the Convair Hypersonic Aerodynamics Prediction program, which is based on modified Newtonian aerodynamic theory. The trim capability of the fixed-wing configuration at a 60-degree angle of attack is shown; approximately 58% of the total horizontal stabilizing area must be removed from the flow (δ_e = -60 degrees) to trim with the center of gravity at 55.5% of body length, with additional control area required to trim at more forward cg locations. (The horizontal stabilizer surface area was sized to produce subsonic stability comparable to the deployable-wing configuration.) Figure 6-8 presents the lift/drag ratio and the static direction stability of the fixed-wing orbiter. It is indicated that the configuration is directionally unstable, even at a 60-degree angle of attack, with the single vertical surface (which has effectively no contribution except at low angles of attack). The increase in directional stability due to an incorporation of vee tails is indicated, although at lower angles of attack the interference between the wing and the tail would reduce the tail effectiveness.

An entry trajectory for the fixed-wing orbiter was generated using a three-degree-of-freedom-trajectory computer program. Figure 6-9 presents the altitude time history of the entry, starting from 400,000 feet with velocity of 25,315 fps and a -1.5-degree flight path angle. With a 60-degree angle of attack and 45 degrees of bank, a cross-range of approximately 175 nautical miles is achieved. A maximum resultant load factor of 2.18g is produced at 185,000 feet. Also shown is a typical

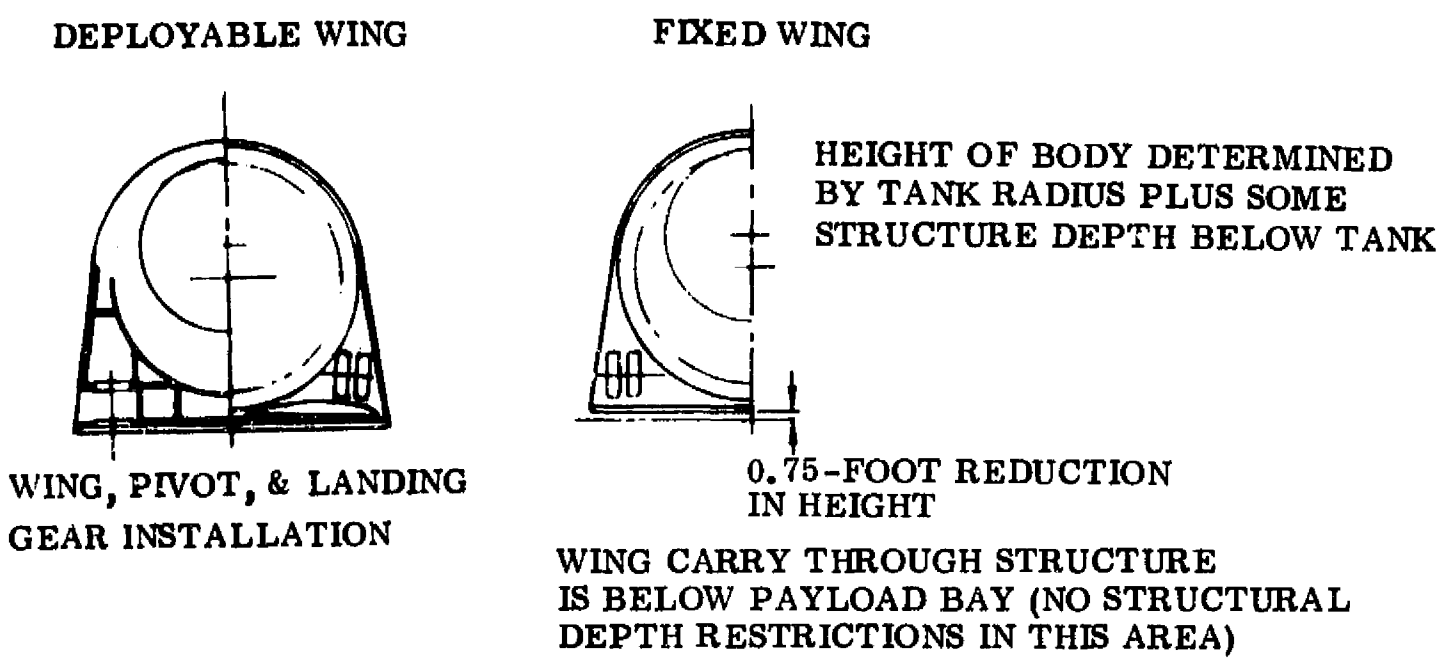

Figure 6-5. Typical Orbiter Cross-Section

$C_{L_{max}}$ entry for the deployable-wing orbiter, which with 35 degrees of final bank achieves approximately 750 nautical miles of lateral crossrange.

6.3 DYNAMICS AND LOADS

Loads at maximum dynamic pressure flight condition were determined by flying the vehicle through 99 percentile Marshall synthesis wind profiles with the maximum wind and gust occurring at the maximum dynamic pressure condition. The trajectory was determined using a three-degree-of-freedom simulation with a control system. The fixed-wing FR-3 configuration requires a cant angle of 8 degrees and a gimbal angle of ±7.5 degrees about the cant angle. The maximum dynamic pressure was 600 psf, and the maximum angle of attack at the maximum dynamic pressure was 10 degrees. No attempt was made to reduce the maximum dynamic pressure by accepting performance losses. Both nose-to-nose and tail-to-tail configurations were analyzed.

The results of the loads analysis are presented in Figures 6-10 through 6-13. These curves indicate that the maximum αq loads of the fixed-wing configuration imposes a penalty on the booster body in both the nose-to-nose and the tail-to-tail arrangements and also on the orbiter of the nose-to-nose arrangement. The next critical loads are the booster burnout condition as shown by the curves. For the orbiter vehicle in the tail-to-tail arrangement, the booster burnout condition remains the critical one, although the maximum αq loads for the fixed-wing configuration are substantially higher than those for the stowed deployable-wing configuration.

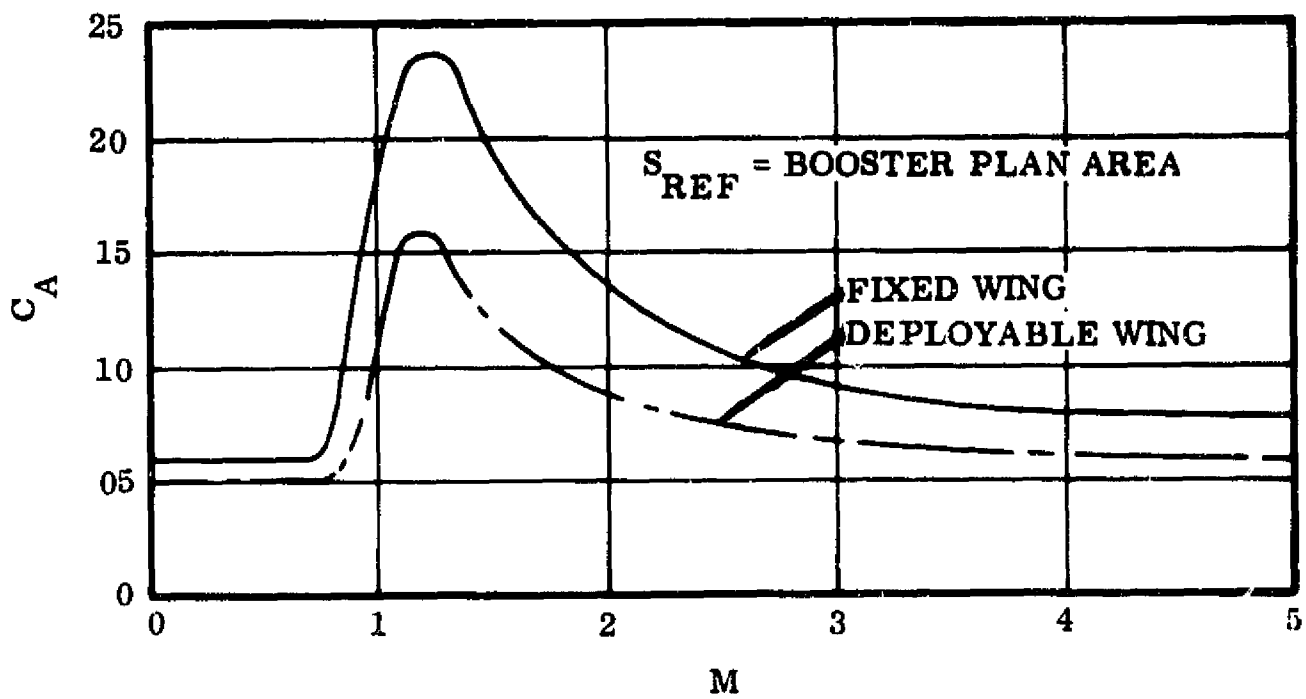

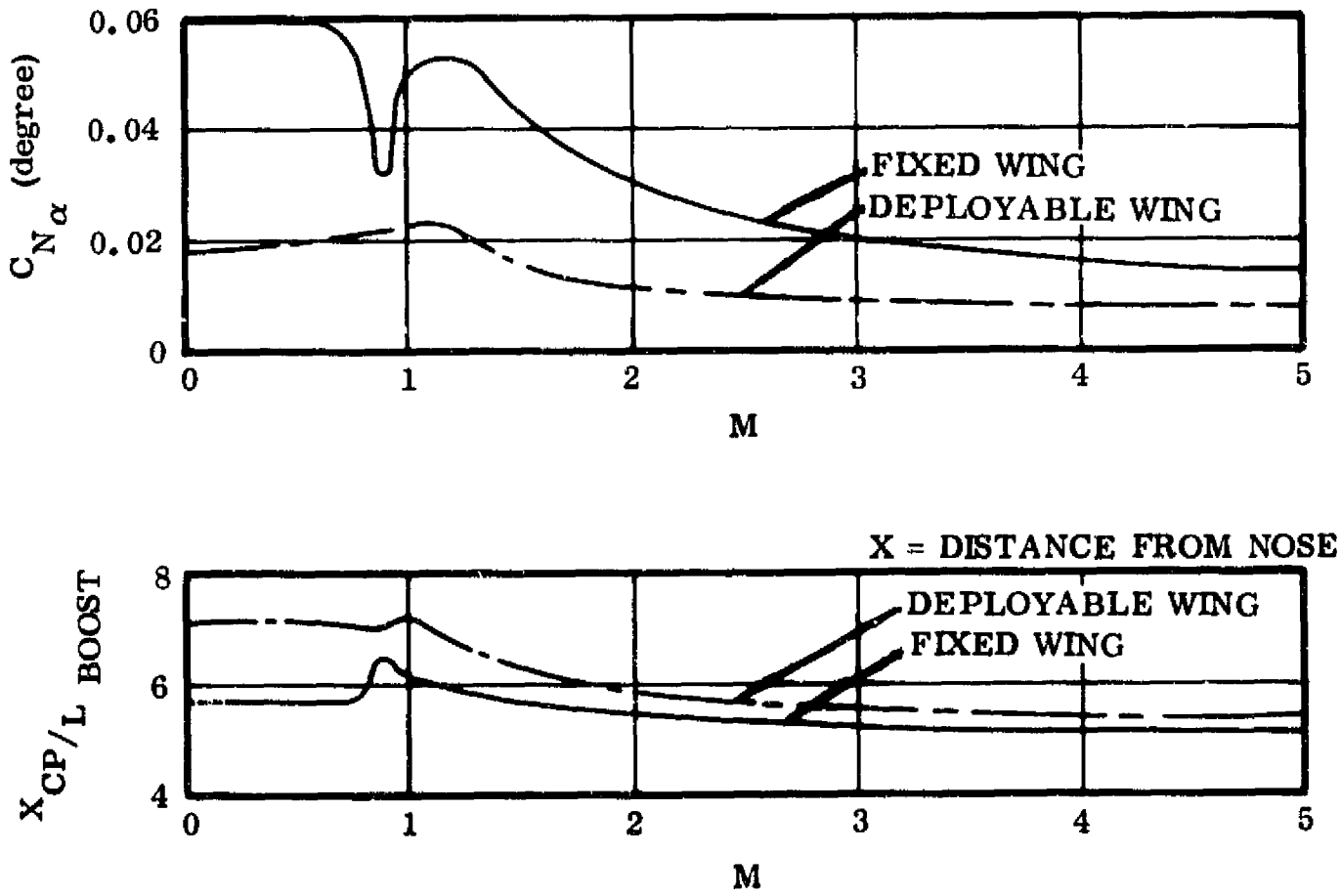

Figure 6-6. Two-Element Vehicle Launch Configuration Aerodynamics

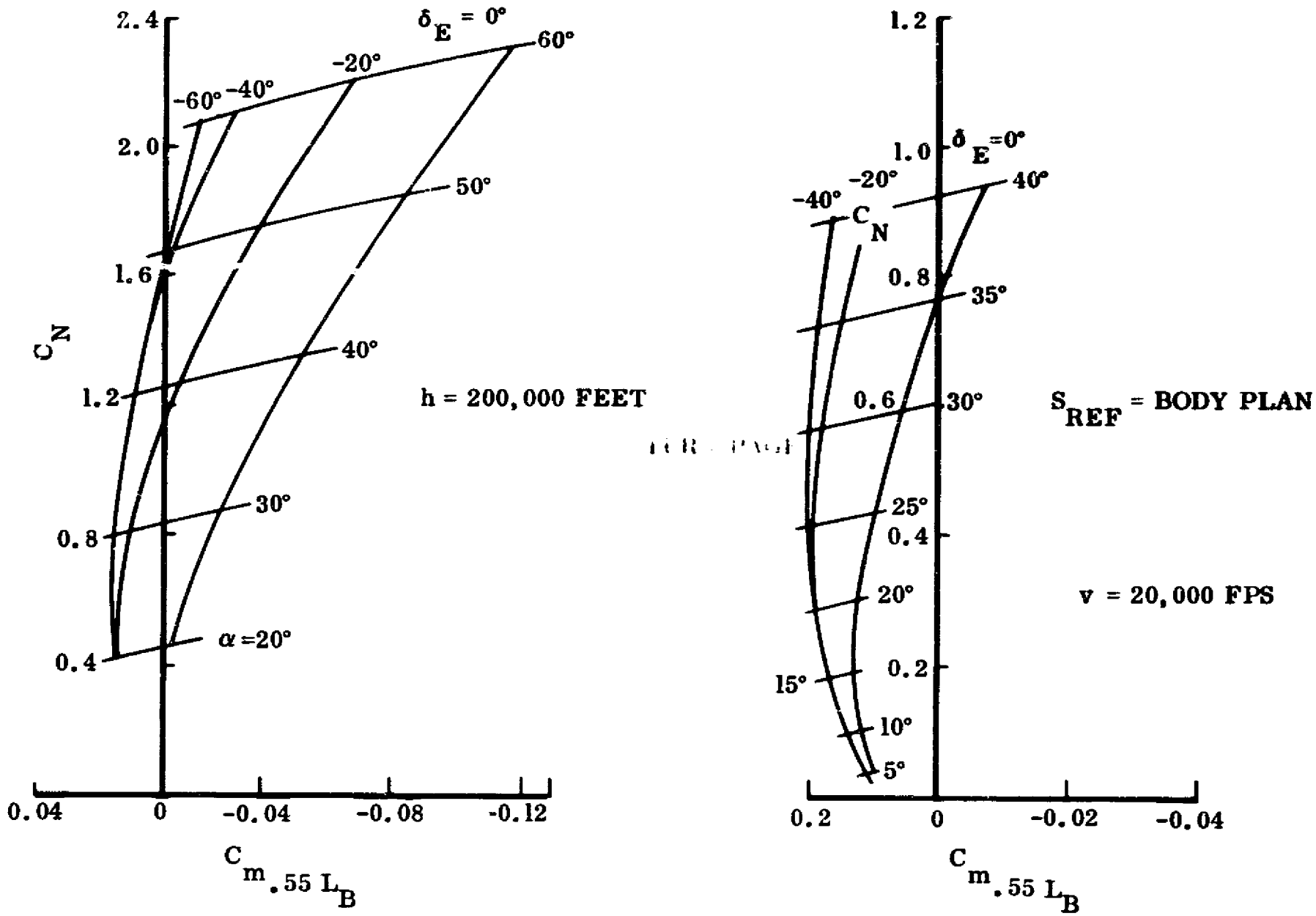

Figure 6-7. Orbiter Hypersonic Aerodynamics

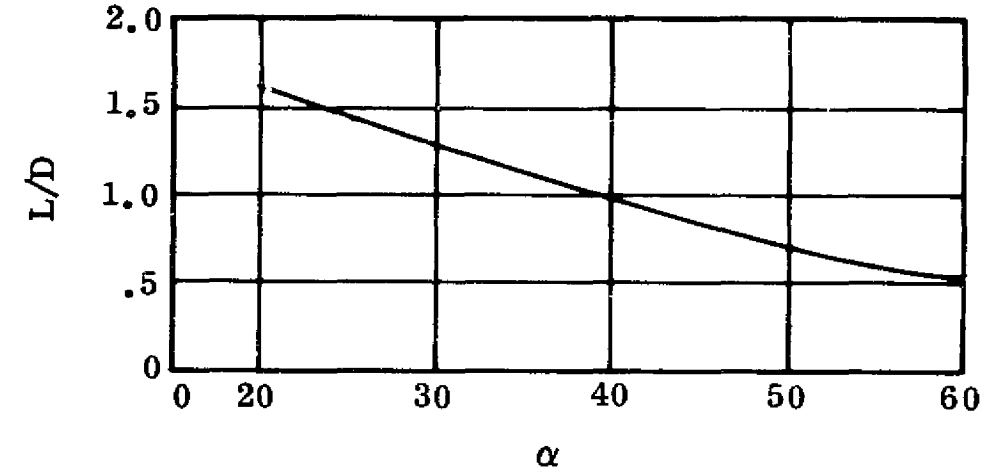

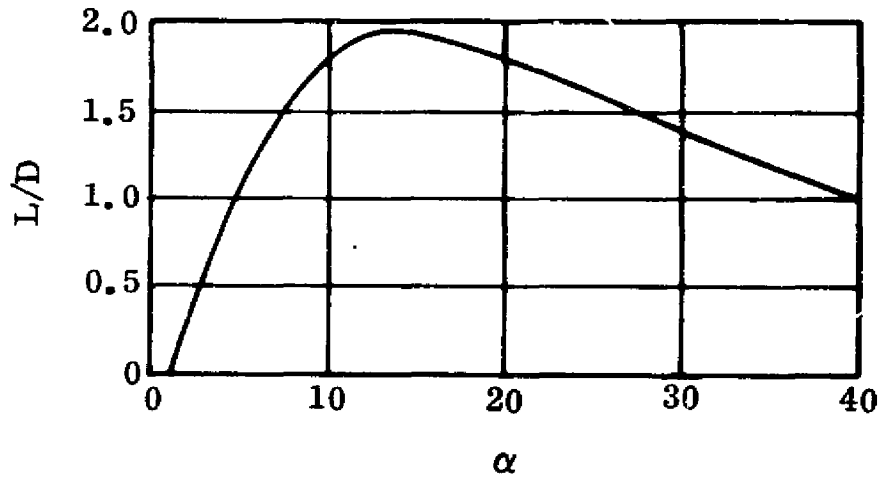

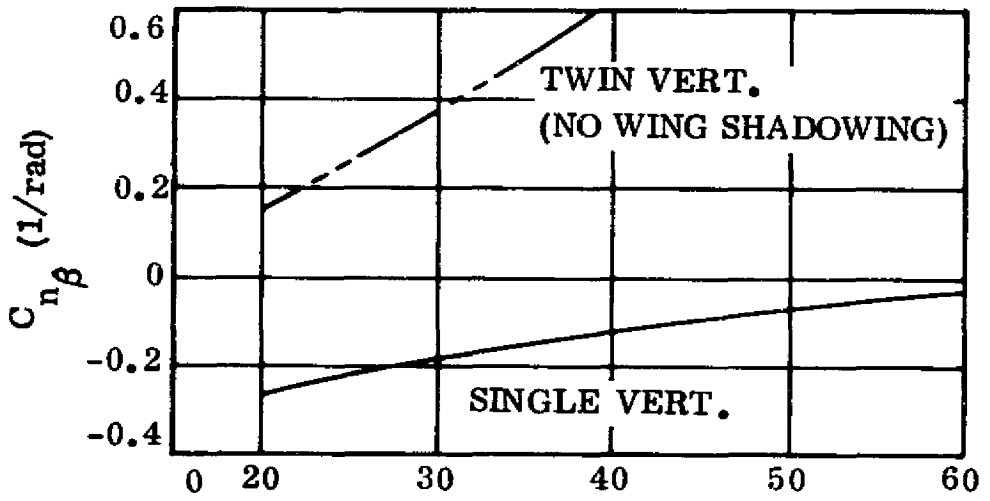

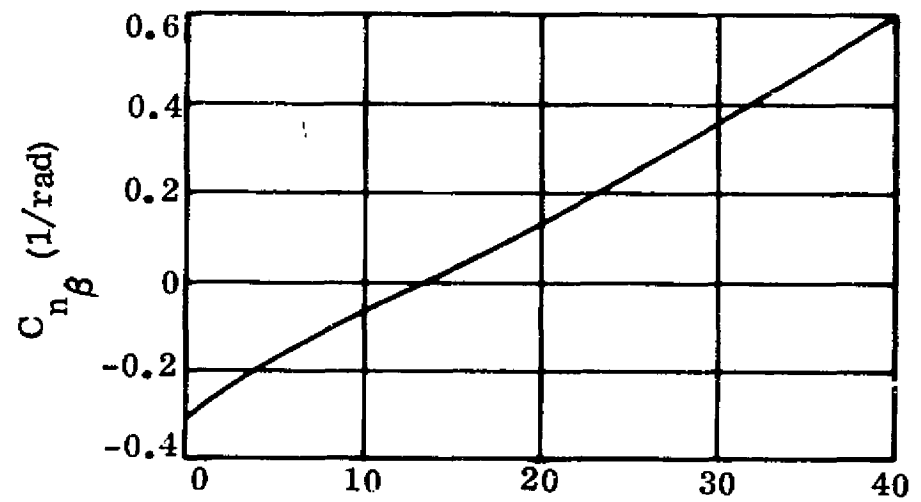

H = 200,000 FEET
V = 20,000 FPS

S_{REF} = BODY PLAN
b_{REF} = BODY SPAN

Figure 6-8. Orbiter Hypersonic Aerodynamics

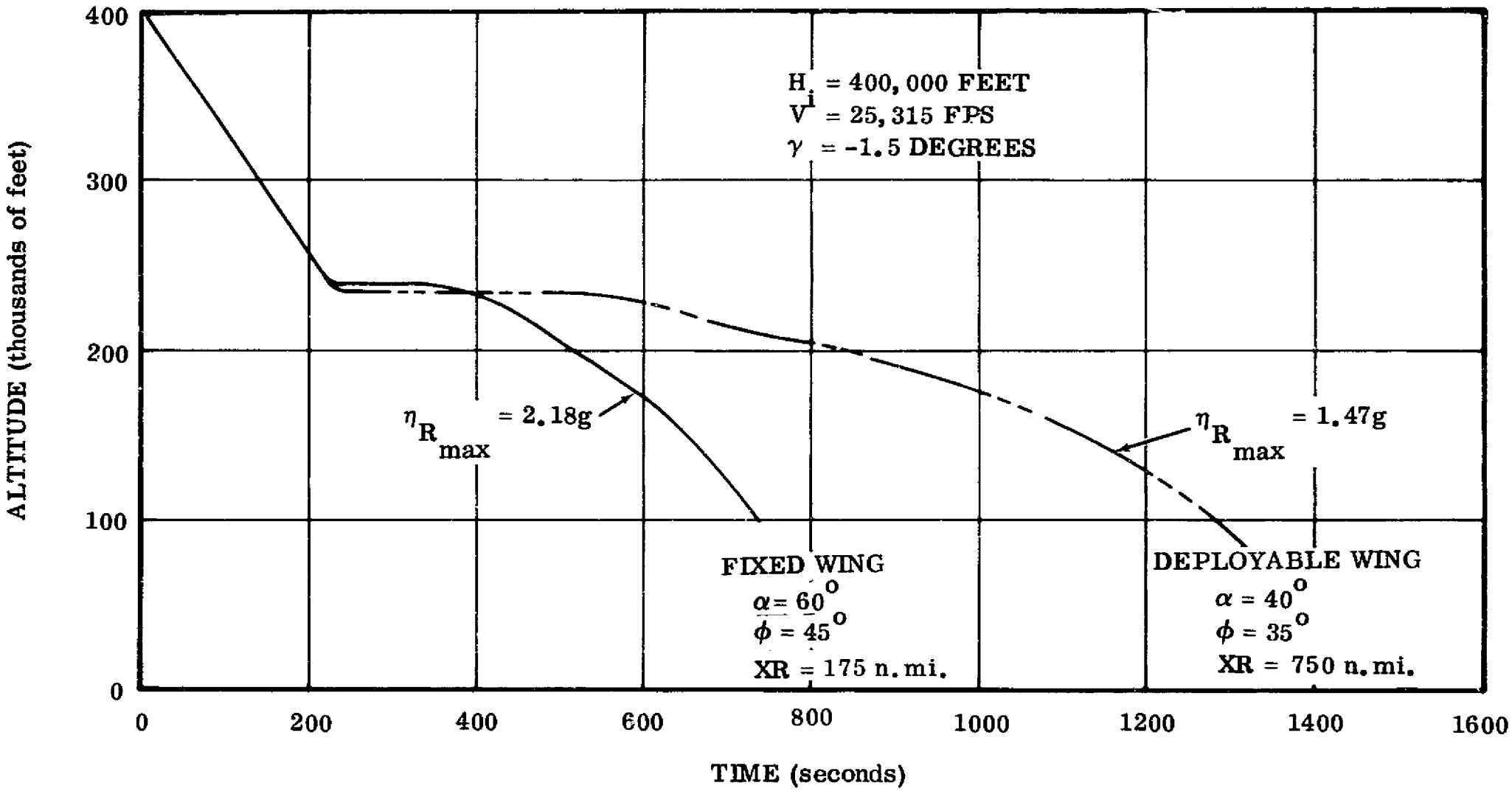

Figure 6-9. Orbiter Entry Trajectory

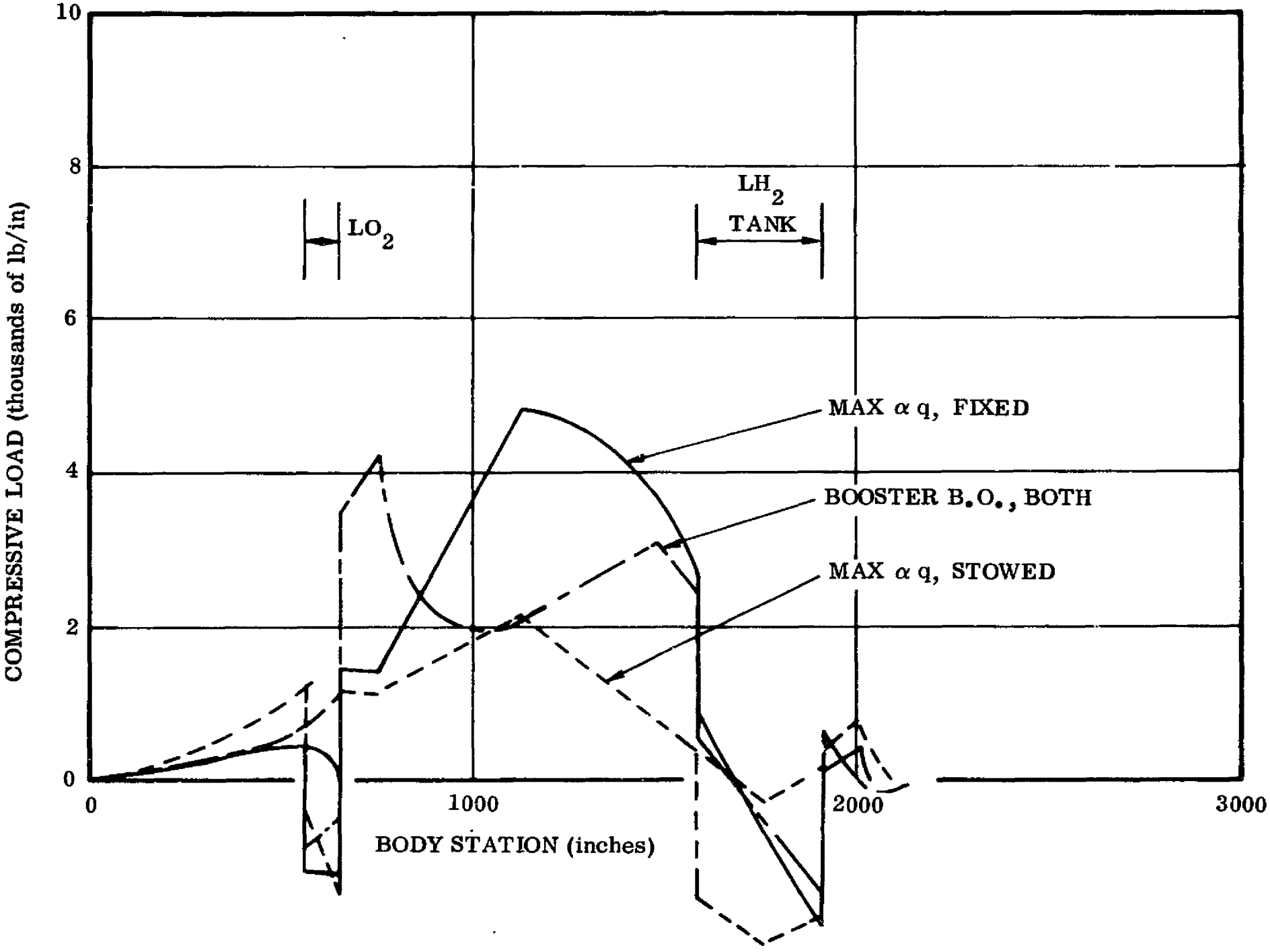

Figure 6-10. Comparison of Orbiter Body Peak Compressive Limit Loads, Nose-to-Nose Configuration

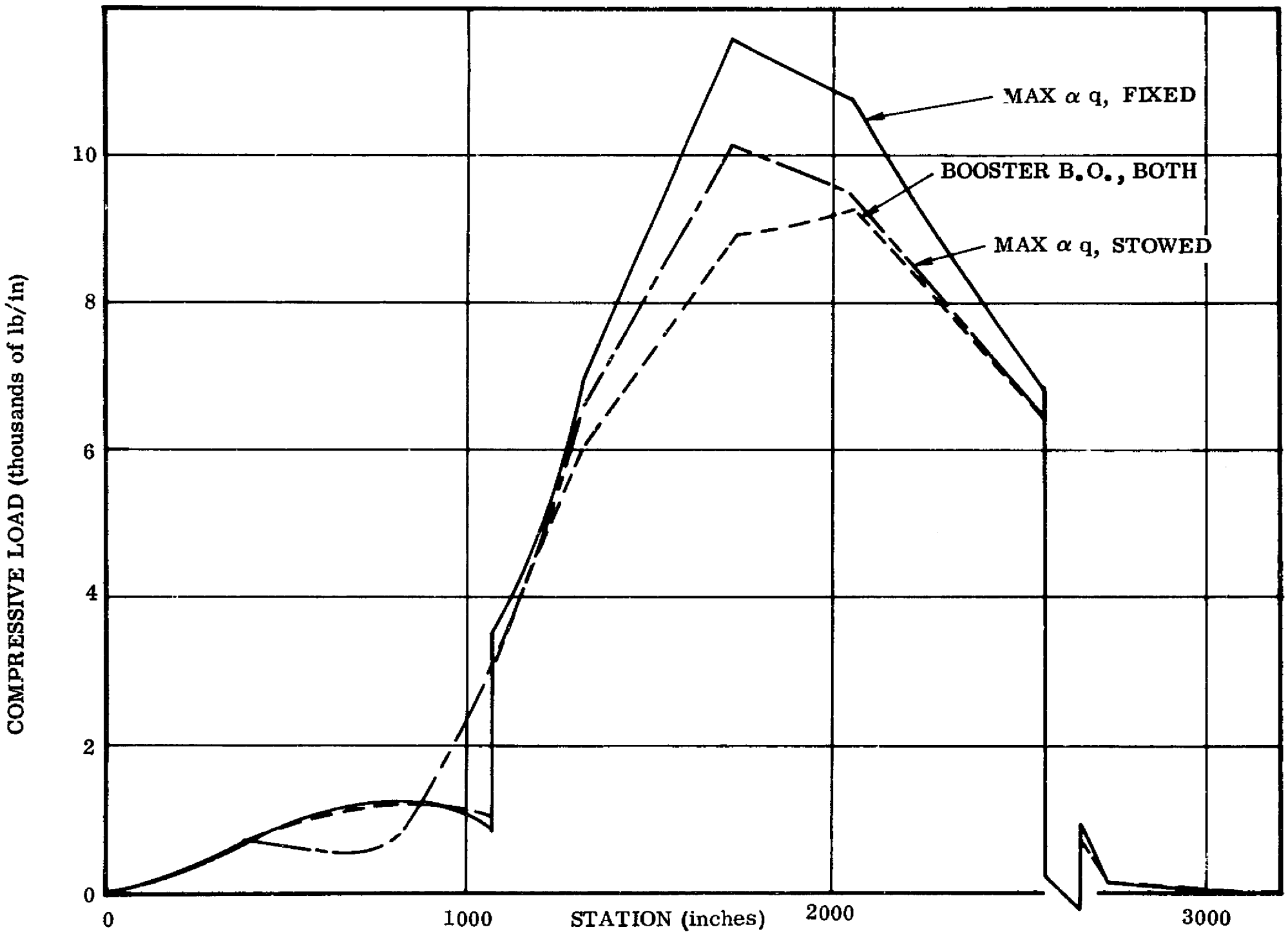

Figure 6-11. Comparison of Booster Body Peak Compressive Limit Loads, Nose-to-Nose Configuration

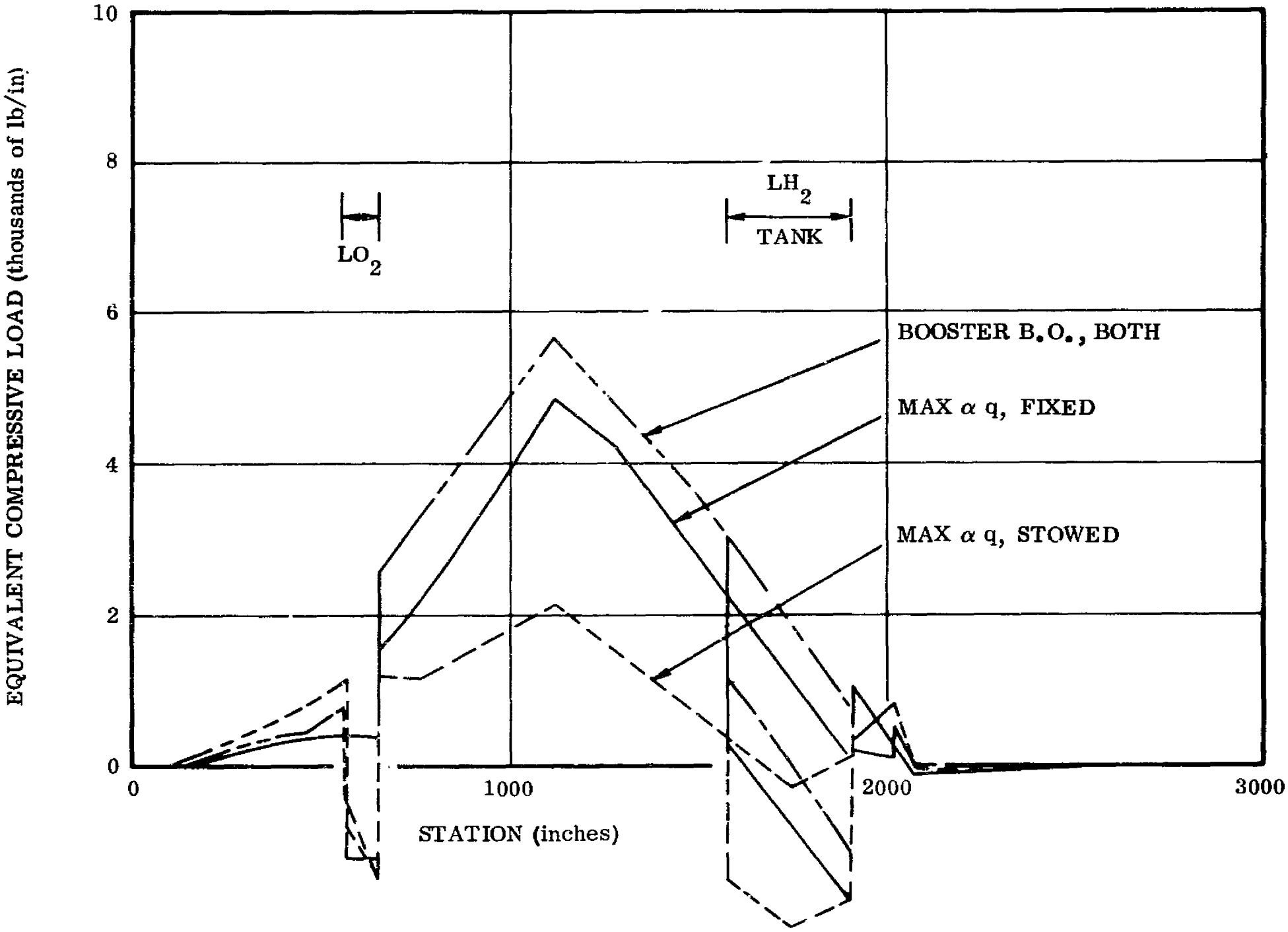

Figure 6-12. Comparison of Orbiter Body Peak Compressive Limit Loads, Tail-to-Tail Configuration

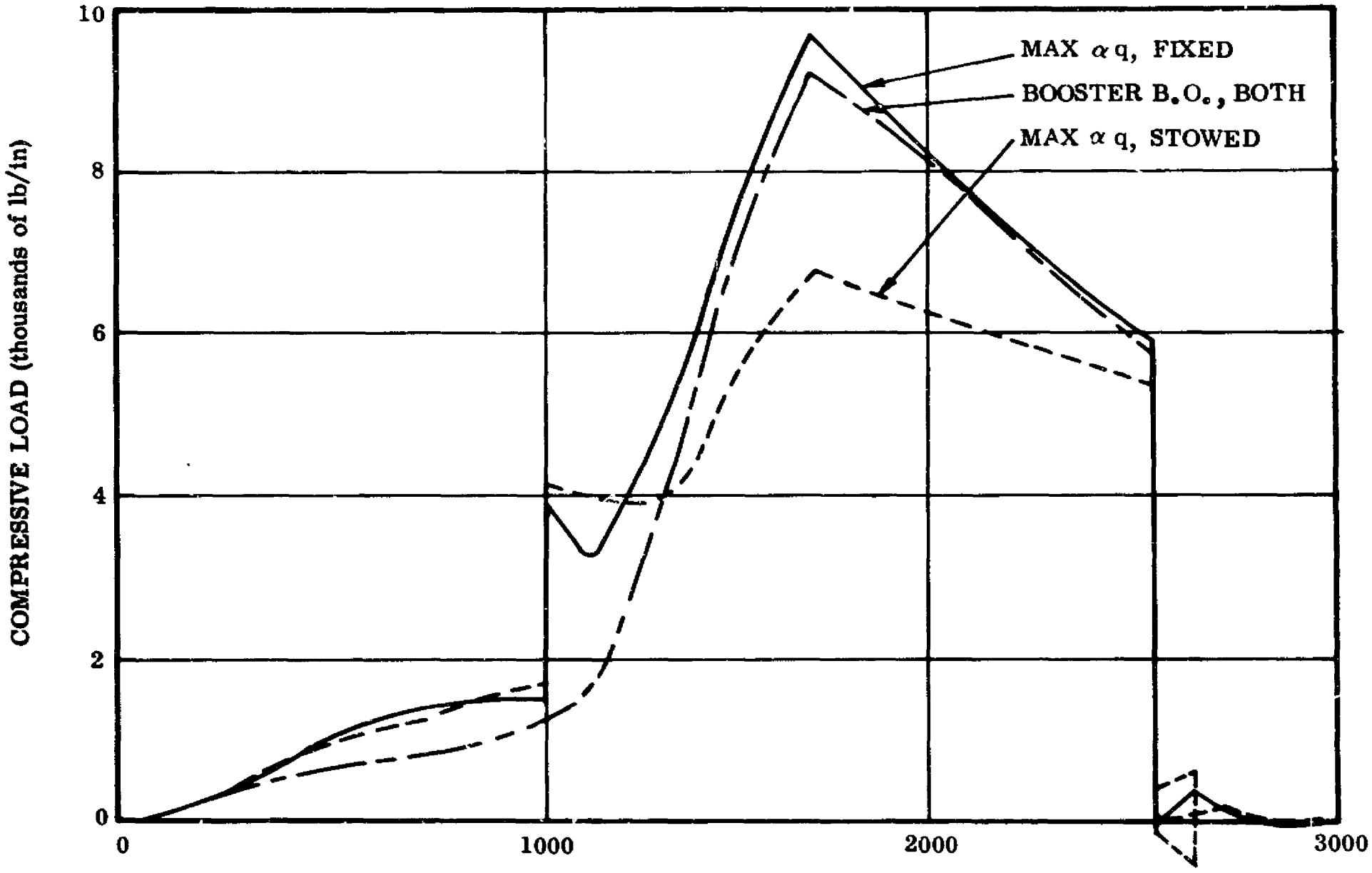

Figure 6-13. Comparison of Booster Body Peak Compressive Limit Loads, Tail-to-Tail Configuration

6.4 AERODYNAMIC HEATING

Figures 6-14 through 6-17 show aerodynamic heating data computed during the study. The following comments note some of the differences between the fixed- and deployable-wing configurations.

a. During laminar heating the average temperature difference is approximately 250°R. This can be attributed to the decreased $M/C_L S$ resulting from increased area, and C_L due to increased angle of attack. Increased angle of attack results in decreased lateral range during entry, and decreased temperature.

b. A 67% decrease in body insulation mass was calculated. However, the lateral range was 800 n. mi. for the deployable wing versus 200 n. mi. for the fixed wing. This difference would decrease for the same lateral range to approximately zero.

c. Fixed wing results in interference heating and reduced radiation heat transfer near the wing/body junction. Interference heating film coefficient ratios of 4.0 are reasonable.

d. Fixed wing at angle of attack of 60 degrees does not lend itself to state-of-the-art heat transfer prediction methods. At other angles of attack, fixed wing requires more experimental investigation than deployable wing.

6.5 SYNTHESIS SUMMARY

Tables 6-2 through 6-5 show the synthesis and weight summaries for both the current fixed-wing and FR-3 deployable-wing designs.

6.6 CONCLUSIONS

From the weights point of view there is very little difference between a fixed-wing and deployable-wing design.

The fixed-wing design is inherently simpler in concept, but surface exposed to complex flow conditions is increased.

Wings are inherently subject to deflections due to loads and flow interactions, requiring a thermal protection subsystem that will be subject to these conditions.

The effects of exposed wings on transonic flow with the possibility of flutter need to be evaluated by considerable wind-tunnel testing.

Fixed-wing design needs to satisfy both subsonic, transonic, and hypersonic aerodynamic requirements, some of which are in conflict with each other. Deployable wings decouple these requirements but at some expense in complexity.

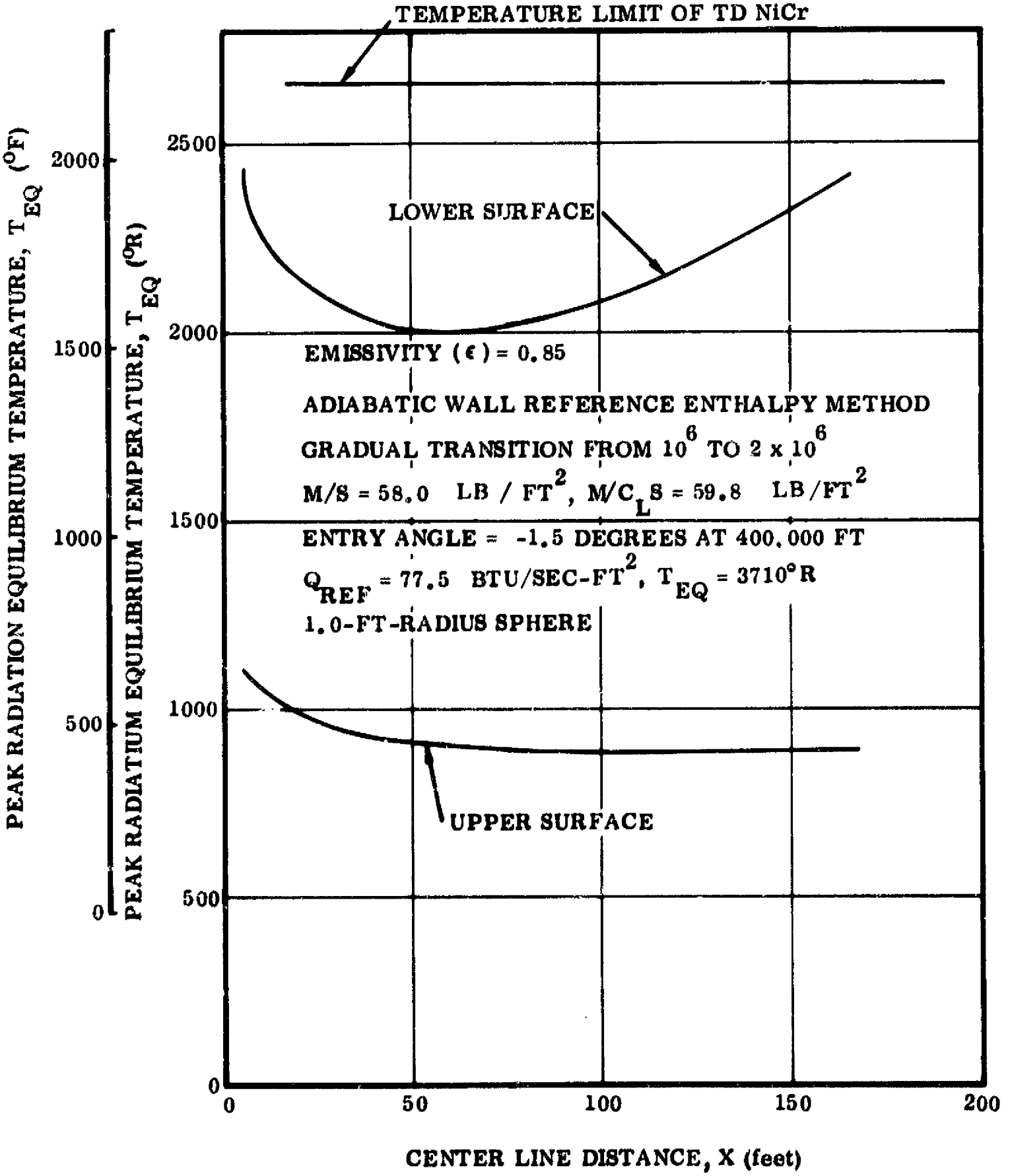

Figure 6-14. Orbiter Fixed-Wing Body-Surface Peak-Temperature Distribution

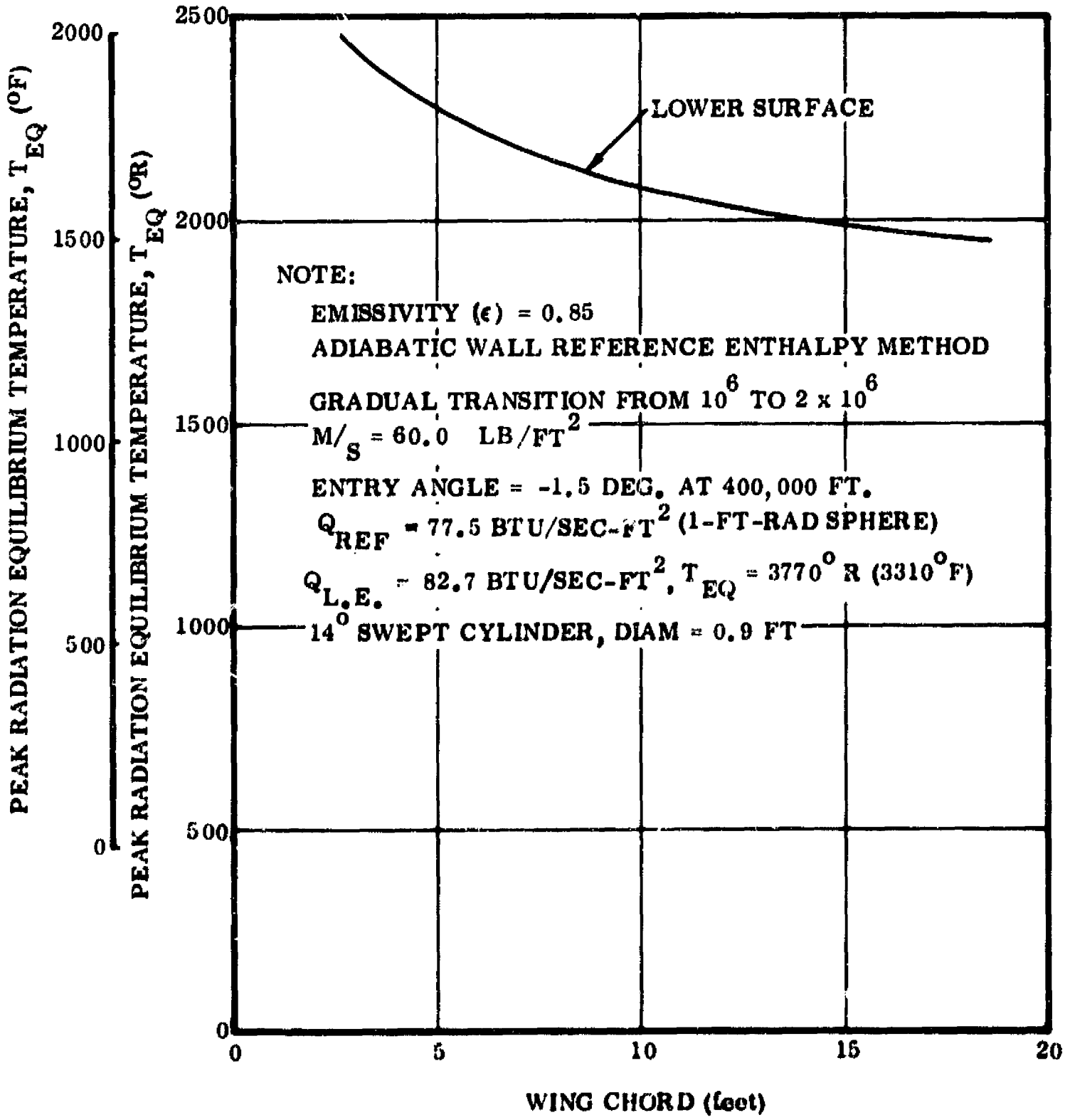

Figure 6-15. Orbiter Fixed-Wing Surface Peak-Temperature Distribution

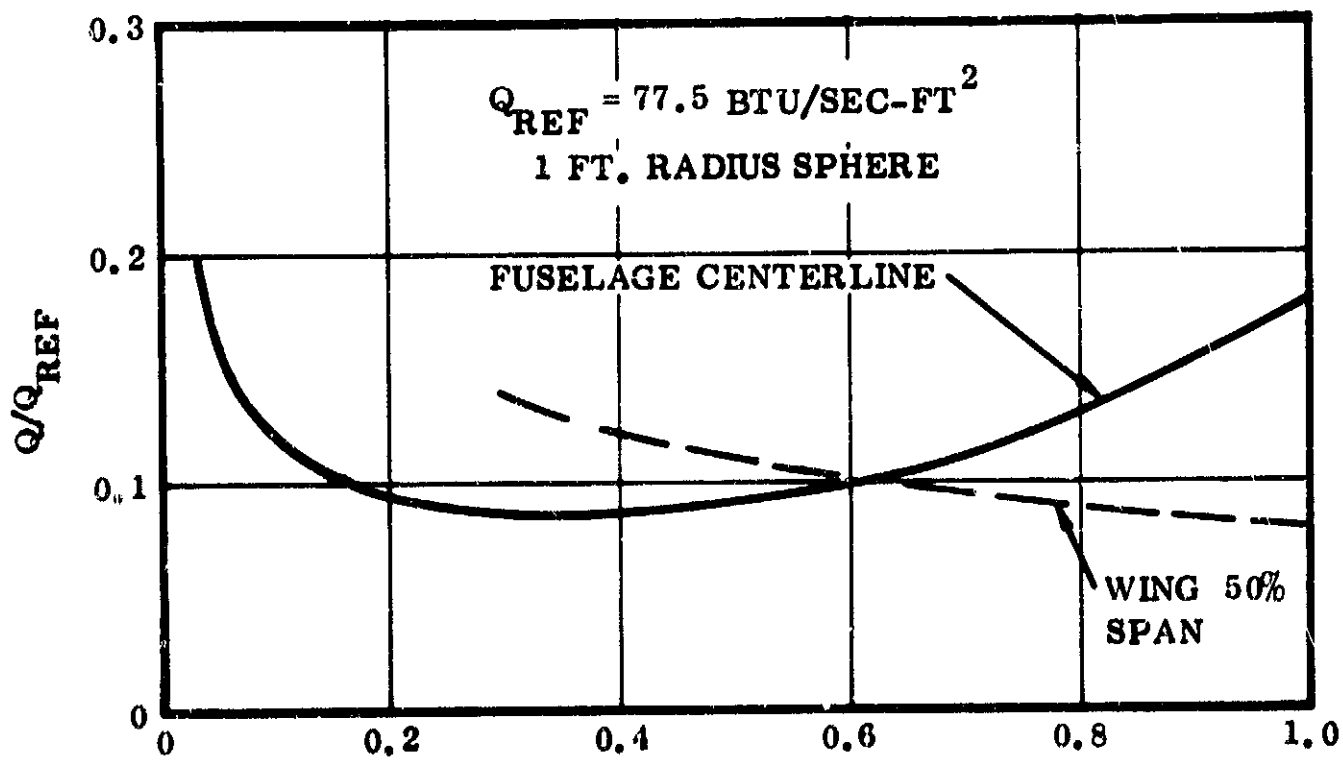

Figure 6-16. Orbiter Fixed-Wing Lower Surface Heating

Crossrange capability is restricted in the fixed wing relative to the deployable wing configuration.

6.7 UPDATING OF THE FR-3 50K POUND PAYLOAD TWO-ELEMENT SEQUENTIAL-BURN VEHICLE SYSTEM

It will be noted that the summary run on the two-element sequential-burn vehicle in Paragraph 6.5 shows a slightly higher GLOW (4.067M lb) than the presentation version shows in Paragraph 2.1 (4.007M lb). This is due to nominal iteration changes in the program, since the design development of the vehicles is a changing iterative process with calendar time.

The FR-1 configuration in Section 4 incorporated two features resulting in higher weight than the presentation vehicle. These were 1) an increase in wing weight due to scaling factors, and 2) an increase in flyback and landing turbofan engine weights due to the cost saving device of using off-the-shelf engines currently available. For comparison purposes these changes were made to the two-stage segmented-burn 50K pound payload vehicle also. The results are generally applicable to all of the other vehicles in the spectrum.

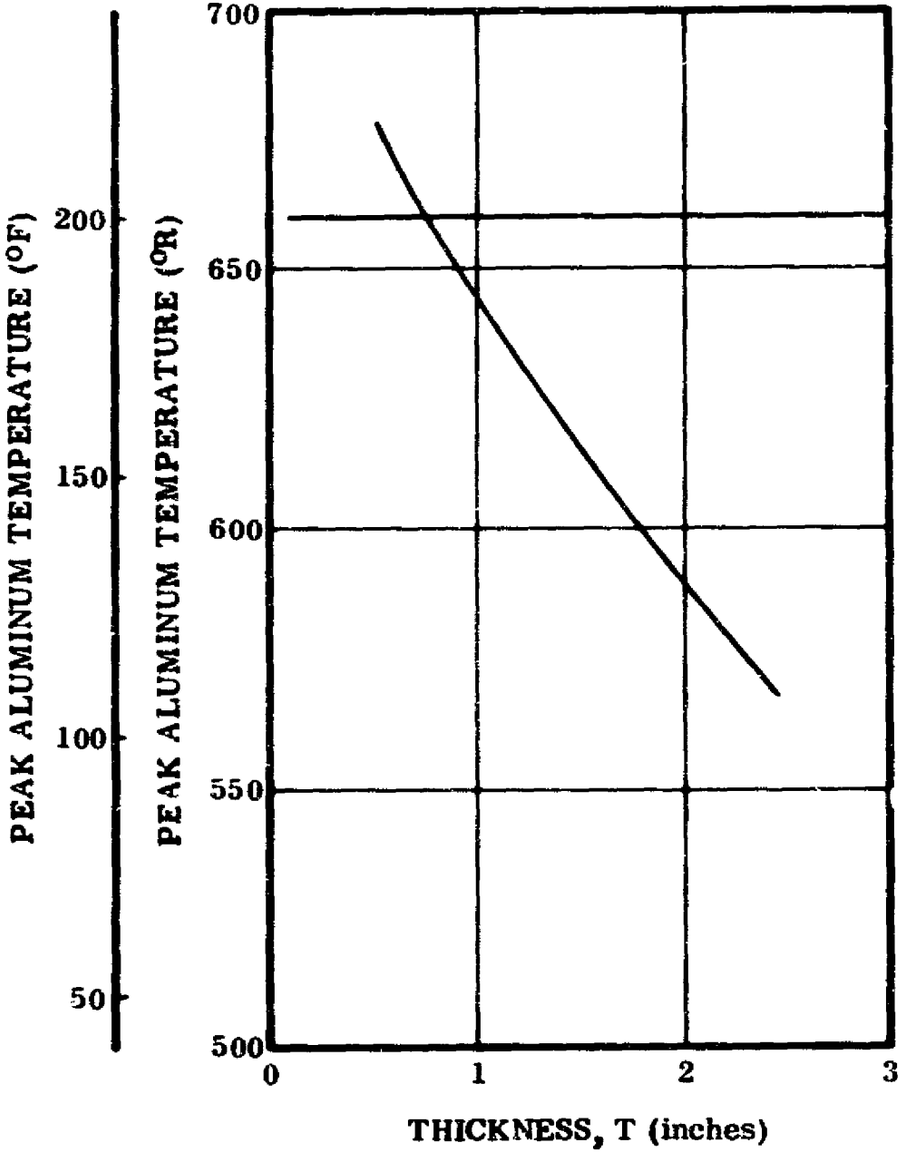

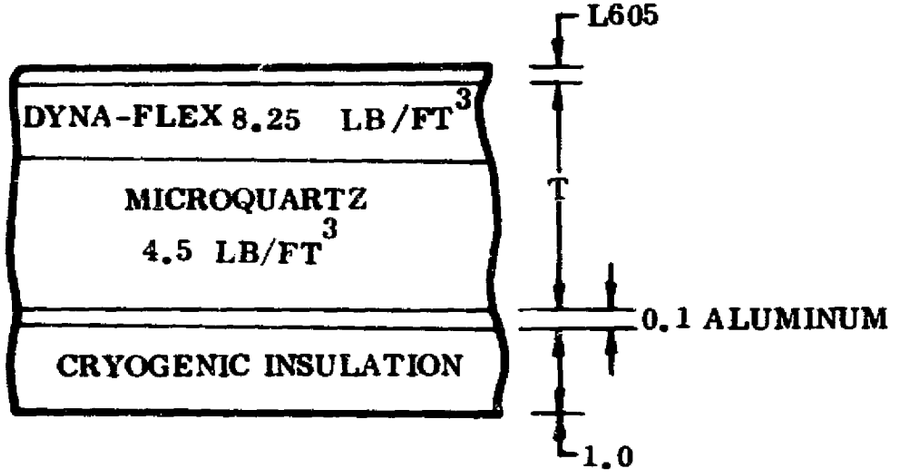

Figure 6-17. Lower Surface Insulation Requirements at 50 Feet

Table 6-6 shows the summary run for the increased wing weights. The gross liftoff weight has increased to 4.12M lb. Table 6-7 shows the added effect of off-the-shelf flyback engines.

The orbiter element of the two-stage sequential-burn vehicle has three Pratt & Whitney TF 33-P-5 turbofan engines. Versions of the TF-33 engine are used on the C-135, the 707, and the DC-8. The TF-33-P-5 has a maximum sea level static thrust of 18,000 pounds and an S. F. C. at maximum power of 0.54 lb/hr/lb. Its bare weight and dimensions are: weight, 4170 pounds; diameter, 53 inches; length, 137 inches.

An alternate airbreathing engine configuration is two General Electric TF 39-F10 turbofan engines. The TF39-F10 engine is a study version of the TF39-1 and was estimated to require approximately $55 million and 38 months to develop through MQT. The TF39-F10 has a maximum sea level static thrust of 26,000 pounds and an S. F. C. at maximum power of 0.365 lb/hr/lb. Its bare weight and dimensions are: weight, 5445 pounds; diameter, 70 inches; and length, 159 inches. Using this configuration would result in a decrease in airbreathing engine system and fuel weight of approximately 2550 pounds.

The gross liftoff weight is now 4.27M pounds, including the updated wing and engine.

6.8 REFERENCES

6-1 D. E. Haak, USAF Stability Control DATCOM, Flight Control Division, AFFDL, WPAFB, August 1968.

Table 6-2. Two-Element Sequential Fixed-Wing Configuration (Single Tail) Synthesis Summary

	BOOSTER ELEMENT	ORBITER	VEHICLE
WEIGHT			
FUEL	355205	67989	
OXIDIZER	2273314	475920	
PROPELLANT	2628519	543908	
FLYBACK FUEL	43250	3055	
PAYLOAD		50000	
STRUCTURE	445395	185111	630505
CONTINGENCY	48539	18511	
OTHER	20598	47253	
TOTAL	3186302	847838	4034140
IN ORBIT		308625	
RETURN CONDITION	557787	299864	
ENTRY	0	258902	
LANDING	494826	254546	
VOLUME			
FUEL	85337	14199	
OXIDIZER	33682	7047	
PROPELLANT	122019	21246	
PAYLOAD		10638	
OTHER	74866	51338	
TOTAL	196885	83223	
GEOMETRY			
LENGTH	241.4	183.7	
BODY WETTED AREA	25504.3	14495.0	
BODY PLANFORM AREA	9305.9	4768.2	
ENTRY PLANFORM LOADING	57.9	54.3	
PROPULSION			
THRUST-TO-WEIGHT		1.67935	1.39258
NO. OF ENGINES	8	2	
THRUST PER ENGINE (SL)	702233	UPRATED	
THRUST PER ENGINE (VAC)		O/F = 6.4 711910	NOMINAL
SPECIFIC IMPULSE (SL)	395.0	357.4	O/F = 7.0 395.0
SPECIFIC IMPULSE (VAC)	451.7	456.5	451.7
TRAJECTORY			
MASS RATIO		2.74773	2.67000
MAXIMUM DYNAMIC PRESSURE			599.4
STAGING DYNAMIC PRESSURE			50
STAGING VELOCITY (RELATIVE)			10852
STAGING ALTITUDE			187287
STAGING FLIGHT PATH ANGLE (RELATIVE)			2.052
INJECTION VELOCITY (INERTIAL)		25897	
INJECTION ALTITUDE		260001	
INJECTION FLIGHT PATH ANGLE (INERTIAL)		-.000	
INJECTION INCLINATION		54.95	
FLYBACK RANGE	277.8		

Table 6-3. Two-Element Sequential Fixed Wing Configuration (Single Tail) Summary Weight

SPACECRAFT SUMMARY WEIGHT STATEMENT

2 Stage Sequential Fixed Wing Configuration (Single Tail) | BY | DATE

CODE	SYSTEM	ITEM OR MODULE A	B	C	D	E	F	SPACECRAFT M	U
1.0	AERODYNAMIC SURFACES	9A478						30936	
2.0	BODY STRUCTURE	213855						67865	
3.0	INDUCED ENVIR PROT	12401						37547	
4.0	LNCH RECOV & DEC	27630						11327	
5.0	MAIN PROPULSION	136666						38264	
6.0	ORIENT CONTROL SEP & ULL	18726						12156	
7.0	PRIME POWER SOURCE	975						1771	
8.0	POWER CONV & DISTR	9994						3038	
9.0	GUIDANCE & NAVIGATION	220						310	
10.0	INSTRUMENTATION	220						275	
11.0	COMMUNICATION	220						242	
12.0	ENVIRONMENTAL CONTROL	330						616	
13.0	(RESERVED)								
14.0	PERSONNEL PROVISIONS								
15.0	CREW STA CONTRL & PAN	220						275	
16.0	RANGE SAFETY & ABORT								
SUBTOTALS (DRY WEIGHT)		493935						203622	
17.0	PERSONNEL	700						920	
18.0	CARGO							50000	
19.0	ORDNANCE								
20.0	BALLAST								
21.0	RESID PROP & SERV ITEMS	19285						4069	
SUBTOTALS (INERT WEIGHT)		20185						54989	
22.0	RES PROP & SERV ITEMS								
23.0	INFLIGHT LOSSES	43663						11455	
24.0	THRUST DECAY PROPELLANT								
25.0	FULL THRUST PROPELLANT	2628519						577772	
26.0	THRUST PROP BUILDUP								
27.0	PRE-IGNITION LOSSES								
TOTALS (GROSS WEIGHT) (LB)		3186302						847838	
DESIGN ENVELOPE VOLUME (FT^3)		196885						83223	
PRESSURIZED VOLUME (FT^3)									
DESIGN ENVEL SURF AREA (FT^2)		25504						15495	
PRESSURIZED SURF AREA (FT^2)									
DESIGN q, MAX (LB/FT^2)		599						599	
DESIGN n, MAX		4						4	
DESIGN POWER, MAX (KW)									
DESIGN NO. MEN/DAYS		2/.1						2/7	

DESIGNATIONS:

CODE, SYSTEM: REF. MIL-M-38310A OR SP-6004

ITEM OR MODULE

A - Booster

B

C

D

E

F

SPACECRAFT

M MANNED LAUNCH - Orbiter

U UNMANNED LAUNCH

NOTES & SKETCHES:

Thrust decay propellants are included in residual weights.
Tanks are over-sized to account for thrust build-up and pre-ignition losses.

NSC Form 1523 (Jul 68)

Table 6-4. Two-Element Sequential Variable Geometry Wing Synthesis Summary

	BOOSTER ELEMENT	ORBITER	VEHICLE
WEIGHT			
FUEL	357849	66067	
OXIDIZER	2290236	462468	
PROPELLANT	2648085	528534	
FLYBACK FUEL	46266	3048	
PAYLOAD		50000	
STRUCTURE	456540	184665	641205
CONTINGENCY	60654	18467	
OTHER	20742	47169	
TOTAL	3232287	831883	4064171
IN ORBIT		308029	
RETURN CONDITION	584205	299279	
ENTRY	0	258393	
LANDING	518108	254040	
VOLUME			
FUEL	88995	13423	
OXIDIZER	33933	6848	
PROPELLANT	122928	20271	
PAYLOAD		10638	
OTHER	75389	46959	
TOTAL	198317	77868	
GEOMETRY			
LENGTH	242.0	177.2	
BODY WETTED AREA	25627.8	13741.9	
BODY PLANFORM AREA	9351.0	4437.3	
ENTRY PLANFORM LOADING	60.4	58.2	
PROPULSION			
THRUST-TO-WEIGHT		1.72434	1.39261
NO. OF ENGINES	8	2	
THRUST PER ENGINE (SL)	707476	UPRATED	
THRUST PER ENGINE (VAC)		O/F = 6.4 717226	NOMINAL
SPECIFIC IMPULSE (SL)	395.0	357.4	O/F = 7.0 395.0
SPECIFIC IMPULSE (VAC)	451.7	456.5	451.7
TRAJECTORY			
MASS RATIO		2.70082	2.87000
MAXIMUM DYNAMIC PRESSURE			668.7
STAGING DYNAMIC PRESSURE			50
STAGING VELOCITY (RELATIVE)			11086
STAGING ALTITUDE			188347
STAGING FLIGHT PATH ANGLE (RELATIVE)			1.864
INJECTION VELOCITY (INERTIAL)		25897	
INJECTION ALTITUDE		260002	
INJECTION FLIGHT PATH ANGLE (INERTIAL)		-.000	
INJECTION INCLINATION		54.96	
FLYBACK RANGE	283.6		

Table 6-5. FR-3 Two-Element, Sequential Burn, 50K Pound Payload Weight Summary

SPACECRAFT SUMMARY WEIGHT STATEMENT

CONFIGURATION: FR-3, Two Stage Sequential, 50K Payload | BY | DATE

CODE	SYSTEM	ITEM OR MODULE A	B	C	D	E	F	SPACECRAFT M	U
1.0	AERODYNAMIC SURFACES	63561						29799	
2.0	BODY STRUCTURE	229528						64269	
3.0	INDUCED ENVIR PROT	28334						41251	
4.0	LNCH RECOV & DKG	30107						11590	
5.0	MAIN PROPULSION	139532						38183	
6.0	ORIENT CONTROL SEP & ULL	19612						12406	
7.0	PRIME POWER SOURCE	1018						1824	
8.0	POWER CONV & DISTR	4292						2092	
9.0	GUIDANCE & NAVIGATION	220						310	
10.0	INSTRUMENTATION	220						275	
11.0	COMMUNICATION	220						243	
12.0	ENVIRONMENTAL CONTROL	330						616	
13.0	(RESERVED)								
14.0	PERSONNEL PROVISIONS								
15.0	CREW STA CONTRL & PAN	220						275	
16.0	RANGE SAFETY & ABORT								
SUBTOTALS (DRY WEIGHT)		517194						203132	
17.0	PERSONNEL	900						920	
18.0	CARGO							50670	
19.0	ORDNANCE								
20.0	BALLAST								
21.0	RESID PROP & SERV ITEMS	19429						4064	
SUBTOTALS (INERT WEIGHT)		20329						54984	
22.0	RES PROP & SERV ITEMS								
23.0	INFLIGHT LOSSES	46679						11435	
24.0	THRUST DECAY PROPELLANT								
25.0	FULL THRUST PROPELLANT	2648085						562332	
26.0	THRUST PROP BUILDUP								
27.0	PRE-IGNITION LOSSES								
TOTALS (GROSS WEIGHT) (LB)		3232287						831883	
DESIGN ENVELOPE VOLUME (FT^3)		198317						77868	
PRESSURIZED VOLUME (FT^3)									
DESIGN ENVEL SURF AREA (FT^2)		25628						13742	
PRESSURIZED SURF AREA (FT^2)									
DESIGN q, MAX (LB/FT^2)		669						669	
DESIGN ε, MAX		4						4	
DESIGN POWER, MAX (KW)									
DESIGN NO. MEN/DAYS		2/.1						2/7	

DESIGNATIONS:
CODE, SYSTEM: REF. MIL-M-38310A OR SP-6004
ITEM OR MODULE
A - Booster
B
C
D
E
F
SPACECRAFT
M MANNED LAUNCH - Orbiter
U UNMANNED LAUNCH

NOTES & SKETCHES:
Thrust decay propellants are included in residual weights.
Tanks are over-sized to account for thrust build-up and pre-ignition losses.

NSC Form 1523 (Jul 68)

Table 6-6. FR-3 Two-Element Sequential Burn, 50K Pound Payload Synthesis Summary

	BOOSTER ELEMENT	ORBITER	VEHICLE
WEIGHT			
FUEL	363009	66766	
OXIDIZER	2323255	447359	
PROPELLANT	2686264	534125	
FLYBACK FUEL	47186	3082	
PAYLOAD		50000	
STRUCTURE	472952	187170	660121
CONTINGENCY	54595	18717	
OTHER	21009	47662	
TOTAL	3282005	840756	4122761
IN ORBIT		311359	
RETURN CONDITION	595749	302511	
ENTRY	0	261190	
LANDING	528458	256808	
VOLUME			
FUEL	90277	13597	
OXIDIZER	34422	6921	
PROPELLANT	124700	20517	
PAYLOAD		10638	
OTHER	76410	47397	
TOTAL	201109	78552	
GEOMETRY			
LENGTH	243.1	177.7	
BODY WETTED AREA	25867.8	13822.3	
BODY PLANFORM AREA	9438.6	4463.2	
ENTRY PLANFORM LOADING	61.0	58.5	
PROPULSION			
THRUST-TO-WEIGHT		1.72915	1.39133
NO. OF ENGINES	8	2	
THRUST PER ENGINE (SL)	717014		
THRUST PER ENGINE (VAC)		726895	
SPECIFIC IMPULSE (SL)	395.0	357.4	395.0
SPECIFIC IMPULSE (VAC)	451.7	456.5	451.7
TRAJECTORY			
MASS RATIO		2.70041	2.87000
MAXIMUM DYNAMIC PRESSURE			667.8
STAGING DYNAMIC PRESSURE			50
STAGING VELOCITY (RELATIVE)			11085
STAGING ALTITUDE			188438
STAGING FLIGHT PATH ANGLE (RELATIVE)			1.864
INJECTION VELOCITY (INERTIAL)		25897	
INJECTION ALTITUDE		260004	
INJECTION FLIGHT PATH ANGLE (INERTIAL)		.000	
INJECTION INCLINATION		54.96	
FLYBACK RANGE	283.5		

Table 6-7. FR-3 Two-Element Sequential Burn, 50K Pound Payload Synthesis Summary

	BOOSTER ELEMENT	ORBITER	VEHICLE
WEIGHT			
FUEL	375913	69839	
OXIDIZER	2405846	489283	
PROPELLANT	2781759	559181	
FLYBACK FUEL	57678	3353	
PAYLOAD		50000	
STRUCTURE	475589	197552	673140
CONTINGENCY	54859	19755	
OTHER	19877	49722	
TOTAL	3389761	879562	4269324
IN ORBIT		325325	
RETURN CONDITION	608009	316054	
ENTRY	0	272879	
LANDING	531362	268225	
VOLUME			
FUEL	93447	14375	
OXIDIZER	35640	7245	
PROPELLANT	129086	21621	
PAYLOAD		10638	
OTHER	78935	49344	
TOTAL	208021	81603	
GEOMETRY			
LENGTH	245.8	180.0	
BODY WETTED AREA	26457.2	14177.9	
BODY PLANFORM AREA	9653.6	4578.1	
ENTRY PLANFORM LOADING	61.1	59.6	
PROPULSION			
THRUST-TO-WEIGHT		1.73877	1.39184
NO. OF ENGINES	8	2	
SL THRUST/ENG NOM/UR	643268/ 742777	598662/	5146145/5942218
VAC THRUST/ENG NOM/UR	747908/ 852615	764678/	5983265/6820922
SL ISP NOM/UR	383.6/392.9	357.0/	383.6/392.9
VAC ISP NOM/UR	446.0/451.0	456.0/	446.0/451.0
TRAJECTORY			
MASS RATIO	2.87000	2.70452	
MAXIMUM DYNAMIC PRESSURE			676.4
STAGING DYNAMIC PRESSURE			50
STAGING VELOCITY (RELATIVE)			11066
STAGING ALTITUDE			188163
STAGING FLIGHT PATH ANGLE (RELATIVE)			1.940
INJECTION VELOCITY (INERTIAL)		25897	
INJECTION ALTITUDE		260004	
INJECTION FLIGHT PATH ANGLE (INERTIAL)		.000	
INJECTION INCLINATION		54.96	
FLYBACK RANGE	283.5		

SECTION 7

FIXED GROSS LIFTOFF WEIGHT VEHICLES

This section summarizes the FR-3 and FR-4 point design vehicles sized to fixed gross liftoff weights of 3.0 and 3.5 million pounds.

FR-3 is a two-element sequential-burn vehicle and FR-4 is a three-element configuration. (Two-stage sequential-burn with the booster being made up of two identical elements arranged on either side of a central orbiter element.) The vehicles do not use crossfeed.

The ground rules established for this vehicle investigation are summarized below:

a. Investigate a 3.0 million pound liftoff weight version of both the FR-3 and FR-4. These were to incorporate the 15-foot-diameter by 60-foot-long payload bays.

b. Investigate a 3.5 million pound liftoff weight version of both the FR-3 and FR-4. These were to incorporate the basic 15-foot-diameter by 60-foot-long payload bay with a 22-foot-diameter by 30-foot-long bay superimposed on it.

c. 400K pound thrust bell nozzle, high P_c engines, sea level nominal were to be incorporated. Only nominal 100% thrust ratings with a mixture ratio of 6.5 to 1 were to be used in all stages.

d. Elimination of go-around in the orbiter was permitted. (In this case XJ-99 engines were used to permit holding a 3-degree glide path on the approach.)

e. Reduction of on-orbit ΔV was allowed within the limits of the mission requirement. (In this respect the nominal 1800 fps in the main maneuver propellant system was reduced to 1480 fps, being made up as follows for the 270 n. mi. orbit mission: circularize at 100 n. mi., 110 fps; transfer to 270 n. mi., 300 fps plus 300 fps; retro 450 fps; reserve 320 fps.)

f. Orbiter burn was required at liftoff, 100% thrust throttled back to 10% thrust during the remainder of the orbiter flight prior to staging.

g. The basic design should have a crossrange capability (inherent in its shape) of 1500 n. mi. with actual TPS for 800 n. mi. The effect of added TPS weight for 1500 n. mi. crossrange was to be shown.

7.1 3.0M POUND GLOW VEHICLES (15-FOOT-DIAMETER BY 60-FOOT-LONG PAYLOAD BAY)

Exploratory data was examined, and it was apparent that to arrive at a system with positive payload some concession must be made in the ground rules. The alternatives seemed to be:

a. Design to less demanding orbit.

b. Reduce payload bay length.

c. Revert to uprated thrust.

d. Eliminate contingency.

The decision was made for this immediate study to eliminate the contingency. This was done on all the point designs, for comparison purposes. To keep the record clear, the effects of the contingency are shown also.

7.1.1 FR-3 POINT DESIGN. This point design is shown in Figure 7-1. The arrangement is tail-to-tail alignment to permit orbiter burn if necessary. The arrangement also reduces loads on the booster. The vehicles are similar to those previously presented in the two-element sequential-burn studies. Table 7-1 gives the point design synthesis outputs for the FR-3 system. Table 7-2 is a weight summary for this system.

7.1.2 FR-4 POINT DESIGN. This FR-4 point design is shown in Figure 7-2. The lines are similar to the previously developed series of fully reusable vehicles at Convair. The synthesis run is summarized in Table 7-3 and weights are summarized in Table 7-4. This final summary is slightly higher in gross liftoff weight than the vehicle used in previous parametric studies, but the difference is small (3.02M versus 2.99M).

7.2 3.5M POUND GLOW VEHICLES

The 3.5M lb GLOW vehicles are summarized in the following paragraphs.

7.2.1 FR-3 POINT DESIGN. To incorporate the payload bay into the vehicle, a certain amount of reconfiguring was required. The orbiter vehicle was the only one affected, the booster being similar to that used throughout. Some advantage was taken of the reduced 1500 n. mi. maximum crossrange shape requirement (versus 2000 n. mi. previously used) to blunt the nose and improve volume-to-wetted-area ratios. The large payload bay area and the smaller payload weights allow a decrease in planform area, since the entry planform loading limits are not approached in these configurations. Since these configurations took cognizance of the smaller gross liftoff weight factors, the volumes have been adequately checked out, and further iteration should

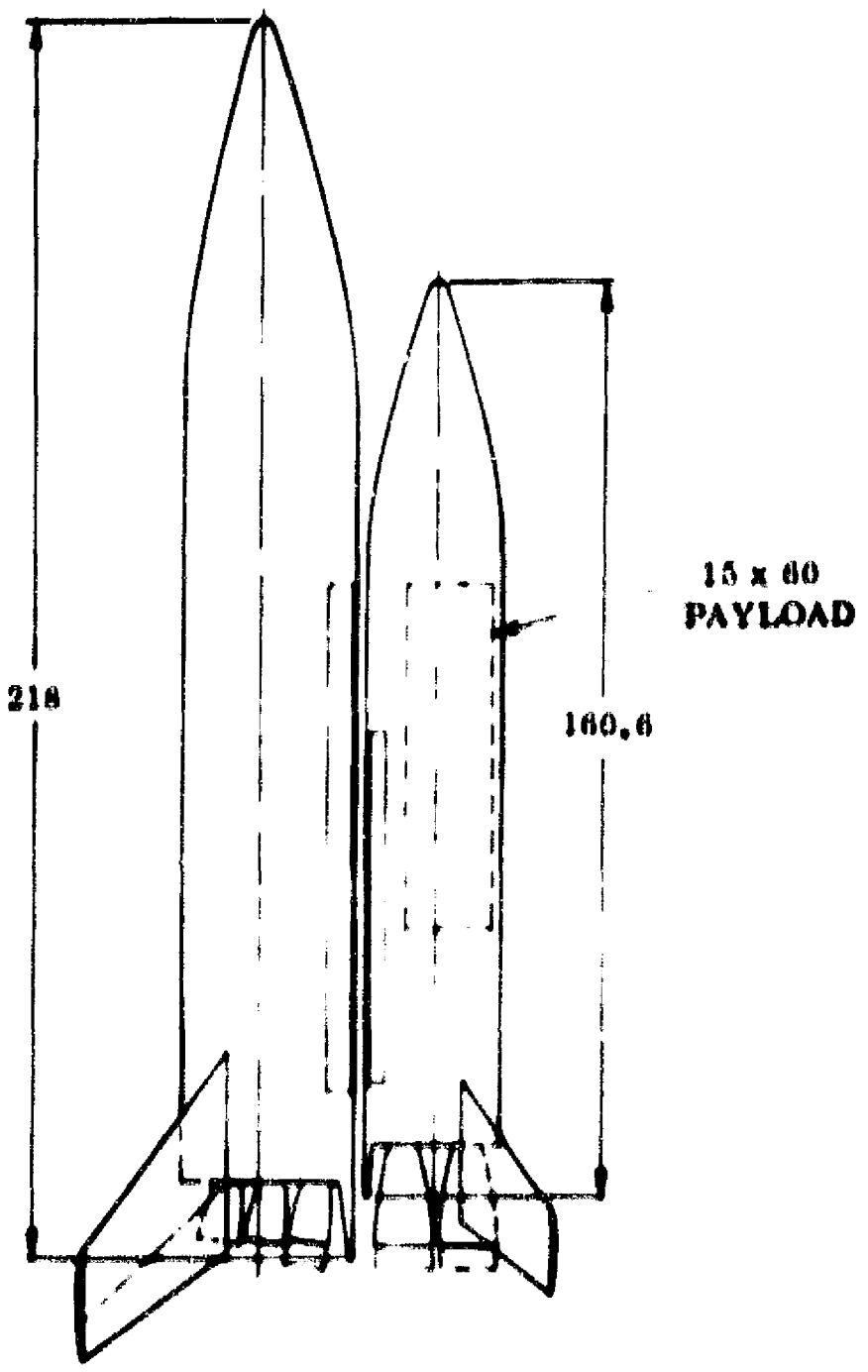

ALL DIMENSIONS IN FEET

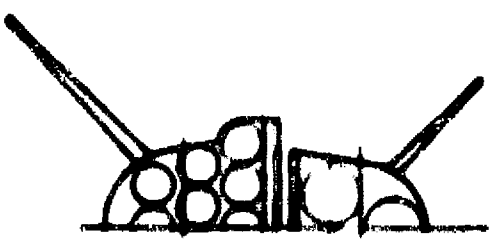

Figure 7-1. FR-3 Point Design Launch Configuration

Table 7-1. 3M-Pound GLOW FR-3 Design Point Synthesis Summary

	BOOSTER ELEMENT	ORBITER	VEHICLE
WEIGHT			
PROPELLANT, ASCENT	1968076	368280	
PROPELLANT, ORBIT MANEUVER		20643	
PROPELLANT, TOTAL	1968076	388923	
FLYBACK FUEL	45227	0	
PAYLOAD		32000	
STRUCTURE	391476	159567	550441
CONTINGENCY	7300	0	
OTHER	17409	11147	
TOTAL	2429486	590637	3020523
[illegible]		275769	
[illegible]	401810	210627	
[illegible]	0	191643	
[illegible]	400075	[illegible]	
VOLUME			
[illegible]	65364	8907	
[illegible]	25277	4728	
PROPELLANT	90986	13636	
PAYLOAD		10638	
OTHER	56503	39862	
TOTAL	165086	60115	
GEOMETRY			
[illegible]	219.0	108.6	
[illegible]	20007.9	11972.3	
[illegible]	7532.3	3906.0	
[illegible]	68.7	60.6	
PROPULSION			
[illegible]		2.39538	1.58969
[illegible]	12	3	
[illegible]	[illegible]	[illegible]	[illegible]
[illegible]	[illegible]	[illegible]	[illegible]
[illegible]	[illegible]	232.[illegible]	[illegible]
[illegible]	[illegible]	456.[illegible]	[illegible]
TRAJECTORY			
MASS RATIO	2.87086	2.81750	
[illegible]			402.2
[illegible]			60
[illegible]			11205
[illegible]			188895
[illegible]			2.988
[illegible]		25987	
[illegible]		253946	
[illegible]		-.001	
[illegible]		55.09	
[illegible]	200.7		

Table 7-2. FR-3 Weight Summary

SPACECRAFT SUMMARY WEIGHT STATEMENT

PROG Point Design, NASA, 12-3 Engines No Contingency Fixed Thrust | BY | DATE

CODE	SYSTEM	ITEM OR MODULE A	B	C	D	E	F	SPACECRAFT B	U
1.0	AERODYNAMIC SURFACES	86468						25788	
2.0	BODY STRUCTURE	160094						49668	
3.0	INDUCED ENVIR PROT	40290						12708	
4.0	LNCH RECOV & DOC	21466						7059	
5.0	MAIN PROPULSION	123061						31787	
6.0	ORIENT CONTROL SEP & ULL	13324						8289	
7.0	PRIME POWER SOURCE	720						1481	
8.0	POWER CONV & DISTR	310						1487	
9.0	GUIDANCE & NAVIGATION	203						407	
10.0	INSTRUMENTATION	203						260	
11.0	COMMUNICATION	501						442	
12.0	ENVIRONMENTAL CONTROL	300						600	
13.0	(RESERVED)								
14.0	PERSONNEL PROVISIONS								
15.0	CREW STA CONTRL & PAN	200						450	
16.0	RANGE SAFETY & ABORT								
	SPACECRAFT DRY WEIGHT	333173						126667	
17.0	PERSONNEL	720						212	
18.0	CARGO							14000	
19.0	ORDNANCE								
20.0	BALLAST								
21.0	RESID PROP & SERV ITEMS	6270						4792	
	SPACECRAFT (INERT WEIGHT)	[illegible]						[illegible]	
22.0	RES PROP & SERV ITEMS								
23.0	INFLIGHT LOSSES	75472						6918	
24.0	THRUST DECAY PROPELLANT								
25.0	FULL THRUST PROPELLANT	[illegible]						148733	
26.0	THRUST PROP BUILDUP								
27.0	PRE IGNITION LOSSES								
	GROSS WEIGHT	[illegible]						[illegible]	
	DESIGN ENVELOPE VOLUME FT³	466807						8445	
	PRESSURIZED VOLUME FT³								
	DESIGN ENVEL SURF AREA FT²	22000						782	
	PRESSURIZED SURF AREA FT²								
	DESIGN W/SREF LB FT²	3.?						242	
	DESIGN L/D								
	DESIGN POWER KW								
	DESIGN NO CREW DAYS								

DESIGNATIONS

ITEM, SYSTEM, SET, etc. IS DESIGNATED BY CODE	
ITEM OR MODULE	
A - Booster	
B	
C	
D	
E	
F	
SPACECRAFT	
B BOOSTED LAUNCH - Orbiter	
U UNBOOSTED LAUNCH	

NOTES & COMMENTS

THRUST DECAY PROPELLANTS ARE INCLUDED IN RESIDUAL WEIGHTS.

THRUSTS ARE OVER-SIZED TO ACCOUNT FOR THRUST BUILD-UP AND PRE-IGNITION LOSSES.

[illegible]

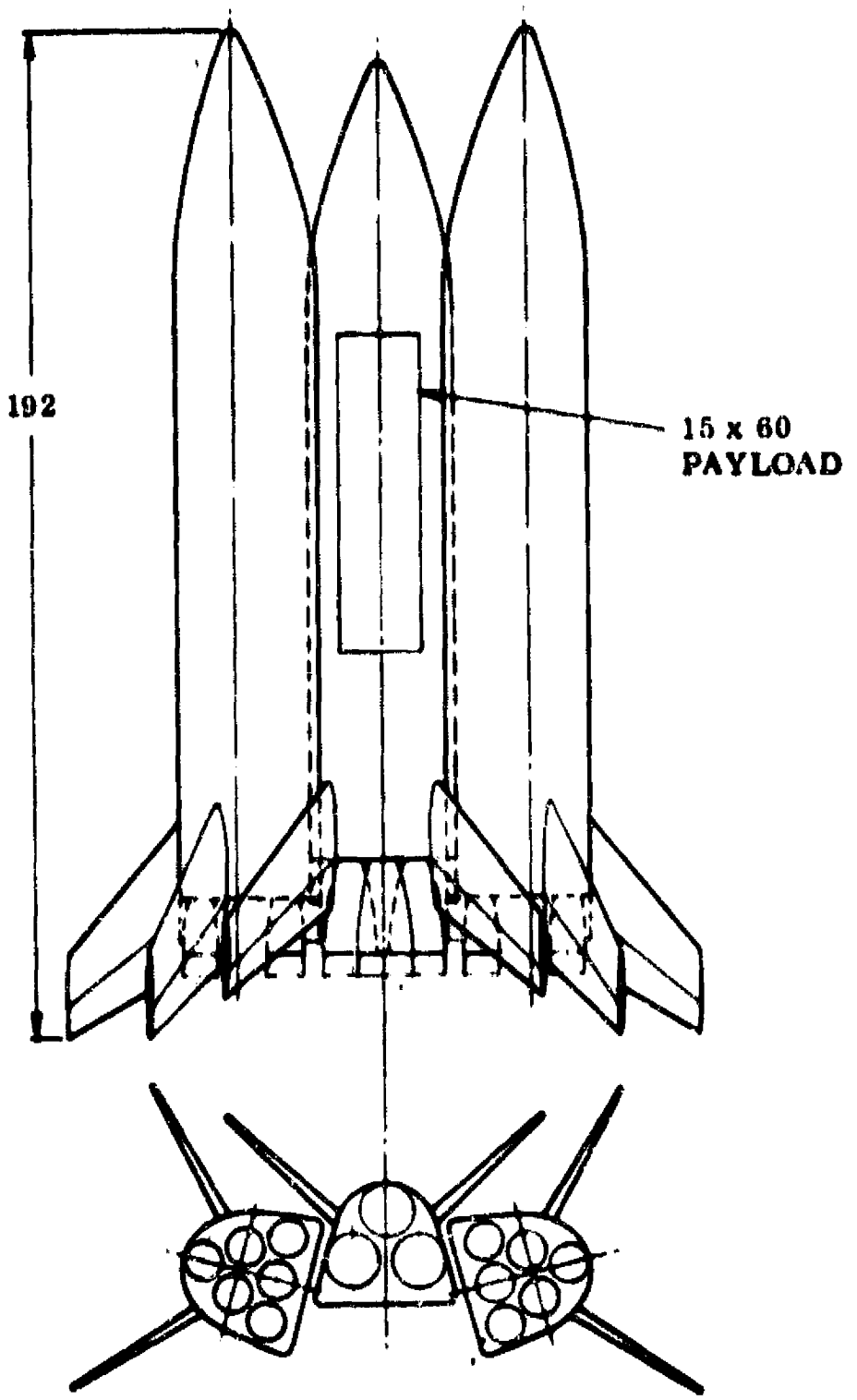

ALL DIMENSIONS IN FEET

Figure 7-2. FR-4 Point Design Launch Configuration

Table 7-3. 3M-Pound GLOW FR-4 Design Point Synthesis Summary

	BOOSTER ELEMENT	ORBITER	VEHICLE
WEIGHT			
PROPELLANT, ASCENT	980288	362783	
PROPELLANT, ORBIT MANEUVER		19199	
PROPELLANT, TOTAL	980288	381982	
FLYBACK FUEL	73521	0	
PAYLOAD		15000	
STRUCTURE	214804	161870	591478
CONTINGENCY	0	0	
OTHER	10481	12293	
TOTAL	1279094	571145	3029333
IN ORBIT		211560	
RETURN CONDITION	248805	203330	
ENTRY	219225	177788	
LANDING	215437	0	
VOLUME			
FUEL	12293	8935	
OXIDIZER	12590	4667	
PROPELLANT	44883	13602	
PAYLOAD		10638	
OTHER	29658	40260	
TOTAL	74542	64500	
GEOMETRY			
LENGTH	174.6	160.9	
BODY WETTED AREA	13347.7	12020.1	
BODY PLANFORM AREA	4870.3	3959.7	
ENTRY PLANFORM LOADING	49.1	44.9	
PROPULSION			
THRUST-TO-WEIGHT		2.47713	1.58447
NO. OF ENGINES	6	3	
SL THRUST/ENG NOM/UR	399996/ 399996	238369/	4799924/ 4799924
VAC THRUST/ENG NOM/UR	661867/ 661867	471600/	5542168/ 5542168
SL ISP NOM/UR	389.3/389.3	232.0/	389.3/389.3
VAC ISP NOM/UR	449.5/449.5	459.0/	449.5/449.5
TRAJECTORY			
MASS RATIO	2.83445	2.69944	
MAXIMUM DYNAMIC PRESSURE			736.4
STAGING DYNAMIC PRESSURE			50
STAGING VELOCITY (RELATIVE)			10685
STAGING ALTITUDE			186354
STAGING FLIGHT PATH ANGLE (RELATIVE)			3.965
INJECTION VELOCITY (INERTIAL)		25897	
INJECTION ALTITUDE		260002	
INJECTION FLIGHT PATH ANGLE (INERTIAL)		.000	
INJECTION INCLINATION		55.05	
FLYBACK RANGE	285.1		

Table 7-4. FR-4 Weight Summary

SPACECRAFT SUMMARY WEIGHT STATEMENT

NASA FR-4, Point Design 6-3-6
Eng. Zero Contingency Fixed Thrust

BY

DATE

CODE	SYSTEM	ITEM OR MODULE A	B	C	D	E	F	SPACECRAFT M	U
1.0	AERODYNAMIC SURFACES	32132	32132					26176	
2.0	BODY STRUCTURE	71282	71282					51045	
3.0	INDUCED ENVIR PROT	33920	33920					33075	
4.0	LNCH RECOV & DKG	7823	7823					8123	
5.0	MAIN PROPULSION	62922	62922					33377	
6.0	ORIENT CONTROL SEP & ULL	3786	3786					6663	
7.0	PRIME POWER SOURCE	437	437					1447	
8.0	POWER CONV & DISTR	1402	1402					1502	
9.0	GUIDANCE & NAVIGATION	200	200					282	
10.0	INSTRUMENTATION	200	200					350	
11.0	COMMUNICATION	200	200					220	
12.0	ENVIRONMENTAL CONTROL	300	300					560	
13.0	(RESERVED)								
14.0	PERSONNEL PROVISIONS								
15.0	CREW STA CONTRL & PAN	200	200					250	
16.0	RANGE SAFETY & ABORT								
SUBTOTALS (DRY WEIGHT)		214804	214804					161870	
17.0	PERSONNEL	900	900					920	
18.0	CARGO							15000	
19.0	ORDNANCE								
20.0	BALLAST								
21.0	RESID PROP & SERV ITEMS	9314	9314					5031	
SUBTOTALS (INERT WEIGHT)		102114	102114					20951	
22.0	RES PROP & SERV ITEMS								
23.0	INFLIGHT LOSSES	23788	23788					6342	
24.0	THRUST DECAY PROPELLANT								
25.0	FULL THRUST PROPELLANT	980288	980288					381982	
26.0	THRUST PROP BUILDUP								
27.0	PRE-IGNITION LOSSES								
TOTALS (GROSS WEIGHT) (LB)		1229094	1229094					571145	
DESIGN ENVELOPE VOLUME (FT^3)		74542	74542					64500	
PRESSURIZED VOLUME (FT^3)									
DESIGN ENVEL SURF AREA (FT^2)		13348	13348					12020	
PRESSURIZED SURF AREA (FT^2)									
DESIGN q, MAX (LB/FT^2)		736	736					736	
DESIGN g, MAX									
DESIGN POWER, MAX (KW)									
DESIGN NO. MEN/DAYS									

DESIGNATIONS:

CODE, SYSTEM: REF. MIL-M-38310A OR SP-6004

ITEM OR MODULE

A - Booster

B - BOOSTER

C

D

E

F

SPACECRAFT

M MANNED LAUNCH - Orbiter

U UNMANNED LAUNCH

NOTES & SKETCHES:

THRUST DECAY PROPELLANTS ARE INCLUDED IN RESIDUAL WEIGHTS.

TANKS ARE OVER-SIZED TO ACCOUNT FOR THRUST BUILD-UP AND PRE-IGNITION LOSSES.

NSC Form 1523 (Jul 69)

not reduce the system capability on that score. Figure 7-3 shows the orbiter configuration, and Table 7-5 shows the synthesis summary. Table 7-6 is the weight summary.

7.2.2 FR-4 POINT DESIGN. The new orbiter configuration was used here also. It is similar to that of Figure 7-3. Table 7-7 shows the synthesis summary of this FR-4 system, and Table 7-8 is its weight summary.

7.3 COMPARISON OF FR-3 AND FR-4 VEHICLES

A comparison of the vehicles defined in Sections 7.1 and 7.2 is summarized in the table below. The FR-3 has approximately twice the payload capability of the FR-4 for both the 3.0 and 3.5M-lb configurations.

Note also that the 17 percent increase in GLOW did not result in a similar payload increase. This was due to the larger payload bay requirement (22-ft diameter) for the 3.5M-lb vehicle.

	3.0M-lb GLOW		3.5M-lb GLOW	
	FR-3	FR-4	FR-3	FR-4
Payload (lb)	32,000	15,000	35,000	17,300
Total Weight — Booster Element (lb)	2,429,886	1,229,094	2,787,324	1,396,323
Propellant — Booster (lb)	1,968,076	980,288	2,281,676	1,131,186
Total Weight — Orbiter (lb)	590,637	571,145	714,499	707,454
Propellant — Orbiter (lb)	388,923	381,982	474,331	482,172

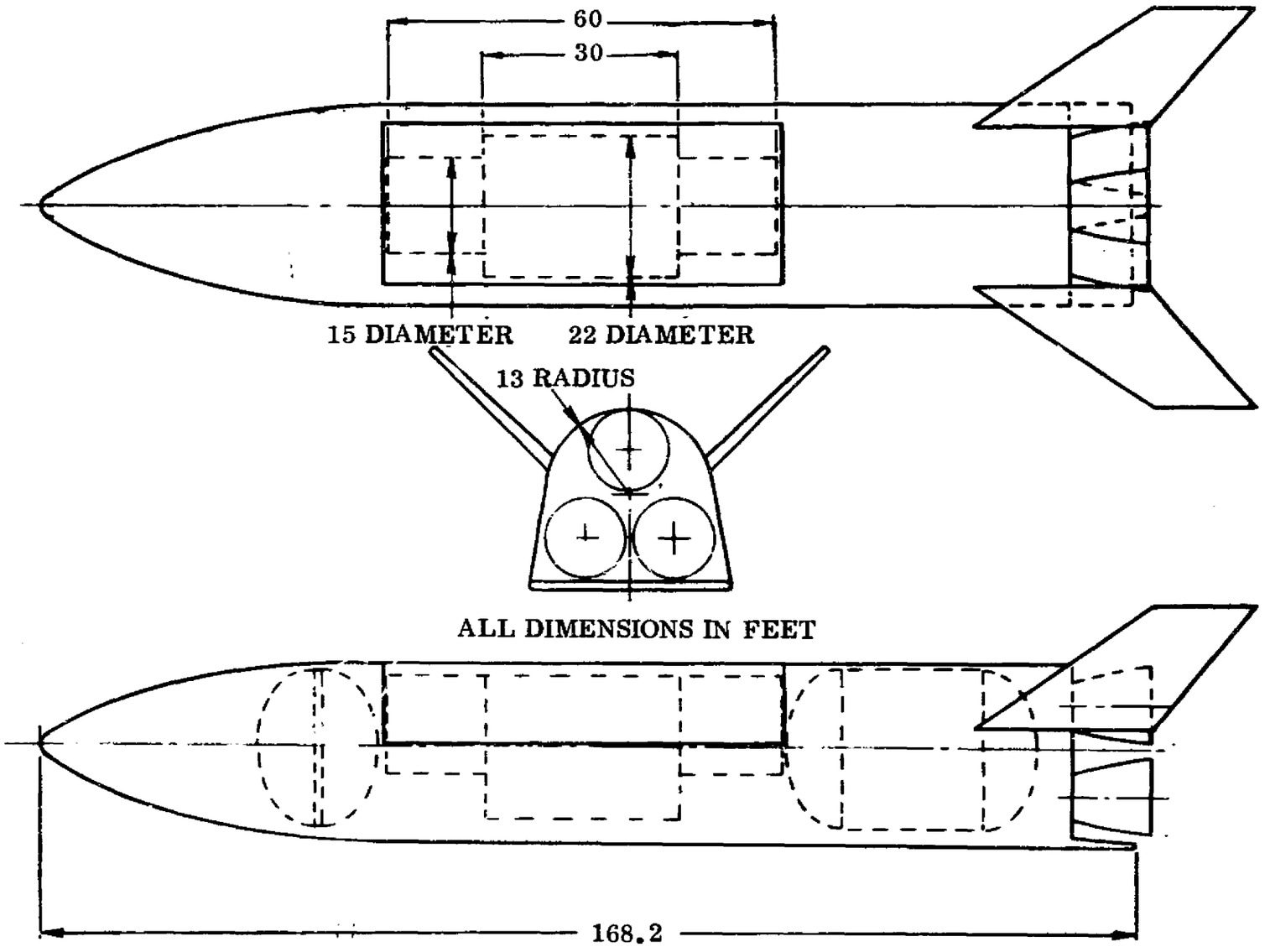

Figure 7-3. FR-3 Orbiter, 22-Foot-Diameter Payload Bay, 3.5M-Pound Gross Liftoff Weight System

Table 7-5. 3.5M-Pound GLOW FR-3 Design Synthesis Summary

	BOOSTER ELEMENT	ORBITER	VEHICLE
WEIGHT			
PROPELLANT, ASCENT	2281676	449694	
PROPELLANT, ORBIT MANEUVER		24637	
PROPELLANT, TOTAL	2281676	474331	
FLYBACK FUEL	48487	0	
PAYLOAD		35000	
STRUCTURE	430839	192483	623722
CONTINGENCY	7300	0	
OTHER	19022	12286	
TOTAL	2787324	714499	3501823
IN ORBIT		268867	
RETURN CONDITION	505648	260920	
ENTRY	0	228795	
LANDING	439040	0	
VOLUME			
FUEL	75693	14897	
OXIDIZER	29302	5772	
PROPELLANT	104995	20669	
PAYLOAD		16720	
OTHER	62543	52111	
TOTAL	167538	89501	
GEOMETRY			
LENGTH	228.7	168.2	
BODY WETTED AREA	22902.5	14353.0	
BODY PLANFORM AREA	8356.6	4698.8	
ENTRY PLANFORM LOADING	58.3	46.7	
PROPULSION			
THRUST-TO-WEIGHT		1.98029	1.48503
NO. OF ENGINES	13	3	
SL THRUST/ENG NOM/UR	400027/ 400027	238388/	5200349/ 5200349
VAC THRUST/ENG NOM/UR	461886/ 461886	471639/	6004512/ 6004512
SL ISP NOM/UR	389.3/389.3	232.0/	389.3/389.3
VAC ISP NOM/UR	449.5/449.5	459.0/	449.5/449.5
TRAJECTORY			
MASS RATIO	2.87000	2.65805	
MAXIMUM DYNAMIC PRESSURE			766.3
STAGING DYNAMIC PRESSURE			50
STAGING VELOCITY (RELATIVE)			11042
STAGING ALTITUDE			189345
STAGING FLIGHT PATH ANGLE (RELATIVE)			2.597
INJECTION VELOCITY (INERTIAL)		25897	
INJECTION ALTITUDE		260002	
INJECTION FLIGHT PATH ANGLE (INERTIAL)		.000	
INJECTION INCLINATION		54.96	
FLYBACK RANGE	298.2		

Table 7-6. 3.5M-Pound FR-3 Weight Summary

SPACECRAFT SUMMARY WEIGHT STATEMENT

CONFIGURATION: FR-3 Point Design, 22 Ft Bay, 13-3 Engines | BY | DATE

CODE	SYSTEM	ITEM OR MODULE A	B	C	D	E	F	SPACECRAFT M	U
1.0	AERODYNAMIC SURFACES	60980						29797	
2.0	BODY STRUCTURE	178879						64803	
3.0	INDUCED ENVIR PROT	23033						39156	
4.0	LNCH RECOV & DKG	23622						9352	
5.0	MAIN PROPULSION	130944						35078	
6.0	ORIENT CONTROL SEP & ULL	15349						9841	
7.0	PRIME POWER SOURCE	809						1574	
8.0	POWER CONV & DISTR	3423						1719	
9.0	GUIDANCE & NAVIGATION	200						282	
10.0	INSTRUMENTATION	200						250	
11.0	COMMUNICATION	200						220	
12.0	ENVIRONMENTAL CONTROL	300						560	
13.0	(RESERVED)								
14.0	PERSONNEL PROVISIONS								
15.0	CREW STA CONTRL & PAN	200						350	
16.0	RANGE SAFETY & ABORT								
SUBTOTALS (DRY WEIGHT)		458139						192882	
17.0	PERSONNEL	900						920	
18.0	CARGO							35000	
19.0	ORDNANCE								
20.0	BALLAST								
21.0	RESID PROP & SERV ITEMS	17709						3880	
SUBTOTALS (INERT WEIGHT)		18609						39800	
22.0	RES PROP & SERV ITEMS								
23.0	INFLIGHT LOSSES	46900						7486	
24.0	THRUST DECAY PROPELLANT								
25.0	FULL THRUST PROPELLANT	2281676						474331	
26.0	THRUST PROP BUILDUP								
27.0	PRE-IGNITION LOSSES								
TOTALS (GROSS WEIGHT) (LB)		2787324						714499	
DESIGN ENVELOPE VOLUME (FT^3)		167538						89501	
PRESSURIZED VOLUME (FT^3)									
DESIGN ENVEL SURF AREA (FT^2)		22903						14353	
PRESSURIZED SURF AREA (FT^2)									
DESIGN q, MAX (LB/FT^2)		766						766	
DESIGN q, MAX									
DESIGN POWER, MAX (KW)									
DESIGN NO. MEN/DAYS									

DESIGNATIONS:
- CODE, SYSTEM: REF. MIL-M-38310A OR SP-6004
- ITEM OR MODULE
  - A - Booster
  - B
  - C
  - D
  - E
  - F
- SPACECRAFT
  - M MANNED LAUNCH - Orbiter
  - U UNMANNED LAUNCH

NOTES & SKETCHES:

THRUST DECAY PROPELLANTS ARE INCLUDED IN RESIDUAL WEIGHTS.

TANKS ARE OVER-SIZED TO ACCOUNT FOR THRUST BUILD-UP AND PRE-IGNITION LOSSES.

MSC Form 1323 (Jul 68)

Table 7-7. 3.5M-Pound GLOW FR-4 Design Point Synthesis Summary

	BOOSTER ELEMENT	ORBITER	VEHICLE
WEIGHT			
PROPELLANT, ASCENT	1131186	459243	
PROPELLANT, ORBIT MANEUVER		22929	
PROPELLANT, TOTAL	1131186	482172	
FLYBACK FUEL	23625	0	
PAYLOAD		17300	
STRUCTURE	230886	194399	656171
CONTINGENCY	0	0	
OTHER	10625	13583	
TOTAL	1396323	707454	3500100
IN ORBIT		252032	
RETURN CONDITION	265136	242828	
ENTRY	255411	212622	
LANDING	231519	0	
VOLUME			
FUEL	37249	15103	
OXIDIZER	14525	5908	
PROPELLANT	51773	21010	
PAYLOAD		16720	
OTHER	33786	52825	
TOTAL	85560	90556	
GEOMETRY			
LENGTH	182.8	168.9	
BODY WETTED AREA	14632.7	14465.3	
BODY PLANFORM AREA	5339.1	4735.6	
ENTRY PLANFORM LOADING	47.8	44.9	
PROPULSION			
THRUST-TO-WEIGHT		1.99953	1.37114
NO. OF ENGINES	6	3	
SL THRUST/ENG NOM/UR	399931/ 399931	238331/	4799170/ 4799170
VAC THRUST/ENG NOM/UR	461775/ 461775	471526/	5541297/ 5541297
SL ISP NOM/UR	389.3/389.3	232.0/	389.3/389.3
VAC ISP NOM/UR	449.5/449.5	459.0/	449.5/449.5
TRAJECTORY			
MASS RATIO	2.82784	2.80707	
MAXIMUM DYNAMIC PRESSURE			518.9
STAGING DYNAMIC PRESSURE			50
STAGING VELOCITY (RELATIVE)			10246
STAGING ALTITUDE			184067
STAGING FLIGHT PATH ANGLE (RELATIVE)			3.343
INJECTION VELOCITY (INERTIAL)		25897	
INJECTION ALTITUDE		260057	
INJECTION FLIGHT PATH ANGLE (INERTIAL)		.004	
INJECTION INCLINATION		54.97	
FLYBACK RANGE	267.4		

Table 7-8. 3.5M-Pound FR-4 Weight Summary

SPACECRAFT SUMMARY WEIGHT STATEMENT

CONFIGURATION: NASA FR-4, Design Point 6-3-6 Engines, 22 Ft Payload Bay | BY | DATE

CODE	SYSTEM	ITEM OR MODULE A	B	C	D	E	F	SPACECRAFT M	U
1.0	AERODYNAMIC SURFACES	32781	32781					30687	
2.0	BODY STRUCTURE	78863	78863					66137	
3.0	INDUCED ENVIR PROT	37171	37171					39701	
4.0	LNCH RECOV & DRG	9355	9355					9655	
5.0	MAIN PROPULSION	64952	64952					35450	
6.0	ORIENT CONTROL SEP & ULL	4586	4586					7954	
7.0	PRIME POWER SOURCE	461	461					1534	
8.0	POWER CONV & DISTR	1618	1618					1718	
9.0	GUIDANCE & NAVIGATION	200	200					282	
10.0	INSTRUMENTATION	200	200					250	
11.0	COMMUNICATION	200	200					220	
12.0	ENVIRONMENTAL CONTROL	300	300					560	
13.0	(RESERVED)								
14.0	PERSONNEL PROVISIONS								
15.0	CREW STA CONTRL & PAN	200	200					250	
16.0	RANGE SAFETY & ABORT								
SUBTOTALS (DRY WEIGHT)		230887	230887					194398	
17.0	PERSONNEL	900	900					920	
18.0	CARGO							17300	
19.0	ORDNANCE								
20.0	BALLAST								
21.0	RESID PROP & SERV ITEMS	9458	9458					5391	
SUBTOTALS (INERT WEIGHT)		10358	10358					23611	
22.0	RES PROP & SERV ITEMS								
23.0	INFLIGHT LOSSES	23892	23892					7278	
24.0	THRUST DECAY PROPELLANT								
25.0	FULL THRUST PROPELLANT	113186	113186					482172	
26.0	THRUST PROP BUILDUP								
27.0	PRE-IGNITION LOSSES								
TOTALS (GROSS WEIGHT) (LB)		1376323	1376323					707459	
DESIGN ENVELOPE VOLUME (FT^3)		85560	85560					90556	
PRESSURIZED VOLUME (FT^3)									
DESIGN ENVEL SURF AREA (FT^2)		14633	14633					14465	
PRESSURIZED SURF AREA (FT^2)									
DESIGN q, MAX (LB/FT^2)		519	519					519	
DESIGN ε, MAX									
DESIGN POWER, MAX (KW)									
DESIGN NO. MEN/DAYS									

DESIGNATIONS:
CODE, SYSTEM: REF. MIL-M-38310A OR SP-6004
ITEM OR MODULE
A - Booster
B - Booster
C
D
E
F
SPACECRAFT
M MANNED LAUNCH - Orbiter
U UNMANNED LAUNCH

NOTES & SKETCHES:
THRUST DECAY PROPELLANTS ARE INCLUDED IN RESIDUAL WEIGHTS.

TANKS ARE OVER-SIZED TO ACCOUNT FOR THRUST BUILD-UP AND PRE-IGNITION LOSSES.

MSC Form 1523 (Jul 69)